United Nations Educational, Scientific and Cultural Organization

International Hydrological Programme

APPLICATION OF SATELLITE REMOTE SENSING TO SUPPORT WATER RESOURCES MANAGEMENT IN AFRICA: RESULTS FROM THE TIGER INITIATIVE

IHP-VII

No. 85

IHP-VII | Technical Documents in Hydrology | No. 85

United Nations
Educational, Scientific and
Cultural Organization

International
Hydrological
Programme

Application of satellite remote sensing to support water resources management in Africa: Results from the TIGER Initiative

IHP-VII | Technical Documents in Hydrology | N° 85
UNESCO, Paris, 2010

Published in 2010 by the International Hydrological Programme (IHP) of the United Nations Educational, Scientific and Cultural Organization (UNESCO)
1 rue Miollis, 75732 Paris Cedex 15, France

IHP-VII Technical Documents in Hydrology N° 85
UNESCO Working Series SC-2010/WS/15

Publications in the series of *IHP Technical Documents in Hydrology* are available from:

IHP Secretariat | UNESCO | Division of Water Sciences
1 rue Miollis, 75732 Paris Cedex 15, France
Tel: +33 (0)1 45 68 40 01 | Fax: +33 (0)1 45 68 58 11
E-mail: ihp@unesco.org
http://www.unesco.org/water/ihp

Printed in UNESCO's workshops
Paris, France

Introduction

Parameters relevant for hydro(geo)logy are spatially distributed and may show significant temporal variability. Earth Observation (EO) data, when used jointly with in situ data, can provide an essential contribution for the creation of inventories of surface water resources, the extraction of thematic maps relevant for hydrogeological studies and models (landcover, surface geology, lineaments, geomorphology…) or for the retrieval of (bio)geophysical parameters (water quality and temperature, soil moisture…) for a more detailed list, refer to Schultz and Engman (2000). The large area coverage of each observation, on the one hand, helps moving beyond the point-based readings provided by gauge networks to –for instance- basin-wide measurements of discharge and storage, and on the other hand derives common databases of inter-country comparable information. Repeatability of observations allows the generation of a time-series of observed parameters and may result in an improved capability to analyse, monitor and forecast the evolution of phenomena, facilitating water resources management.

In Africa, where a 90% decline in available infrastructure at water stations was reported (Brown, 2002) and where there are issues related to occurrence, distribution, protection and management of available water resources as well as to the management of competing demands for such resources (ECA et al., 2000), exploitation of EO data has been marginal in the past. Only in 2002 the European Space Agency (ESA) in the context of the Committee of Earth Observation Satellites (CEOS) started the TIGER initiative as a concrete action following the resolutions of the World Submit on Sustainable Development held in Johannesburg. The initiative aims at assisting African countries to overcome problems faced in the collection, analysis and dissemination of water related geo-information by exploiting the advantages of EO technology.

In the last few years, under the leadership of the African Ministerial Council on Water (AMCOW), TIGER has evolved with main contributions by ESA, UNESCO and the Canadian Space Agency (CSA) and with collaboration of other partners such as the Economic Commission for Africa (UN-ECA), the African Development Bank (AfDB) and other African and International organizations.

During the first implementation period, the initiative followed a three-step approach — from research to pre-operational and operational stages — aimed at preparing the ground for further activities (Fernandez-Prieto and Palazzo, 2007). This resulted in:

- Successful implementation of fifty research projects focusing on the status of water resources in Africa and Integrated Water Resources Management (IWRM) exploiting Earth Observation data provided by ESA. These projects involved partnerships between numerous universities, technical centres and water authorities. Research teams were supported with dedicated training, capacity building actions and tools.

- Support of sixteen pre-operational projects (development and demonstration projects) funded by ESA and CSA at 6 Million Euro and involving more than 30 African water authorities working with technical consortia involving African, European and Canadian companies. The projects developed EO-based water information services adapted to specific user needs and demonstrated their real applicability in Africa. The result of this

activity was a solid portfolio of potential operational services ready to be transferable to a full operational level.

- On the basis of the results from successful demonstration projects, trans-boundary or national projects led by African water authorities are being implemented, aimed at supporting the transition from a pre-operational stage to a sustainable operational phase in partnership with development partners. The first TIGER operational project, the GEO-AQUIFER which is a successor of the AQUIFER pre-operational project, is ongoing and is co-funded by the African Water Facility (AWF) and the Sahara and Sahel Observatory (OSS). Other projects are under evaluation.

This approach was complemented by:

- A strong capacity building component involving dedicated training support for African partners (water authorities, technical centres, universities, remote sensing centres) to develop skills in the utilization of EO technology to support IWRM. More than 20 training sessions have been organized under the TIGER umbrella, focusing on the needs of both the different TIGER research and pre-operational projects.

- The TIGER Capacity Building Facility was activated in 2006, led by the International Institute for Geo-Information Science and Earth Observation, ITC (www.itc.nl), and has provided further support to a number of African teams involved in the Research stage (Vekerdy et al., 2008). Capacity building efforts of the facility have benefited more than 90 African scientists with tailor-made courses in four basic activities: basic training, applied short courses, project-oriented supervision of researchers and advanced courses.

UNESCO through its International Hydrological Programme, IHP, agreed to publish the results provided by several different groups involved in the TIGER research and pre-operational projects in the series *IHP Technical Documents in Hydrology*. It is our hope that this publication will stimulate researchers worldwide to perform additional in-depth work and analysis on the exploitation of space borne remote sensing technology for water resources in Africa. The papers in this special issue fall under four interrelated themes: (1) use of multi-source EO data to facilitate analysis and management (through ingestion in Decision-Support Systems or models) of large aquifers (transboundary such as SASS and SAI and national such as Sous-Massa); (2) exploitation of EO data to derive information about catchment characteristics (lineaments and geology, landcover and land use etc.); (3) extraction of water bodies from multi-temporal datasets for the creation of inventories and assessment of flooding patterns; and (4) the derivation of soil moisture information on a dynamic basis from satellite data.

ACKNOWLEDGEMENT

We wish to thank all authors for submitting their manuscripts for consideration for publication and CSA and ITC for their support in the release of this special issue. We further extend our deepest appreciation to the reviewers who spent precious time from their busy schedules to review the papers submitted to this special issue. The reviewers are listed below in alphabetical order: Abou Amani, Bo Appelgren, Emanuel Balloffet, Lieven Bydekerke, Chris Bremmer, Ian Cluckie, Steve Iris, Chris Mannaerts, Chris Stewart, Bob Su, Giovanna Trianni, Zoltán Vekerdy.

REFERENCES

Brown, K. 2002. Water Scarcity: Forecasting the Future with Spotty Data. *Science* 9 August 2002: Vol. 297. no. 5583, pp. 926 – 927.

ECA, AU and AfDB, 2000. *The Africa Water Vision for 2025: Equitable and Sustainable Use of Water for Socioeconomic Development.* Economic Commission for Africa, African Union and African Development Bank, Addis Ababa.

Fernandez-Prieto, D. and Palazzo, F. 2007. The role of Earth Observation in improving water governance in Africa: ESA's TIGER initiative. *Hydrogeology Journal,* Vol. 15, No. 1, pp. 101-104.

Schultz GA and Engman ET (eds) 2000. *Remote Sensing in Hydrology and Water Management.* Springer-Verlag, Berlin.

Vekerdy, Z., Su, B. v. Lieshout, A., Fernandez-Prieto, D. and Stewart, C. 2008. TIGER Capacity Building Facility - Phase 1, lessons learnt. *Space Applications*, Toulouse, France, ESA.

Diego Fernandez Prieto

Siegfried Demuth

Annukka Lipponen

Francesco Palazzo

TABLE OF CONTENTS

Earth Observation in support of Management of Internationally Shared Groundwater Resources in Africa: the AQUIFER Project

Stefan Saradeth[(1)], Abdel Kader Dodo[(2,3)] and Djamel Latrech[(2)]

[(1)] GAF AG, Arnulfstr.197, D-80634 Munich, Germany, E-mail: info@gaf.de
[(2)] OSS, Boulevard de l'environnement, BP 31 - 1080 Tunis Cedex – Tunisia, E-mail: sass@oss.org.tn
[(3)] University Abdou Moumouni, Faculty of Science, Department of Geology, BP. 10666, Niamey – Niger, E-mail: dodoabdelkader@yahoo.fr

Abstract This paper sets out to report key results and experiences obtained during the execution of the AQUIFER project. AQUIFER focuses on the development of Earth Observation based products and services and demonstrating their use in support of national authorities and international institutions in transboundary groundwater management. Two prominent, internationally shared groundwater resources (aquifers) in Africa, the SASS (North-Western Sahara Aquifer System) and SAI (Iullemeden Aquifer System) have been addressed, and a number of Earth Observation based information products have been developed, demonstrated and validated.

1. INTRODUCTION

Cooperative management of internationally shared aquifers aims at ensuring the sustainable provision of water to the population and avoiding international conflicts. The AQUIFER project (below referred to as AQUIFER) focuses on the development and demonstration of Earth Observation based products and services which support national authorities and international institutions in the transboundary management of two prominent, internationally shared groundwater resources - aquifers - in Africa, the North-Western Sahara Aquifer System referred to as SASS (acronym from the French "Système Aquifère du Sahara Septentrional") and the Iullemeden Aquifer System, referred to as SAI (from the French "Système d'Aquifère d'Iullemeden").

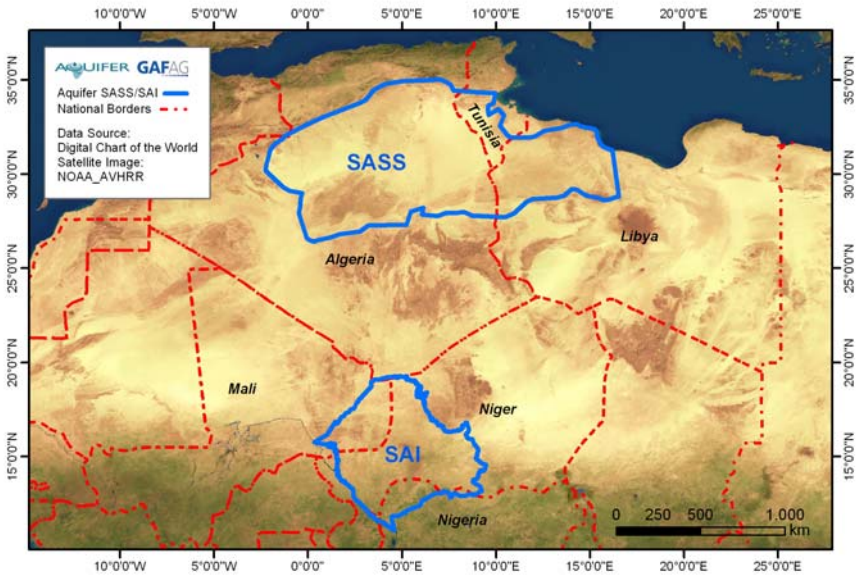

Figure 1 Delineation of the SASS and SAI groundwater basins in Northern Africa

AQUIFER is one of the demonstrator projects of the joint ESA - UNESCO TIGER initiative, which focuses on "Earth Observation for Integrated Water Resources Management in Africa". After 3 years of implementation, the project was concluded in September 2007.

2. AQUIFER OBJECTIVES AND APPROACH

The main objective of the AQUIFER project is to support the users in the management of internationally shared water resources and aquifers by means of Earth Observation (EO) as well as to strengthen overall and integrated water management practices. In the project, a number of tailored and GIS-compatible demonstration products and services are generated and integrated into work-flows. The following principles apply:

- The project is defined and its success measured in terms of implemented and delivered products and services – different from other, more process-oriented technical assistance approaches
- An initial review of the information requirements has been performed in the project, bringing together user's demand and the supply side (taking into account the capacities and limitations of Earth Observation technology and project resources)
- Some AQUIFER products, the so-called "science" products, are not primarily addressing user requirements but are driven by the desire to demonstrate future capabilities of EO in support of aquifer management
- Capacity strengthening in generating products, delivering and using services is the key to sustainability. Emphasis is put on the joint project performance by African, Maghrebian and European partners as well as on extensive on-site training interventions and know-how transfer.

3. THE AQUIFER PROJECT TEAM AND ROLES

AQUIFER involves institutions from Africa, the Maghreb and Europe: user organizations in charge of water management in 6 countries as well as product and service providers (see Table 1).

The user organisations play a critical role in the project – they are involved in the definition of the products and services, in the delineation of the geographical priority areas as well as in the assessment and validation of results. User involvement is coordinated by OSS ("Observatoire du Sahel et du Sahara": the Sahara and Sahel Observatory) in Tunis. Product providers comprise institutes and specialists in Earth Observation, geo-information and water resources management, with each partner having a specific expertise and product responsibility. The local providers from Africa-Maghreb play a crucial role, being in charge of the land use/cover mapping and monitoring product, as explained below.

4. EARTH OBSERVATION AND GROUNDWATER: CAVEATS

Earth Observation (EO) or satellite remote sensing offers unique capabilities: its simultaneous area wide and transboundary coverage provides a uniform spatial information layer to correlate or extrapolate isolated field data. It thus can be a cost efficient and objective mapping and monitoring instrument. There are two caveats:

- EO is not a stand alone tool but requires ground truthing and needs to be integrated and assimilated by means of geographical information systems, data modelling and decision support systems with other available information and data like well information or geological maps.
- Additionally and in the context of groundwater management it is important to note that EO is confined to the land surface: optical remote sensing sensors measure the reflectance of surface features, radar and thermal sensors allow only to detect and to identify features at or very close to the surface. For application to groundwater management this implies that Earth Observation can usually work only indirectly by means of proxy information or secondary effects.

Both points are expanded in the following discussion of the AQUIFER products and services

5. TWO AFRICAN TRANSBOUNDARY AQUIFERS

The project work is performed on two large transboundary aquifers in Africa. The groundwater basins give the overall geographical frame of work; specific areas of interest are defined according to the requirements and priorities of the user organisations. In each basin, 2-3 areas of interest with a total size of approximately 100,000 km² are selected as key work areas. Both basins are characterized by in large parts poor accessibility, harsh climatic conditions and by the limited or very heterogeneous availability of ground truth information- all this making remote sensing a tool of particular interest.

5.1 SASS: North-Western Sahara Aquifer System

The SASS is a groundwater resource and freshwater reserve underlying parts of Algeria, Libya and Tunisia. It occurs at varying depths (as deep as 1000 m) and has negligible recharge. The SASS groundwater resource is sufficient for many centuries to come (500-600 years at projected consumption rates), but intense development by the three countries in the past thirty years has exposed the aquifer to a serious risk of groundwater table drawdown, loss of artesian pressure, salinisation, salt water intrusions along the coast, and deterioration of water quality across the national borders. The situation is aggravated by growing population pressure and a strong development of irrigation schemes. A comprehensive characterisation of the SASS is given in the literature, for example OSS (2003).

Table 1 AQUIFER partnership

User Group	**Project team of expert institutions / product & service providers**	
	African – Maghrebian Partners	**European Partners**
ANRH: Agence Nationale des Ressources Hydrauliques, **Algeria**	CNTS: Centre National des Techniques Spatiales, **Algeria**	GAF AG, **Germany** – lead partner and project responsible
GWA: General Water Authority, **Libya**	LCRSS: Center for Remote Sensing & Space Science, **Libya**	C-S SCOT, **France**
Le Ministère des Mines, de l'Energie et de l'Eau, **Mali**		Institutes of "Water Resources Management" and "Digital Image Processing"; Joanneum Research, **Austria**
Le Ministère de l'Hydraulique, de l'Environnement et de la Lutte Contre la Désertification, **Niger**	The AGRHYMET Regional Centre, **Niger** – provider for SAI	Telespazio SpA, **Italy**
Federal Ministry of Water Resources, **Nigeria**	NASRDA: National Space Research Development Agency, **Nigeria**: provision of NigeriaSat imagery	University of Jena, Department of Geoinformatics and Remote Sensing, **Germany**
Direction Générale des Ressources en Eau, **Tunisia**	CNT: Centre National de Télédétection, **Tunisia**	Vista Geowissenschaftliche Fernerkundung, **Germany**
Observatoire du Sahel et du Sahara (OSS), Tunis – user coordinator		

5.2 SAI: Iullemeden Aquifer System

The Iullemeden Aquifer System is a transboundary sedimentary groundwater basin representing one of the major freshwater reserves of West Africa. It covers parts of Mali, Niger and Nigeria and extends over

an area of 500,000 km². The SAI is a multi-aquifer system composed of two major aquifers: the Cretaceous "Continental intercalaire" and the Tertiary "Continental Terminal" sedimentary formation. There are a number of major threats to the aquifer and the related ecosystems. These include the change in water levels, a loss of water resources, groundwater depletion, water quality degradation and salinisation and land degradation. The stress on the aquifer and the environment in the SAI basin is further pronounced by recent climatic changes with reduced precipitation and increased evaporation. The Niger River crosses the basin and is also fed by the groundwater resources. More information on the SAI can be found in the literature (e.g. ESRIN, 2003; OSS, 2007a,b,c).

6. AQUIFER PRODUCTS AND SERVICES

The AQUIFER portfolio consists of eight spatial information products, based on EO:

1. Land use and land cover mapping and change monitoring
2. Water abstraction estimate in respect of crop water demand estimates for irrigated areas
3. Refined land use/cover mapping
4. Surface water bodies or water pools (called "mare" in French) - their location, extent and dynamics
5. Digital elevation models and derived products
6. Estimates of basin-wide evapotranspiration and precipitation as key parameters for water balance
7. Water and vegetation monitoring over the entire aquifer
8. Ground subsidence monitoring and its correlation with groundwater abstraction

Each of the products is shortly discussed in the sections below. All products and related documentation are presented in full detail on the AQUIFER project website (GAF, 2007). Results are generated in two phases: in a prototype phase, a first set of products is developed and tested in small prototype areas. Subsequently all products are generated in extended areas. Results are delivered in the form of GIS compatible files and paper maps with related metadata and documentation. Around 1000 Earth Observation satellite image data sets dating from 1992 to 2006 - were acquired and analysed in the framework of AQUIFER and made available to project partners.

6.1 Land use and land cover mapping and change detection

Multitemporal satellite data from optical and multispectral as well as radar sensors were combined and augmented with ancillary information (thematic maps) and ground truth information. The data was processed using a combination of automated classification steps and visual interpretation. Maps of land use (LU) / land cover (LC) and their changes in time were compiled covering parts of Algeria, Tunisia, Libya, Niger, Nigeria and Mali.

The LULC mapping and monitoring product was selected by the users for implementation within AQUIFER because of the following uses and applications:

- Improved location and definition of areas subject to water use for irrigation purposes and better detection of illicit abstraction
- Improved and up-to-date information on surface water bodies and wetlands and their role in recharge of aquifers
- Monitoring of soil deterioration and evolution of the agricultural sector

Specifically by the SASS user organisations:

- Provision of information on irrigated areas and crop patterns for the determination of crop water requirements and estimates of groundwater abstraction (as further described below)
- Provision of objective and trans-boundary comparable information for decision making within the legal and institutional consultation mechanism among the countries of the SASS region

and for the SAI basin:

- Monitoring of the changes in LULC occurring in important recharge areas due to population pressures and the use of this information as input to groundwater recharge modelling
- Location, extent and development of wetlands as important ecological assets
- Determination of areas at risk from possible groundwater contamination by pollutants

The EO based land use and land cover mapping is an operational product since many years, both in the public and commercial sector. It is genuinely multipurpose with applications particularly in agriculture, environment and natural resources management. The relevance of this product to the SASS users is underlined by the fact that the product generation is continued and expanded in the follow-up Geo-Aquifer project. "Reconnaissance mapping" with few thematic classes at lower geometric resolution must be clearly separated from "detailed mapping" at scales up to 1:10,000. Limiting factors in the SASS proved to be parcel sizes sometimes too small in relation to the sensor resolution and "intercropping" practice where crops are cultivated multi storey, for example vegetables under date palms.

The work has been performed in the different countries through the respective local providers, coordinated by C-S SCOT with the support of the user's organisations.

6.2 Water abstraction estimates

Measurement of irrigation water volume consists primarily of measuring surface-water withdrawals from rivers, lakes and streams, groundwater withdrawals, and diversions and conveyance losses in surface-water-delivery systems. However, determining irrigation water use over large areas, which may include hundreds or thousands of irrigation units (irrigated areas, oasis), requires reliance on data from other sources, or developing methods to derive irrigation water-use values from coefficients related to power consumption, or estimating water use through irrigated acreage and crop consumption coefficients.
The later approach has been applied here: Water abstraction estimation for irrigation is an estimation of the optimal amount of water to be extracted from the aquifer (or from other water resources) and applied to the irrigation scheme to satisfy the crop water demand during the growing season. The CROPWAT decision-support system, developed by the Land and Water Development Division of the Food and Agriculture Organization of the United Nations (FAO) for irrigation planning and management, is used together with the land use/cover maps to determine spatial distribution of water abstraction estimates. In addition, climatic data and crop parameters are used. CROPWAT is a tool to carry out standard calculations for reference evapotranspiration, crop water requirements and crop irrigation requirements, water abstraction estimation and more specifically to assist in the design and management of irrigation schemes (see Figure 2).

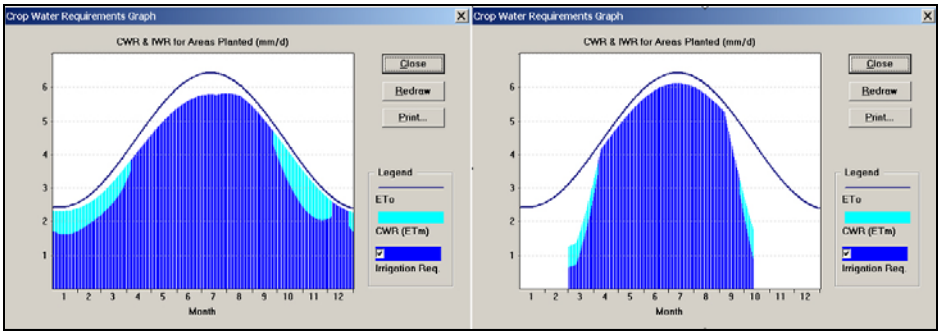

Figure 2 Examples of crop water requirement graphs for date palm (left) and alfalfa (right). Shown are the reference crop evapotranspiration (ET0), the crop water requirement (CWR) and the irrigation water requirement (IWR) in mm/d. The difference between the CWR and IWR is made up by the effective rainfall. Graphs prepared by Joanneum Research.

The product 'Water Abstraction Estimation' is an estimation of the optimal amount of water to be extracted and applied to the irrigation scheme to satisfy the crop water demand during the growing season. The advantage is applicability of the method for estimating water abstractions from an internationally shared aquifer. Results are given in the form of GIS data and of maps. The generated maps show water abstraction estimates, expressed as mean annual discharge per unit area in litre/second/hectare for two demonstration sites in the SASS (see Figure 3).

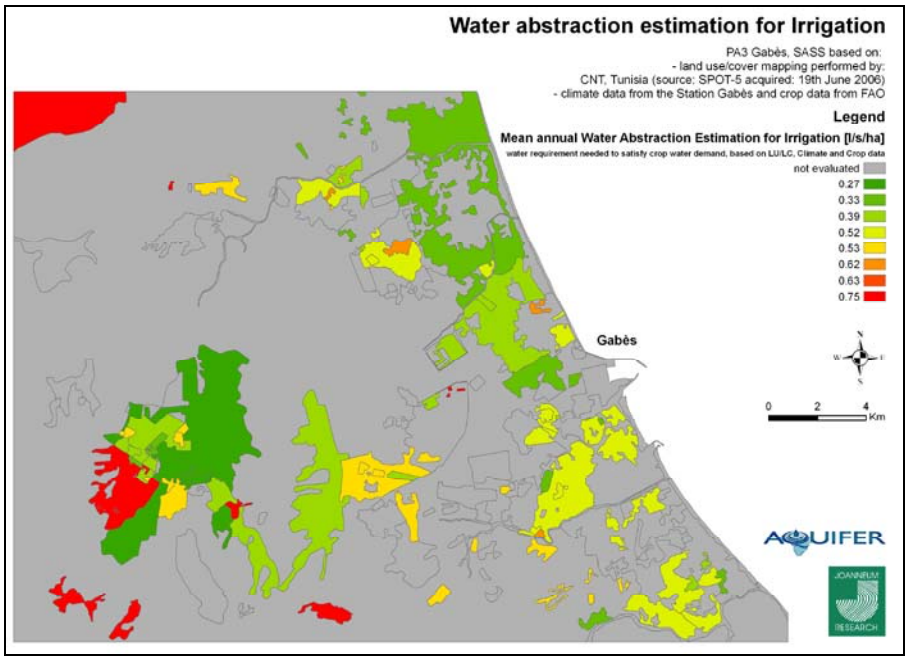

Figure 3 Map of irrigated areas in the demonstration area Gabès, Tunisia with the mean annual water abstraction estimation for irrigation as amount of water needed to satisfy crop water demand during growing period 2006, given in litre per second per hectare derived from the AQUIFER land cover/use map and crop specific irrigation water requirements. Map prepared by Joanneum Research on the basis of land use mapping performed by CNT.

The following applications of the product were aimed at:

- Estimation of water needs for selected crops and other vegetation taking into account their morphology, phenology, growing rate and local meteorological parameters.
- Optimizing the use of water for irrigation and optimize irrigation schedules
- Reducing waste of water recourses for the agricultural activities
- Monitoring water abstraction, reducing over-exploitation of the aquifer and improving groundwater management

This product for the SASS has received highest user attention and interest. Results remain confined to two test and demonstration areas in the SASS. Comparison of results with ground truth data and a first error assessment are only performed in one area. Crop water demand can serve as a first estimate for the actual groundwater abstraction, the latter being also determined by irrigation practice, supply and drainage losses as well as human and industrial use. Future work should aim at the full development in two modes: a detailed assessment for irrigation schemes versus a transboundary reconnaissance mode.

The work has been led by Institute of Water Resources Management, Joanneum Research, based on selected AQUIFER LULC maps, as described above.

6.3 Refined land use/land cover mapping

The goal of this research and development activity within AQUIFER is to demonstrate the future capabilities of satellite EO. Airborne data was acquired in 2005 through the dedicated AquiferEx campaign for two test sites in Tunisia (Gabès and Ben Gardane) by a polarimetric, 2 band radar sensor and a hyperspectral optical sensor, and were accompanied by a field campaign. The AquiferEx data are complemented by radar and optical satellite images ENVISAT ASAR – alternate polarisation and CHRIS PROBA – a research sensor for hyperspectral, multi-angular observations).

Several approaches for the synergistic processing, analysis and classification using optical and SAR data have been applied and bio-geophysical parameters like soil moisture, surface moisture, soil roughness and leaf area index are retrieved. A GIS-based decision-support system combines the obtained geophysical parameters, resulting in refined multisensory classification and land use map.

The work for this product has been led by Vista GmbH.

6.4 Open surface water mapping and dynamics

The mapping and monitoring of water bodies and wetlands is based on satellite data from different sources including multitemporal optical and radar image data, satellite derived global land cover data sets and radar image derived maps of water surfaces (watermask from the Shuttle Radar Topography Mission - SRTM). A multisensor and multitemporal processing and analysis workflow has been adopted using automatic and semiautomatic processing steps combined with visual interpretation.

Work has been focused on the open water surfaces – "mare" – in the SAI basin: a basin-wide mare inventory of water bodies with a resolution of 30 meters × 30 meters has been generated. In order to describe intra-annual dynamics an area of approximately 120,000 km² has been mapped in the dry as well as in the rainy seasons.

The product was selected by the users in expectation of the following applications and objectives:

- Mapping of "mares" as areas of groundwater recharge and surface water resources (e.g. for cattle)
- Mapping of wetlands as recharge/discharge areas and important ecological phenomena
- Inter- and intra-annual monitoring of the mare dynamics; some of them are ephemeral, some permanent

A compromise had to be found in AQUIFER combining a basin-wide approach with the high temporal and geometric resolution. Limiting factors proofed to be the geometric resolution of the used image data and their temporal revisit time: mapping of the inter- and intra-seasonal dynamics of the permanent and ephemeral ponds necessitates a dense temporal coverage. Many water bodies go undetected due to their small size by the medium resolution sensors used. In some cases mares are not detected, since the used C-band radar is sensitive to water surface roughness which during windy conditions can prevent the detection of mares. New L-band SAR sensors with improved geometric resolution have the potential to overcome both these limitations.

The users assessed the product as very useful, giving information that considerably exceeds the previous status of knowledge. Sub-classification of the water bodies into rivers, mare, dams, and floods is desired as well as additional ground truth verification. A basin-wide - supranational inventory with improved geometric accuracy for the SAI plus continued inter-annual monitoring is highly desired by the users in SAI.

The work for this product has been led by GAF.

6.5 Digital elevation models and derived products

Satellite remote sensing can provide operationally digital elevation models (DEM) through radar interferometry or stereoscopic optical satellite images. DEMs form the basis for contour line-, slope- and aspect maps and can be further analysed through Geographical Information System (GIS) technology to define watersheds, stream-networks and order (see Figures 4 and 5).

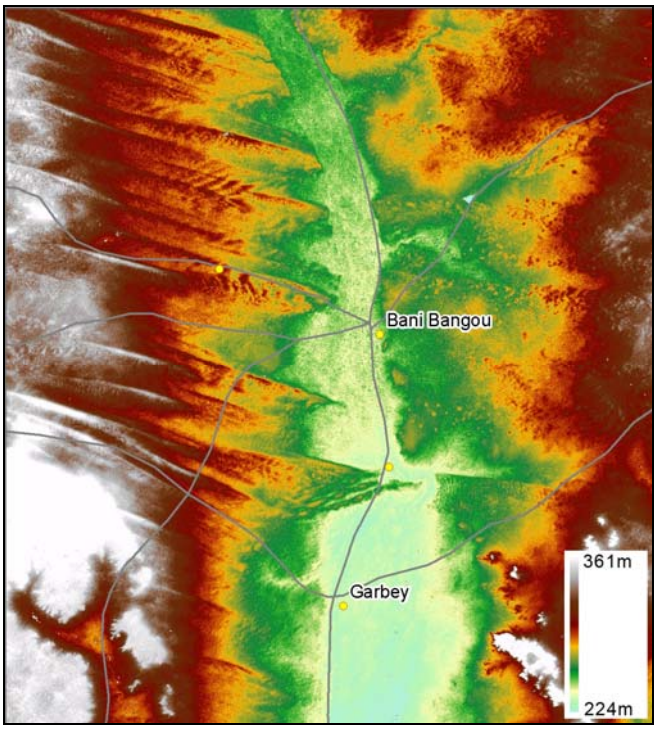

Figure 4 Digital elevation model (colour coded) interferometrically derived from EO radar data for the area around Bani Bangou, SAI. Dunes and other geomorphological structures become evident, which are not shown on existing topographical maps. DEM generated by Telespazio, cartography by GAF.

Data for high resolution (30 m) DEMs are derived interferometrically from ERS SAR for two demonstration areas in Oued Rhir, Algeria and Banibangou, Niger. For the full basin-wide DEM coverage a publically available medium (90 m) resolution DEM (Shuttle Radar Topography Mission - SRTM) has been introduced.

DEM and derived products are used as input to groundwater models, to improve accuracy and modelling of regional aspects. Users cited the following reasons for their interest in DEMs:

- Determination of flow of drainage waters from oases
- Determination of flow accumulations (local depressions) controlling groundwater recharge
- Delineation of watersheds which aids in modelling of mare inflows
- Correlating the location of mares and local depressions in topography. Depressions without mapped mares are indicators for zones of fast infiltration

The high resolution interferometric DEM received much user interest and positive feedback. The accuracy and resolution of the 90 m SRTM DEM appears too limited. Additionally in the SASS basin the interferometric DEM is affected by large no-data areas, limiting their use considerably. Basin-wide high

resolution DEMs exist but are still not available outside the military domain or could be produced at costs far out of the means of the users in SAI.

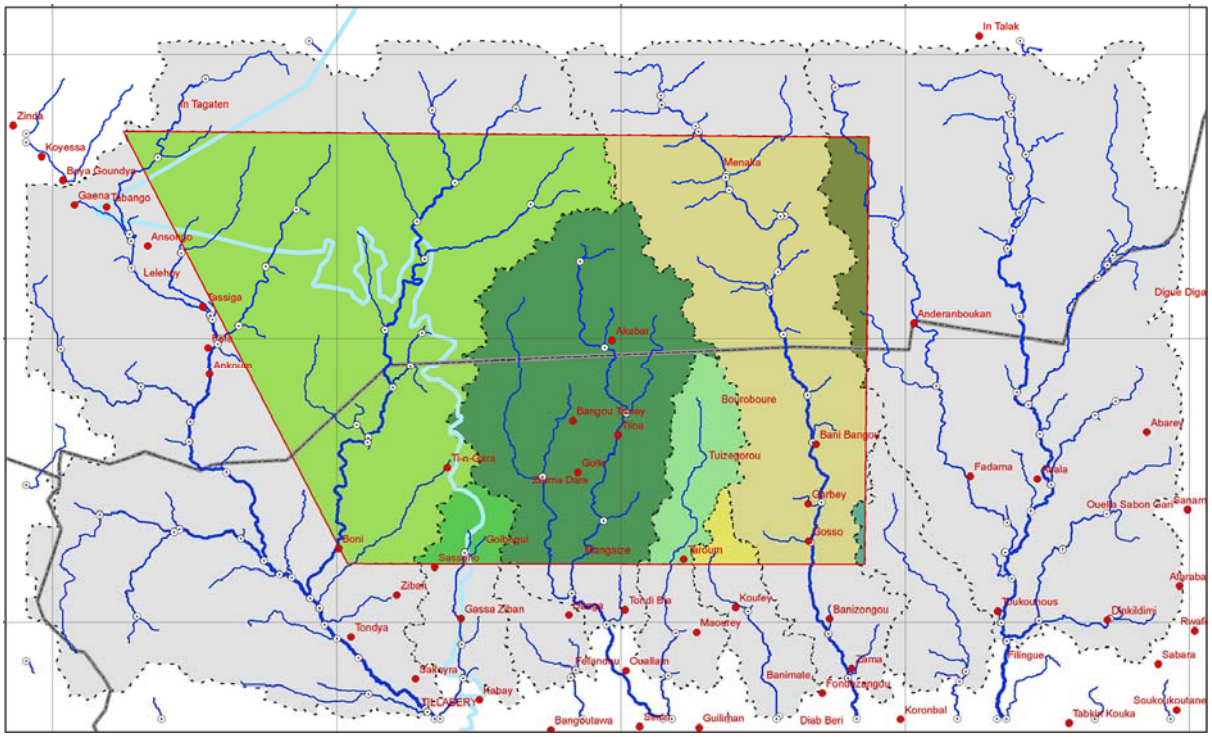

Figure 5 Delineation of watersheds (in colour) derived from digital elevation model (here SRTM DEM with 90 m resolution) for the area of interest in SAI. Map prepared by GAF.

The work for this product group has been led by Telespazio (interferometric DEMs) and GAF (DEM and derived products).

6.6 Water and vegetation monitoring over the entire aquifer

Both basins were analysed using optical and radar satellite (ENVISAT, MERIS and ASAR) augmented by ground truth and ancillary data like DEMs. Multiscale, object-oriented and rule-based land cover classification is applied. The analysis took into account the specific climate conditions and typical vegetation types. Different reference data were used for an assessment of the quality of the classification accuracy. Biophysical vegetation variables like fAPAR (Fraction of Absorbed Photosynthetically Active Radiation), fCover (Fraction of green vegetation covering a unit area of horizontal soil)] and indices like NDVI (Normalized Differenced Vegetation Index), MTCI (Meris Terrestrial Chlorophyll Index)] were used to describe and map vegetation phenology. Results show land use at different time periods. Target classes adhere to FAO LCCS (Land Cover Classification System) with subclasses defined depending on the specifics of the mapped region. Specific context information was used to derive an irrigated vegetation map for the SAI region.

The basin-wide product is by its nature limited in geometric accuracy but is a suitable tool for large area; high temporal resolution land cover + land cover change analysis. Time series analysis will allow mapping effects of climate change and overexploitation (e.g. desertification, disappearance of vegetation, mare and wetlands). The product has the potential to be used in SASS transboundary consultations as a tool to promote transparency and for future treaty monitoring. In the SAI context, the application focuses

on mapping and monitoring of wetlands, mares and desertification within the limitations of geometric and temporal resolution.

The work has been led by the Department of Geoinformatics and Remote Sensing, University of Jena.

6.7 Basin-wide evapotranspiration and precipitation

Water balance information is important for watershed management and in aquifer management showing regions with water surplus and deficit. Information on basin-wide precipitation and actual evapotranspiration are key parameters for the assessment of a basin-wide water balance. For large scale, basin-wide precipitation assessment, meteorological satellite data is used to improve spatial interpolation between sparse data from rainfall stations. Actual evapotranspiration (ET_a) cannot be measured directly; the combined application of energy balance modelling and meteorological satellite data analyses is applied to determine spatial extents of basin wide evapotranspiration. For this purpose, a pre-processed time series of 2005 METEOSAT 7 first generation data is used (36 ten-day intervals in 2005 in low spatial resolution of 5 km). Meteorological station data from World Meteorological Organisation (WMO) network is used for calibration, verification and quality control.

Annual precipitation, actual evapotranspiration and water balance were determined for the entire SAI basin and parts of the SASS basin. Water balance was computed as a difference between rainfall and actual evapotranspiration. Positive values predominantly observed in the SAI indicate that not all rainfall water was used by vegetation, but it has contributed to surface runoff or infiltrates to the aquifer. Large negative values indicate irrigation as the rainfall alone accounts for only a portion of the observed actual evapotranspiration. The developed and demonstrated approach can be extended to the new Meteosat Second Generation (MSG) EO data.

This “science” product has raised much interest among users. Improved accuracy by better calibration and ground truthing is needed as well as the expansion to a long (multiple years) time series analysis and the full assimilation of the data sets into agro-meteorological models.

The work for this product has been led by Vista GmbH.

6.8 Subsidence monitoring and correlation with water abstraction

Surface subsidence monitoring using radar satellite data and the method of differential interferometry allow to measure and monitor land subsidence over large areas and over years with an accuracy of less than 1cm. Herein interferograms are generated between datasets of various acquisition dates, forming multiple temporal baselines. The magnitude of land subsidence is determined by the phase shift in the interferograms, which is proportional to the line of sight displacement of the surface.

Since time series of SAR data are evaluated, the method’s success is highly dependent of persistent and coherent surface scattering of radar signals in the target area over time. A high level of coherence (or stable phase correlation of SAR data) guarantees a reliable measurement. Thus temporally varying land surface types, such as forest or vegetation cover, sand or sand dunes can pose problems. The temporal instability inside these areas leads to decorrelation of the phase resulting in increased noise. The noise level plus the atmospheric artefacts and the limited accuracy of the geometry acquisition knowledge set limits to the method.

Subsidence mapping and monitoring can be of interest in areas with intensive groundwater extraction (but also in hydrocarbon exploitation or mining settings) for risk assessment and prediction, for mapping and assessing the surface impact of lowered water tables as a result of groundwater abstraction.

The interferometric analysis was carried out for the study area Oued Rhir in Algeria with a size of 20,000 km² and for the time period from 1992 to 2006 using data from the ESA ERS-1/2 satellites and the ENVISAT satellite. The area of Oued Rhir was selected because of ongoing significant groundwater extraction and some known subsidence effects. Water abstraction information and well data have been provided by ANRH/ABHS for verification. Measured subsidence was compared to known water extraction information by means of GIS and statistical analysis and presented in a number of maps:

- Land subsidence as mean velocity per year for the time period 1992-2006 (see Figure 6)
- Water extraction including information on well depths, well density and pumping rate
- Qualitative comparison between measured surface subsidence and known water extraction

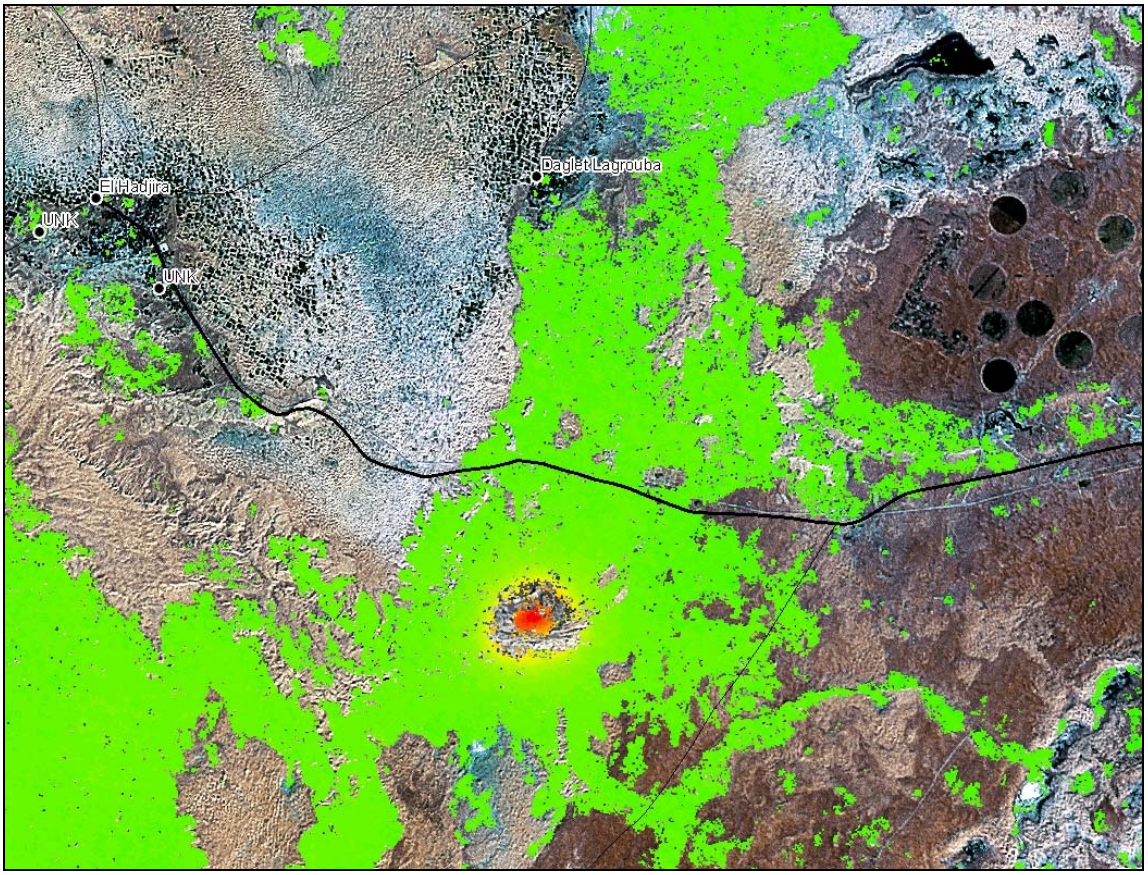

Figure 6 Subsidence in area SE of El Alia, Algeria which can be linked to now defunct oil exploration and water production well. Subsidence is shown in color code ranging from green (subsidence < 1mm/yr) over yellow to red (20 mm/yr) – in transparent no-data areas because of decorrelation. Background: Landsat satellite image. The area shown is approximately 20 km ×20 km in size and a subset of the total test area. Map prepared by GAF with inputs from Telespazio and ANRH.

The inclusion of data on the lowering of the water tables is recommended for a future analysis. Space-borne land subsidence mapping is an operational tool and has been successfully demonstrated in the test area. The observed subsidence values and velocities are in general small, and a significant part of the studied region is affected by temporal decorrelation due to effects of for example sand movements, vegetation cover, water surfaces or shadow effects resulting in no-data areas. A fairly good correlation is recognized between areas of considerable water abstraction and the observed land subsidence. It must be noted that particularly the irrigated and vegetated areas are affected by the decorrelation noise. The

objective to use in the future subsidence measurements to improve estimates of water abstraction appears as overly ambitious.

The work has been led by Telespazio (subsidence mapping and monitoring) and the Institute of Water Management, Joanneum Research (interpretation and correlation with water abstraction).

7. CONCLUSIONS

7.1 Summary of Results

The project accomplishments can be summarized as follows:

- Although the groundwater resources are hidden up to more than a kilometre below the surface, AQUIFER has demonstrated that observations from space of the Earth's surface can provide useful and effective information to decision-makers and strengthen cooperative management of internationally shared aquifers.
- AQUIFER has implemented products and services based on satellite data, such as land-use and land-cover maps, change maps, surface water extent and dynamics, digital terrain models, and derived information relating to water consumption for irrigation, subsidence, basin-wide water and vegetation monitoring, and water balance.
- Products have been delivered and their use demonstrated to and assessed by national authorities in groundwater management in 6 countries. User assessment is constructive and generally positive. The assessment ranges from full usability and confirmed interest by users to low relevance and assignment to the science demonstration product category. It provides valuable guidance for future improvements and enhancements.
- Intensive training and on-site consultations with partners in Maghreb and Africa have been delivered and intensive know-how exchange has started.
- AQUIFER has helped its Maghrebian partners to successfully conceive and formulate a follow-up project "Geo-Aquifer" and in securing funding from both the African Water Facility (AWF) and OSS.
- All results and reports prepared in the framework of AQUIFER are available on the AQUIFER website (GAF, 2007).

7.2 Recommendations

A number of recommendations for future follow-up work can be derived:

1) Complete and thorough understanding of user work flows is important. Full integration of the EO based information products into groundwater management and decision-making requires a comprehensive value adding chain including the integration of surface and sub-surface information together with data assimilation, modelling and interpretation in a multidisciplinary cooperation of EO, GIS, modelling and water resources and management experts (see Figure 7). This can be exemplified by the crop water demand product as introduced in Chapter 6.2. The crop water demand product relies on EO (e.g. crop pattern and land use), field and laboratory data (e.g. meteorological data, irrigation practice, crop coefficients) and modelling (the CROPWAT model for data assimilation). In the wider perspective, the crop water demand product itself takes a role in the water balance and overall decision-making.
2) Strong emphasis must be put on aiming at products which offer fast benefits to users in groundwater management in their day-to-day operations, which can in turn create a sustainable demand (and budgets) for the EO based services and generate business cases for local providers.

3) The following EO based products are of particular interest and have good potential for becoming fully operational tools in support of cooperative groundwater management:
    - "Estimate of water abstraction respectively crop water demand of irrigated areas": The topic is considered to have high potential for application in groundwater management, but it needs further work in the fields of demonstration, verification and validation. Important inputs to this product are the EO based land use/land cover maps.
    - "Surface Water Extension and Dynamics" has a very good potential and high relevance, specifically in the SAI.
    - "Digital Elevation Models and derived products" are inherently multipurpose and considered as fully mature and operational EO based products
    - "Evapotranspiration and precipitation for a basin-wide water balance": will be instrumental for water balance estimations and yield forecasts after a full assimilation of the data sets into agro-meteorological models.

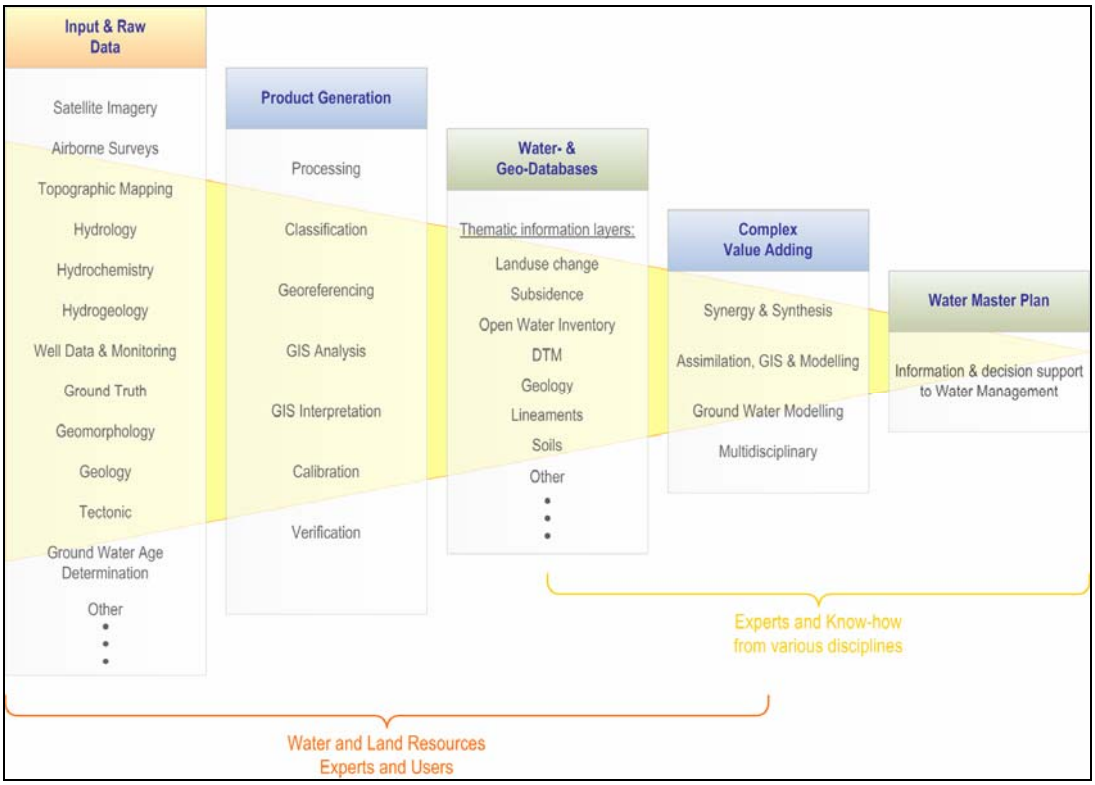

Figure 7 Successful application of Earth Observation information products in groundwater management depends not only on the assimilation of field observations and ancillary data but also on a comprehensive value adding chain.

8. ACKNOWLEDGEMENTS

The following principal co-workers in the AQUIFER project are gratefully acknowledged: Abdurahim Abughuffa, Alio Agoumo, Job Andigue, Heike Bach, Pibgnine Bazie, Nick Butler, Mario Costantine, Christian Crepeau, Yousfi Djaffar, Tahar Iftene, Reik Leiterer, Ruth Krause, Federico Minati, Johannes Reiche, Pierpaolo Saccon, Mathias Schardt, Christiane Schmullius, Bacha Sinan, Salem A. Sola, Ulrich Steiner, Sylvia Stockhammer, Christian Thiel and Thomas Weissmann.

The valuable support and contributions by the users group in the involved 6 countries is acknowledged: Algeria : Agence Nationale des Ressources Hydrauliqes: Rachid Taibi, Abderrazak Zahrouna, Ben

Brahim Lazhar; Libya : General Water Authority: Sadek Kadri, Mali : Ministère des Mines, de l`Energie et de l`Eau: Séïdou Maïga; Niger : Le Ministère de l'Hydraulique de l'Environnement et de la Lutte Contre la Désertification: Abdou Guero, Abdoul Moumine Moussa; Nigeria : Federal Ministry of Water Resources: Mr John Chabo; Tunisia: Direction Générale des Ressources en Eau: Mekki Hamza, Rachid Khanfir, Brahim Ben Baccar.

The project has been supported by ESA - Ref. AO/1-4645/04/I-LG; ESRIN/Contract No. 18481/04/I-LG under the Data User Element (DUE) programme. We gratefully acknowledge the provision of remote sensing data and ground truth information through the AQUIFEREX Optical and Radar Campaign (ESRIN/Contract No. 18746/05/I-LG), performed by DLR and partners. ESA Earth Observation image data has been made available through the TIGER announcement of opportunity AO nr. 2978. The useful comments of the anonymous reviewers are gratefully acknowledged.

9. REFERENCES

ESRIN, 2003. Final Report on Development of Water Resources in the Iullemeden Aquifer System, Project Coordination Meeting, IAEA Headquarters, 5 - 8 May 2003. ESA Centre for Earth Observation (ESRIN).

GAF, 2007. AQUIFER project website. URL: www3.gaf.de/aquifer, GAF.

GAF – OSS, 2007. AQUIFER Users Handbook. GAF and Observatoire du Sahel et du Sahara.

Dodo, A., 2007. Analyse Diagnostique Transfrontière du Système Aquifère d'Iullemeden (SAI) – rapport régional– PNUE/FEM. Observatoire du Sahel et du Sahara, Tunis – March 2007.

OSS, 2003. Système Aquifère du Sahara Septentrional – Rapport de Synthèse. Observatoire du Sahel et du Sahara.

OSS, 2007a. Modèle mathématique du Système Aquifère d'Iullemeden (SAI). Observatoire du Sahel et du Sahara.

OSS, 2007b. La base de données du Système Aquifère d'Iullemeden (SAI). Observatoire du Sahel et du Sahara.

OSS, 2007c. Système Aquifère d'Iullemeden: synthèse des principaux résultats. Observatoire du Sahel et du Sahara.

Implementation of an Integrated Decision Support System for the Souss-Massa Watershed, Morocco

Prévil C.[(1)]; Dolcine L.[(2)]; Brahm A.[(2)]; Er-Raji A.[(3)] and Qaimi A.[(4)]

[(1)] Department of Geography, University of Quebec at Montreal (UQAM), Canada, prévil.carlo@uqam.ca;
[(2)] Info-Electronics Systems (IES), Canada leslie@info-electronics.com;
[(3)] Royal Centre for Remote Sensing (CRTS), Morocco er-raji@crts.gov.ma;
[(4)] Hydraulic Agency of the Watershed of Souss-Massa (AHBSM), Morocco.

Abstract This paper presents the results of the implementation of an Integrated Decision Support System (IDSS) designed specifically for the Souss-Massa Hydraulic Basin Agency (AHBSM). Using Earth Observation products, this project has been developed to provide AHBSM with an updated spatial database, the appropriate tools and the know-how for a better support in the management and allocation of precarious water resources. The conceptual model of the database has been designed to take into account the entire role and mission of the water agency. The development of the IDSS has been successfully completed by providing the water agency with a spatial geodatabase with an updated and high resolution DEM, land cover map and modelling tools. The application developed proposed a global-local way of solution to different problems identified with the heads of the Agency. The modelling tools developed by the implementation and integration of applications meet some specific requirements designed with global-local objectives such as: dam and reservoir management, erosion mapping and flood risk area in a water demand management (WDM) perspective.

Résumé Ce papier présente les résultats de la mise en œuvre d'un système intégré d'aide à la décision (SIAD) au profit de l'Agence (de gestion) du Bassin hydraulique du Souss-Massa (ABHSM) au Maroc. La conception du SIAD a considéré l'ensemble de la mission de l'Agence et les applications ont visé cinq problématiques de gestion identifiées avec les responsables de l'Agence. Cette mise en œuvre a été réalisée à travers trois étapes principales: la formalisation du modèle décisionnel, son utilisation à travers des applications intégrant prioritairement des produits d'observation de la terre et sa facilitation grâce à la programmation d'une barre d'outils. Les applications traitent de problématiques avec des portées globales (ensemble du bassin) et locales (site d'un barrage, un sous bassin) sur: 1) la cartographie de l'érosion; 2) la répartition des zones menacées par les inondations torrentielles; 3) la gestion des barrages. Les détails de chacune des applications feront l'objet de publications distinctes. Le développement du SIAD_TIGERS a aidé l'Agence à se doter d'une base de connaissances territoriales, à jour, et d'un savoir-faire approprié, pour une meilleure prise en charge de la gestion de la demande en eau (GDE) avec des aspects relatifs à : l'arbitrage des changements dans l'occupation du sol et de la gestion des ressources précaires disponibles en eau (région aride du Maghreb).

1. PROJECT BACKGROUND

The countries of the Southern Mediterranean region, including Morocco, are exposed to multiple challenges with regard to the management of the water resources. Decision-makers on water issues have to find original and accurate solutions to tackle the increasing demand for water to satisfy the regular consumption of the population and the farm irrigation (large farms and intensive crop technologies level). Since 1995, the management of water in Morocco is governed by the Law 10-95 (1995), in accordance with the resolutions of the first World Water Summit, in Marrakech (Morocco, 1995). The basin agencies have the responsibility to enforce the law and they have to rely on several principles among which are the following: a) the public character of the water resources; b) the socio-economic planning and the

distribution of the resources based on the public participation; c) the settlement to mitigate uncertainties, vulnerabilities and risks inherent to exploitation of water hydro resources.
The complex and various interrelations between activities on the territory of the watershed cause that any considerable change of affectation of the land can have impacts on the management and the availability of the water in the basin; the production of goods, services and the prosperity of the general population (Lasalmil and Boulal, 2003). The Agency of watershed, in this context inherited from a complex problem (high level of organization; uncertainty of the environment; impossibility to know and understand all the holding relations). In such situation, the solution requires an integrated, interdisciplinary approach, based on the availability of better territorial information for elaborating scenarios, conducting debates with the public and for educating the stakeholders, in brief, for the aid of the territorial decision-making process. This solution implies a learning curve, based on a socio-constructivist axiology for an adaptive management of the resources (Prévil et al., 2004).

1.1 Helping the decision-making process

The mission of the agency with regard to the water resources demand covers all the aspects of basin management, quantity, quality (pollution), infrastructure (dam), distribution, risks (floods), royalties (userpays), and education (communication, popularization, awareness and participation). To embrace such a mission, the agency has to take into account social, spatial dimensions, space-time dynamics as well as legal and institutional framework of the problem (Keith and Said, 2004). Therefore, the Agency as the lead-institution has to deal with a whole set of problems affecting various levels of the decision-making process. The obligation of cooperation between the groups of users requires availability of synthesized territorial information to help to discuss, to negotiate or to convince the partners about the management of water, the legitimacy of a way of making with regard to the other alternative (Hanna, 2000). In this spirit, we can quote: updated information about the state of the resource, tools, not only to follow and model the evolution of the resources, but also to estimate the likely effect of the management scenarios.

It is to this set of challenges that we suggested answering, with the cooperation of the Agency, by a system of solutions (Leveque, 2001) based on the methods of decision support, the graphical representations and the systematic modelling integrated based on geo-information products (Longley et al., 2005). This system of solutions became a reality through the realization of an IDSS (called for the project SIAD_TIGERS). In this IDSS, we tried to increase the general understanding of the system of problems affecting the management of the water resources in the watershed of Souss-Massa. The organization of these solutions within the SIAD_TIGERS guarantees the fact that these solutions are not isolated, but are systematic with the functions of interaction, global nature, organization and a structure capable of tackling the complexity of the questions expressed previously (Prévil et al., 2004; Simonovic, 2007).

This system will have to help to answer aspects related to: a) the territorial economic planning; b) the (spatiotemporal) territorial information; c) the management of reservoirs; d) the protection against the risks of flood; e) the best exploitation of the ground water resources and f) the organization of the knowledge of the territory.

1.1.1 Definition and scope of the IDSS

The realization of an IDSS is located in the whole evolution of the methods and tools of the geographical information science. There is no formal method of production of IDSS for watersheds. Prévil et al. (2004) remind that a real IDSS adapted to the watershed management should not come down to an integrator of models in which the understanding of the decision-making problem is neglected. The IDSS must not be treated as a tool of simply overlaying of features of territorial data and even less as an interface press-

button to excite a set of algorithms in more or less sophisticated simulation software. The IDSS has to answer fundamentally to territorial decision-making problems. Numerous so-called integrated systems neglect simply the underlying decision-making problem and do not often constitute anything more than a platform where the only effort of integration applies to the format of the data in a way that the user does not have to go through too much trouble to make one interface compatible with the other (Cesur et al., 2004; Andreu et al., 1998; Dieulin and Boyer, 2003).

The application of the IDSS comes along with technological, organizational and important social implications for the AHBSM (called the Agency) involved its application. The IDSS joins a course of research on Coupling Human and Environmental Systems (CHES, Biosphere Data project, 2004), covering the following operational specificities a) socio-constructivist and contextualist aspects of learning, b) multicriteria approaches to decision theory, and c) methodologies concerning the science of geographical information. In this project, the IDSS is treated as a way of learning (water demand management) and a territorial long-term realization, aiming at giving to decision-makers and stakeholders of the management of the Souss watershed, a complex system, based on the management of the territorial information (Longley et al., 2005). This system integrates modules which were made operational quickly to fit the business model of the Agency.
The method of implementation of an IDSS is not intended to replace the political debate or the human decision. The end aims at first at taking into account the limited rationality by the territorial decision (Rosenhead, 2001), to inform the steps of a decisional territorial process (Carver et al., 1998) and to organize the actions of the decision-making (Heywood et al., 2006). In this way, the Agency can justify the legality and improve the legitimacy of the debates, the negotiations and even the decision, when it is possible (Roy, 1985; Longépé, 2006).
The application of an IDSS requires a patient and rigorous work which has to start with the construction of the decision-making stakes followed by an effort to structure the objects of territorial processes. In the case of a territorial problem, the geomatics tools and modelling can help in putting together the main facts, actions, flows or phases of activities of the territorial processes (Heywood and Carver, 1994; Hill et al., 2005). The objective of appropriation by the stakeholders of the territorial decision must be always present in all the steps (Prévil et al., 2004).

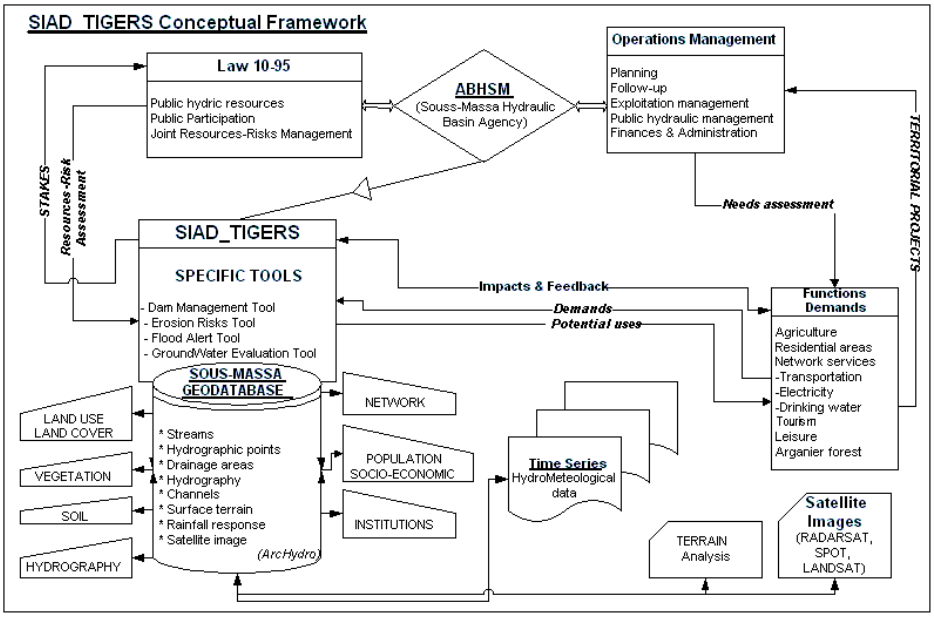

Figure 1 Conceptual Framework of the IDSS (SIAD_TIGERS)

1.1.2 Steps of structuring of the IDSS

The know-how in the elaboration of IDSS includes three intrinsic dimensions: generic, functional and structural. Various decision-making problems of proximity (from simple to complex) which face the Agency were analyzed, in cooperation with the Agency analysts. For example, all the operations subject to a license were reviewed. These operations concern activities such as the digging of wells or drilling, the setting up water intakes on streams or abstraction of groundwater beyond certain pre-established thresholds, etc.

After this stage, it was allowed to work in a way deepened with the aim of the realization of the geomatic tools. This implementation was realized according to three axes:

1) An axis of formalization which integrates the constitution of the various phases of data modelling, data provided and IDSS contents.
2) An axis of use which consists of the demonstration of the accuracy of the IDSS through the simulation of solutions for various territorial problems.
3 An axis of facilitation which corresponds to the programming of a toolbar to facilitate the update and development of the applications of the previous axis by the officials of the Agency.

The realizations concerned various additional aspects. The application of the IDSS required the realization of a set of activities. This paper addresses only the main realizations ensuing from these activities. Specific and detailed publications presenting the main applications of the project will be developed in other papers (Prévil et al., 2008; Dolcine et al., 2008; Er-Raji et al., 2008).

2. EARTH OBSERVATION PRODUCTS AND GEOMATICS FOR BETTER TERRITORIAL INFORMATION

2.1 Constitution of the territorial model and definition of the scope of the IDSS (Axis of formalization)

The realization of the axis of formalization of the IDSS aims at answering two questions: How to improve the decision-making in the watershed and to ensure good management of the water resources of the watershed? Furthermore, how to improve knowledge on the short and long-term trends and the effect of changes in the use of the natural resources?

The method of understanding concludes with the elaboration of a decision tree to represent the main relationships between the services delivered by the Agency, its mission and the data required to define the available options for these services (Figure 1). This stage allowed the elaboration of a conceptual data model (CDM). It is a simplistic representation of the territorial data independent of any technological consideration. Relational standard object tool for ArcGIS was used (Maidment, 2002; Bedard et al., 2004) by progressively transforming a map of knowledge organized using the standard Unified Modelling Language object formalism, adapted to a Database Management System, so that the procedure remains accessible to non-specialists (Paquette, 2002). Hence, on the occasion of a field activity, this draft was discussed in a workshop with the representatives of organizations forming the Board of directors of the Agency and the revised editions were regularly submitted for comments to the executives of the Agency. The CDM of the watershed of Souss-Massa represents the territorial entities relevant to the management of the water resources of the basin as well as the relationships between these entities, in addition to the attributes characterizing these entities. ArcHydro constituted an excellent synthesis of geospatial and temporal data to support the hydrological modelling (quantity and quality) and the decision-making process, in its entirety (Maidment, 2002).

2.2 Implementing the geodatabase and updating the territorial information

The content of the Bill 10-95 devoted a very large mandate to the ABHSM. The Agency has to address at the regional level the main priorities of the National Water Policy. Like that, they have to formulate plan and strategy for a better use of infrastructures (dams, channel) and availability of water in the Souss-Massa area. The water challenge is related in the National Policy with the Environmental Management, including administrative, economic, and financial and information objectives. It is also related also to the sustainable resources plan, the Rural Water Table Plan, the Improvement of Irrigation Plan and the Sanitary Plan (relative to diseases associated with water) and Natural Risks, Pollution and Taxation matters. With such a large mandate, it is necessary to consider on what facts, data, information or knowledge the ABHSM works to deliver day by day or strategic decisions need to be made (ABHSM, 2002).

A large inquiry administrated to staff and partners of ABHSM permitted to assess the state of the art regarding to spatial data and capacity available. Presently, the informed decision-making process concerning the territory and the environment is one the weakness observed in the Souss-Massa region. Mainly, there are the following weaknesses: a) a lack of information to characterize and understand the spatial context of activities in the watershed; b) Decision makers and engineers have difficulty to catch the impact of their decisions and cumulating aspects of concurrently projects; c) the socio-economic and environmental processes are not adequately monitored. With all these challenges, one could feel a somewhat low level of planning or "laisser-faire" approach in some of the key objectives of the Agency.

Still recently, after different projects led by USAID, French or Swiss cooperations, it was not possible to get a basic geodatabase encompassing the metrical aspects of activities in the watershed. Only a set of administrative, hydrographical and roads features completed with location of the township was used for cartography. Some basic geophysical data (geology, pedology, fault and hydrogeology) were available on analogical format (paper maps). Most of these analogical data come from studies conducted in the sixties and were not updated since that time. Scale, accuracy and precision are variable. Meteo-climatologic data are available with cost. Flow data (gauging station) were irregular; piezometric data (groundwater levels) from 1975 and 2003 are available. Reported data from well exploration are available with analogical location (place names). Spatial data for territorial processes were not effective, software or knowledge varies from one service to another when present; data available were not documented and finally there are no enterprise envisioning regarding to spatial data for informed decision and water demand management.

2.3 Improving the Souss-Massa geodatabase (impact and challenges)

The approach followed in designing the SIAD_TIGERS allowed the basin Agency to develop and update its spatial database, particularly due to the usage of remote sensing images (Ziad et al., 2007). Realization of the IDSS aimed at improving the territorial knowledge on the realities and tendencies (short term and long term) in the effect of the alterations of the process and the land use. Data available from different sources and dates and of different precision and accuracy had to be integrated, structured and prepared for this kind of purpose. To help resolve this problem of availability of territorial information, existing data were collected first. The construction of the database integrates digitalization, preparation (geo-processing) and structuring according to the adopted data model (§ 2.1). Next Earth Observation products were considered. Satellite data, RADARSAT, Landsat and SPOT images were handled to establish the land cover and land use (lot and crop) as well as the analysis of terrain and territorial processes.

2.3.1 DEM, terrain analysis and associated products

Radar images are very useful in agriculture, forest, crop and ecological applications (Brown et al., 1993). Potential for monitoring grassland and biophysical properties constitute emerging fields in remote sensing

science. The radar image (RADARSAT) was used for the extraction of the digital elevation model (DEM). Radar images (*RAdio Detection and Ranging*) provide information about the location of an object by transmitting signals and measuring the time it takes for them to bounce off the targeted object and return. It is an active sensor system.

A total of twelve images (20 m resolution) acquired in standard mode for the whole territory of the basin have been ordered. With a swath of 100 km each, we had an adequate set of pairs of images for the DEM recovery. Processes were elaborated in PCI Geomatica with the component OrthoEngine through the ASAR/Radarsat algorithm. Images were processed with a rigorous model, using level 1B data. A set of 12 ground control points (CGP) and some tie points by images are used. The radiometric Terrain correction is activated during the preparation of the orthoimages. Finally, the DEM was extracted from epipolar images and saved. Some additional characteristics are tuned for failed pixel (-100) and background value (-150). Different levels of DEM were produced with resolution of 10m, 30m, 50m, and 100m. For the further hydraulic and hydrological modelling, DEM with a resolution of 30m or higher are recommended (Maidment, 2002). A resolution of 100m and 50m help to carry out a quick test of the process before trying it out for final results. Resolution of 30m gives DEM pixels a resolution equal to Landsat images which will be used later. A fine resolution of 10 m gives in theory more accurate result in modelling. Special attention must be paid to the 20m resolution Radar images before their use.

TAUDEM (Terrain Analysis and Using DEM), a specific algorithm, was used for improving quality of the DEM (Taborton and Ames, 2001). TAUDEM verifies the consistency of the DEM for hydrological purposes. This algorithm tries to validate the drain functions from all point of the territory. The main results are: pits filled a complete River network Raster, Network delineation and finally a new DEM hydrologically correct for eight possible directions for flow. Later, TAUDEM and ArcHydro functions were used to extract primary attributes of the DEM which are the following: stream order, network of drainage, watershed and sub-watershed, slope area, flow distance to stream, hillside, and exposure of the hillside and view sight.

Specific secondary attributes of the terrain – in this case features of lineaments – were elaborated also from the DEM with the LINE function in PCI Geomatica (Samih et al., 2006). These lineaments are associated to surface morphology and the structure of main faults known. These images were also used afterward for the generation of the maps of fault and lineament.

2.3.2 Land use/land cover and change detection analysis

Once the GeoDataBase constitution and update was completed, it was possible to proceed to a second step of elaboration of new information concerning the dynamics of the evolution of the land use in the watershed between the years 1987 and 2006, notably, using analysis of Earth Observation products. In the SIAD_TIGERS, land use/land cover (LULC) was expected to satisfy various demands.

LULC is a key element in all territorial decision-making processes in watershed management. At the Agency, there is a real knowledge gap in the land/soil use et also in the related change process (sites at risk, tendency, direction and pattern). In fact, planning methods or permit allowance was based only on temporal water/rain gauge data and perceptions or political decision. Although the task council wanted to make informed decisions in the management process, data, information, knowledge and tools were simply inadequate. The realization of the LULC and the change detection analysis formed the second part of the improvement of the GeoDatabase. Landsat images for about twenty years on three dates were used. The start point was 1987 with Landsat 5 TM. For 2002 and 2006, Landsat 7 ETM was retained. Limits of the watershed can be contained in three scenes (Table 1). The process includes different steps:

1. Preprocessing for radiometric and geometric correction. Radiometric correction was based on complementary data coming from the provider of Landsat images. Geometric correction was image to image based on SPOT images from the study area, georeferenced earlier with ground control points and level contour from topographical maps (1:50,000). At least twelve points were collected on each scene for a second degree polynomial correction. Finally, the nearest neighbour algorithm was used to keep the aspect of the pixels. This correction was applied to each band (visible, infrared and near infrared) available for each scene. Errors admissible were less than a pixel. Pixels maintain their size (no re-sampling) and projection adopted (Lambert Conformal Conic, Datum Merchich) is conformal for the whole geodatabase.
2. Mosaicking with all scenes pertaining to a same year was competed. The result is a set of multiband images. The assembly was specific for each time period (1987, 2002 and 2006).
3. The next step lays in radiometric balance (cross track) and final standardization for a good balance of colors in a mosaic.
4. Original mosaics were multiband (5 to 7). Principal component analysis helped to reduce band numbers (to 3) producing a kind of compression of information: less bands, but more significant set of information (90 % pertinent).
5. In an image or mosaic, there is an infinite amount of information with a large number of tones or intensity of colours. A set of pixels with similar reflectance characteristics with concordant localization could represent a class of fact in the territory (Girard and Girard, 1999). At this step it is important to keep a significant number of events or fact to synthesize territorial information. A supervised classification was applied, based on the maximum likelihood. This method is commonly recommended in general LULC elaboration (Girard and Girard, 1999). Due to the resolution of images, a set of eight to ten classes was studied in a diachronic manner (Table 2). Specific details on the approach applied and sensibility analysis are given in Ziad et al. (2007).

Table 1 Images used for the LULC (SIAD_TIGERS)

Sensor	Path	Row	Date	Category
Landsat 5 TM	203	40	02/03/87	L1G single NLAPS
Landsat 5 TM	202	39	27/03/87	L1G single NLAPS
Landsat 5 TM	203	39	02/03/87	L1G single NLAPS
Landsat 7 ETM+	203	39	19/03/02	SLC-ONSingle LPGS
Landsat 7 ETM+	203	40	19/03/02	SLC-ONSingle LPGS
Landsat 7 ETM+	202	39	24/02/02	SLC-ONSingle LPGS
Landsat 7 ETM+	202	39	23/03/06	SLC-OFF Gap fill- L1G
Landsat 7 ETM+	203	39	14/03/06	SLC-OFF Gap fill- L1G
Landsat 7 ETM+	203	40	14/03/06	SLC-OFF Gap fill- L1G

Table 2 Class distribution in LULC (SIAD_TIGERS)

Class (%)	1987	2002	2006
Water surface	6,26	2,44	5,43
Snow	1,91	0,08	3,00
Cloud	0,00	0,00	5,27
Gravel / Sand	7,75	5,63	5,49
Urban area	6,03	3,15	3,31
Greenhouse	0,00	1,97	4,65
Agricultural lot	6,16	3,60	4,85
Natural vegetation : low density	52,03	13,48	23,23
Natural vegetation : medium density	12,70	62,26	28,98
Natural vegetation : high density	7,16	7,41	15,78
Total (100 % = 28000 ha)	100 %	100 %	100 %

Main drivers for LULC are related to agriculture, natural vegetation and urban area. Greenhouses appeared in 2002 and sprawl significantly in 2006. The urban area in the plain of Souss competes with agricultural lots, river bank and beach area. Natural vegetation modifications are affected by agriculture front (Oulad Berhil) and climatic variation. In this last situation, changes inside the class (density of vegetation) were significant (Figure 2).

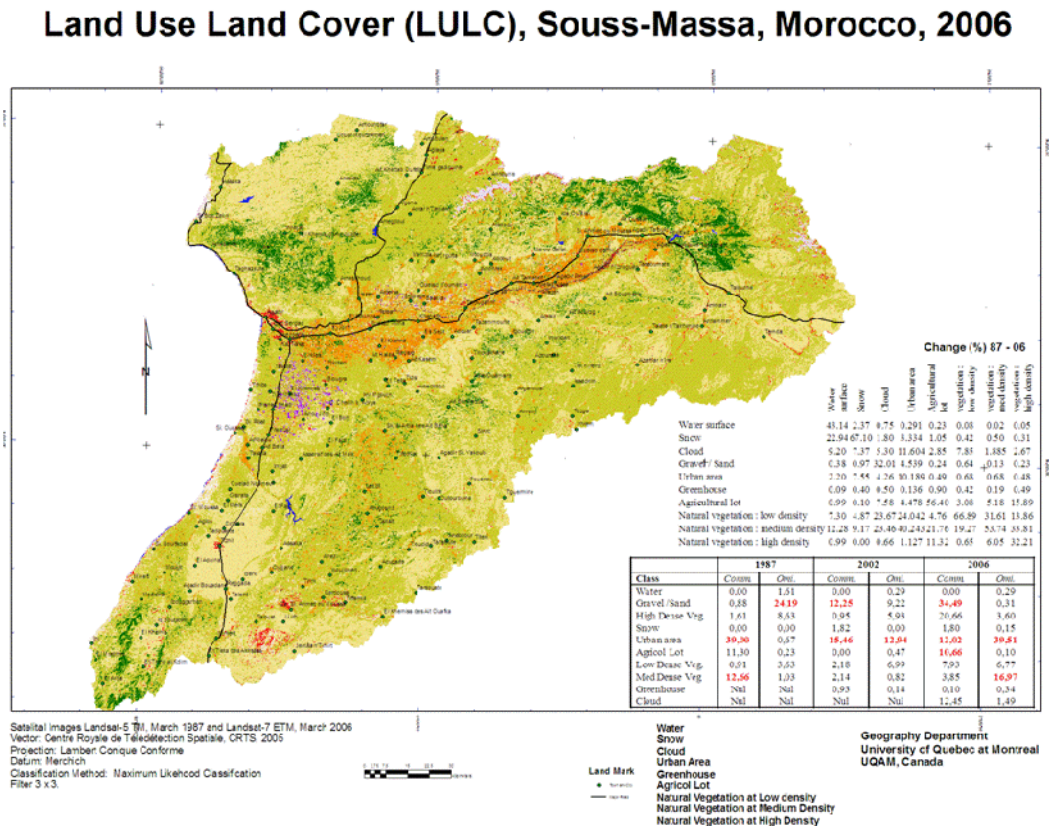

Figure 2 Spatial Class distribution in LULC (SIAD_TIGERS)

Change analysis helps in detecting area and intensity of change within and between classes between the three dates (February 1987, June 2002 and June 1987). Medium levels of change are observed in more than 50% of the watershed in February 1987 and close to 20% for June 2002. Strong to very strong changes are notable in some specific places (3.6% for February 1987 and 1.3 % for June 2002). These strong changes are localized in the Agadir and Imi n'Tghoula urban areas, but also in the area of the Youssef ben Tachfine, Abdel Mounem dams, and curiously in the mountain areas of Tiznit for February 1987. For June 2002, there are some new places close to Ouled Teïma and Ouled Berhil and also the Imi n'Tghoula and Tiznit. Analysis of these facts (direction, speed, and pattern), combined with field and socio-economic inquiry, will help the Agency to better understand how LULC transformation process proceeds in the watershed both at the level of whole watershed and locally (Figure 3).

This study could be improved with the use of images coming from other detectors (ASTER, SPOT) available at the CRTS. Radar images also could be added in most advanced integrated data approach. ASTER and Radarsat images have a higher resolution and could help to have better result on number of class of occupation and lot dynamics. Other approach could help also to better discriminate specific areas like road network and agricultural lot (textural analysis); Additional techniques such as decision trees and

neural networks added to work field could help to improve deeply the all set of products (Ziad et al., 2007). Finally, at the local level (like at Oulad Berhil), where significant changes are detected, high resolution imagery would be used for a local scheme of occupation of irrigated zones extension (Er-Raji et al., 2007).

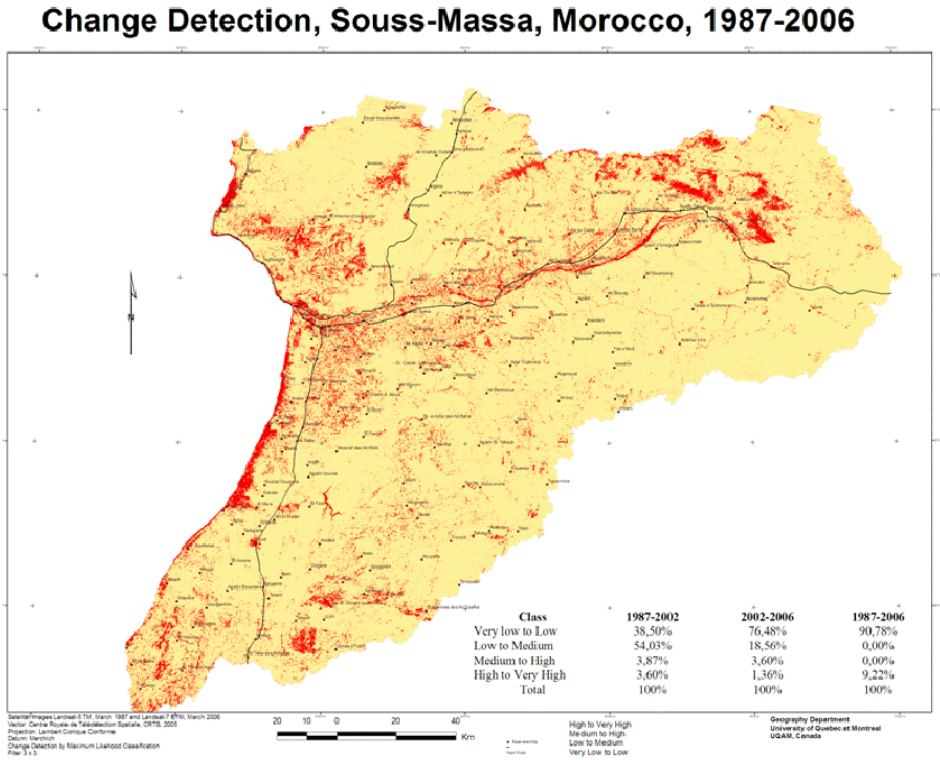

Figure 3 Spatial Class Changes in LULC (SIAD_TIGERS)

3. APPLICATION

Discussion with the Agency laid on the opportunity given with the LULC and the Geodatabase. There, structuring of the data was realized so as to ensure that their access can be made according to three approaches: a) thematic; b) spatial and c) temporal (Zeiler, 1999; Maidment, 2002). A set of strategic data concerning biophysical, administrative, economic or socio-cultural aspects of the management of the watershed were collected.

3.1 Exploitation and operational capabilities of the IDSS (Axis of use)

The operational capabilities of the IDSS were set up in a way to show to the Agency the usefulness of the SIAD_TIGERS to solve real problems on a day to day (local) or strategic (global) basis. It includes the use of the information system, the development of specific tools for the watershed and reservoir management, and additional tools developed specially for the Souss-Massa context. All the applications presented include the DEM, the LULC and derived products as corner piece. They showed on one hand strong pertinence of the use of Earth Observation products for water demand management in Souss-Massa; on the other hand, these products demonstrate how far these products associated with the IDSS could help the Agency to advance informed decision-making processes. The applications allowed the construction, the stages step by step development of a set of products supplying a better territorial knowledge with regard to: the dams and reservoirs management (sites of Youssef Ben TachFine and AbdelMoumen), the vulnerability of the environment to floods at the scale of the whole basin and local scale (at Taroudant check point); and erosion (the whole watershed of Souss-Massa, watershed of

reservoirs). These various applications show the potentialities of the IDSS (SIAD_TIGERS) as like a framework tool for the Agency.

The method used in the development of all the applications contains generally five stages. The first three stages concern the activities of designing, implementing and improving the GeoDataBase. The third one corresponds to specific activities of updating the GeoDataBase with the production of the LULC, the DEM and other Earth Observation derived products including the generation of lineaments, density of drainage or distance from lineaments, etc. (Vieux, 2001).

3.2 Management of dams

Eight dams with variable capacity have been set up in the Souss-Massa watershed. The management of dams constituted, until very recently, the dominant activity of the Agency. The administrators were always interested to see how the Earth Observation products and the IDSS can help them in the management of dams for: a) the planning of the demand for the irrigation, the urban and rural consumption, the leisure activities; b) the hydrological balance at the level of the reservoirs of dams (inflow, releases, evaporation, infiltration lateral losses) according to pre-established scenarios of management; c) the distribution between the categories of users (drinking water, open channel irrigation, recharge); d) the follow-up of drilling and well licenses.

Although hydrology and hydraulics are well founded since the nineteenth century, there were still a lot of emerging issues on scientific challenges to better understand the link with the diversity of climates, territories or the way water could flow and other part technical advances coupling physics, statistic, stochastic to deterministic approaches. Tools coming from informatics and geomatics offer new ways to renew understanding and application of global, half-distributed and distributed models (Dolcine et al., 2008). Due to the variability of results expected from dams and reservoir managers, it became important to evaluate how to integrate continuous modelling process in a way to include a whole set of components like flow (direct or indirect), long or short-term process affecting moist of soil between rainfall events. Cunderlink (2003) and McKinney (2004) in Dolcine et al., (2008) present an exhaustive description of these models and their impact with GIS tools and LULC data. In the SIAD_TIGERS, a framework approach is adopted to better take advantage of the geodatabase and existing tools. Water managers in Souss-Massa area have to face decisional problems relating to supplies of reservoir, consumption estimation, water resources sharing, concurrent uses or exploitation planning. The Hydrologic Engineering Center's set of tools (HEC, from the U.S. Army Corps of Engineers) linked to ArcGIS could support this tough challenge. It includes simulation component (HEC-HMS), reservoir management component (HEC-ResSim), Hydraulic component (HEC-RAS) and organization-visualization component (HEC-DSS). The data used are debit, flow, rain, watershed, dam and reservoir characteristics. Data related to watershed or sub-watershed comes essentially from precedent steps of activities (LULC, DEM and attributes). A more precise DEM with 3m of resolution was also elaborated for hydraulic simulation, based on local elevation data for these areas.

This application helped to show how the management of dams, instead of being an isolated activity of a service, can interfere with all the other missions of the agency. The various data modeled in the IDSS are put in relation with the hydro-meteorological series, in particular the water elevation in the dam, rain, solar radiation, flow, and temperature. The evaporation as well as the other parameters can be estimated to determine the infiltration rates, the water release for irrigation and potable water. Visualization tools, data export, the calculation of connected derived parameters like evapotranspiration, potential evapotranspiration, water demand and spatial interpolation of these data were also estimated for a better management of dams and reservoirs within IDSS.

The implementation of these modules requires the interaction of the hydraulic and hydrological models with the other data modules within the IDSS. The management scenarios and the real-time control and monitoring of dams and reservoirs are largely improved. The IDSS allows the Agency to appreciate the interaction effects of some of the localized factors (category of hillside, land-cover/landuse class, soil conservation practices). Much more, the IDSS allows estimating in real time the accuracy of management scenarios for water releases according to the rain gauge on pluviometer, for example.

Although the Agency had separately in different services a lot of pertinent data, through the SIAD_TIGERS and with the feeding of Earth Observation products, they could upgrade their strategic and tactic (day to day) manner to decide in watershed management on subjects related to a) irrigation demand plan, the urban and rural consumption; b) the reservoir balance (inflow, releases, evaporation, infiltration lateral losses); c) distribution between the categories of users; d) follow-up of drilling and well licenses.

3.3 Water or Hydro Erosion

The specialization of the Souss-Massa region's economy in intensive export-oriented agriculture and international, mass tourism implies a serious environmental impact at the same time to ensure investment in these activities and to tackle the impact of these activities. This application is dedicated to one of these environmental impacts: soil erosion. It occurs when fine particles of soil are extracted by actions of water or wind. It leads to a reduction of the productive quality of agricultural land by taking away elements favouring the aggregates and containing the nourishing materials for plants. On the other hand, the extracted particles contribute to diffuse pollution, eutrophication (oligotrophy) and turbidity of surface waters, destabilization of sand dunes, change of local environments and especially the silting of dams and reservoirs (Simonovic, 2007). The Agency needs dedicated tools for analyzing, monitoring and even evaluating effects of counter measures. In this application, the question was first to help the basin Agency to use the capacities of Earth Observation products and IDSS to better estimate and monitor the vulnerability and the risks of water-induced erosion on soil at the regional and local scales for a better environmental decision making process within the basin. Various methods are available to study the soil sensitivity to the water-induced erosion. The works of Wishmeier and Smith (1978) were for a long time the main reference for agricultural soil erosion since the formulation of the universal soil loss equation (USLE), shown in eq. 1

$$\mathbf{A = R * K * LS * C * P} \qquad (1)$$

In this equation, erosion or loss of soil (A) is estimated from a combination of factors in a composite index coming from factors related to rain aggressivity (R), soil erodibility (K), slope and length slope (LS), soil cover (C) and anti-erosion practices known (P).

Morris and Therivel (1995 in Prévil, 2000) have modeled soils sensitivity to erosion in a way represented with predictive models of waters flow. From USLE, they got various factors of how soil cover and soil use (LULC) should be considered in an artificial ecosystem. Other researchers have evaluated behavior of ecosystem regarding to specific spatial factors. It permits the development of complementary methods for soil erosion capable to give more accurate estimation of soil erosion in particular circumstances. Relatively popular are: revised USLE (RUSLE), agricultural non-point source (AGNPS) and a real non-point source watershed environmental response simulation (ANSWERS) (respectively: Renard et al., 1991; Young et al., 1987; Beasley and Huggins, 1991; reviewed in Hickey et al., 2001; Moehansyah et al., 2004).

At present time, the use of Earth Observation products and GIS opens new avenues for a GIS-based implementation of all these known models (Duchemin et al., 2001; Mitasova et al., 1996). Field evaluation of the main factors combined to their estimation using GIS and spatial analysis method are considered like imperative way to study and monitor soil erosion (Moehansyah et al., 2004).
For this application, the USLE model has been chosen. It is one of the best known models and has been extensively used in Morocco by the Environment Minister (Khatouri, 2003).

The various data used to estimate the factors of the universal soil loss equation come directly from GeoDataBase. This approach was applied globally and locally in the various sub-watersheds upstream of the man dams and with change in factors like DEM resolution.

Table 3 presents the repartition of value for different factors. R factor comes from rainfall documentation; K factor is established by pedology map; primary attributes needed for LS factor come from DEM and terrain analysis; C factor is a value from LULC. Finally, the P factor must be linked to specific field data.In absence of reliable data this results in the assignement of a value 1.

Table 3 Factors used in soil erosion modelling

Factor R	Factor K		Factor LS	Factor C		Factor P
	Value	Pedologic Code		Value	Landuse Code	
Min 0 Max 727	0.15	1, 3, 31, 33, 34	Min 0 Max 56	0	0, 219, 255	Constant = 1
	0.17	12		0.06	112	
	0.20	2, 32_34, 37, 40, 42, 5, 9		0.13	204	
	0.25	20, 23, 24, 25, 41, 43, 45, 47, 52, 55, 56, 57, 58, 59, 60, 62, 7, 8_55		0.32	227	
	0.27	63		0.70	32	
	0.30	00, 01, 3_55, 8		0.80	138	
	0.35	16, 18_47		1	75	
	0.36	10, 30		No Data	240	
	0.37	22				
	0.38	18, 19, 21, 29_44, 29_47, 29_55				
	0.40	28				
	0.42	26, 27, 6				

The erosion rate generally varies according the slope gradient of hillside, being low in plain and higher in mountainous areas. This fact allows verifying the coherence of the USLE model used in the project. Value resulting from this application could be used both quantitatively and qualitatively. The amount of soil loss varies considerably by site location and local environment. In the Souss-Massa, data revealed sectors where soil loss could be higher than 2000 T/ha/yr. According to Wishmeier et al. (1978) at an experimental site in the United States, a loss lower than 8 T/ha/yr can be considered nil. Such a loss results from natural processes in soil evolution. A loss higher than 20 T/ha/yr could be adequate to start investigating what is going on. Rank of acceptability can vary with regional condition across the world. So all measures must be interpreted in relation to the national system where modelling data are compared with field data (Khatouri, 2003; Sadiki et al., 2004). A qualitative interpretation shows across a watershed which sites are more exposed than others. In the case of Souss-Massa, some specific locations like the

head of the dams are locations to be watched closely. A watershed-scale evaluation helps to appreciate how a specific dam could be more exposed to erosion than another (Figure 4).

Furthermore, an analysis of the erosion map generated shows that about 35 % of the Souss-Massa area is exposed to strong erosion (Figure 4). The information on the local scale allows appreciating the context of certain environments and community facilities, like habitat, facilities, dams and reservoirs. From there, the Agency is able to refine the method to study the erosion at the local level, particularly in the watershed upstream of the dams.

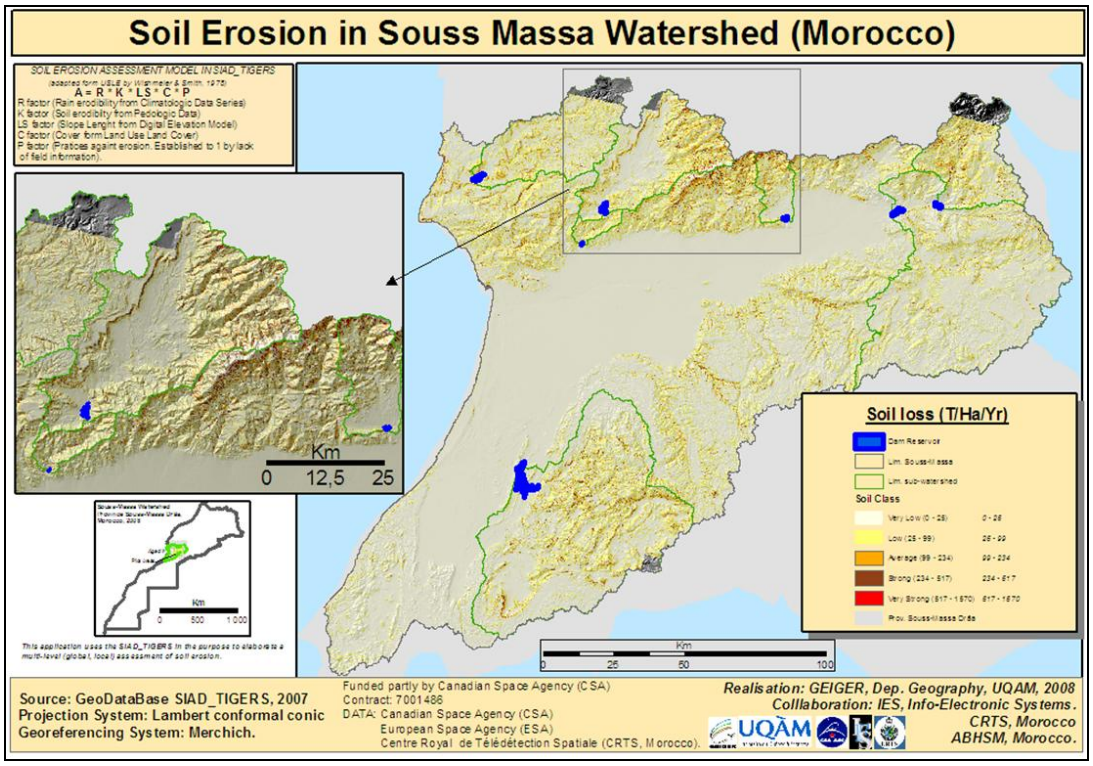

Figure 4 Soil Erosion in Souss-Massa (Morocco).

3.4 Flood risk Zones

Even if the region of Souss and Morocco in general evoke an idea of uncertainty of water availability and desert, it is nevertheless important to retain that this region is also exposed annually to torrential rains and flash floods. These can cause considerable damages to human lives and property. The protection against the floods is effective thanks to measures before, during and after the floods. Being flood-prone is a serious challenge in the Souss-Massa area. Planners in the urban service are very concerned and have even ordered a basic study to better understand the problem after serious flood events in the past years. A set of 138 hot spots have been identified and the planners wanted to collaborate with the Agency to realize a real regional plan.

Flood risk results from a combination of the occurrence of a non-ordinary climatological event (rain), vulnerability of the environment, exposition of a good (dam, house) and vulnerability of human beings or biota. Flood is the more common of territorial risks. Impacts are evaluated considering loss of money or goods, biodiversity and human lives. Traditional approach is based on probabilistic comeback time and hydraulic line data regarding to relation between debit and cross-section analysis of channels (§ 3.2, *Dam-reservoir application*). Based on this, flood hazard maps can be constructed with global and deterministic

models. For planners, it is necessary to complete this information with on one hand sites of interest (where the occurrence of the event can cause damage) and on the other hand, environmental factors or amenities that could speed up or break the risk. These include, among others, morphology, land use, type of soil, vegetation, distance to channel or soil moisture, population density, annual rainfall, size of watershed, basin slope, gradient of main drainage channel, drainage density and type of soil (Bapalu and Sinha, 2005; Yalcin and Akyurek, 2004). Therefore, it is much more a matter of territorial process depending on multiple criteria. Modelling these criteria could help simulate flood-prone on real time, assess the probability of danger and finally sketch measures like a precocity alert system which can help in the management of the crises of a real-time flood (Yalcin and Akyurek, 2004).

In this application, a model based on a multi-criteria evaluation (MCE) and GIS was adopted to take advantage of the content of the IDSS for flood area management in Souss-Massa. Factors affecting flood area are multiple, varying in scale, amplitude and importance (weight). MCE is dedicated to integrating the impact of various factors, quantitative or qualitative, dependant or independent. MCE includes a ranking method and pair-wise comparison to help calculating the weights of each factor to a random perspective. In the flood problematic, it includes at the first step mainly biophysical factors. An analytical hierarchy process (AHP) such as MCE technique is recommended to be used (Saati, 1980 in Prévil, 2000).

An empirical multi-criteria model combining the geomorphological features, elevation, vegetation, land cover, distances to active channels, and population density was applied to develop a flood risk map for the area (Bapalu and Sinha, 2005). Most of these data come from processing of Earth Observation products described in section 2; others were included in the Geodatabase at the structuring step of the SIAD_TIGERS. For all the criteria, a sub-factor is specified. Each criterion is ranked under analytical and decision-maker's preference and knowledge. Values for evaluation unit come from significance for implying flood risk. Linear standardization technique help to establish comparison between maps with a consistent numeric range (Malczewski, 1999). The pair-wise comparison method helps to determine the weights of the criteria. This method helps to convert linear importance into a linear set and allows the comparison of two criteria at once (Prévil, 2000).

Once the first results are obtained, it is recommended to go through a sensitivity analysis. Sensitivity analysis helps examining the stability of the choices and if they will be modified, light variations are introduced in the weight of the criteria. This analysis is very useful in a situation where decision-makers are not confident about the importance of some criteria (Prévil, 2000).

The watershed was assigned in five classes of risk according to the performance of each pixel and the organization of the area: high / medium-high / medium-low / low. About 70% of the watershed is classified at a low or low-medium level of flood risk. 12% is at a medium-high level of risk and 1% is at a high level of flood risk.

On a local scale, the resulting maps were refined using the 138 ground observation points (hot spot) of flood risk zones identified by the regional planning service. One of these hot spots, which is on the Souss River (Souss, at Taroudant check point), was retained for a detailed study with hydraulic simulation established in the first application (Dam Reservoir management). By including the rainfall-runoff management systems at this point as additional criteria according to the empirical model of Yalcin and Akyurek (2004), it is possible to adapt the static Flood risk map to flood alerts with SIAD_TIGERS. This model includes rainfall as a key criterion and, with HEC-HMS value for rainfall, can be adapted in real-time to manage the variation of meteorological factors and produce a risk map on the fly. This part of the

application incorporates the HEC-HMS model for hydrological forecasting and the HEC-RAS model for hydraulic simulation.

4. DEVELOPMENT OF THE TOOLBAR (AXIS OF FACILITATION)

A tool bar is implemented within the GIS platform with the aim of monitoring the integrated use of IDSS within the Agency and between the Agency and its partners. It is a question of wondering how to assure the coherence, information sharing and the use of the spatial knowledge for a better cooperation among the basin stakeholders. The tool bar was designed as the method of choice. It represents an organization of the different integrated modelling tools (erosion, flood, groundwater, etc.) at the global and local scale (Figure 5).

This toolbar developed in ArcGIS covers the whole concept of IDSS, including the features of Arc Hydro, Model Builder and features programmed in Bow Object / Visual Basic. This bar integrates all the modules used for the generation of the products described previously as well as intermediary products such as time series, data visualization through cartography (of precipitation, evapotranspiration and water balance), the contextual and spatial information about the groundwater potential, surface waters availability, etc., as described in the dam management section.

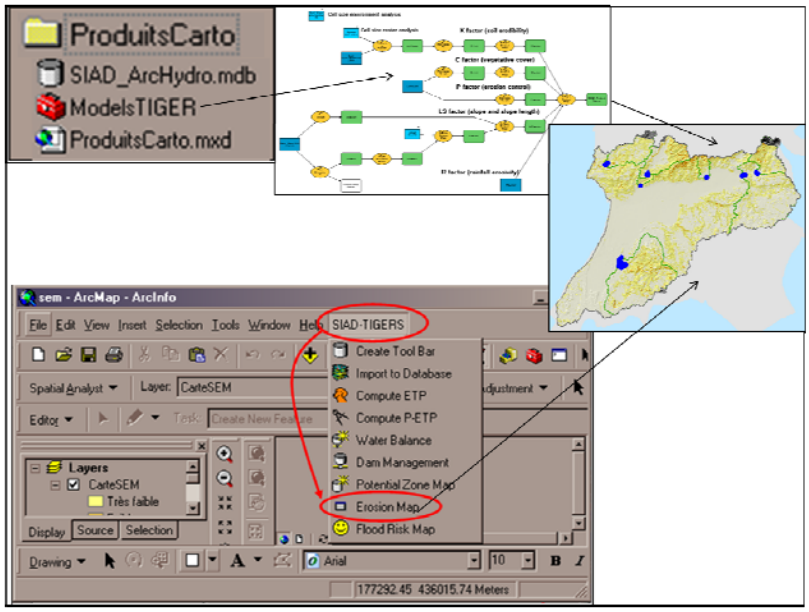

Figure 5 Facilitation with the Toolbar

5. CONCLUSIONS AND PERSPECTIVES

The SIAD_TIGERS project for watershed management represents a good illustration of the usefulness of knowledge development and know-how for the appropriate use of the Earth Observation data from GIS and modelling tools for water management. The various applications developed during the project achieve two major goals with regard to the application of the IDSS, besides the staff training objective. On one hand, verify the global-local coherence of the IDSS information system for water management; on the other hand, generate new territorial information on the global and local scales. The last part of the work done was the development of a toolbar which represents a synthesis of the mechanisms of modelling technologies. The main design concept behind the toolbar is the automation of the most

recurring tasks in the preparation and the update of derived products generated by the various developed applications.

This implementation of the IDSS has the ultimate goal of improving the management and the decision-making in the Souss-Massa basin with regard to: soil erosion and silting of dams; the management of dams and reservoirs; the vulnerability and the risks of flood; etc., besides the monitoring of changes in land cover and land use patterns. The methodology used in this project constitutes a good illustration for various applications based on the integration of Earth Observation products with structured multi-source, multi-date spatial data and multi-criteria analysis. in SIAD_TIGERS implementation for the water demand management (WDM) and other natural resources like agriculture, forests, soil, territorial risk management, and the various categories of territorial decisional processes faced by many developing countries and for which they lack the capacities for informed and sustainable decisions.

THANKS: This project benefited from a financial support of the Canada Space Agency (CSA). The authors also thank Info-Electronics Systems, the Morocco Royal Centre for Remote Sensing and the Souss-Massa Hydraulic Agency for their collaboration. We thank also the reviewers for constructive suggestions.

6. REFERENCES

ABHSM 2002. *Stratégie d'intervention de l'Agence pour la période 2004-2007*. Royaume du Maroc, Min. chargé de l'aménagement du territoire, de l'eau et de l'environnement. Agadir, Maroc.

Andreu, J., Capilla, J., and Sanchis, E. 1996. AQUATOOL: a generalized decision support-system for water-resources planning and operational management. *Journal of Hydrology*. Vol. 177, pp. 269-291.

Bapalu, G. V. and Sinha, R**.** 2005. GIS in Flood Hazard Mapping: a case study of Kosi River Basin, India. *GIS@Development* online edition (October, 2005).

Bédard, Y., Larrivée, S., Proulx, M.J. and Nadeau, M. 2004: "Modeling Geospatial Databases with Plug-Ins for Visual Languages: A Pragmatic Approach and the Impacts of 16 Years of Research and Experimentations on Perceptory". S. Wang et al. (eds.): *Conceptual Modeling for Geographic Information Systems (COMOGIS) Workshop ER2004*, LNCS 3289, pp. 17-30.

Carver, S., Kingston, R. and Turton, I. 1998. Accessing GIS over the web: an aid to public participation in environmental decision making. *GISRUK 98*, Edinburgh, Scotland (web only), http://www.ccg.leeds.ac.uk/vdmisp/publications/paper1.html.

Cesur D., Beene K. N. and Englehart S. T. 2004: Integrated GIS based Modeling System for watershed Resources. Proceedings of the 2004 AWRA Spring Conference: *GIS and Water Resources III*. Nashville (Te), American Water Resources Association.

Dieulin C. and Boyer, J. 2004. SIEREM Système d'Informations Environnementales sur les Ressources en Eau et leur Modélisation. UMR, HydrosSciences, Montpelier. <http://www.hydrosciences.fr/sierem/produits/dieulin/dieulin.htm> (Accessed in December 2007.)

Dolcine, L., Prévil, C., Ahluwalia, H. and Bouguenouch, B. 2008. Modélisation des apports et gestion des barrages du bassin de Souss-Massa (Maroc). Submitted to *Géo-Observateur*.

Duchemin, M., Lachance, M., Morin, G. and Lagacé, R. 2001. Approche géomatique pour simuler l'érosion hydrique et le transport des sédiments à l'échelle des petits bassins versants. *Water Qual. Res. J. Canada*, 36 (3), 435-473.

Er Raji, A., El Hadani, D., Sefiani, S., El Faskaoui, M. and Bouguenouch, B. 2007. Données Geospatiales pour l'évaluation de l'impact de l'utilisation des eaux souterraines sur la dynamique territoriale dans le bassin hydraulique du Souss-Massa (Agadir, Maroc). *Géo-Observateur*, No.16, pp. 3-10.

Hanna K. S. 2000. The Paradox of Participation and the Hidden Role of Information. A Case Study. *APA Journal*, 66(4), pp. 398 - 410.

Heywood, I., Carver, S.J. 1994. Decision Support or idea generation: the role for GIS in policy formulation. *Procedings Symposium fuer Angewandte Geographische*.

Heywood, I., Cornelius, S. and Carver, S.J. 2006. *An Introduction to Geographical Information Systems*. 3rd edn. Prentice Hall/Pearson Education.

Hickey, R., Smith, A. and Jankowski, P. 1994, Slope length calculations from a DEM within ARC/INFO GRID, Computers, *Environment and Urban Systems*, Vol. 18, No. 5, pp. 365–380.

Hill, M.J., Braaten, R., Lees, B. and Veitch, S. M. 2005. Multi-criteria decision analysis in spatial decision support: the ASSESS analytic hierarchy process and the role of quantitative methods and spatially explicit analysis". *Environmental Modelling and Software* 20, pp. 955-976.

Malczewski, J. 1999. *GIS and Multicriteria Decision Analysis*. New York, John Wiley and Sons.

Keith, J. E. and Ouattar S., 2004. Strategic planning, impact assessment and technical aid: The Souss Massa integrated water management project. *Journal of Environmental Assessment Policy and Management,* 6(2).

Khatouri, 2003. *Evaluation of soil erosion rates in the Dou Tama watershed using a Geographical Information System (GIS).* USAID. Morocco WPM Watershed Protection and Management.

Lasalmil, A. and Boulal, R. 2003. *Schéma d'aménagement territorial de l'aire métropolitaine d'Agadir* (Projet SATAMA). Rapport synthèse. Coopération Franco-Marocaine et Min. délégué de l'habitat et de l'urbanisme. Agadir, Agence urbaine d'Agadir.

Lévêque, C. 2001. *Écologie : de l'écosystème à la biosphère*. Paris, Dunod.

Longépé, C. 2006. *Le projet d'urbanisation du S.I.* Management des SI. Paris, Dunod.

Longley, P. A., Goodchild, M., Maguire, D.J., and Rhind, D. 2005. *Geographic Information Systems and Science,* 2nd edn. New York Wiley & Sons.

Maidment, D. R. (ed) 2002. *Arc Hydro: GIS for Water Resources*. Redlands (Ca), ESRI Press.

Mitasova, H., Hofierka, J.,Zlocha, M. and Iverson, R.L. 1996. Modeling topographic potential for erosion and deposition using GIS. *Int. Journal of Geographical Information Science*, Vol. 10, No. 5, pp. 629-641.

Moehansyah, H., Maheswari, B. L. and Armstrong, J. 2004. Field Evaluation of Select Erosion for Catchment Management in Indonesia. *Biosystems Engineering*, Vol. 88, No. 4, pp. 491-506.

Murthy, K. S. R. 2000. Groundwater potential in a semi-arid region of Andhra Pradesh: a geographical information system approach. *Int J Remote Sens,* Vol. 21, No. 9, pp. 1867-1884.

Paquette, G. 2002. *La modélisation des connaissances et des compétences, un language graphique pour concevoir et apprendre*. Presses de l'Université du Québec.

Prévil, C., St-Onge, B. and Waaub, J.-P. 2004. Aide au processus décisionnel pour la gestion par bassin versant au Québec : Étude de cas et principaux enjeux. *Cahiers de Géographie du Québec*., Vol. 48, No. 134, pp. 209-234.

Prévil, C., Dolcine, L., Brahm, A., Erraji, A. and Qaimi, A. 2008. Mise en œuvre d'un système intégré d'aide à la décision pour la gestion du bassin Souss-Massa (Maroc). In review.

Prévil, C. 2000. *Approche méthodologique pour la préparation de plans d'aménagement axés sur les préoccupations environnementales*. Pd.D. thesis, Department of geography, Laval University, Québec, Canada.

Rao Srinivasa, Y. and Jugran, K. D. 2003. Delineation of groundwater potential zones and zones of groundwater quality suitable for domestic purposes using remote sensing and GIS. *Hydrogeol Sci J* 48, pp. 821-833.

Rosenhead, J. 2001. *Rational Analysis of a problematic World, Revisited*. New York, John Wiley and Sons.

Roy, B. 1985. *Méthodologie multicritère d'aide à la décision*. Paris, Economica.

Sadiki, A., Bouhlassa, S. and Auajjar, J. 2004. Utilisation d'un SIG pour l'évaluation et la cartographie des risques d'érosion par l'Equation universelle des pertes en sol dans le Rif oriental (Maroc): cas du bassin versant de l'oued Boussouab. *Bulletin de l'Institut Scientifique, Rabat, section Sciences de la Terre*, Np. 26, pp. 69-79.

Samih Al Rawashdeh, Bassam Saleh et Mufeed Hamzah, The use of Remote Sensing Technology in geological Investigation and mineral Detection in El Azraq-Jordan, *Cybergeo*,Systèmes, Modélisation, Géostatistiques, article 358, mis en ligne le 23 octobre 2006, modifié le 06 février 2007. http://www.cybergeo.eu/index2856.html.

Simonovic, S. P. 2007. Sustainable Floodplain Management - Participatory Planning in the Red River Basin. A. Castelletti and R. Soncini-Sessa (eds), Topics on *System Analysis and Integrated Water Resources Management*. Amsterdam, Elsevier, pp. 173–189.

Taborton, D. G. and Ames, D.P. 2001.Advances in the mapping of flow networks from digital elevation data. *World Water and Environmental Resources Congress*, Orlando, Florida, May 20-24, ASCE http://hydrology.neng.usu.edu/taudem/.

Vieux, B. E. 2001. *Distributed hydrologic modelling using GIS*. Dordrecht, Kluwer Academic. (Water Science and Technology Library, 38.)

Wischmeier, W. M. and Smith, D.D. 1978. Predicting Rainfall Erosion Losses - a Guide to Conservation Planning. *Agricultural Handbook*, No 537, Washington D.C., U.S. Dep. of Agric.

Yalcin, G. and Akyurek, Z. 2004. Analyzing Flood Vulnerable Areas with Multicriteria Evaluation *XXth ISPRS Congress*, Istanbul, Turkey, 12-23 July

Zeiler, M. 1999. *Modeling Our World*: The ESRI Guide to Geodatabase Design. Redlands, CA, ESRI Press.

Ziad, A., Baudouin, Y. and Prévil, C. 2007. *Analyse diachronique pour l'étude des changements dans l'occupation globale du sol, Souss-Massa, Maroc, 1987-2006. Research report*, Université du Québec à Montréal UQAM.

Données Geospatiales pour l'Evaluation de l'Impact de l'Utilisation des Eaux Souterraines sur la Dynamique Territoriale dans le Bassin Hydraulique du Souss-Massa (Agadir, Maroc)

A. Er Raji[(1)], **D. El Hadani**[(1)], **S. Sefiani**[(1)], **M. El Faskaoui**[(2)] **& B. Bouguenouch**[(2)]

[(1)]Centre Royal de Télédétection Spatiale (Maroc) er-raji@crts.gov.ma ; elhadani@crts.gov.ma ; sefiani@crts.gov.ma
[(2)]Agence du Bassin Hydraulique du Souss-Massa (Maroc) elfasskaoui_mhamed@yahoo.fr ; adbsouss@iam.net.ma

Résumé Ce travail s'insère dans le cadre d'une étude qui vise à introduire, à l'échelle du bassin hydraulique du Souss–Massa, Maroc une approche intégrée incluant l'exploitation des données satellitaires, des données préexistantes et des Systèmes d'Information Géographique (SIG) comme sources d'information et outils d'analyse dans le processus de gestion des ressources en eau. L'utilisations des images satellitaires multi-capteurs (optique et radar) a permis de mettre en évidence de nouvelles informations sur la situation actuelle de l'occupation / utilisation du sol et en particulier sur l'étendue des zones agricoles irriguées, ceci pour la période allant de 1987 à 2006. L'analyse de l'évolution de cette situation a révélé d'importants changements, notamment en ce qui concerne l'espace agricole. Ces changements sont de deux formes: Ils sont soit dans le sens de disparition ou dans le sens d'apparition d'activités agricoles irriguées. Dans le premier cas, ils sont pour l'essentiel liés à la pression de l'urbanisation (partie occidentale), à la dégradation des sols (partie Sud) et à la surexploitation/épuisement des eaux souterraines (El Guerdane). Dans le deuxième cas, considéré comme le plus dominant, ils prennent la forme d'extension en terme d'apparition de nouvelles exploitations agricoles irriguées ce qui continue à faire pression sur la ressource malgré la réduction des ressources renouvelables suite à la succession des années de sécheresse. Bien que le constat général à l'échelle du bassin est marqué par une tendance à l'accroissement des superficies irriguées, localement les zones irriguées continuent à disparaître. Par ailleurs et contrairement à ce qui est communément supposé, la mise en place de nouvelles zones irriguées est quasi-généralisée à l'échelle de toute la plaine et ne se limite pas uniquement à la zone amont, ce qui menace le potentiel agricole de toute la région.

Abstract This paper presents a part of the results of an ongoing project, which aims at developing in the Souss-Massa hydraulic basin, Morocco an integrated approach including the exploitation of satellite data, pre-existing data and Geographical Information Systems (GIS) as sources of information and tools of analysis in the water management process. The use of multiple sensors and multi-temporal satellite images (optics and radar) enables to highlight new information on the current situation of the land cover/land use, particularly in the agricultural zones, during the period 1987 - 2006.
The land cover/land use changes analysis shows the surface expression of the groundwater over-exploitation by generating an intensive dynamic, with regards to different aspects of land cover changes, in particular in terms of irrigated zones extension. These changes are of two forms: 1) closely related to the reduction (disappearance) or 2) the extension (appearance) of irrigated agricultural activities. In the first case, they are essentially related to the urbanization pressure, soil degradation, and groundwater overexploitation. In the second case, considered as more dominant, these changes take the form of appearance of new irrigated farms where groundwater is better available. Although the general trend at the basin-scale shows a continuous increase in irrigated surfaces, locally these irrigated zones are

disappearing. The extension seems to be more general in the whole plain region and not simply limited to the upstream as it was expected.

1. INTRODUCTION

Ce travail a été réalisé dans le cadre de l'initiative TIGER en partenariat avec l'Agence du Bassin Hydraulique du Souss-Massa et avec le soutien de l'Agence Spatiale Européenne (ESA). Il vise à introduire à l'échelle du bassin hydraulique du Souss–Massa une approche intégrée incluant l'exploitation des données satellitaires, des données préexistantes et des Systèmes d'Information Géographique (SIG) comme sources d'information et outils d'analyse pour le processus de gestion des ressources en eau. Etant marquée par la faiblesse des apports superficiels et de la surexploitation des eaux souterraines, cette zone est aujourd'hui confrontée à une réduction continue de la disponibilité de ses ressources en eau. Ainsi, toute la problématique de développement de la région est actuellement centrée autour de la préservation et la durabilité des ressources hydriques. Etant un important pôle agro-économique, le secteur de l'agriculture consomme à lui seul près de 95% des ressources en eau mobilisées dont les eaux souterraines constituent l'essentiel. Selon plusieurs études, au Maroc l'année 2020 est considérée comme seuil de pénurie et de dépassement de la demande par rapport à la ressource mobilisable du pays (MATEE et al., 2004). D'ailleurs, la ressource est passée de 1,200 m^3 à 950 m^3 par an et par habitant entre 1990 et 2000. Malheureusement la région du Souss semble anticiper sur cette échéance et doit aujourd'hui faire face à une situation déficitaire très critique (MATEE et al., 2004**)**, sachant que cette région est considérée comme la première zone « primeuriste » et agrumicole au niveau national par une importante agriculture irriguée moderne. Quoique dans certaines exploitations les pratiques agricoles soient à un niveau technique très avancé, toutes les potentialités agricoles de la région restent fortement dépendantes des conditions climatiques et de la disponibilité des eaux souterraines. Ainsi, la durabilité de ce potentiel est actuellement menacée par la disponibilité de cette ressource, ce qui oblige à réfléchir à de nouvelles sources d'informations et à de nouvelles approches pour sa gestion et sa préservation (ABHSM, 2007).

Notre contribution pour faire face à cette situation vise à introduire à l'échelle de cette région (bassin hydraulique du Souss–Massa), une approche intégrée en s'appuyant sur l'apport des nouvelles technologies de l'information (données d'observation de la terre et les Systèmes d'Information Géographique (SIG)). Cette approche permettra d'aborder la gestion de l'eau sous plusieurs aspects tant en termes scientifiques et techniques qu'en termes socio-économiques. L'action de coopération avec l'ABHSM a permis le développement des produits cités ci-dessous :

- La mise en place d'une base de données SIG sur l'ensemble du bassin hydraulique du Souss-Massa.
- La cartographie multi-dates de l'occupation/utilisation des sols (1987- 2006).
- La cartographie des changements et l'analyse de la dynamique territoriale.
- L'intégration de produits dérivés des images satellitaires (géologie, géomorphologie et humidité des sols) pour la caractérisation du contexte hydrogéologique en milieux fissurés.
- Modélisation probabiliste pour la cartographie du potentiel aquifère dans la zone d'Ighrem.

Dans cet article, nous traiterons uniquement la partie ayant trait à la cartographie de l'occupation des sols et l'analyse de la dynamique territoriale. La prospection des eaux souterraines et l'aspect base de données et système d'aide à la décision feront l'objet d'articles séparés (Er-Raji et al., 2007 ; Er-Raji et al., 2008).

2. APPROCHE METHODOLOGIQUE

Le besoin croissant d'estimer et de surveiller l'extension des zones irriguées tend à faire ressortir la nécessité de mettre à jour de façon périodique les informations concernant la couverture de l'occupation/ utilisation du sol à l'échelle de la région. Ainsi, l'apport des nouvelles techniques d'acquisition et de production de l'information nous a permis de caractériser et mieux appréhender la dynamique de

l'occupation du sol survenue dans le bassin pendant les dernières décennies. Une série de documents cartographiques ont été élaborés à partir des images satellitaires optiques et radar, des observations de terrain et des documents existants (CRTS, 2001). Ces documents ont servi de base à une analyse de la dynamique de l'évolution du milieu dans l'espace et dans le temps afin d'identifier les facteurs qui influencent la relation entre l'occupation du sol et l'utilisation des eaux souterraines dans la zone. Cette analyse a été faite selon une fréquence temporelle variée afin de permettre une meilleure connaissance des tendances passées et futures de l'occupation du sol et des besoins en eau.

La méthode utilisée a été réalisée en deux étapes. La première consiste en l'élaboration d'une carte de référence d'occupation/utilisation du sol, couvrant tout le bassin hydraulique du Souss-Massa, selon une nomenclature détaillée. Cette carte de référence a été mise à jour à une fréquence temporelle variée permettant d'une part le dégagement des grandes tendances à l'échelle du bassin pour la période 1987-2006, et d'autre part le suivi saisonnier des nouvelles apparitions des zones irriguées. La deuxième étape a été consacrée à l'analyse des changements survenus pendant cette période selon une méthode incluant des informations intermédiaires afin de mieux discriminer entre changement permanent et changement temporaire. L'analyse et l'interprétation de ces changements avait été faite par l'intégration des résultats du modèle hydrodynamique des principales nappes permettant ainsi de mieux comprendre les grandes tendances que connaît la région en terme d'occupation/utilisation des sols et son impact sur la situation des nappes.

3. SUIVI DE L'EXTENSION DES ZONES IRRIGUEES

En vue d'assurer une meilleure détermination des thèmes de la nomenclature adoptée, notamment l'identification des zones irriguées, nous avons fait appel à des données de différents capteurs (Landsat, Aster, Spot et ASAR) et ayant des résolutions spatiales rapprochées. Un intérêt particulier avait été donné à l'apport de l'imagerie radar en mode de polarisation alternée pour compléter le jeu de données utilisé vu sa sensibilité pour le couvert végétal (Kuntz et al., 1999) ; Onana et al., 2003; Ballester-Berman et al., 2004). Ces images nous ont permis une meilleure discrimination entre les terrains de cultures et les terrains de plantations. La carte de référence élaborée à partir d'images acquises en 1987 nous a servi comme document de base. La mise à jour de cette carte de référence à l'aide d'image plus récentes a permis l'élaboration des cartes selon les dates et saisons suivantes : été 2001, printemps 2006 et été 2006 (Fig. 1). La nomenclature adoptée avait été arrêtée en commun accord avec les utilisateurs finaux de ces cartes, notamment l'Agence du Bassin Hydraulique du Souss-Massa (ABHSM) et l'Office Régional de Mise en Valeur Agricole du Souss-Massa (ORMVA-SM). La nomenclature adoptée comporte les thèmes suivants:

1 Irrigué Public Moderne
2 Irrigué Public Traditionnel
3 Irrigué Privé
4 Irriguée de Haute Montagne
5 Terrain Potentiellement en Bour
6 Arganier
7 Forêt de Haute Montagne
8 Parcours et Incultes
9 Bâti
10 Plan d'Eau
11 Cours d'Eau.

L'exploitation de données satellitaires multicapteurs et multidates a permis d'une part, la mise en évidence de nouvelles informations sur la situation actuelle de l'étendu des zones irriguées dans la région, et d'autre part, de faire le lien entre les grandes tendances que connaît la région en terme de superficies irriguées et leur relation avec l'évolution de la situation des nappes, notamment celles du Souss et de Chtouka.

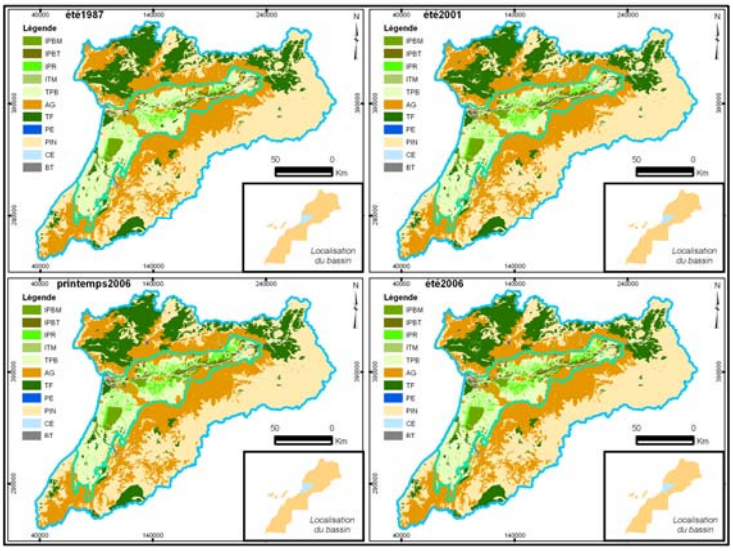

Figure 1 Cartes de l'occupation du sol

Une première lecture des cartes élaborées révèle une importante dynamique, notamment en ce qui concerne l'espace agricole. Cette dynamique est évidente sur les images couvrant la période 1987-2006 (Fig. 2). Dans ce laps de temps (1987-2006) le constat général, à l'échelle de tout le bassin, est marqué par un net accroissement des superficies irriguées. Ces superficies passent de 120 000 ha en 1987 à 152 000 ha en 2006, soit une augmentation de plus de 26 %. Toutefois dans certaines régions les parcelles irriguées continuent à disparaître plus particulièrement à Sebt El Guerdane.

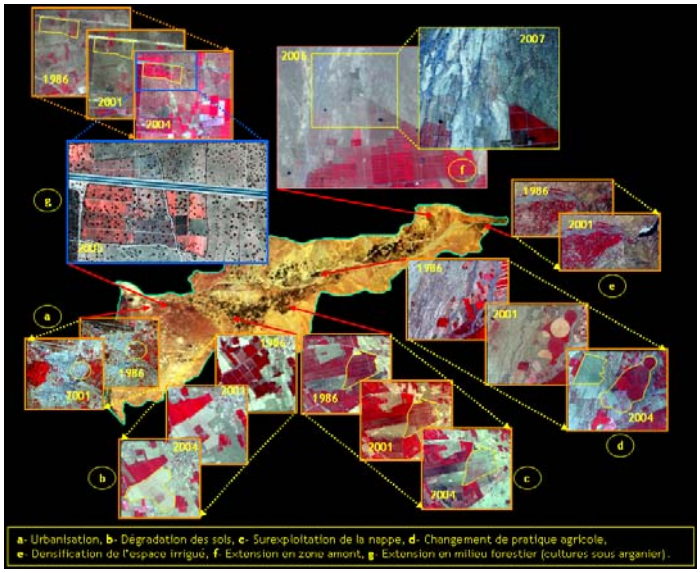

Figure 2 Extraits d'images montrant différentes formes de la dynamique de changement dans les zones irriguées

4. DETECTION ET ANALYSE DES CHANGEMENTS

Afin de mieux apprécier la dynamique de ces changements, notamment en ce qui concerne la discrimination entre changement permanent et changement temporaire, nous avons adopté une méthode d'analyse permettant d'intégrer toutes les situations d'occupation/utilisation du sol élaborées pour les quatre dates à savoir l'été 1987, été 2001, printemps 2006 et été 2006 (Fig. 3). La combinaison des différents documents nous a permis de dégager dans un premier temps 305 situations de changements possibles. Suite à une phase de regroupement entre classes de changement en se basant sur leur affinité, notamment en ce qui concerne l'apparition ou la disparition des zones agricoles irriguées, nous avons fait ressortir onze formes de changements dominants dans la région.

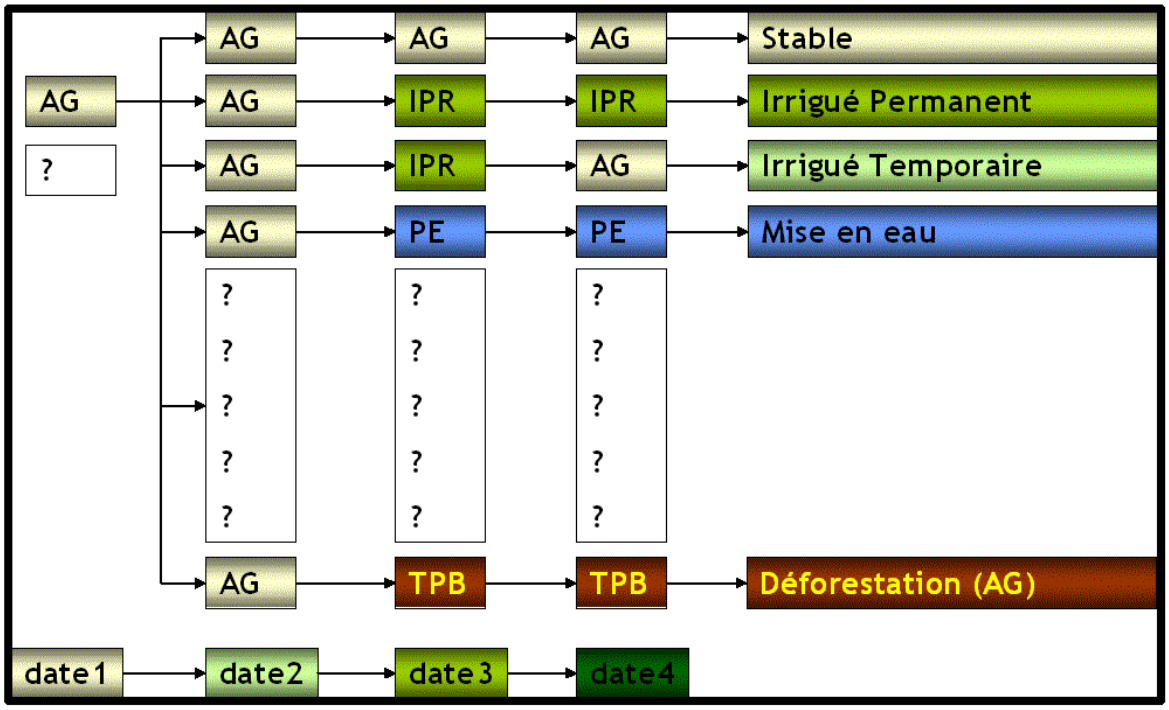

Figure 3 Méthodologie adoptée pour la détection des changements : AG : Arganier ; IPR : Irriguée Privé ; PE : Plan d'Eau ; TPB : Terrain Potentiellement en Bour.

L'analyse de ces changements montre que l'essentiel de la dynamique territoriale est concentré dans la zone de plaine. Ailleurs dans les zones montagneuses, les changements sont relativement peu prononcés. Les changements en termes d'accroissement concernent les zones irriguées et l'espace bâti. Ce dernier a enregistré pendant la période de l'étude (1987-2006) une hausse d'environ 7 000 ha concentrée pour l'essentiel dans la partie occidentale du bassin (Grand-Agadir). Quant aux changements en termes de disparition (réduction), ils touchent le domaine forestier (arganeraie) et les espaces cultivés en bour. Ceci s'explique par la pression démographique et économique que connaît la région pendant ces décennies engendrant ainsi l'apparition de nouvelles zones agricoles irriguées (exploitations) et une forte pression de l'urbanisation qui dans certaines régions s'étend au détriment de terres agricoles. D'ailleurs, cette région a présenté pendant cette période le taux d'accroissement de population le plus élevé au niveau national soit 3,7 %**.** Dans les communes urbaines du Grand Agadir le taux a été de 5,76 % soit un résultat largement supérieur à la moyenne urbaine nationale qui est de l'ordre de 3,6 % (MATEE et al., 2004).

5. IMPACT DE L'UTILISATION DES EAUX SOUTERRAINES SUR LES DYNAMIQUES TERRITORIALES

Bien que les possibilités actuelles de la télédétection ne permettent pas un accès direct à des informations du sous-sol profond, il est toutefois possible reconnaitre certains phénomènes du sous-sol à travers leur expression en surface. Dans notre étude et en vue de mieux comprendre la dynamique des changements qui concernent l'espace agricole irrigué, nous nous sommes appuyé sur leur relation avec l'utilisation des eaux souterraines dans la zone sachant que ces eaux forment la principale source pour l'irrigation. En effet, leur rôle dans la dynamique des changements que connaît la région est bien marqué par le fait que ces changements sont pratiquement concentrés dans la zone de plaine et épousent la distribution spatiale des principaux aquifères: Chtouka et Souss (Fig. 4).

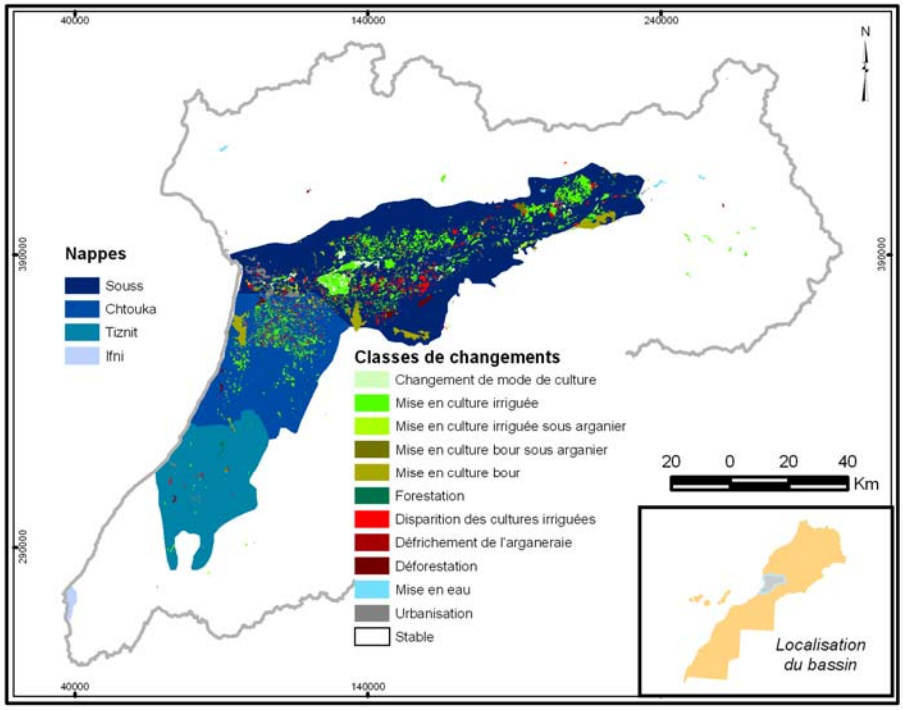

Figure 4 Carte des changements et distribution spatiale des aquifères

Par ailleurs, l'évolution des bilans de ces deux nappes montre clairement que leurs situations déficitaires vont de pair avec l'accroissement des superficies irriguées pendant ces dernières décennies (Fig. 5). L'intégration des produits du modèle mathématiques dont dispose l'ABHSM a permis aussi de mieux comprendre les grandes tendances que connaît la zone (ABHSM, 2004a). Ainsi, la densification de l'espace irrigué dans le Chtouka-Nord et la situation alarmante que connaît la région de Sebt El Guerdane explique bien l'évolution locale de ces nappes entre 1968 et 2005. Cette évolution se matérialise par un rabattement du niveau piézomètrique variant de 40 à 60 mettre (Hsissou, 1999; ABHSM, 2004b). Quant à la région de Oulad Berhil, elle subit actuellement une forte pression par l'installation de nouvelles exploitations agricoles irriguées venant pour la plupart des zones en situation déficitaire, notamment Sebt El Guerdane après l'abandon des exploitations et coupe à blancs de leurs agrumes (Fig. 6). En raison de sa situation en zone d'alimentation de l'aquifère du Souss, la région de Oulad Berhil suscite plus d'intérêt. En effet, et selon le résultat du scénario « catastrophes » élaborés à l'aide du modèle hydrogéologique (ABHSM, 2004b), cette région subira un rabattement allant jusqu'à 50 m au cas où les extensions agricoles continueront à s'y installer, ce qui provoquera le tarissement de certaines zones en aval.

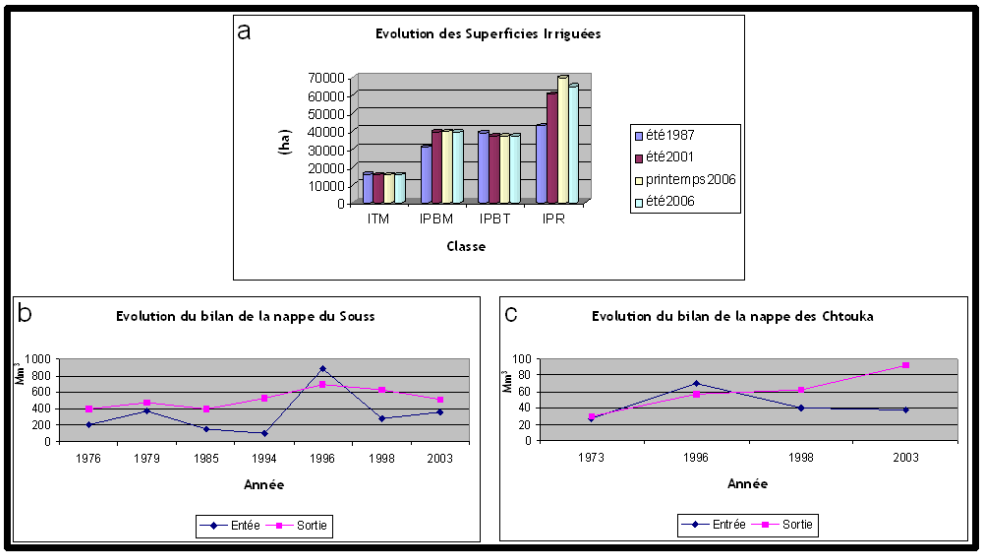

Fiure 5 Graphe a: Evolution des superficies irriguées; ITM: Irriguée Traditionnel de haute Montagne; IPBM: Irrigué Public Moderne ; IPBT : Irrigué Public Traditionnel; IPR: Irrigué Privé. Graphes b et c: Bilans des nappes Souss et Chtouka. (Source: Graphes b et c, ABHSM (2004b)).

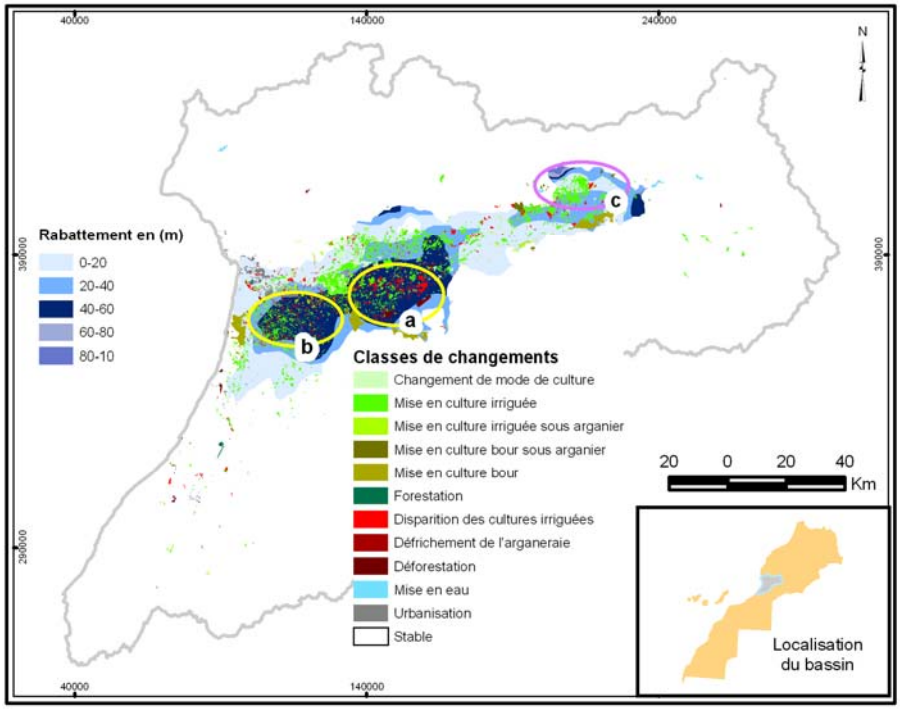

Figure 6 Localisation des grandes tendances et leur impact sur les nappes.
a: Sebt El Guerdane, b: Massa Nord, c:Oulad Berhil

6. CONCLUSIONS

L'utilisation des données satellitaires multicapteurs et multidates (optiques et Radar) a permis de mettre en évidence de nouvelles informations sur la situation actuelle de l'occupation / utilisation du sol en particulier l'étendue des zones agricoles irriguées. Ces informations nous ont permis de mieux appréhender la dynamique des changements survenus pendant les dernières décennies, et de mieux dégager les grandes tendances que connaît la région en terme de superficies irriguées et leur relation avec l'évolution de la situation des nappes.

Il est irréfutable que le moteur essentiel derrière toute cette dynamique de changement est le potentiel hydrogéologique de la zone quelque soit son emplacement dans le bassin. Les formes de changements les plus dominantes sont étroitement liées à l'apparition ou la disparition des activités agricoles irriguées. Les disparitions sont pour l'essentiel liées à la pression de l'urbanisation, à la dégradation des sols et à la surexploitation/épuisement des eaux souterraines. Quant aux extensions, et contrairement à ce qui est communément supposé, la mise en place de nouvelles zones irriguées est quasi-généralisée à l'échelle de toute la plaine et ne se limite pas uniquement à la zone amont, ce qui menace le potentiel agricole de toute la région. La région amont (Souss amont), et en particulier la région de Oulad Berhil, constitue une destination privilégiée pour les nouvelles exploitations agricoles venant pour la plupart des zones situées plus en aval. Etant située en zone d'alimentation de la nappe du Souss, l'exploitation excessive des eaux souterraines dans cette zone risque de mettre en péril tout l'avenir du potentiel agricole de la région.

Par ailleurs, l'irrégularité très marquée du climat et l'alternance de séquences d'années pluvieuses et de séquences de sécheresse d'une part ; et l'accroissement des besoins en eau, la dégradation de la qualité des eaux et la surexploitation accrue des eaux profondes d'autre part, menacent sérieusement les ressources en eau au niveau de tout le bassin hydraulique du Souss-Massa et imposent le besoin en informations fiables et objectives pour mieux assurer la protection et la gestion intégrée de cette denrée cruciale. En effet, la planification et la gestion de cette ressource sont devenues de plus en plus difficiles en raison de facteurs complexes dont les professionnels du domaine doivent en tenir compte. Avec les contraintes mises en place par la loi pour l'utilisation des ressources en eau, une nouvelle approche de gestion s'est mise en place surtout que les opérateurs du domaine sont devenus plus sensibles et plus impliqués dans la prise de décisions notamment celles qui risquent d'avoir des impacts sur leurs activités. Tous les acteurs impliqués dans la gestion de l'eau, posent actuellement de façon accrue le problème de la durabilité. Ainsi, les méthodes traditionnelles de gestion des ressources s'avèrent insuffisantes pour répondre à cette situation. C'est une gestion intégrée de ces ressources qui constitue l'approche la plus prometteuse. Notre contribution à cette gestion intégrée se fera à travers le développement d'un Système Intégré d'Aide à la Décision. Le système que nous proposons disposera d'une base de données geospatiales et descriptives et d'une interface SIG qui permettra la visualisation, la manipulation et l'extraction d'informations facilitant la prise de décision.

Nous recommandons que l'exploitation des images satellitaires soit étendue pour l'extraction de paramètres comme l'évapotranspiration (ET) surtout que plusieurs études ont montré leur intérêt dans des régions similaires (EL-Magd et al, 2005 ; Zwart et al, 2007). La combinaison de ce paramètre avec des cartes de détails sur les cultures irriguées pourrait améliorer davantage la caractérisation du bilan hydrologique à l'échelle du bassin.

7. BIBLIOGRAPHIE

Agence du Bassin Hydraulique du Souss-Massa. 2007. *Etude de révision du plan directeur d'aménagement intégrée des ressources en eau (PDAIRE) des bassins du Souss-Massa*. Bulletin de communication n°1.

Agence du Bassin Hydraulique du Souss-Massa. 2004a. *Etude de la stratégie de gestion des ressources en eau dans le bassin du Souss-Massa : Rapport de modélisation hydrodynamique*. Rap. Inédit.

Agence du Bassin Hydraulique du Souss-Massa. 2004b. *Stratégie de la préservation des ressources en eau dans le bassin du Souss-Massa : Plan d'action 2005-2020.* Rap. Inédit.

Ballester-Berman, J. D., Lopez-Sanchez, J. M., et Fortuny-Gausch, J. 2004. Estimation of extinction coefficients and its implications in crop monitoring with polarimetric SAR interferometry. *Proceeding of EUSAR workshop,* Vol. 2, pp. 737-740.

Centre royal de télédétection spatiale. 2001. *Carte de l'occupation du sol de l'aire couverte par le projet SATAMA*. Rap. Inédit.

El-Magd, I. A et Tanton T. 2005. Remote sensing and GIS for estimation of irrigation crop water demand. *Int. Jour. Remote Sensing*, 26 (11), pp. 2359-2370.

Er Raji, A., El Hadani, D., Sefiani, S., El Faskaoui, M. et Bouguenouch, B. 2007. Données Geospatiales pour l'évaluation de l'impact de l'utilisation des eaux souterraines sur la dynamique territoriale dans le bassin hydraulique du Souss-Massa (Agadir, Maroc). *Geo Obs*, N°16, pp. 3-10.

Er-Raji, A., D. El Hadani D., Tajdi A., Sefiani S. et Qaimi, A. 2008. Intégration des données d'observation de la terre dans une approche probabiliste pour la prospection des eaux souterraines dans la boutonnière d'ighrem (Anti-Atlas, Maroc). *Geo Observateur*, soumis.

Hsissou, Y. 1999. *Impact de l'environnement naturel et anthropique sur la qualité des eaux alluviales en zone semi-aride : cas de la plaine du Souss (Maroc)*. Thèse d'état, Université d'Agadir.

Kuntz, S., Siegert, F., Rucker, G. 1999. ERS SAR images for tropical rainforest and land use monitoring: change detection over five years and comparison with RADARSAT and JERS SAR images. *Geoscience and Remote Sensing Symposium*, Proceedings. Vol. 2, pp. 910 – 912.

Ministère de l'Aménagement du Territoire, de l'Eau et de l'Environnement, UN-HABITAT et PNUD. 2004. *Profil environnemental d'Agadir*. Rap. Inédit.

Onana, V. P., Trouve, E., Mauris, G., Rudant, J. P., et Frison, P. L. 2003. Change detection in urban context with multitemporal ERS-SAR images by using data fusion approach. *Geoscience and Remote Sensing Symposium, 2003, Proceedings.* Vol. 6, pp. 3650 – 3652.

Zwart, S J., et Bastiaanssen, W. G. M. 2007. SEBAL for detecting spatial variation of water productivity and scope for improvement in eight irrigated wheat systems. *Agricultural Water Management,* N° 89, pp. 287-296.

Inflow Modelling and Reservoir Management in Souss-Massa (Morocco)

Dolcine L.[(1)], Prévil C.[(2),] Brham A. [(1)], Ahluwalia H.[(1)] and El-Menaoui[(3)]

[(1)] Info-Electronics Systems (IES), Canada. Email: leslie@info-electronics.com
[(2)] Département de Géographie, Université du Québec à Montréal (UQAM), Canada.
[(3)] Agence du Bassin Hydraulique du Souss-Massa (ABHSM), Maroc

Abstract This paper presents an application dedicated to the management and inflow modeling of the Souss-Massa dams and reservoirs in Morocco and the use of Earth Observation in water management. The watershed is the site of seven major dams. Presently, to assess the loss and the release of water, ABHSM conducts periodic calculation of reservoir budget, from measurements of water level. Thus, the reservoir inflow is deducted as a by-product of the reservoir balance. The approach proposed in this paper models the flow using a hydrological rainfall-runoff model coupled with a reservoir simulation model, and the flood mapping is done by coupling the hydrologic model with a hydraulic simulation model.
This paper analyses several hydrological models according to a set of criteria determined by the constraints and the requirements of the project. The reservoir management model has been selected on the basis of its good performance, its ability to meet the requirements of the ABHSM and its integration with the rainfall-runoff model for estimation of the reservoir inflow.
The hydrological model is calibrated and validated on daily measurements of rainfall and flow observed in the reservoir catchments and the estimated inflow from the reservoir budget. The reservoir management model has been validated on the assessment made from manual balance budget for two reservoirs. The results show that the hydrological model reproduces well the volume and peak of floods observed despite intermittent periods of drought. The reservoir model simulates exactly the elevation and storage estimated in the reservoir in the same conditions of inflow, losses and water releases. This project was made possible through a grant from the Canadian Space Agency (CSA).

Résumé Ce papier présente une application dédiée à la modélisation des apports et la gestion des réservoirs du SoussMassa au Maroc et traite de l'application des données satellites dans la gestion de l'eau. Cette application est insérée dans le système intégré d'aide à la décision (SIAD_TIGERS) réalisé pour accompagner l'Agence (de gestion) du Bassin hydraulique du Souss-Massa (ABHSM). Le Sous-Massa connaît depuis ces quinze dernières années un développement très important de ses activités économiques et une évolution rapide de l'habitat. Ces multiples développements s'accompagnent d'une forte pression sur les ressources en eau.
Le bassin versant est le site de 7 importants barrages dont celui d'AbdelMoumen (ABD) d'une capacité, à retenue normale de 20100 million de m^3 (Mm^3), et le réservoir de Youssef Ben TachFine (YBT) d'une capacité de 303515 Mm^3 à retenue normale. Actuellement, pour évaluer les pertes et les volumes des lâchers d'eau, l'ABHSM effectue des bilans périodiques des réservoirs, à partir des mesures de niveau d'eau dans le barrage. Ainsi, l'apport est déduit comme un sous-produit du bilan du réservoir. L'approche proposée dans ce texte est progressive et s'inscrit dans le cadre d'une planification proactive pour la gestion et le suivi des réserves en eau des réservoirs. Elle consiste à modéliser les apports en utilisant un modèle hydrologique pluie-débit suivi d'un modèle de simulation de réservoir, les cartes d'inondation et la prévision des crues sont réalisées en couplant le modèle hydrologique à un modèle de simulation hydraulique.
Cet article revoit et discute différents Systèmes d'Aide à la Décision et analyse plusieurs modèles hydrologiques selon un ensemble de critères déterminés par les contraintes de gestion et les besoins de l'ABHSM (échelle spatio-temporelle, processus modélisés, coût, interface utilisateur etc.). Le modèle de

gestion de réservoir a été retenu en fonction de sa bonne performance, sa capacité à répondre aux besoins du projet et son intégration avec le modèle pluie-débit d'estimation des apports.
Le modèle hydrologique est calé et validé sur des mesures journalières, de pluie et de débit, observées dans le bassin d'alimentation ainsi que les apports estimés à partir du bilan des réservoirs. Le modèle de gestion des réservoirs a été validé sur les bilans réalisés sur les deux réservoirs ABD et YBT. Les résultats montrent que le modèle hydrologique reproduit bien le volume et la hauteur de crues observées en dépit des périodes intermittentes de sécheresse. Le modèle de réservoir simule exactement la hauteur et le volume d'eau dans le réservoir en tenant compte des apports, des pertes et des lâchers d'eau. Le modèle permet de simuler différents scénarios (pessimiste, conservateur, optimiste, et variantes) et d'établir des priorités dans les besoins à satisfaire. Ce projet a été réalisé grâce à une subvention paritaire de l'Agence Spatiale du Canada (ASC).

1. INTRODUCTION

The Souss-Massa region in Morocco is facing a major development challenge relative to the sustainable management of its water resources. Most of its agricultural exports are produced by irrigated agriculture, which consumes a large part of the region's freshwater. Over the last fifteen years, the Souss-Massa region has seen a very important development of its economic activities and a rapid evolution in the habitat. These multiple developments have a direct impact and increase the pressure on the already scarce water resources.

Nowadays, society demands a safe water supply for drinking and other socio-economic activities as well as protection against the adverse impact of floods and droughts (Andreu, 2004). The region of Souss-Massa and Morocco generally evoke a sense of precariousness of water availability, it is however important to note that this region is also exposed to torrential rain and flash floods that can cause considerable damage to human life and property. The problem in Souss-Massa is far from unique, as water managers world-wide are under pressure as many river basins have been plagued by extreme hydrologic conditions ranging from severe droughts to catastrophical flood events (Labadie, 2006).

The basin area of Souss-Massa covers approximately 28,000 km^2, of which some 250,000 ha is potential irrigable land. The region is served by a set of seven dams of capacity ranging from 2 Mm^3 to 180 Mm^3 allowing a maximum storage in surface waters of more than 450 Mm^3. In addition, these plains host two continuing aquifers with a capacity estimated at 467.7 Mm^3 (Carlo et al., 2008).

The region of Souss-Massa produces around 30% of citrus exports and 25% of vegetable production in Morocco. Along with the strength of its agricultural development, the region of Souss-Massa, especially the Agadir urban region, is also the leading tourist destination in Morocco.

Facing a conflict between stakeholders for water use and important decisions, managers usually rely on tools to support and aid in the decision making process. Different definitions of Decision Support System (DSS) are proposed in the scientific literature (Sprague and Carlson, 1982; Adelman, 1992; Poch et al., 2003; McKinney, 2004).

2. RIVER BASIN DECISION-SUPPORT SYSTEMS

Labadie (2006) presents a robust river basin DSS as one which can provide both a planning framework for development and management as well as aid in real-time river basin operations and controls. In practice, some river basin DSSs are more suitable for network simulation and planning and some others for real-time operations. River basin DSS suitable for real-time operations like flood control, reservoir management, disaster management require more detailed physics and hydraulics in their definition and implementation.

River basin Decision Support Systems used in water resources management have received special attention and have been reviewed by several authors (Yeh, 1985; Wurbs, 1993; Wurbs, 1994; Labadie, 2006 and McKinney, 2004). Yeh, (1985) proposed a comprehensive review of models and methods used in reservoir system operations. Wurbs (1993) also reviewed reservoir system simulation and optimization models. Wurbs (1994) proposes an extensive review of computer models for water resource planning and management covering all aspects from water demand, water distribution, ground and surface water, hydraulic and reservoir simulation models. Labadie (2006) proposed his definition for a DSS and stressed that a DSS should have general applicability and not be hardwired to a particular river basin configuration and management structure and reviewed the most commonly used DSS for water resource planning. McKinney (2004) underlined the fact that DSS for water management range from fully data oriented models to fully process oriented models. In describing the most popular water management DSSs, McKinney (2004) grouped the existing systems in two main classes: flood management decision support system and water allocation decision-support. Only the DSSs of interest for the project (WEAP and MODSIM) are discussed in this article, and the readers can refer to Labadie (2006) or McKinney (2004) for a more detailed description.

The Water Evaluation and Planning WEAP is a microcomputer tool for integrated water resources planning. It provides a comprehensive, flexible and user-friendly framework for planning and policy analysis. WEAP implements an integrated approach to simulating both the natural and engineered components of water systems. The result is an effective tool for examining alternative water development and management options (http://www.weap21.org/). WEAP is relatively straightforward and user-friendly for testing the effects of different water management scenarios. The main disadvantage of WEAP is the link with a GIS. However, WEAP does have a GIS-based graphical interface which allows the user to import an Arcview shapefile as a background picture (Lancaster, 2004).

MODSIM-DSS is a generalized river basin Decision Support System and network flow model developed at Colorado State University designed specifically to meet the growing demands and pressures on river basin managers today. MODSIM-DSS was designed for this highly complex and constantly evolving river basin management environment, and with a graphical user interface (GUI) allowing users to create any river basin system topology. Through the GUI, the user represents the components of a water resource system as capacitated flow network of nodes (diversions points, reservoirs, point of inflow/ouflow, demand locations, stream gages etc.) and arcs (canals, pipelines, and natural river reaches) (Labadie, 2006).

MODSIM-DSS can perform daily scheduling, weekly, operational forecasting and monthly, long-range planning. MODSIM-DSS can be used with a geographical information system (ArcGIS) to generate input data for the model based on spatial databases and to provide an interface for the user to modify input parameters and to display the results of the model.

For short-term operation and emergency water management decision-support systems, CWMS is not available to the general public, Mike-Basin and WMS require expensive licensing fees. These systems are close and tightly integrated making it impossible to add new models. Water management DSSs have been developed according to two general approaches (Mckinney, 2004):
Stand-alone approach - where a DSS is created from scratch as stand-alone system with a unified input data set and a core of modelling tools that tightly couple to each other.
Framework approach - where a DSS is created by taking a series of existing models and creating an interface that allows a user to execute the modelling procedures in a sequence passing outputs of one model to another as input in a manner that is transparent to user.
The development of the Souss-Massa system follows the latter approach. The next section presents the methodology used in the choice of the best models to integrate in the system.

3. CHOICE OF THE SIMULATION MODELS

Managers of the Souss-Massa basin have always been interested in seeing how the products of Earth Observation, geomatics and simulation models could help in the management of basin reservoirs with the objectives of achieving: a) a better understanding of the reservoir inflow, b) a better balance of the water stored in the reservoirs based on pre-established scenarios; and c) a better distribution of water available among the different categories of users. Furthermore; the region is also exposed to torrential rain and flash floods that can cause considerable damage to human lives and property during the rainy season, a fourth objective is d) mapping of flood risk zones for flood forecasting and warning. Groundwater is an important alternative source of water for consumption, agriculture and recreation. The Souss Massa basin contains one of the largest aquifers in Morocco. The Souss-Massa water managers have to assure that e) groundwater will remain a long-term reliable source of water of adequate quality and quantity and f) monitor the effect of pumping and recharge on groundwater level.

The implementation of water resource management for Souss-Massa implies interaction between hydrologic and reservoir simulation models with hydraulic models for flood forecasting and mapping and simulation of groundwater scenarios.

Deterministic hydrologic model can be classified into three main categories:

- ***Lumped models.*** Parameters of lumped hydrologic models do not vary spatially within the basin and thus, basin response is evaluated only at the outlet, without explicitly accounting for the response of individual sub-basins.
- ***Semi-distributed models.*** Parameters of semi-distributed models are partially allowed to vary in space by dividing the basin into a number of smaller sub-basins.
- ***Distributed models.*** Parameters of distributed models are fully allowed to vary in space at a resolution usually chosen by the users

According to the hydrologic processes model, hydrologic models can be further divided into ***event-driven models***, or ***continuous process models***, or models capable of simulating both short-term and continuous events.

To choose the best hydrologic model meeting the project requirements a number of existing hydrologic models including HEC-HMS, TR-20, TR-55, SWMM, MIKE-11, IHACRES, SRM, HBV-96, HFAM, HSPF, SSARR, SWAT, TOPMODEL, GSSHA, CEQEAU, HYDROTEL, WATFLOOD have been analyzed. The description of these models is beyond the scope of the present paper. Interested readers are referred to McKinney (2004) for a more detailed description of these models.

A two-level selection methodology is used for the comparison and selection of models for the project. At the first level, a large number of existing models have been reviewed, and at the second level the models are ranked according to several evaluation criteria reflecting different aspects of the project requirements. The objective of the selection methodology is to choose the best model fulfilling the projects requirements in an operational context in term of spatial and temporal scales, ease of use and user interface. The selection process is not a classical model inter-comparison where the objective is to assess the scientific capabilities of the models to represent different hydrologic conditions.

The main criteria included in the evaluation process are summarized in the rest of this section. Lumped, semi-distributed and fully-distributed models are compared separately, since they reflect different approaches to hydrologic modelling. An additional point is given however to model package containing different types of models. A comparison table is developed after analyzing the different models, most of them are open source or freely available. The selected models are compared according the following criteria:

1. *Spatial scale* evaluates the basin size the model is developed or recommended for.

2. *Temporal scale* evaluates the time step used in the model.
3. *Processes modelled* evaluate the processes modelled that are important for the project.
4. *GIS connection* evaluates if the model is or can be included in GIS package.
5. *Hydraulic simulation* evaluates if the model comes with a package for hydraulic simulation.
6. *Multiple models* evaluate if the model comes in a package with different types of model (lumped, semi-distributed or distributed).
7. *Cost* evaluates the model cost.
8. *Set-up time* evaluates the approximate time needed to set the model into operational use
9. *Expertise* evaluates the scientific expertise required to use the model adequately.
10. *Technical support* evaluates the support available for setting up the model, calibration and use.
11. *Documentation* evaluates what documentation is available about the model.
12. *Ease-of-use* describes computer related user-friendliness of the model, taking into account GUI, input-output (I/O), and visualization options
13. Operating System evaluates the computer operating system required by the model to run [Linux, Windows].
14. *Total score* gives the sum of all ranked criteria [0-36].

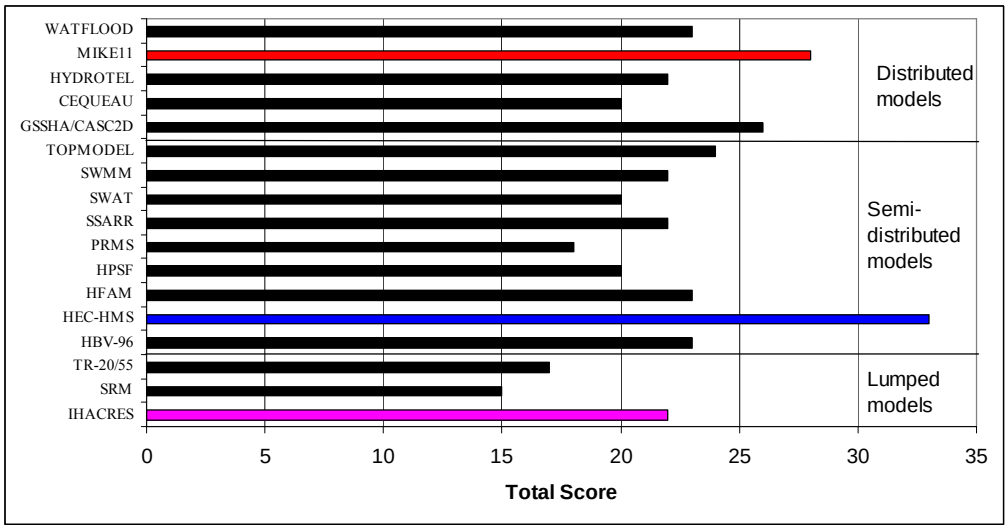

Figure 1 Hydrologic models score

Figure 1 gives a condensed view of the comparison table. As shown in the figure, IHACRES model received the best score among the lumped models. Among the selected semi-distributed models; the HEC-HMS has the best score of all. This model represents the state-of-art of public domain model for hydrologic modelling. The model comes with the HEC-GEOHMS for the watershed data inputs and delimitations, the output of the model can be input directly in HEC-RAS for hydraulic and flood plain analysis. The HEC-ResSim package can be use also as an alternative for reservoir simulation. Among the selected distributed models MIKE11 is the best in this category; it is a suite of hydrologic and hydraulic modelling tools integrated in a GIS system (Mike11 GIS).

3.1 Hydraulic Models for Flood Forecasting and Mapping

In practical applications, flood forecasting involves two steps. First, a hydrologic model is used to obtain the flood peak. This flood peak must then be inserted as input into a hydraulic model based on detailed channel geometry in order to forecast water levels at key sites along the river.

Hydraulic models generally fall into six classes, 1-dimensional, 2-dimensional (vertically integrated) and 3-dimensional, either steady or unsteady state. 3-Dimensional hydrodynamic models are used only for lakes, reservoir and lagoons.
From the project perspective, HEC-RAS is a good choice for 1D food plain modelling, it is available free of charge, has an easy to use user interface. Its GIS application companion HEC-GEORAS makes it easier to gather physical data required by the model from a high resolution DEM. For a complex 2D simulation, MIKE 2D or MIKE FLOOD is the appropriate choice. MIKE FLOOD combines the best features of 1D and 2D flood modelling technology.

3.2 Reservoir Simulation and Groundwater simulation models

The problems facing reservoir managers include among others the prediction of inflows, the estimation of demand, the allocation of water to meet the conflicting demand of various users, and the development of operating policies (Loucks at al., 1981). Asante et al. (1997) developed a GIS-based reservoir planning for the Souss-Massa Basin. The reservoir simulation model, which was completely integrated in the GIS, was limited to the monthly time-step. A currently available tool like MODSIM, which was discussed previously, offers a better alternative for the overall network simulation and planning. The model ResSim which is well integrated with HEC-HMS, and allows simulation at different time steps, defining rules and setting priorities for the reservoir release, will be the reservoir simulation model of choice.

For groundwater simulation, the agency has developed experience in using MODFLOW; this model is retained as the groundwater simulation.

4. SYSTEM ARCHITECTURE

The architecture of the system is described in the following section (Figure 2). The central component of the system is the database containing spatial and time-series data. As the integration of spatial and temporal data in the GIS follows the Archydro approach (Maidment, 2002), the GIS is also used for spatial data visualization and analysis tools. The simulation models include HEC-HMS for hydrologic simulation, HEC-ResSim for reservoir management, HEC-RAS for hydraulic simulation and flood mapping, HEC-DSS for data visualization and MODFLOW for groundwater simulation. The time-series data are converted to the DSS file format to be used as inputs to HEC models. For long-term planning and network simulation the best choices are considered MODSIM and WEAP.

5. IMPLEMENTATION ON PILOT SITES

The study area is the Souss-Massa basin presented in Figure 3 for an estimated area of 28000 km^2.
The watershed is the site of seven major dams including the pilot reservoirs of AbdelMoumen (ABD) with a nominal capacity of 201,100 Mm^3, and the reservoir of Youssef Ben TachFine (YBT) with a nominal capacity of 303,515 Mm^3.
The areas of the reservoirs' inflow catchments are given in Table 1.

Table 1 Souss-Massa Main dams and reservoirs

Dams	**Area (km^2)**
Youssef ben Tachfine	3755.06
Abdelmoumen	1307.36
Aoulouz	4441.26
Dkhila	111.77
Imilkheng	287.63
Mokhtar Soussi	977.07
AitAmoud	1167.41

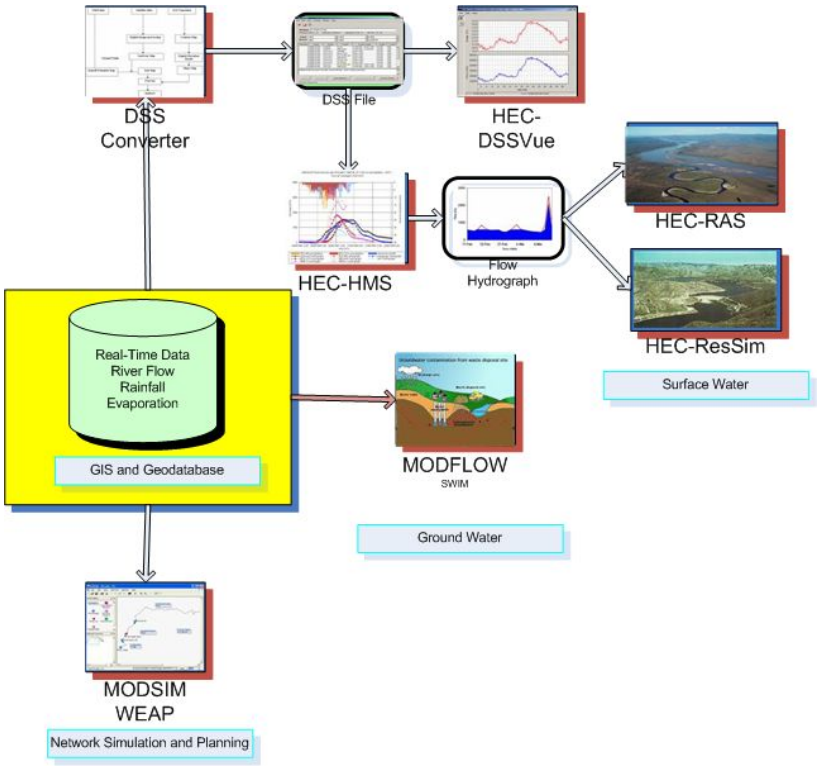

Figure 2 Architecture of Water resource management models in SIAD_TIGERS

YBT is modeled with four sub-basins: Amagouzh 97533 km^2, Nguerf 60599 km^2, Ouijane 88950 km^2, and Massa Aval 2,470 km^2

A water management decision-support system to be useful must be accompanied by a supporting database. In this section, we discuss only the data required for the simulation models; the development of the geodatabase is the focus of another paper in this publication (Prévil et al., Implementation of an Integrated Decision Support System for the Souss-Massa Watershed, Morocco).

5.1 Remote sensing data and water management

The DEM for the entire basin is developed using the radargrammetry technique from RADARSAT-1 images. The DEM is used to obtain the reservoir catchments size, characteristics and the hydrographical network using the GIS tools incorporated in ArcHydro. The land use/land cover for the entire basin is generated from LANDSAT and SPOT images. The land cover map is used to characterize the response of the hydrologic basins and the map is later used in the determination of the Manning coefficients for the hydraulic simulation model. A higher resolution landcover map will certainly improve the river cross-sections and the hydraulic model results. A higher resolution map will also be very useful in post-disaster estimation, a very important aspect of flood mapping and disaster management. The high resolution DEM for the determination of the channel geometry is obtained from remote sensing data complemented by terrain data. With the development of new space-borne radar like RADARSAT-2 (3 m resolution) and TERRASAR-X (1 m resolution), there are great potentialities to use these data for high resolution DEM generation for flood mapping and post-disaster evaluation.

The data supplied by the basin Agency is used in defining the storage-elevation and storage-area curves for each of the reservoirs. The hydraulic simulation for one reach of the Souss River at Taroudant is done using a three-meter resolution DEM developed for the project needs.

The groundwater model has been developed in a separate project and is not discussed in this section. The data required includes runoff, rainfall, evaporation, seepage, water release, dams and reservoirs properties. The Runoff and Rainfall data contain daily time-series of flow and rainfall for the entire Souss-Massa basin. The daily and monthly time-series of reservoir data include water level measured in the reservoir, temperature, solar radiation, evaporation, wind speed and wind direction measured at the dam sites. The dam and reservoir data contains the dams' technical properties, estimated inflow to the reservoir, estimated seepage, storage, elevation and water allocation data covering the period of operation of the reservoirs. The estimated inflow to and seepage from the reservoir are obtained from a balance budget operation, the inputs being the reservoir elevation, the reservoir surface and storage; and the evaporation.

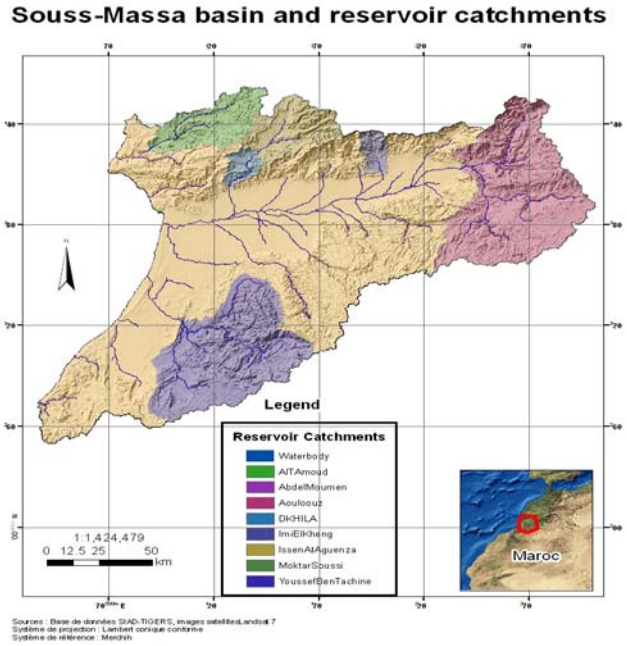

Figure 3 Study area Souss-Massa basin (Morocco)

6. SIMULATION RESULTS

The model HEC-HMS uses several components to simulate the hydrological behaviour of the basin. The basin model includes a weather component, a control specification and data entry components. The basin model represents the natural catchments and is developed by adding and connecting several hydrologic elements (sub-basins, reaches, and junctions). These hydrological elements use mathematical functions to describe the physical processes in the watershed. The simulation model calculates the response of the basin according to the entries provided by the meteorological model. The control specification allows the user to define the start and end of the simulation period, and the time step.

The model was calibrated and validated on the reservoir basins of ABD and YBT. ABD is modelled as a single basin using the flow data from a station upstream of the entrance to the reservoir and the estimated inflow to the reservoir and YBT with four sub-basins. Three rain gages and one flow gage are currently available for ABD; four rain gages and three flow gages for YBT respectively.

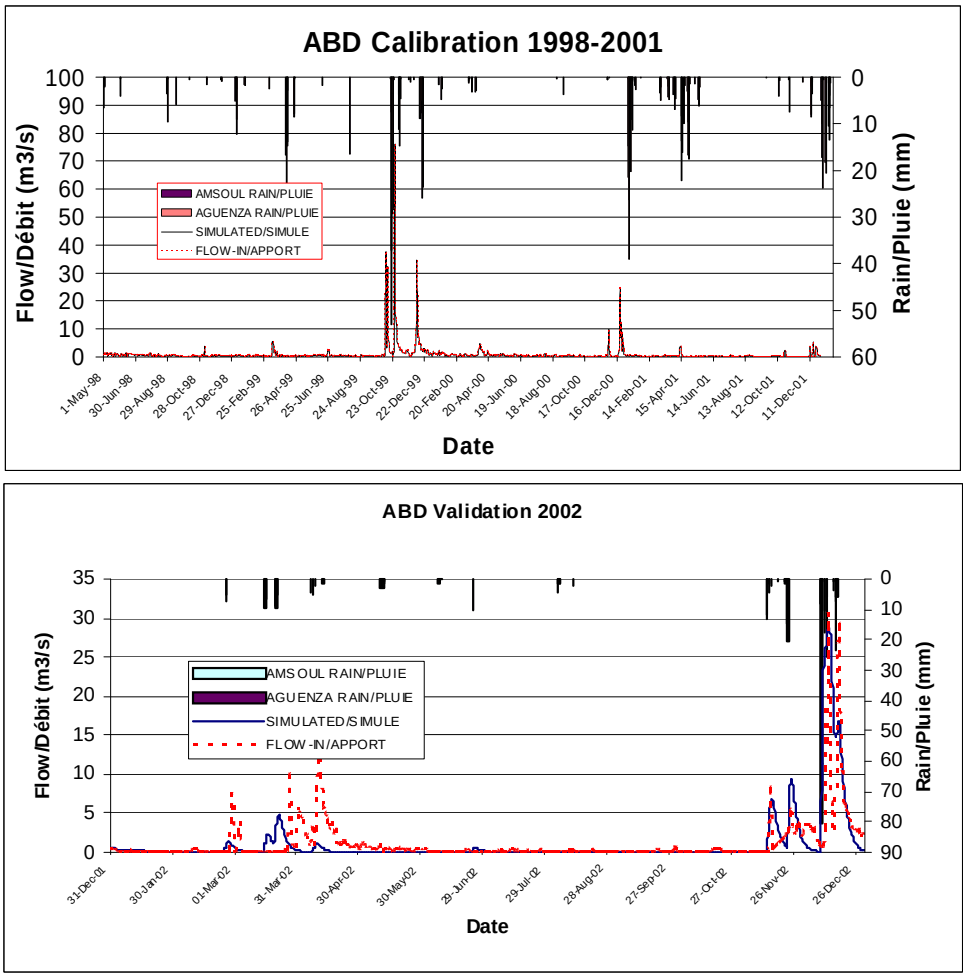

Figure 4 Hydrologic Model results ABD basin (a) and (b)

In validation on ABD basin, the model reproduces both the peak flow and the volume of water observed over the one year period (Figure 4 and Table 2). The Root Mean Square Error (RMSE) is 3.25 m^3s^{-1} in calibration and 2.93 m^3s^{-1} in validation, respectively. The estimated inflow is generally undervalued compared to the flow simulated by the model. On the other hand for YBT, the RMSE is 8.66 m^3s^{-1} in calibration; and 34.66 m^3s^{-1} in validation. This degradation is mainly due to the quality of the observed data. The estimated inflow is generally overestimated compared to the observed rainfall and simulated inflow for the same period. Even with an imperfect calibration on the basin, the simulated inflow is a better representation of the observed rainfall in the basin than the estimated inflow obtained by the balance budget. The size and physical configuration of the two reservoirs, 128.12 Mm^3 for YBT against 75.05 Mm^3 for ABD explains the different behaviour: an error in the measurement of reservoir water elevation will have more serious consequences on the estimation of the storage and the inflow for YBT than ABD.

Table 2 Model results for ABD in calibration and validation

Validation ABD	Observed	Simulated
Peak Flow (m^3s^{-1})	31.71	30.0
Volume (Mm^3)	34.554	31.554
Volume (mm)	26.10	24.15
RMSE (m^3s^{-1})		2.93
Calibration ABD		
Peak Flow (m^3s^{-1})	75.90	30.0
Volume (Mm^3)	94.035	96.449
Volume (mm)	71.95	73.79
RMSE (m^3s^{-1})		3.25

The reservoir simulation model has been tested on both ABD and YBT using the balance budget over the year 2006 as the reference. The objective is to be able to reproduce the reservoir elevation and storage in the same conditions of inputs and releases as for the reference year. The figure 5 shows (for ABD) the reservoir simulation model results using an inflow obtained from the balance budget. These results are obtained under the same conditions of evaporation, seepage losses, water allocation and release. The reservoir model is capable of simulating over a period of a year the behavior of the two reservoirs. ResSim allows the users to create and test different alternatives and analyze the consequences of these alternatives on the reservoir storage. The simulation model will allow the water managers to analyze and simulate different water allocation scenarios potable water, irrigation, power generation (if any) and plan accordingly.

As mentioned earlier, the Souss-Massa region is also confronted during the rainy season to flash floods. An inundation map supported by empirical data has been developed. One reach of the Souss River was chosen as a pilot site to test the HEC-RAS flood mapping model. A high resolution DEM was generated and used to model the river geometry: channel right and left banks, cross sections, and Manning coefficients (Figure 6). The Manning coefficient table was deduced from the landuse map.

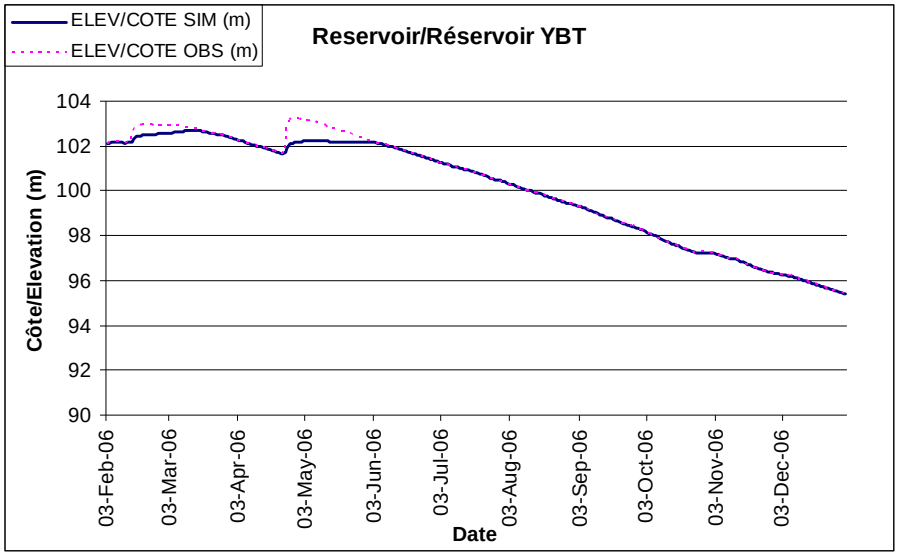

Figure 5 Observed and simulated elevation for YBT for the year 2006

The river geometry developed from the GIS is imported in the hydraulic simulation model (Figure 7). Water levels and flood maps for three return periods 10, 25, and 50 years, are simulated using the hydraulic model

and exported back to the GIS. Figure 8 shows an example of flood risk mapping for the entire basin and for the Souss reach at Taroudant. The flood maps are overlaid on top of the DEM.

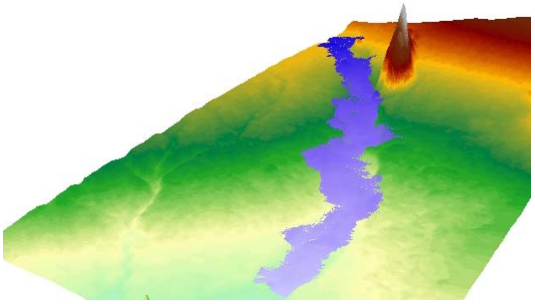

Figure 6 High resolutions DEM for the definition of the channel geometry (not at scale)

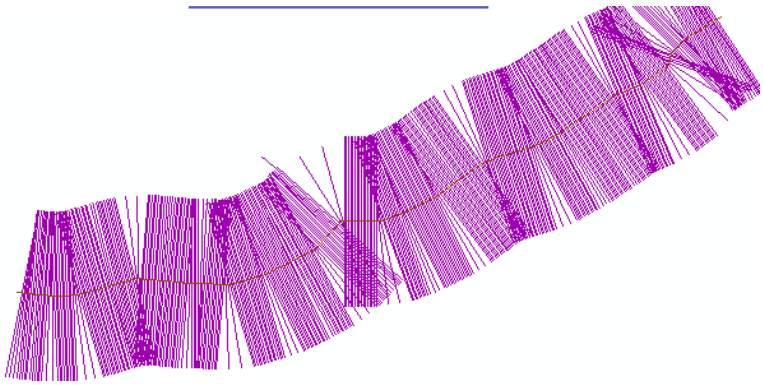

Figure 7 River channel cross-sections obtained from the DEM

7. CONCLUSIONS

This paper reviewed and discussed the different water resource management decision support systems available in order to help water managers choose the appropriate tools from the overwhelming existing DSS and models. The DSS's are grouped in two main classes based on their functionalities: water resources planning systems and real-time operation and control systems. For water resources simulation and planning, the paper presents the two best systems of choice for Souss-Massa: the Water Evaluation and Planning (WEAP) and MODSIM. MODSIM presents some advantages over WEAP and is better integrated in available GIS package. For real-time operation and control, two approaches are possible: 1) a *Stand-alone approach* where a DSS is created from scratch and 2) a *Framework approach* where a DSS is created by taking and integrating a series of existing models. The authors choose the second approach for Souss-Massa, discuss the choice of models to build the system and present the architecture of the system. The different components of the system are tested on pilot sites in the basin for hydrologic simulation, reservoir inflow, reservoir management, hydraulic simulation and flood mapping.

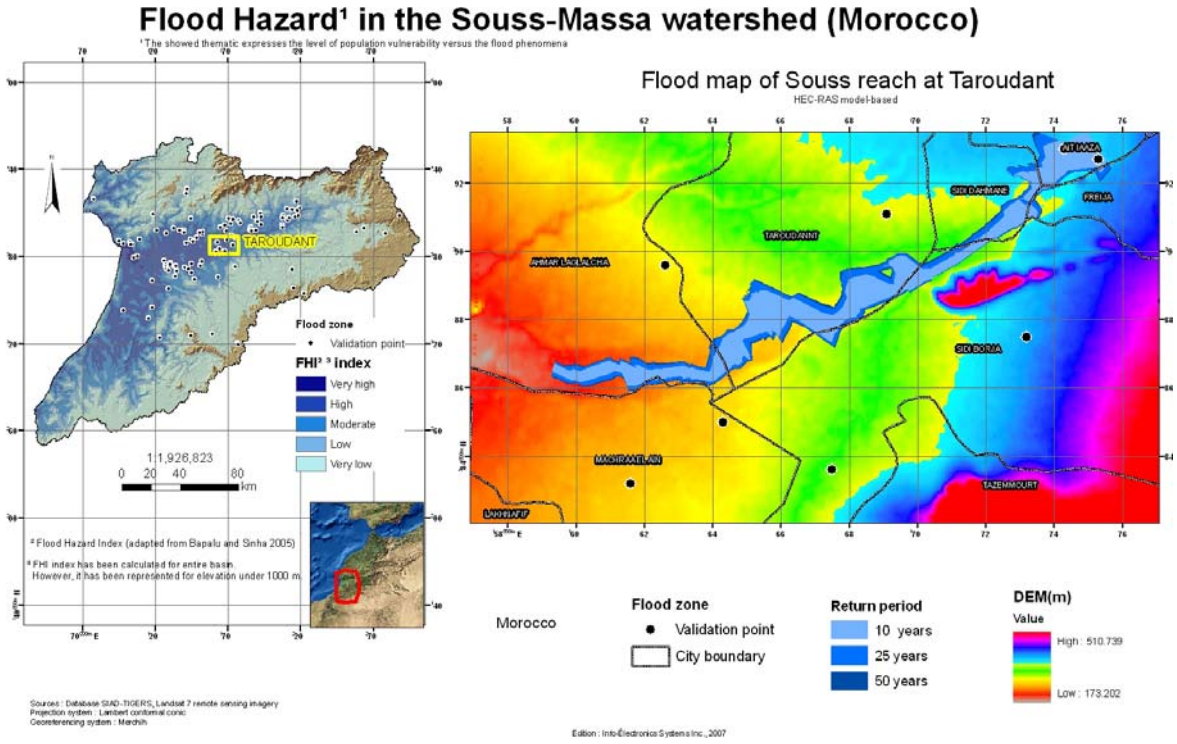

Figure 8 Flood hazard and flood mapping in the Souss-Massa basin

8. ACKNOWLEDGEMENTS

This project has been made possible by financial support of the Canada Space Agency (CSA). The authors also thank the European Space Agency (ESA), the Université du Québec à Montreal (UQAM), the Centre Royal de Télédétection Spatiale (CRTS) and the Agence de Bassin Hydraulique de Souss-Massa (ABHSM) for their collaboration.

9. REFERENCES

Adelman, L. 1992. *Evaluating Decision Support and Expert Systems*, 1st edn. Wiley-InterScience New York, NY, USA 232 pages.

Andreu, J. 2004. *AQUATOOL: Decision Support Systems for integrated water resources planning and management*. Universitat Politècnica de València. http://www.upv.es/aquatool/index_E.htm.

Asena, K. and Maidment, D. 1997. GIS based reservoir planning for the Souss Basin in Morocco, Center for Research in water resources, the University of Texas at Austin. http://www.ce.utexas.edu/centers/crwr/reports/online.html

Bapalu GV and Sinha R (2005) GIS in Flood Hazard Mapping: a case study of Kosi River Basin, India *GIS@Development* online edition, 1–3 (October, 2005 http://www.gisdevelopment.net/application/natural_hazards/floods)

Gibbens, G. and Goodman J. 2000. *Integration of GIS and the River Basin Network Flow Model MODSIM*, Department of Civil Engineering, Colorado State University, Fort Collins, CO. May 2000.

Lancaster, C. 2004. *Application of WEAP and GoldSim models to a simplified schematic of the Rio Conchos river basin.* M.Sc. report, University of Texas at Austin, United States.

Poch. M., Comas, J., Rodríguez-Roda, I., Sànchez-Marrè, M. and Cortés U. 2003. Designing and building real environmental decision support systems, *Environmental Modelling and Software*, Vol. 19, No. 9, pp. 857-873.

Quinn, N., Brekke, L., Miller, N., Heinzer, T., Hidalgo, H. and Dracup, J. 2004. Model integration for assessing future hydroclimate impacts on water resources, agricultural production and environmental quality in the San Joaquin Basin, California. *Environmental Modelling & Software* 19: 305-316.

Labadie, J.W. 2006. MODSIM: Decision Support System for integrated river basin management. *3rd Biennial meeting of the International Environmental Modelling and Software Society*, July 9-13, 2006 online http://www.iemss.org/iemss2006/papers/w5/MODSIMpaper.pdf

Loucks, D.P. Stedinger, J.R., Haith, D.A 1981. *Water resource planning and analysis*, Englewodd Cliffs, NJ, Prentice-Hall Inc.

Maidment, D. 2002. *Arc Hydro: GIS for water resource*. ESRI Press, New York Street, Redlands, California.

McKinney D.C. 2004. *International survey of decision support systems for integrated water management, Technical Report*, IRG Project No: 1673-000.

Sprague, R., and Carlson E. 1982. *Building effective Decision Support System*. Englewood Cliff, NJ, Prentice Hall,

Wurbs, R. 1993. Reservoir-system simulation and optimization models, *Journal of Water Resources Planning and Management,* 119(4): pp. 455-472.

Wurbs, R. 1994. *Computer models for water resources planning and management,. IWR Report 94*-NDS-7, Institute for Water Resources, US Army Corps of Engineers, Alexandria, VA.

Yates, D., Purkey, D., Siebert, J., Huber-Lee, A. and Galbraith H. 2005. A demand, priority and preference-driven water planning model: Part1: Model characteristics. *Water International*, 30(4), pp. 487-500.

Yeh, W.1985. Reservoir management and operations models: A start-of-the-art review. *Water Resour. Res.* 21(12): pp. 1797-1818.

Utilisation de l'Imagerie satellitaire Optique et Radar pour la Cartographie Géologique dans le Secteur de Sebt Brikyne (Bordure Orientale de Doukkala, Maroc): Contribution à la Compréhension Hydrogéologique

Kamal Labbassi [(1)], Loubna Sbih [(1)], Alain Sandoz [(2)].

[(1)] Faculté des Sciences, El Jadida, Maroc, kamal_labbassi@yahoo.fr, sbih.loubna@yahoo.fr
[(2)] Centre de recherche pour la conservation des zones humides méditerranéennes de la Tour du Valat, France, sandoz@tourduvalat.org

Résumé L'objectif de cette recherche est une caractérisation de la géologie régionale comme pivot permettant de comprendre l'hydrogéologie de la région de Doukkala. Le site choisi dans cette étude est considéré comme une zone de recharge qui alimente la plaine de Doukkala en eaux. Un MNT d'une grande résolution (maille de 30 m avec intervalle de 25 m) a été établi et a permis d'extraire des produits dérivés qui vont contribuer à la caractérisation hydrologique et géomorphologique du secteur. L'utilisation des données de télédétection spatiale multi-source (image Spot, Landsat et ERS radar) a rendu possible : la production d'une esquisse de cartographie géologique, qui fourni d'avantage d'informations, en raison du détail qu'elle apporte (1/100 000) par rapport aux documents cartographiques existants (1/200 000) ; (ii) l'élaboration d'une carte structurale des fractures et des linéaments qui affectent la zone. La réalisation d'une telle carte géologique permettra la caractérisation de la géométrie des structures et des couches géologiques en profondeur d'où une meilleure compréhension de la circulation des eaux superficielles et souterraines et les liens entre les points de pertes et de sortie.

Abstract The objective of this research is a characterization of the regional geology and surface hydrology, both key features for understanding the hydrogeology. The study area is regarded as a groundwater recharge zone that feeds the populated plains. A high resolution DEM (30 m pixels and 25 m contour intervals) is needed to derive maps of slope steepness, hydrographical network and to delimit drainage basins. These maps contributed to the hydrological and geomorphological characterization of the study area. The geological setting is being mapped using remote sensing, notably the interpretation of imagery from SPOT, Landsat, and ERS radar data. This has produced: (I) a lithological map at 1:100,000 scale: a big improvement on the existing 1:200,000 maps; (II) a structural geology map, showing fractures and folds. Geological mapping based on remotely sensed imagery has allowed the characterization of the regional structures, aquifers and aquicludes for a better understanding of water circulation and pathways between the zones of recharge and sites of abstraction.

1. INTRODUCTION ET PROBLEMATIQUE

Le bassin des Doukkala, connaît, depuis les années soixante, un important essor économique avec un développement important des activités agricoles et industrielles associées à une forte expansion démographique. Ce contexte fait que le besoin en eaux ne cesse de croître dans cette région semi aride du Maroc. Au cours des deux dernières décennies de nombreux travaux ont mis en évidence l'importance de l'apport de la télédétection et des Systèmes d'Information Géographiques sur les études de ressources en eau (El Hadani, 1992, 1997 ; Bannert, 2004).

Malgré de nombreux travaux de recherche effectués dans la région (Choubert, 1965 ; Cornée et al. 1984 ; El Kamel et al. 1987 ; labbassi, 1998 ; Oaudia, 1998 ; El Attari, 2001 ; Echarfaoui, et al 2003) l'état de la cartographie géologique, dans la bordure du bassin (massif des Rahamna), reste insuffisant. Les études hydrogéologiques se sont concentrées aux eaux souterraines dans la plaine des Doukkala par un suivi

ponctuel de piézomètres et d'analyses chimiques. La mise en œuvre de modèles de fonctionnement des nappes, pour tenter de prévoir l'effet des différentes mesures ou interventions réalisées dans la région, est de plus en plus préconisée. Une approche scientifique intégrée où la maîtrise du cadre géologique s'impose est donc nécessaire. Le contexte géologique dans la région de Sebt Brikyne, qui constitue l'une des principales zones d'alimentation de la plaine des Doukkala, est l'un des points importants pour la compréhension de l'hydrogéologie de la région.

Les images satellitaires optiques et radar, constituent des données d'entrée complémentaires et une source d'information très utile pour valider les modèles. En effet, les données optiques permettent d'améliorer la perception successible de révéler des variations lithologiques (Barrett et al., 1990 ; Delpont et al., 1998), tandis que les images radar possèdent un grand potentiel dans la reconnaissance et la cartographie des linéaments géologiques (Desjardins et al., 2000).

Par l'utilisation des images satellitaires comme source de données, on se propose, dans cette étude, de réaliser une esquisse de cartographie géologique pour contribuer ainsi à la géologie régionale et mieux comprendre l'hydrologie et l'hydrogéologie de la plaine des Doukkala. La réalisation d'une telle carte permettra la caractérisation de la géométrie des structures et des couches géologiques en profondeur d'où une meilleure compréhension de la circulation des eaux et de l'hydrogéologie de la région.

2. CADRE REGIONAL DE LA ZONE D'ETUDE

La région de Sebt Brikyne (Fig.1), est comprise entre les latitudes N32°12' et N32°39' et entre les longitudes W8°26' et W7°49', et a une superficie de 137 516,4 km^2. Le climat est continental aride à semi aride et est fortement influencé par l'altitude et l'éloignement de la mer. Les précipitations sont faibles, avec une moyenne de 220 mm par an.

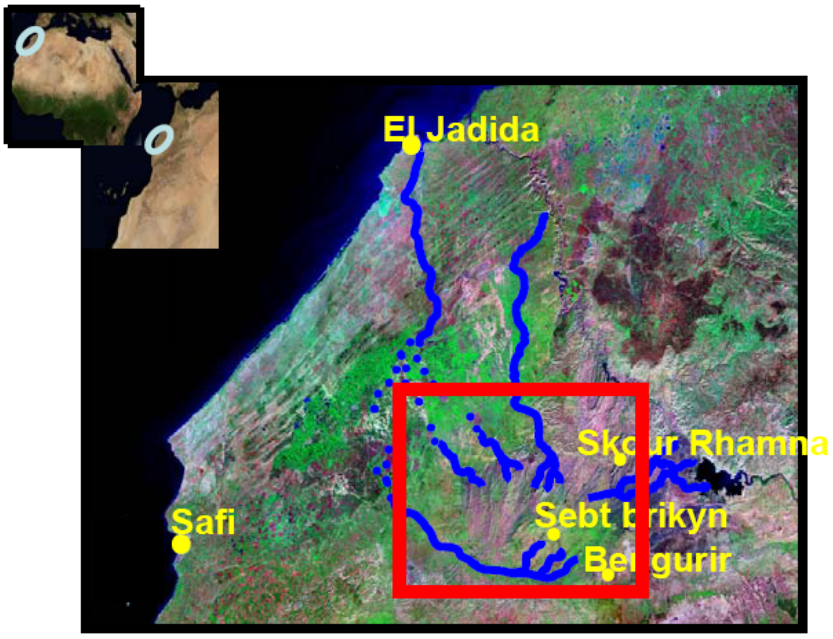

Figure 1 Situation géographique du site de Sebt Brikyne.

La région étudiée appartient à la grande unité géologique du « Môle côtier », caractérisé par un régime tabulaire des dépôts secondaires et tertiaires reposant sur des terrains primaires fortement plissés par l'orogenèse hercynienne. Ces déformations ont été accompagnées par la mise en place d'un massif granitique et de son auréole de métamorphisme (massif de Brikyne). L'histoire géologique commence par une activité tectonique distensive au Cambrien et au Dévonien. Les déformations hercyniennes dont l'amplitude varie

d'un point à l'autre semblent plus affirmées vers l'est dans la zone centrale des Rehamna, au delà de la faille d'Oulad Ziane qui constitue la limite orientale du môle côtier (Michard, 1976 ; Corné et al. 1984 ; El Attari, 2001).

Le socle paléozoïque est constitué en majorité par des terrains attribués au Cambrien moyen et supérieur (Fig.2). Ils sont représentés par des faciès relativement uniformes, subdivisés en trois formations (Gigout, 1965 ; Michard, 1976 ; El Attari, 2001):
- Formation de « schistes à Paradoxides », formée par des schistes argileux feuilletés verdâtres et de grauwackes, avec localement des intercalations volcaniques et volcano-détritiques,
- Formation des « quartzites d'El Hank », constituée par des grès et des quartzites,
- Formation des pélitiques supérieur.

L'épaisseur de la série cambrienne varie du Nord au Sud, est passe de 2000 m à Sidi Saïd Maachou et plus de 4000 m à Imfout. La série paléozoïque se poursuit par des dépôts argilo-gréseux et carbonatés d'age Ordovicien-Silurien et Dévonien avec des d'épaisseurs relativement moins importantes

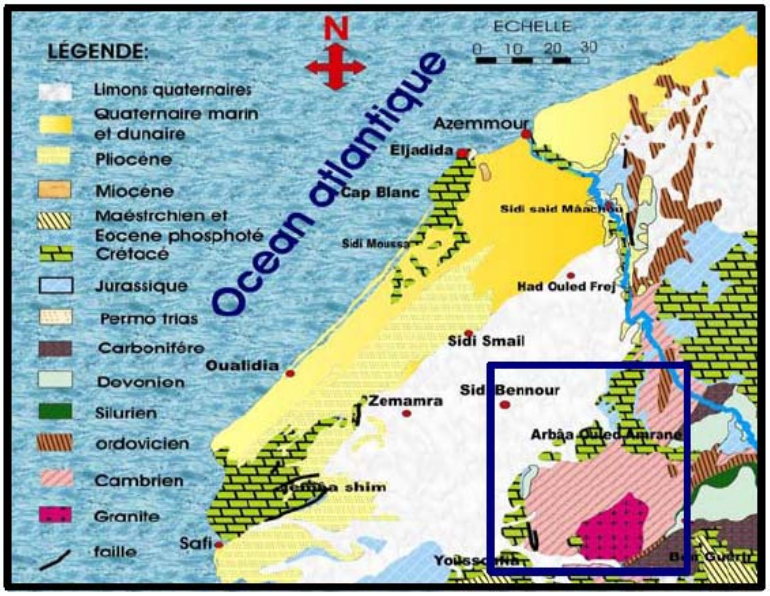

Figure 2 Carte géologique des Doukkala (d'après la carte géologique du Maroc au 1:500 000, feuille d'El Jadida, en encadré : le secteur de Sebt Brikyne).

D'un point de vue hydrogéologique, la région de Sebt Brikyne, est définie comme site amont qui alimente la plaine des Doukkala. Les terrains, à l'exception du granite altéré, sont imperméables. La perméabilité du granite est médiocre et est liée à l'altération et aux fractures. Dans les Rehamna, il n'y a pas de nappe continue et étendue, les écoulements d'eaux souterraines se font à faible profondeur dans les alluvions et dans la frange altérée du substratum. De ce fait, elles subissent de fortes évaporations et se chargent en sels au cours de leur trajet (Ferre et al., 1975; Chtaini, 1987; Guessir, 1995; El Achheb, 2002).

3. DONNEES UTILISEES ET METHODOLOGIE DE TRAVAIL

Les données de télédétection utilisées, dans cette étude, sont multiples: image Landsat TM (path 202, row 37, résolution de 30m du 4 juin 1987; image Spot4 multi spectrales (path 29-30, row 284-285, résolution 20 m) du 6 Mars 2007, et des données radar SAR (track 137, fram 2943-2961, résolution 25 m) du 6 septembre 1995. Ces images sont géoréférencées dans le système UTM, WGS-84, zone 29.

La méthodologie de travail suivie (tableau 1) consiste a : (i) une exploitation de données topographiques et la production d'un modèle numérique de terrain et ses produits dérivés, (ii) un traitement des images satellitaires et des données existantes pour générer de nouveaux produits cartographiques.

L'établissement d'un Modèle Numérique de Terrain d'une grande résolution (pixels de 30 m et 25 m de résolution altimétrique) sur la zone d'étude et l'extraction de produits dérivés ont contribués à la caractérisation du secteur du point de vue de l'hydrologie de surface et ont permit de préciser la géomorphologie du site.

Tableau 1 Approche méthodologique

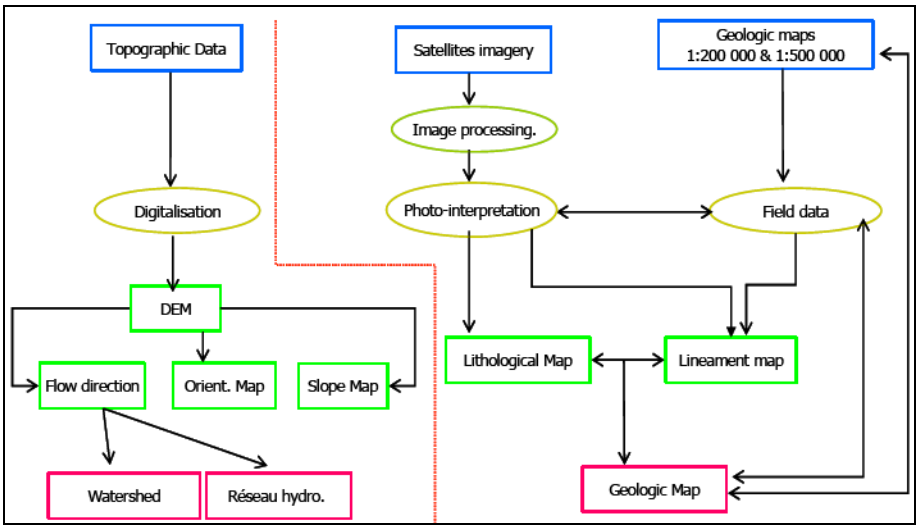

4. TRAITEMENT DES DONNEES ET RESULTATS

4.1 Cartographie des linéaments

L'analyse des linéaments, constitue une étape importante dans la cartographie géologique. L'extraction des linéaments est établie par numérisation des structures linéaires présentes sur les documents cartographiques préexistants, ainsi que par photo-interprétation des images satellitaires. Elle a été appuiée par l'utilisation de données SAR de ERS, par l'application de filtres directionnels (Labbassi et al., 2007). La carte des linéaments obtenue par photo-interprétation (Fig.3), montre que la région est parcourue par un réseau de failles où deux directions ressortent : N-S et NE-SW.

Nos résultats ont mis en évidence l'existence d'un grand linéament de direction NE-SW; la faille de Jbel Lakhder-Guerrandou qui coupe le secteur en deux compartiments: l'un au Nord Ouest représenté par les failles de direction N-S (Fig. 3A) et l'autre au Sud Est où la direction NE-SW prédomine (Fig. 3A). La nature tectonique du contact entre le massif des Rehamna et la plaine des Doukkala est précisée. Elle est exprimé en surface par le monoclinal des Aounate de direction E-W et la flexure de M'tal de direction N-S et s'intègre dans l'ensemble structural nommé « flexure de la Meseta », qui sépare la Meseta côtière au Nord-Ouest de la Meseta centrale au Sud-Est.

Les failles majeures qui affectent le secteur sont exprimées en surface par réseau de diaclase très dense qui guiderait les circulations en profondeur. Le tracé des linéaments tectoniques coïncide avec le réseau hydrographique des principaux oueds qui traversent la région.

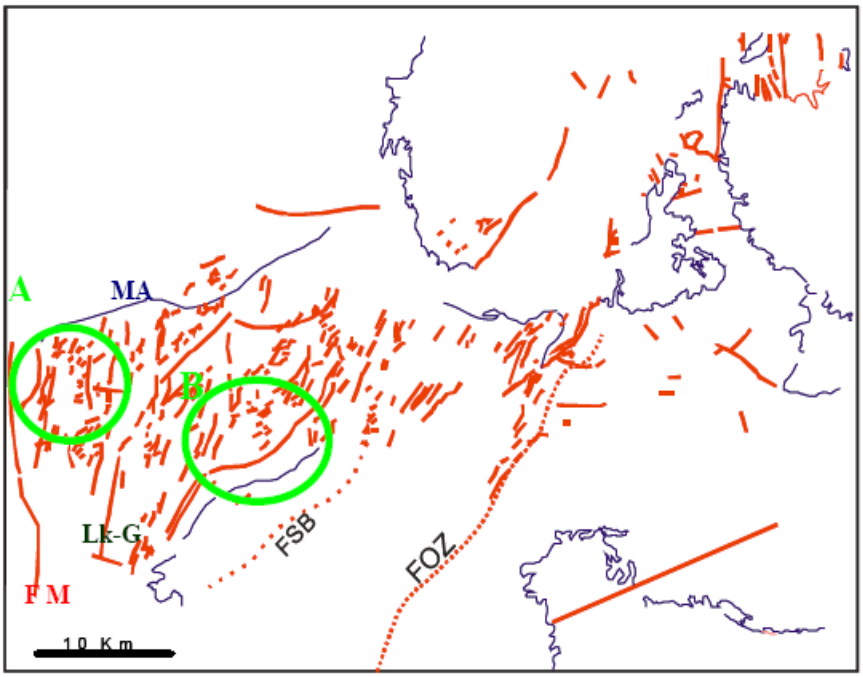

Figure 3 Carte des linéaments dans la région de Sebt Brikyne.
(FOZ : faille Oulad Ziane, FSB : faille des Sebt Brikyne, Lk-G : faille de Jbel Lakhdar-Gerrandou, MA : monoclinale des Aounate, FM : flexure de M'tal)

4.2 Cartographie lithologique

Dans la zone de Sebt Brikyne, les différentes roches (sols) montrent des propriétés spectrales relativement similaires. Différentes techniques de traitement des images numériques, tels que l'analyse en composantes principales, les ratios de bande et la transformation en IHS ont été appliqués aux données Landsat TM et Spot 4 pour appuyer la photo-interprétation des images et la classification lithologique supervisée.

La photo-interprétation, est appliquée sur les données de Landsat TM et Spot images, par l'utilisation de l'Analyse en Composantes Principale (Principal Component Analysis) pour extraire l'information pertinente des différentes bandes. Cette méthode utilisée pour la réduction de la dimension de données qui existe entre les bandes est appliquée sur les six bandes de TM, à l'exception du canal thermique et les quatre bandes de Spot 4.

Pour la classification lithologique, une nouvelle image est produite par l'utilisation de 10 niveaux d'information: Canal TM4, TM5, TM7, Clay minéral (TM5 / TM7), ferrous minerals (TM5 / TM4), ACP1, l'IHS et le canal 3 de Spot4. Le but de cette tentative est une meilleure discrimination lithologique entre les surfaces.

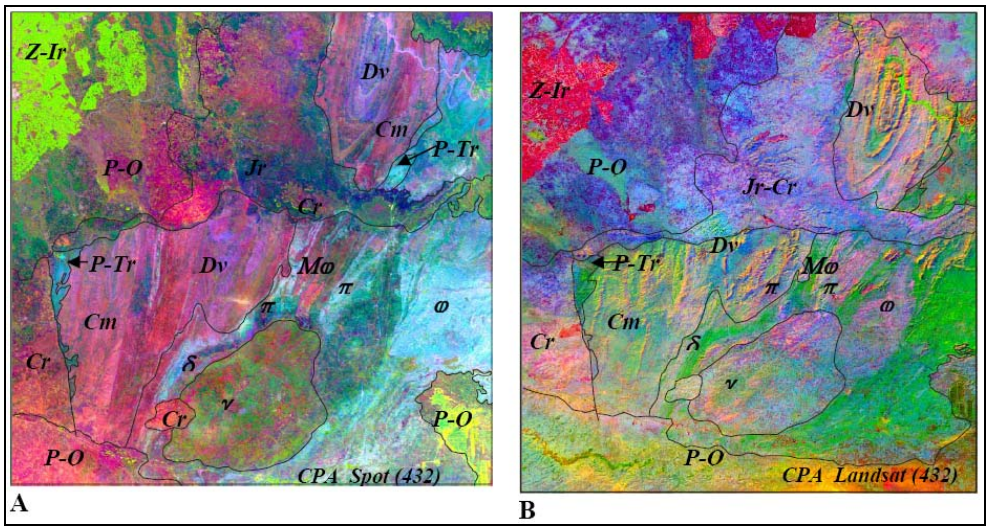

.Figure.4 Analyse en composante principale des données Spot 4 (A) et Landsat TM (B). (4, 3,2 dans le système RGB). Distance E-W: 59 Km environ. [Cm :Cambrien ; Dv :Dévonien ; P-Tr : Permo-Trias ; Jr :Jurassique supérieur ; Cr : Crétacé ; P-Q : Plio-Quaternaire ; Z-Ir : Zone Irriguée. γ : granite ; ζ : gneiss, Mφ: micaschiste ; π : cipolin ; φ : schiste]

Sur la figure 4 sont représentés les résultats de la photo-interprétation. Celle ci donne une première estimation des ensemble lithologiques rencontrés et fait apparaître les grandes unités morpho-structurales dans la région: le granite et son auréole de métamorphisme, les schistes et quartzites cambro-ordoviciens et les terrains sédimentaires jurassico-crétacés et plio- quaternaires. Les résultats montrent la diversité lithologique que présente le terrain étudié.
La classification dirigée consiste à produire des images thématiques en utilisant des classes modélisées par un processus de décision. Une connaissance préalable de la zone à cartographier s'impose. Elle consiste à identifier et classer les pixels en fonction de leur valeur numérique. Cette technique a donné des résultats satisfaisants dans des régions similaires dans le monde (Gomez et al. 2005 ; Gad et al. 2006 ; Inzana et al, 2003).

Le produit de la classification (fig. 5) montre des résultats relativement satisfaisants et les faciès reconnus dans la région sont bien individualisés. Les grands ensembles lithologiques se dégagent clairement. Par apport aux documents cartographiques existants, le massif granitique et les ensembles métamorphiques qui lui sont associés sont bien distincts et leurs extensions paraissent plus intéressantes. On note la présence de terrains permo-triasiques au Nord et au Nord-Est de la carte, ainsi que des formations du Jurassique supérieur et Crétacé inférieur, intercalées entre les roches métamorphiques, ce qui est en conformité avec les données de terrain. Néanmoins des confusions entres les classes lithologiques persistent encore. En effet, mise à part les affleurements de M'tal à l'Ouest de la carte, l'extension des terrains attribués au Permo-Trias au Nord-Ouest da la carte n'est pas validé.

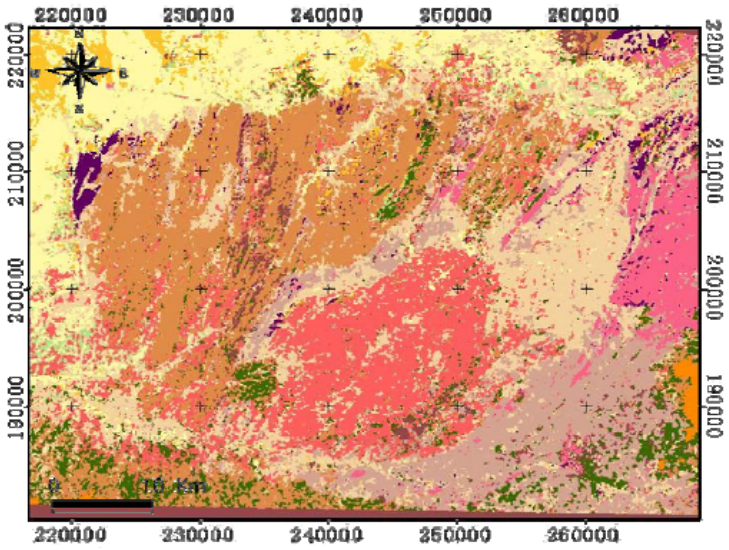

Figure 5 Produit de la classification supervisée appliquée à l'image à 10 niveaux.

Sur le plan de l'interprétation des thèmes contenus dans l'image classifiée, les grands aspects lithologiques se distinguent. Bien évidemment, avec une surestimation ou une sous-estimation des formations obtenues, le résultat de la classification dirigée fournie un produit fiable avec un indice de cartographie supérieure à 90%.

5. CONCLUSIONS

Le présent travail est une contribution à la cartographie géologique par l'application de la télédétection spatiale multi source. Il a permis la production d'une carte lithologique et des linéaments, qui fourni davantage d'information, en raison du détail qu'elle apporte (1/100 000) par rapport aux documents existants (cartes géologiques au 1/200 000 et 1/500 000). En comparant les données recueillies sur le terrain, celles empruntées des documents préexistants ainsi que le temps consacré à la réalisation de cette production, on peut conclure que l'apport de l'imagerie satellitaire peut être estimé à 60-65%. La réalisation d'un tel produit va contribuer à la caractérisation de la géométrie des structures et des couches géologiques en profondeur d'où une meilleure compréhension de la circulation des eaux souterraines et des liens entre les points de pertes et de sortie.

Par rapport aux documents préexistants, le granite et les ensembles métamorphiques qui lui sont associés sont bien distincts et leur extension parait intéressante. L'extension des formations du Jurassique supérieur et Crétacé inférieur, intercalées entre les roches métamorphiques, est en conformité avec les données de terrain. Par contre, celle des terrains du Permo-Trias dans le Nord et au Nord-Est de la carte lithologique est relativement exagéré et mériterait plus d'investigations. La validation de la carte géologique a été effectuée à partir des données de terrains.

La technique de la classification utilisée s'avère intéressante. Cependant et afin d'éviter parfois des confusions entre les classes, d'autres techniques doivent être explorées. L'introduction d'autres types de données satellitaires, une vérification sur le terrain ainsi qu'une étude quantitative sur la base d'une matrice de confusion élaborée à partir d'échantillons terrain apporteront certainement des améliorations aussi bien qualitatives que quantitatives.

L'esquisse d'une carte géologique peut être élaborée par la combinaison du produit issu de la cartographie lithologique et la carte des linéaments. Elle constituera un document de base incontournable pour toute étude géologique et hydrogéologique dans la région. Elle est à l'origine d'une carte de friabilité des roches, utilisée dans un modèle qualitatif de l'érosion hydrique dans le bassin versant des oueds qui alimentent la plaine des Doukkala (Sbih, 2007).

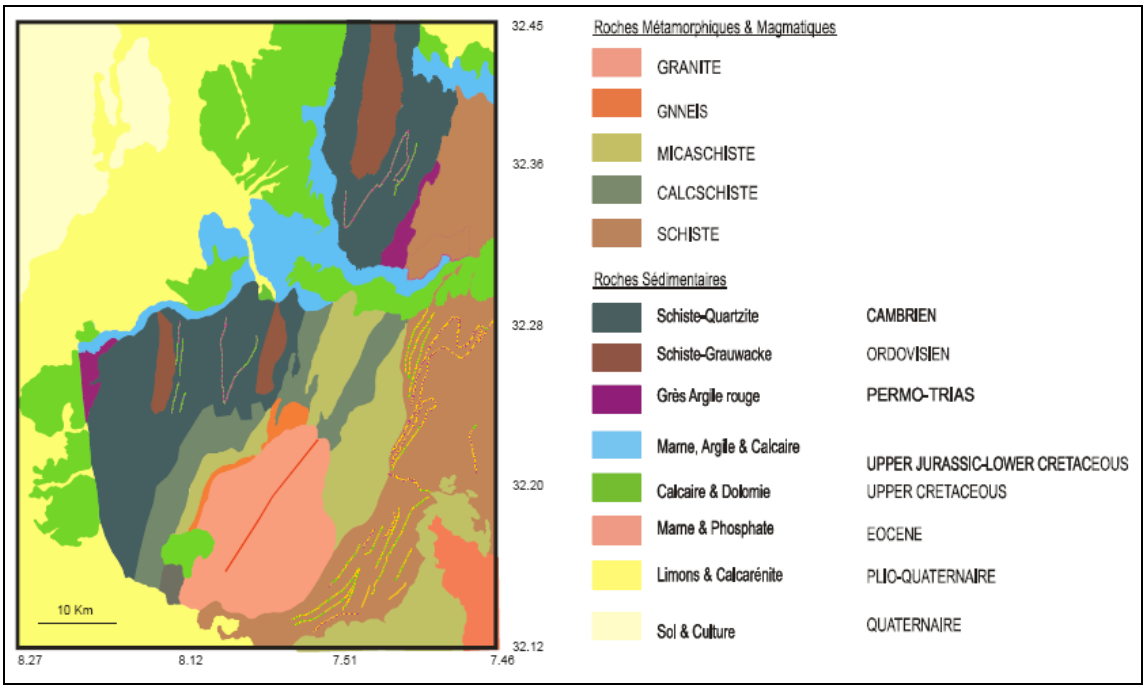

Figure 6. Carte lithologique établie à partir des données la télédétection multi source.

Remerciement : Ce travail est réalisé dans le cadre du projet TIGER. Il a bénéficié du soutien financier du programme volubilis (AI_MA/07/171) et de la fondation internationale des sciences (IFS).

6. BIBLIOGRAPHIE

Bannert, D. 2004. Hydrologeology, water and remote sensing. Actes du Symposium MARISY 2004, Rabat, Maroc, *Géo Observateur,* N° 13.

Barrett, E.C., Beaumont, M.J. et Hershy, R.W. 1990. Satellite remote sensing for operational hydrology: present needs and future opportunities. *Remote Sens. Reviews*, 4(2), pp. 451-466.

Choubert, G. 1965. Evolution de la connaissance du Quaternaire au Maroc. Notes. *Mém. Serv. Geol. Maroc*, 25 (185), pp. 9-27.

Chtaini, A. 1987. *Etudes hydrologiques du Sahel des Doukkala (Maroc)*. Thèse Doctorat, Université de Grenoble, France.

Cornée, J.J., Costagliola, C. et Leglise, H. 1984. Litho stratigraphie et tectonique des terrains Anté-Cénomanien d'El Jadida, Meseta marocaine hercynienne. *Bull. Fac. Sci. Marrakech.*

Delpont G. et Fily M. 1998. *Synthèse des travaux du groupe ad hoc Spot 4 MIR: Hydrologie et hydrogéologie*. Paris, Ed. CNES.

Desjardins, R.› Iris, S.› Roy, D. W.› Lemieux, G. H. et Toutin, Th. 2000. Efficacité des données de RADARSAT-1 dans la reconnaissance des linéaments: un bilan. *Can. J. Remote Sens.*, Vol. 26, N° 6, pp. 483-565

Echarfaoui, H., Hafid, M. et Aït Salem, A. 2003. Structure sismique du socle paléozoïque du bassin des Doukkala, Môle côtier, Maroc occidental: Indication en faveur de l'existence d'une phase éo-varisque. *Comp. Rend. Geosciences,* Vol. 334, N° 1.

El Achheb, A. 2002. *Etude hydrogéologique et hydro chimique de la plaine des Doukkala (Maroc occidental)*. Thèse Doctorat. Fac. Sci. Université El Jadida.

El Attari, A. 2001. *Etude litho stratigraphique et tectonique des terrains paléozoïques du Mole côtier (Meseta occidental, Maroc).* Thèse de Doctorat es Sciences. Fac. Sci. Université Rabat.

El haddani, D. 1992. Application de la télédétection à la prospection Hydrologique an Milieux Fissurés. Actes du Symposium MARISY 92, Rabat, Maroc, Octobre 7-9, *Géo Observateur.*

El haddani, D. 1997. Télédétection et systèmes d'information géographique pour la gestion et la recherche de l'eau. *Géo Observateur*. (Les rapports thématiques, N°1.)

El Kamel, F. et Muller J. 1987. Sédimentation et tectonique dans le basin molassique permo-carbonifère de Mechraa ben Abou (Rehamna). *Bull. Int. Sci. Rabat*, N° 11.

Ferré, A. et Ruhard, J.P. 1975. Les basins des Abda-Doukkala et du Sahel de Azemmour à Safi. Ressources en eau du Maroc, Tome 2, Plaines et basins du Maroc atlantique. *Notes. Mém. Serv. Géol.* Maroc, N°231.

Gad, S. et Kusky, T. 2006. Lithological mapping in the Eastern Desert of Egypt, the Barramiya area, using Landsat thematic mapper (TM). *Journal of African Earth Sciences,* Vol. 44, N° 2, pp. 196-202

Gigout, M. 1965. Carte géologique de la Meseta marocaine entre Settat et Mazagan (El Jadida) (Doukkala et Chaouia occidentale). Notice explicative. *Not. Mém. Serv. Géol.* Maroc, N° 75 bis.

Gomez, C., Delacourt, Ch., Allemand, P., Lerdu, P. and Wackerle, R. 2005. Using ASTER remote sensing data set for geological mapping in Namibia. *Physics and chemistry of Earth*, 30, pp. 97-108.

Guessir, H. 1995. *Etude de l'impact de l'irrigation par les eaux usées brutes sur la qualité physico-chimique du sol et de la nappe phréatique dans la région de Sidi Benn Our (Maroc)*. Thèse de 3° cycle, Fac. Sci. Université El Jadida.

Inzana, J., Dusky, T., Higgs, G. et Tucker, R. 2003. Supervised classifications of Landsat TM band ratio images and Landsat TM band ratio image with radar for geological interpretations of central Madagascar. *Journal of African Earth Sciences* 37, pp. 59–72.

Labbassi, K. et Sbih L. 2007. Use of satellite data and GIS for lithological and geomorphological mapping in groundwater studies in the Sebt Brikyne area (Doukkala) western Morocco. *GRSG. Ann. Conf.* Geol. Soc. of London, December 2007.

Labbassi, K. 1998. *Subsidence et histoire thermique du bassin d'El Jadida-Agadir : Implications géodynamique dans le cadre de la cinématique de l'Atlantique Central*. Thèse de Doctorat, Fac. Sci. Université El Jadida.

Michard, A. 1976. Eléments de Géologie marocaine, *Notes Mém. Serv. Géol*. Maroc, N° 252.

Ouadia, M. 1998. *Les formations plio-quaternaires dans le domaine mesetien occidental du Maroc entre Casablanca et Safi: Géomorphologie, sédimentologie, paléoenvironnements quaternaires et évolution actuelle.* Thèse Doctorat. Fac. Sci. Rabat.

Sbih, L. 2007. *Erosion Hydrique dans le Bassin de l'oued Faregh : Plaine de Doukkala.* Master, Centre Africain pour les Sciences et Technologies de l'Espace en Langue Française (CRASTELF), Rabat.

The contribution of EO data in the identification and management of hydro-geological risks in the lake Nyos region of West Cameroon

Tchindjang Mesmin [(1)], Bizenga Jean François [(2)], Kah Elvis Fang [(3)], Menga Francis Vincent [(4)], Nankam Appolinaire [(5)], Mphoweh Jude Nzembayie [(6)], Nghonda Jean Pierre [(7)]

[(1)] Department of Geography, University of Yaounde I, PO BOX 30464 Yaoundé Cameroon mtchind@yahoo.fr
[(2)] PO BOX 125 Brazzaville, Congo jfbizenga@yahoo.fr
[(3)] Ministry of Environment and Protection of Nature, PO BOX, 13138, Yaoundé kah_elvis@yahoo.fr
[(4)] Department of Geography, University of Yaounde I, PO BOX 755 Yaounde e_menga@yahoo.fr
[(5)] Ministry of Forestry and wildlife, apponankam@yahoo.fr
[(6)] Department of Geography, University of Yaounde I mphowehjude@yahoo.fr
[(7)] National Institute of cartography, Ministry of Scientific Research and Innovation, enpcam@yahoo.com

Abstract Environmental threats are common around the world and they can be classified into various types. The Lake Nyos region, where this study is based, faces a volcanic threat. This type of threat has been assessed with the use of Earth Observation (EO) data. With water accumulation estimated at 3 billion m^3, Lake Nyos witnessed a gas explosion in 1986 which led to the death of 1786 people. A lot of research was carried out in order to determine the origin of the gas which confirmed that the gas explosion was of volcanic origin, coming from the mantle through fractures. Field observations were carried out in order to define the extent of the gas movement, validate field data, determine the lineaments and make an appraisal of the risk zone. This information was then later analysed in the laboratory. Multi-source data (topographical maps, aerial photographs, satellite images, SRTM data) have been compared and used to generate DEM lineaments. This revealed that in case of the rupture of the dam and/or another gas explosion, the floods that will result may spread from Cameroon into Nigeria through streams and about 10,000 people may be under threat.

1. INTRODUCTION

The Cameroon Western Highlands is organized into a series of plateaux, broken hills and major undulations which have been partitioned by tectonic activity and are characterized by imposing volcanic edifices (Mount Bamboutos – 2740 m, Mount Oku – 3011 m). These structures are covered by lava and pyroclastic projections that are interspersed by depressed basins (Mbo plain) and highly dissected valleys. Alain Le Maréchal in the 1970s was the first to have studied thermo-mineral springs and groundwater along fractured axes in Cameroon. However, his study was limited to collection and sampling as well as biochemical aspects of these springs leaving out the tectonic relation to the groundwater or wells. More than 200 thermo-mineral springs have been identified and mapped in the volcanic regions of Cameroon as a whole. These springs are mostly concentrated along the main fractured lines of the country. Geologically, four main lineament or fracture directions have been identified by various authors:

- SW – NE, being the Cameroon Volcanic Line (CVL)
- WSW – ENE direction otherwise called the Adamaoua direction
- The Somalian Direction
- And the Krenkel also known as Eritrean direction.

Lake Nyos region is located to the North West of the Cameroon highlands, specifically in the north of the Mount Oku region (Fig.1).

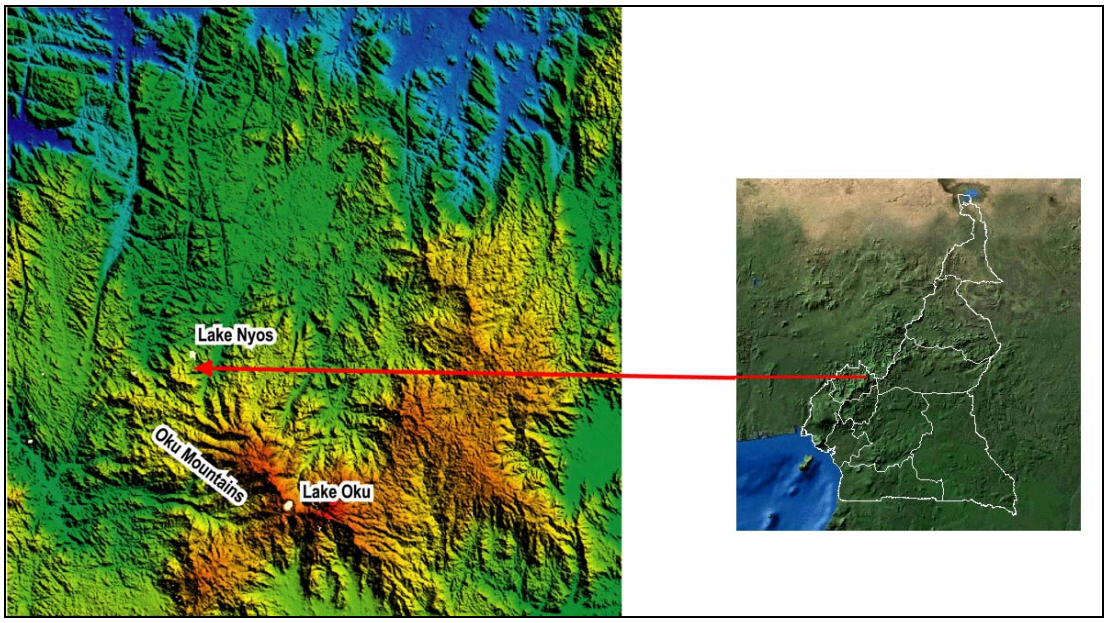

Figure 1 Location of the Lake Nyos region in Cameroon

2. STATE OF THE PROBLEM

It is from the works of Baumann (1887), that the Cameroon line became known as a geological structure in central Africa. This line is an alignment of oceanic and continental volcanic massifs and of orogenic plutonic complexes trending N30°E from Pagalu Island to Lake Chad (Gèze, 1941). It is now considered as a pan African lineament more or less permanently reactivated from the Precambrian to the present (Moreau et al., 1987). Generally the resurgence of thermo-mineral water in this region mostly occurs at lineaments, fault intersections or along depressed topographical lines (Launay, 1899) as it is here where water can easily flow. This flow of springs generally follows the inclination of the landscape and is fast flowing by nature. In this Lake Nyos region, most springs lie parallel to lineaments and this is similar to what is found in the Ngaoundere region where most springs flow parallel to the lineaments of N 117° E direction of the quaternary volcanoes. This situation can still be likened to that of the Mamfe region (to the SW of this region) where springs line up following the N 105° direction of the cretaceous rocks. All these features prove the contribution of thermal-mineral spring prospecting in the study of regional tectonic activity and lead to the determination of tearing and compressing faults. Thus the fractures that are flanked by resurgences have to be open enough for easy water circulation. It should be noted that these fractures generally resulted from the extensional tectonic movements and not from compressive tectonic movements. Satellite images of this region reveal three main lineament directions: which had earlier been identified by Le Marechal (1971, 1976). They include:

- SW-NE, Cameroon Volcanic Line (N28°E)
- NW-SE called Wum Direction (N140° E)
- WSW-ENE called pan African or Foumban direction (N58°E).

Most springs identified by Le Maréchal in this study area lie along the SW – NE direction while lakes are found on the other two directions, that is, WSW – ENE and NW– SE. These springs are directly located at the intersection of fractured zones which are inclined SE-NW. Thus, Lake Nyos exerts pressure on one direction following its inclination under the force of gravity. The scouring action of water has greatly thinned the lake's dam there by threatening it by rupturing. In case the dam ruptures as a result of an earthquake or another emission of toxic gases from the lake, the entire population of the region would be eliminated.

3. METHODS AND TECHNIQUES

The first major stage focused on lineament detection (risk zones) on the satellite images that cover the Lake Nyos region. This consisted of the search of the first drift local extremes or the passing by zero of the second drift using the ENVI software. Such an operation is generally realized by applying a high-pass filter followed by a smoothing operation (low-pass filter) in order to eliminate noise (elimination of wrong contour points). This operation of sensing contours can be realized by two separate methods: 1) the gradient method, which uses derivation operators of the first order; and 2) the Laplacian method, which uses derivation operators of the second order (Horaud et al., 1993). These were carried out on the radar image.

3.1 Methods of applying derivation operators of the first order

These methods can generally be grouped into two. The first one is based on convolution masks of approximating gradient operator by finite difference; the second rely on sophisticated techniques, based on optimal approaches (search for an ideal contour). Techniques of the first group were applied: the gradient was calculated and local extremes of the gradient norm were extracted. An example of a signal is represented by a diagram (in one dimension) in Figure 2. The contour is shown by an abrupt change of intensity.

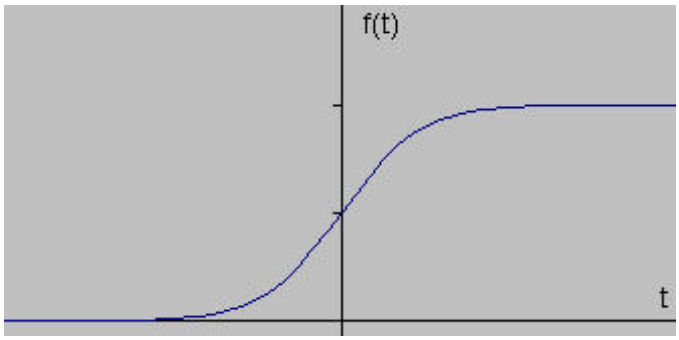

Figure 2 Graphical representation of f(t) signal.

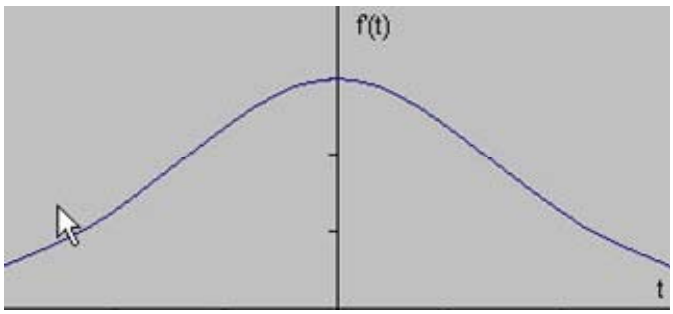

Figure 3 Graphic representation of the first drift of f(t)

The gradient of this signal is the first drift of the f(t) function (see Figure 3). In Figure 3, a local maximum clearly exists at the centre of the contour produced in the diagram in Figure 2. Based on the analysis of a single dimension, the theory can be transported to the second dimension as a calculated approximation which can also be obtained from the first drift in the second dimension. The gradient approach leads us to the determination of a linear filter enabling an approximation of the gradient. The gradient of a digital image is a vector that is characterized by its amplitude and its direction. Amplitude is directly linked to the quantity of local variations of the grey level.

The gradient of an image is calculated thus as follows:

$$G_x(x,y) = \frac{\delta I_f(x,y)}{\delta_x} \quad (1)$$

$$G_y(x,y) = \frac{\delta I_f(x,y)}{\delta_y} \quad (2)$$

Where: G_y = Gradient δI_f = Amplitude δ_y = Direction

At each point (x, y) of the image, we can then calculate the gradient vector.

Within the framework of this study, the max norm was chosen as it has the advantage of less computation time. In a discreet case, the approximation of a gradient is done by image convolution with specific convolution masks. In literature there are many masks of this type amongst which we can cite:

1) **Roberts** Mask:

$$W_x = \begin{bmatrix} 0 & 0 & 0 \\ 0 & 1 & 0 \\ 0 & 0 & -1 \end{bmatrix} \quad W_y = \begin{bmatrix} 0 & 0 & 0 \\ 0 & 0 & 1 \\ 0 & -1 & 0 \end{bmatrix}$$

2) **Sobel** Mask:

$$W_x = \begin{bmatrix} -1 & 0 & 1 \\ -2 & 0 & 2 \\ -1 & 0 & 1 \end{bmatrix} \quad W_y = \begin{bmatrix} -1 & -2 & -1 \\ 0 & 0 & 0 \\ 1 & 2 & 1 \end{bmatrix}$$

3) **Prewitt** Mask**:**

$$W_x = \begin{bmatrix} -1 & 0 & 1 \\ -1 & 0 & 1 \\ -1 & 0 & 1 \end{bmatrix} \quad W_y = \begin{bmatrix} -1 & -1 & -1 \\ 0 & 0 & 0 \\ 1 & 1 & 1 \end{bmatrix}$$

4) **Kirsh** Mask**:**

$$W_x = \begin{bmatrix} -3 & -3 & 5 \\ -3 & 0 & 5 \\ -3 & -3 & 5 \end{bmatrix} \quad W_y = \begin{bmatrix} -3 & -3 & 3 \\ -3 & 0 & -3 \\ 5 & 5 & 5 \end{bmatrix}$$

Where: W_x = Horizontal direction
W_y = Vertical direction
And their respective directional masks.

All these operations were carried out to determine the main lineaments in the region, their directions and their lengths. The operations were complimented with the use of aerial photographs, topographical maps, GPS points and field observations to determine their depths.

Using the database of the hydrographical network of Cameroon, a new table with rivers and lakes of the study area was created in MapInfo. This was superimposed with the geo-referenced radar image used above to create another table that was used to determine the lineaments. 12 aerial photographs obtained in 1964 by UAG mission (NB32 XVI-XVII) were equally geo-referenced (series No. 524 - 529 line 1; and 586 – 591 line 2) and the layer of lakes alongside wells were created and also imported into the MapInfo tables. The location points of the wells were obtained thanks to GPS measurements taken during fieldwork. The resulting map (Fig.5) from the above combination shows a juxtaposition of fault lines, lakes and springs. Since the rocks are generally of granitic nature in a region characterized by tensional forces and undulations, the superimposition of the hydrographical network on a three-dimensional surface clearly shows the general inclination of the region.

4. RESULTS AND INTERPRETATION

4.1 Detection of lineaments

Figure 4 presents the result of lineament detection by applying the first method mentioned above on radar images. But the result obtained through this method was considered insufficient.

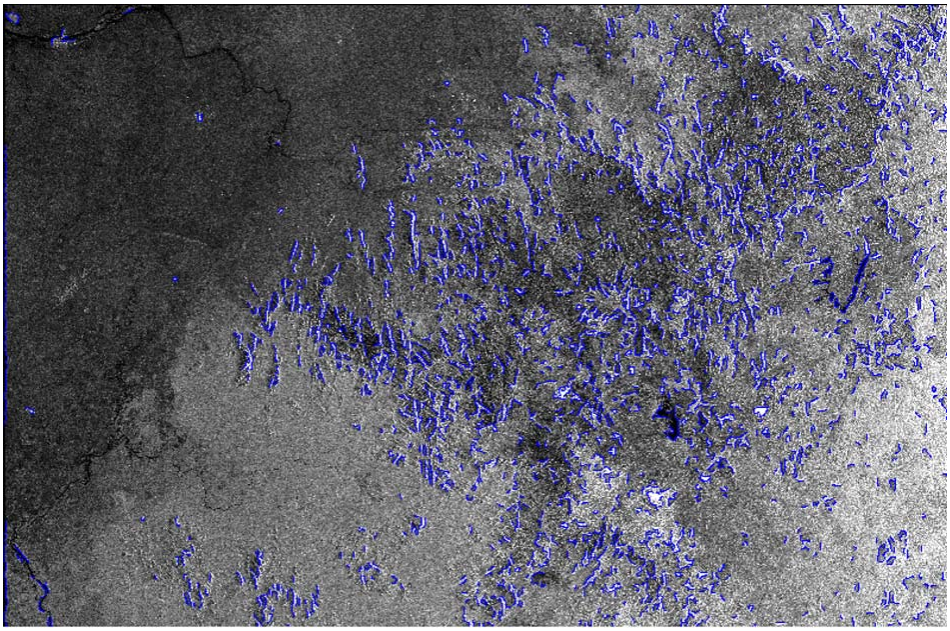

Figure 4 Lineament detection through derivation method of the first order

Unlike the aerial photographs, the processing of radar images using ENVI software, version 4.0 produced quite good results with Laplacian and High pass filters (Fig.4a, b, c, d)

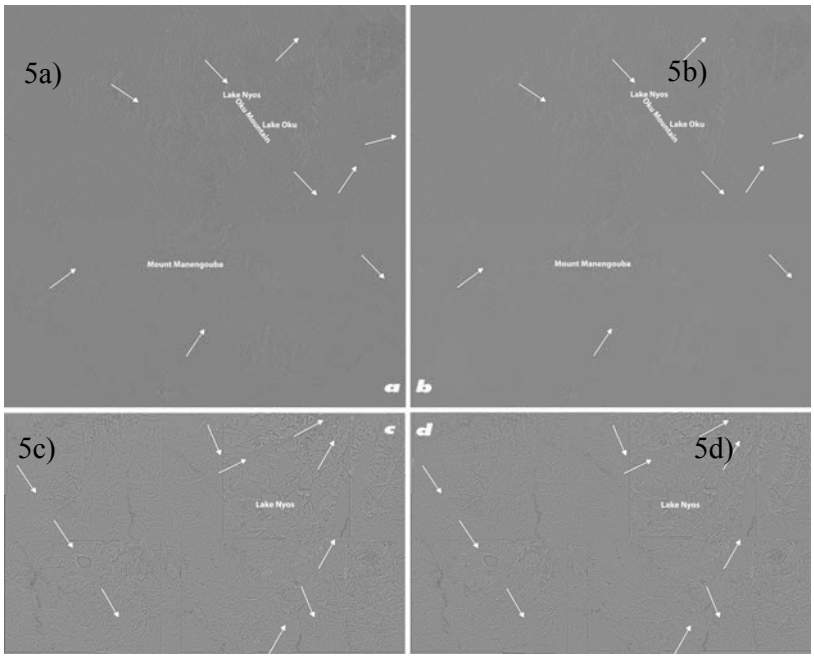

Figure 5 Lineament detection through the signal methods with four main directions (0°,45°,90° and 135°): High-pass and Laplacian filters on a radar image (a, b) and on aerial photographs (c, d).

The above-mentioned techniques of processing for the different databases were then combined and imported into Mapinfo as shown on Fig.6

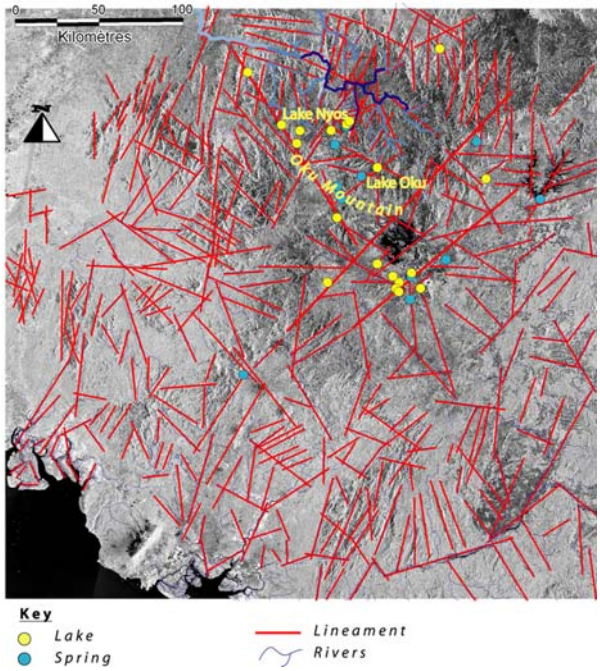

Figure 6: Superimposition of JERS radar image and the hydrographical network.

It should be noted that most springs in Cameroon take their recharge from mountainous and volcanic regions. Gèze (1943) presents three main volcanic phases in Cameroon which produced the host rocks of these springs:

- Basaltic phase that covered the west Cameroon plateau with Hawaiian trapp;
- derived intermediary acid phase (trachytes, rhyolites, phonolites, ignimbrites and tuff) or "white series";and
- Recent volcanoes phase, otherwise called "superior black series" with pyroclastic material.

In Cameroon as a whole, about 70% of groundwater occurs in volcanic regions. Of these occurrences, about 60% are concentrated in major fault lines, and about 15% are salty springs spread along the coast. The formation of rock pedestal mostly occurs in fractured zones. Figure 7a shows the main directions of the lineaments within the Lake Nyos region on a mosaic of aerial photographs. Those indicated in black extend beyond 1 km in length while those in red are less than 1 km. On the other hand, Figure 7b covers a much wider surface on a radar image and represents the thematic analysis of lineaments. The thick lines represent lineaments more than 10 km long while the thin ones are below 10 km long.

Generally, if there is an important aquifer in faulted zones, it becomes easy to locate a well, but if the aquifer is mediocre the only means is to place the forage at zones of intersection. It should also be noted that main fractured zones are sometimes dry with no aquifer (Engladenc 1978, 1979 and 1981) but this is not the case of the Lake Nyos region. The detected lineaments show that the main directions lie parallel to the most active volcanic line in Cameroon today. Most of the springs identified are located at the intersection points of fault lines. It is these springs that later constitute the main rivers in the region which in general take a SE-NW direction flowing into Nigeria to form part of the Niger basin. Out of the 44 volcanic lakes in Cameroon, more than a half, that is, 23, are found in this volcanic province, while the lake Nyos region alone has 13

such lakes. This confirms what Tchindjang (1996) estimated by stating that this region falls within one of the most active fault lines if not the most active fault in Cameroon.

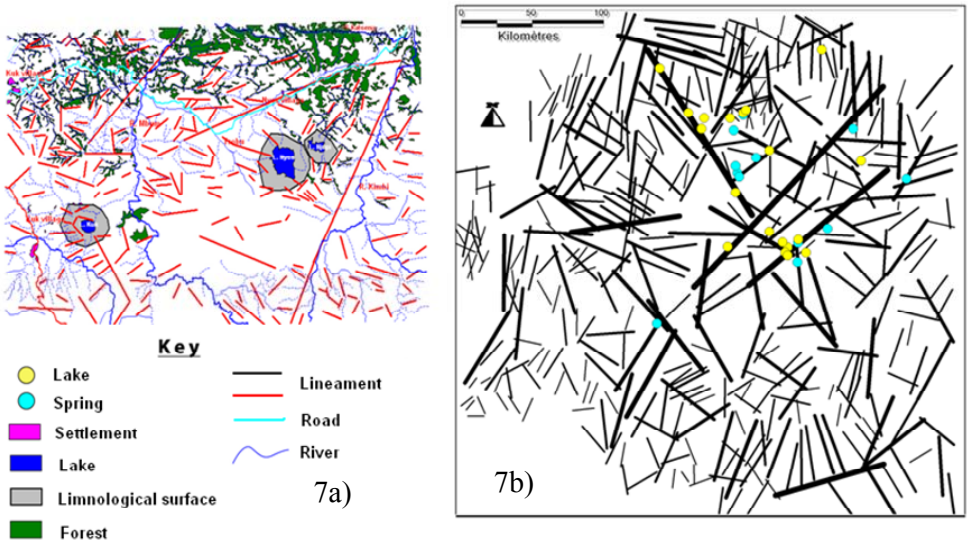

Figure 7 Thematic analysis of lineaments based a) on aerial photographs and b) on radar images

4.2 Evaluation of risks

Determining the extent of the risk depended upon the proper use of the existing data. The distribution of lineaments and the evolution of the vegetation were analysed. Field observations revealed that fractures exist on the pyroclastic dam (Fig.8a) of the lake since 2001. These are accompanied by widening potholes dug by the process of erosion. Thus, the main risk is linked to the pyroclastic dam that surrounds the lake presented in Fig. 8.

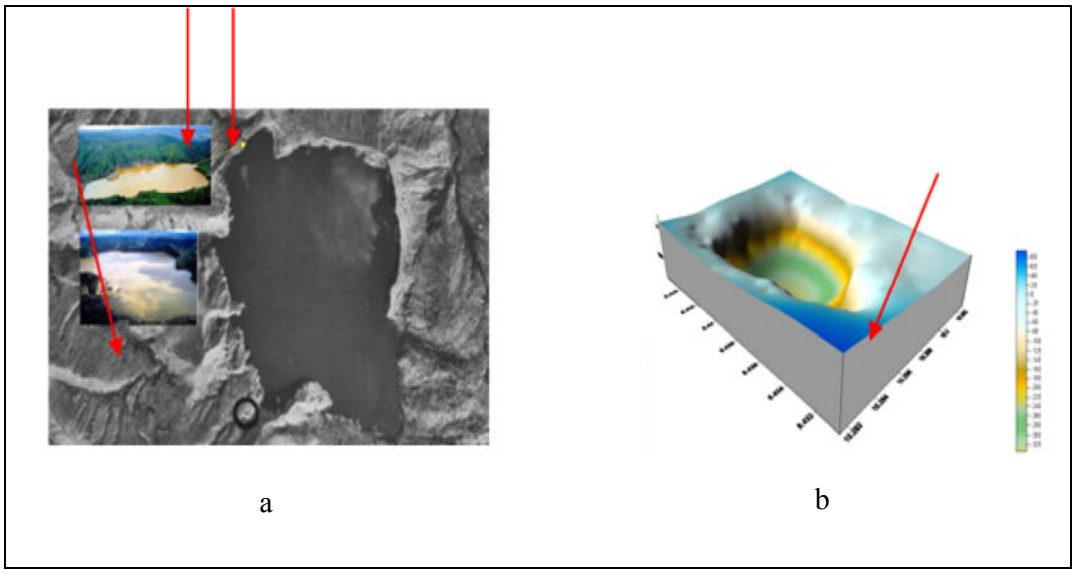

Figure 8 a) Lake Nyos with indications of the pyroclastic dam; b) Digital Elevation Model of Lake Nyos

In case of an earthquake, this dam is likely to break off releasing about 3 billion m^3 of the lake's water along the valleys which will flow right to Nigeria. It should be noted that these valleys are oriented by the fault

lines and they principally form the River Katsina basin. Apart from straightness, the angle of bifurcation of the main river (Katsina and its tributaries) is an indication that drainage lines follow fractures.

Another risk is linked to an increasing number of exposed people to risk in this region. The return of the local population, who for the past 20 years had been living in Bua Bua and other resettled localities, is feared most. This return, it is expected, will certainly orchestrate underground water change, deforestation and the re-conquest of savannah in the present forested zones. Besides, since one cannot predict the occurrence of natural hazards, the returning population will still be exposed to the same danger as of 1986. This means that more deaths will be registered in case of another explosion, which is imminent as many studies have proven that the fault lines are still very active. The degasification process which is still in process, points to this fact. It should also be noted that the gas emitted during the 1986 explosion mostly flew across fault lines and the population settled along these lines were the most affected.

5. DISCUSSION

The lake Nyos region which falls within the Cameroonian dorsal remains the most active fault line in Cameroon. This fault line stretches from the Atlantic Ocean to the Adamawa plateau. To this effect therefore, the region needs to be constantly surveyed as one cannot predict which volcanic eruption can take place at any given moment in time. Apart from the tectonic activities, the frequency of landslides, especially during the rainy season, constitutes another risk to the population, and it is rather this factor that was taken into consideration for the resettlement of the survivors. Thus the Bua bua site, a relatively flat area to the east of Lake Nyos where the survivors of the lake Nyos gas explosion were resettled, cannot be considered to be final. This is due to the fact that from mid June to October, the general wind circulation in this region is West-East. As was the case in 1986, any explosion from the lake will carry the gas to the East following principally the fault lines. This factor was actually not taken into consideration during the resettlement process. This can be proven by the fact that the accompanying measures were never implemented. Multi-date satellite images are well adapted to diachronic approach which is of prime importance in determining the distribution of lineaments and the management of risks. Therefore the powers that be have to rethink the resettlement process in light of remote sensing data.

Because the thickness of the dam is 20 m, it cannot be detected through images of low resolution (one pixel being 25 m). Thus, from field work and the generation of a DEM, it became possible to obtain viable and acceptable information on the dam's fragility. It is observed that if the dam continues to thin down due to the scrubbing action of the lake's water generating potholes, the natural dam might break in the near future. In case of collapse of the dam (due to earthquake or volcanic eruption), given the quantity of water contained in the lake, four categories of risk zones were identified: high, moderate, low and very low risk zones. Most of the population is settled in the high risk zones (valleys or tectonic corridors). After the gas explosion in 1986, the resettlement concentrated the survivors in those zones. The generated DEM with a topographical map at 1:50,000 (Fig. 9) shows that the landscape is highly undulating and the hydrographic network is dense and sinuous. Watercourses directly follow the tectonic orientation.
The map of exposure to floods drawn from this DEM will certainly provide an important basis for decision-making (Fig. 10).

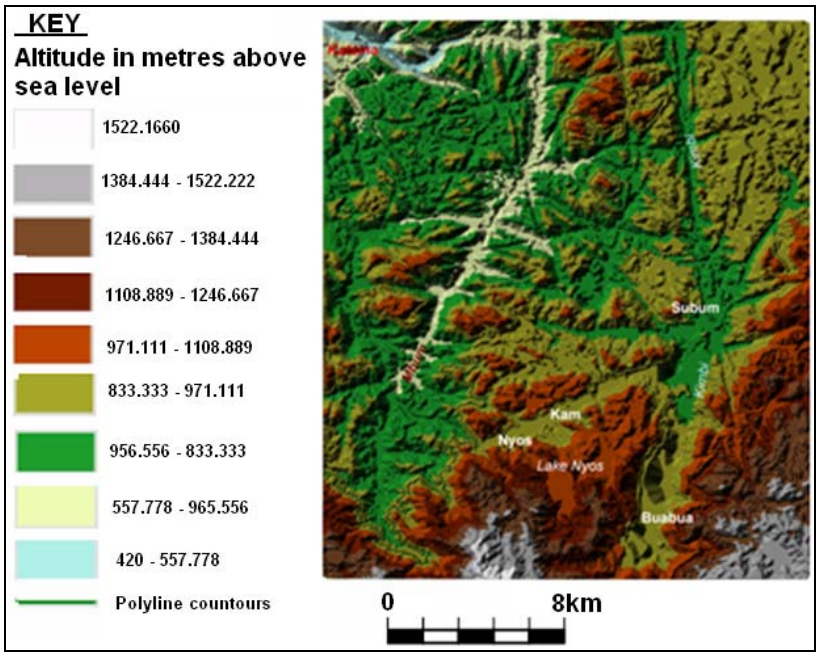

Figure 9 Digital elevation model of Lake Nyos region

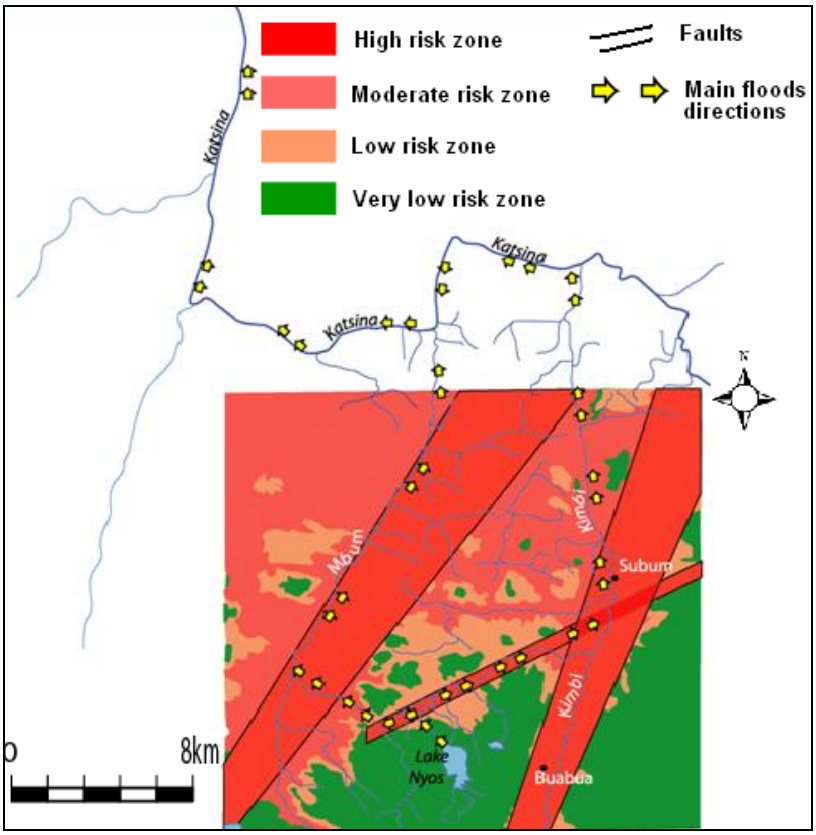

Figure 10 Determination of zones exposed to floods

6. CONCLUSION

The Lake Nyos region, which lies along the Cameroon volcanic line, is subject to various types of risks which are devastating both to the environment and to human lives. To assess these risks, different databases were used - satellite images, aerial photographs, hydrographical network of Cameroon - and complimented with ground-based measurements. Most important use of the radar satellite image was the detection of lineaments using derivative methods of the first and second orders while the optical satellite image served in determining vegetation change in the region. The geo-referenced aerial photographs were useful for zooming in on the area to specify and characterize the lineaments. Inferences cannot be drawn from these operations alone. It is for this reason that these had to be complimented with ground based measurements, in the form of photographs and GPS points. The results then showed that there is still a potential zone at risk, i.e. the resettled sites of the local population created after the gas explosion in 1986 are not safe. The surviving population returned to their original site: in addition to their exposure to risk, the environment will be made more fragile. Lastly, a rupture of the pyroclastic dam holding the lake's water may cause floods that could threaten about 10,000 people along the fractured lines. Much attention is therefore needed in this region to mitigate if not avert the occurrence of any disaster.

7. REFERENCES

Baumann Von O. 1887. Berträge zur physischen geographie von Fernando Poo. *Petermanns Mitt Justus Perthes'Geograph* Anst. 33, pp. 265-269.

Engladenc 1978. *Méthode d'étude et de recherches de l'eau souterraine des roches cristallines*. Paris, Comité inter africain d'études hydrauliques T.1.

Engladenc 1979. *Méthode d'étude et de recherches de l'eau souterraine des roches cristallines*. Travaux complémentaires sur le milieu fissuré T.2, Paris.

Engladenc 1981. *Méthode d'étude et de recherches de l'eau souterraine des roches cristallines*. Atlas de photo interprétation T.3, Paris.

Gèze B. 1941. Sur les massifs volcaniques du Cameroun Occidental. *Compte Rendu Académie des Sciences*; Paris, No. 212, pp.498-500.

Gèze B. 1943. *Géographie physique et géologie du Cameroun occidental. Contribution à l'étude pétrographique du Cameroun Occidental.* Edition du Muséum, Paris. (Mémoire du Muséum d'Histoire Naturelle, 17.)

Horaud, R. et Monga, O. 1993. *Vision par ordinateur. Outils fondamentaux*. Hermès, Paris.

Launay (De), L. 1899. *Recherche, captage et aménagement des sources thermominérales*. Paris, Librairie Polytechnique Baudry.

Maréchal (Le), A. 1971. *Les sources thermominérales du Cameroun*. Yaoundé, ORSTOM.

Maréchal (Le), A.1976. *Géologie et géochimie des sources thermominérales du Cameroun*. Paris. (Travaux et Documents de l'ORSTOM, 69).

Moreau, C.; Regnoult, J-M.; Deruelle, B. et Robineau B.1987. A new tectonic model for the Cameroon line Central Africa. *Tectonophysics*, 139, pp. 317-334.

Tchindjang, M. 1996. *Le Bamiléké central et ses bordures. Etude géomorphologique*. PhD thesis, University of Paris VII, France.

Land Use / Land Cover Mapping of the Kuils-Eerste River Catchment (Western Cape) Through an Integrated Approach Using Remote Sensing and GIS

Abraham Thomas[(1)] and James Ayuk[(1)]

[(1)] Department of Earth Sciences, University of the Western Cape, Bellville 7535, P.Bag X17, Cape Town, South Africa; athomas1965@gmail.com;jaayuk@gmail.com

Abstract Two rivers of the Cape region, the Kuils and the Eerste, flow through urban and agricultural areas and apparently their waters are perceived to be polluted through point source and non-point source (NPS) pollution. In order to assess the NPS pollution in the Kuils-Eerste River catchment, a detailed landuse/land cover map was prepared through an integrated approach using Remote Sensing and GIS techniques. The approach involved: formulation of a landuse/land cover classification scheme, extraction of landuse information from ancillary data including aerial photos, use of knowledge of the area, orthorectification, classification of SPOT5 and Landsat images employing both supervised and unsupervised methods, post-processing of the classification results (classes merging and speckle removal), visual interpretation and manual digitisation of certain features that could not be classified, raster conversion and merging of all layers within a GIS resulting in a final raster grid (10m cell size) having 36 classes. The final map reflected the complex land cover character of the catchment ranging from urban, suburban settlements, industry and commerce in the western portion, large agricultural fields (vineyards) in the central part, to mainly tree plantations, naturally vegetated areas and some urban areas (Stellenbosch) in the eastern part of the catchment.

1. INTRODUCTION

The Kuils and Eerste River catchments, located in the Cape region of the Western Cape Province of South Africa, jointly cover an estimated surface area of over 650 square kilometres (Petersen, 2002 and Taylor, 2000). This catchment is a very complex one in terms of the diversity in surface characteristics (land use activities). This catchment is mostly urban in character and harbours various activities such as business, administrative, industrial and agricultural activities. The two major rivers, the Kuils and the Eerste, flow through urban areas and are therefore influenced in their quality by urban activities. For an assessment of the extent of the influence of these urban activities on the water quality of these rivers, a thorough determination of the surface characteristics or land use activities of the catchment has to be made. One of the products which could duly express the surface character of the catchment is the land use/land cover of the catchment. This paper summarises in brief the main procedures that were followed during the process of creating a detailed land use / land cover map for the Kuils-Eerste River catchment.

2. METHODOLOGY AND RESULTS OBTAINED

The procedure that was used in this study for extracting land use/land cover information was generally based on a methodology/approach that was introduced by Thomas (2001) for Birmingham, UK. The approach was an integrated land use/land cover mapping procedure, based on a specially formulated land use/land cover classification scheme, during which thematic map layers that built up the final map were obtained through digital image classification of acquired remotely sensed digital images, visual interpretation and manual on-screen digitisation supported by local knowledge of the area and use of other data that was readily available in GIS format and further GIS analysis and data conversion. This approach also involved multiple image processing algorithms provided by different software packages to obtain the best results. The following

sections will explain in greater details how the above approaches were implemented for the Kuils-Eerste River catchment.

2.1 Spatial Data Acquisition and Evaluation

In the beginning of the project, a digital copy of a generalized land use map was procured from the City of Cape Town but this map was found to be inappropriate for the use of the project mainly for two reasons. Firstly, the data covered just a portion of the catchment, i.e. the section that basically fell under the administrative jurisdiction of the Cape Town Metropolis; the Stellenbosch municipality area was left out. And secondly, the nature of the map was not appropriate for the purpose of assessing pollutant fluxes emanating from the diverse activities in the catchment. It was found that an improved and more detailed land use/ land cover map is needed for assessing non point source pollution. In the face of the above difficulty, an alternative approach was to produce a detailed land use/land cover map for the catchment through an integrated approach that would suit the purpose of pollutant flux modelling. For this purpose, it was decided to formulate a detailed land use/land cover classification scheme that can help in delineating potential areas of non-point source pollution through runoff processes and use existing spatial data, satellite images and aerial photographs and extract land use features from them using various approaches. Some spatial data sets such as roads, railways etc were obtained from the City of Cape Town and Provincial Government and they were found to be suitable for use in the land use map preparation. Satellite imagery is acquired from remote sensing satellites that retrieve imagery from digital data captured from platforms hundreds of kilometres above the Earth. These images have the advantage of covering an extensive surface area at a time or wide surface aerial coverage. They are also periodic, meaning the same surface could be captured several times during a year. The principle behind these images is that land cover characteristics are recorded as spectral reflectance values in the image.

Digital images consist of an array of discrete picture elements (pixels) or grid cells, which are ordered in rows and columns. Each pixel has a digital number (DN) that represents the intensity of the received signal reflected or emitted by a given area of the Earth's surface. The size of the area belonging to a pixel is called the spatial resolution. The image also consists of spectral bands or layers created by the sensor and that collect energy in specific wavelengths of the electromagnetic spectrum. Therefore, variations in these reflection values will reflect variations on the local surface.

Two sets of multispectral satellite imagery were used during the process of production of a land cover/land use map for the catchment: Landsat-ETM imagery (2002 summer scene) and SPOT 5 imagery (2005 summer scene). Landsat imagery is acquired by the US (NASA) Satellite Remote Sensing programme. Landsat ETM (Landsat Enhanced Thematic Mapper) imagery acquired by Landsat 7 sensors has a spatial resolution of 30 metres in all its seven bands. SPOT imagery is provided by the SPOT (Satellite Pour l'Observation de la Terre or Earth Observing Satellites) programme set by France, Belgium and Sweden. SPOT incorporates a high resolution imaging instrument. SPOT 5 imagery has a very high resolution of 10 m in all 4 spectral bands in the visible and near infra-red ranges.

2.2 Digital Image Processing of Satellite Imagery

Digital image processing involves various steps; the major steps used in this project are the following: image rectification, image enhancement, image classification and post processing of classified images. Both Landsat and SPOT imagery were subjected to certain image processing techniques (rectification, projection changes, clipping and classification techniques) within different remote sensing software such as PCI Geomatica, ILWIS, ENVI and ArcView Image Analysis.

2.2.1 Digital Image Rectification/Orthorectification

Most of the time, when digital images are procured, they do not possess the relationship between the rows/columns and the real world coordinates (UTM, geographical coordinates, or any other reference map projection). In order to use these images within a GIS along with other spatial data sets, it is necessary to correct and adapt them geometrically so that they have comparable resolutions and projections as other data sets. It becomes therefore essential for the image to be converted from the pixel coordinate system to a map coordinate system or another pixel coordinate system in a process known as rectification. This is easily done by correcting the pixel geometry of the image with that of an existing map of the same coverage. In image rectification, a number of control points can be used to transform the image from a pixel coordinate system to a map coordinate system. Orthorectification using an elevation layer (Digital Elevation Model or DEM) to account for the height difference of surface objects gives better rectified images which do not possess any geometric distortion. The orthorectification of the SPOT image was performed using PCI Geomatica OrthoEngine software with the help of digital topographical maps for ground control points' selection and 90 m SRTM DEM data. The road network junctions and large building corners obtained from topographical maps were used as main control points for georeferencing. At various stages during this procedure, care was taken to keep the levels of error in linking control points on the georeferenced image to points on the new image by one or two pixel distance. These levels of error were expressed by the root mean square indices (RMS) of the image processing software. By general procedure it is recommended that the RMS values remain below one for the rectification process to be qualified as accurate. Around 25 well identifiable ground control points were chosen and a final RMS value of 0.6 was obtained while orthorectifying the satellite image covering Cape Town.

2.2.2 Digital Image Enhancement

Image enhancement techniques provide procedures for making a raw image easier to interpret. In other words, these techniques improve the visual impact of the raw remotely sensed data to the human eye. Some image enhancement tools available in ArcView GIS were used to improve the appearance of the image by adjusting contrast and brightness and using various contrast-stretch methods such as standard deviation, histogram equalization, maximum-minimum and density slicing. In addition to this, selection and de-selection of the different combinations of red, green and blue bands of the multi spectral image in the display window using the legend editor tool of image analysis, revealed different visual results or false colour composite (FCC) scenes from the image. Selection of the thermal infra-red band as the 'red band', the near infra-red as the 'green band' and the red band as the 'blue band' in ArcView Image Analysis was found to be the most suitable display option for identifying and discriminating all cultural features, vegetation types, non vegetated areas and all water features.

2.2.3 Classification of Satellite Imagery

Digital image classification is the means through which information on the relationship between land cover and measured reflectance values from an image could be extracted. Two kinds of image classification approaches are available: supervised image classification and unsupervised image classification. Supervised classification is the process of using samples of known identity (training samples) to classify pixels of similar identity/digital number while unsupervised classification is the identification of natural groups, or structures within multi- spectral data by the algorithms available in the remote sensing software. For performing supervised classification, the software is trained on the features or pixels identified earlier to look for similar pixels throughout the image during the classification procedure. These training sets are clusters of homogenous pixels that designate a particular feature on the ground. Therefore, identification of similar pixels in the image automatically identifies similar existing ground surface features. A prior knowledge of the area of interest is, however, vital. Knowledge of the catchment characteristics was acquired through many ground-truthing field trips. For unsupervised classification on the other hand, there is no need to

identify training sites of the area under study. The operator is allowed to specify a number of categories desired and the software classifies the image data into a number of groups of similar pixels corresponding to the number of categories stated earlier. Both the supervised and the unsupervised methods of digital image classification have advantages and disadvantages over each other. For this project, it was decided initially to use the supervised image classification technique.

As it was planned in the beginning to use the supervised approach in image classification, a set of training sites were selected following the land use classification scheme that was generated earlier as a guide to identify the class level from which these land use features would be selected. The classification of both Landsat and SPOT imagery using supervised approaches (classifier algorithms) in ENVI and ILWIS software was later found to be inappropriate or inaccurate after a few trials of classification on the image. A couple of classified features were inappropriate to use because of their appearance in certain regions where they were not supposed to be. For instance, it was discovered that, most of the high density residential areas appeared as water features on the map or some residential areas appeared on the mountainous regions because of their similar spectral reflectance values; some agricultural crop plots could not be differentiated clearly.

To solve this problem of insufficient spectral differentiation of the image, a more integrated approach of image classification was used. This approach involved the use of both supervised and unsupervised methods to select individual thematic layers or single land use features, and then adds these to other correct existing land use classes rightly detected by the previous classification attempts and by manual digitisation.

As such, using the Categorize menu/method in ArcView Image analysis extension, a categorisation of the pixel values in different satellite bands was carried out which resulted in a single thematic grid data layer having specified a number of land use classes. The categorisation process in ArcView Image Analysis extension employs an unsupervised approach using the Iterative Self-Organizing Data Analysis (ISODATA) technique (ESRI, 1998).

The supervised approach was later used to correct all the errors that occurred in terms of inappropriate display or assigning of spectral values to certain thematic layers. Such problematic layers were selected using the 'Find Like Areas' algorithms in ArcView's Image Analysis extension which is a parallelepiped classifier. During this method, a Seed tool is used to create a polygon-like graphic which identifies areas with similar characteristics in the image. The 'Find Like Areas' command is later applied on the imagery by which all pixels having similar DN values/ranges were identified from the whole imagery based on the values or ranges identified under the newly created polygon graphic, regardless of where they are located in the image.

The above techniques were applied on both a Landsat ETM (2003) and SPOT5 (2005) image. By using visual inspection and comparing the results with available ground truth data, errors were revealed in the classified image obtained from the Landsat image. The classified layer derived from the SPOT5 image was later preferred to the Landsat image because it had better resolution (10m) and was also a more recent image that would better reflect current land cover/land use trends in the catchment.

2.3 Post Processing of the Classified Image

All the thematic layers accumulated by means of unsupervised and supervised classification algorithms were saved in tiff file format and then converted into grid file format for a final merge with other previously extracted map features. All the classified layers and the other subsequently identified thematic layers in grid forms were merged into one land use/land cover grid map.

After applying the classification algorithms to the satellite images, it was found that pixels from the same ground surface feature were classified as different features. These have been termed as problematic pixels/layers and such pixels/layers were eliminated by simply regrouping the problematic pixels through a merging-routine. Problematic layers which could not be properly distinguished during the classification processes were merged to adjacent pixels within the same surface feature. This procedure was done using the 'merge' request and 'Con' request in the Map Calculator interface of ArcView Spatial Analyst extension. In doing this, individual grid codes were assigned to each layer and these codes noted, as the codes later formed the basis through which these layers would be identified after the merging. The Avenue syntax for the Con request is expressed in the ESRI online help menu as follows:

aGrid.Con (yesGrid, noGrid)

For a cell in a grid, this request returns the value found in yesGrid if aGrid is non-zero (TRUE), otherwise it returns the value found in noGrid. For instance the layers with a grid cell value of 6 in them (data layer 6 'commercial and industrial units' in the classified image) were merged into cells having a value of 2 as follows:

([landuse12cls]=6).Con(2.AsGrid, ([Landuse12cls])

The classified output had island pixels referred to as speckle that did not fall into the bigger class surrounding them. The appearance of island (speckle) cells can be minimized through the majority filtering technique using GIS or remote sensing software. After eliminating all problematic spectral regions and layers, a Majority Filter request was applied on the merged grid map for minimising the speckled appearance of the data through the elimination of island pixels. At the end of this process a total of 23 land use grid classes were generated. The *Reclass* command in ArcView Spatial Analyst extension was used to reclassify the resulting land use grid map into a new land use grid with a corresponding number of grid layers that would have all these cell values in sequence. The various thematic layers were later identified, labelled or assigned land class names using information obtained from ground truthing, and other reference spatial data documents like topographical maps, aerial photographs and the Cape Town and Peninsular Street Guide document.

2.4 Extraction of Other Features to Complete Land Use Map

Image classification alone could not be used to successfully identify all the features that constitute the catchment area. Some of the linear features (minor roads, railway line, etc. 6-8 m wide) were too narrow to be grouped because of the image's spatial resolution and polygon features like industry and residential settlements, etc, could not be differentiated due to their very diverse spectral characteristics.

The linear features like the roads, railways and rivers were obtained in ESRI shapefile format from the City Council. These line features were all converted into polygon features using the buffering technique in ArcView. Different buffering distances were identified by measuring the road widths of different road types that exist in the study area. Similarly a unique buffer distance of 10 m was chosen for buffering railway lines and major river channels. The polygon width that was attained had a minimum width of 10 m to enable the final grid to have a grid cell size of 10 m. All these buffered polygons were converted into grid layers by choosing a grid cell of 10 m and assigning appropriate cell values for each layer using the reclassify command.

The different residential areas, industrial areas, commercial areas (institutional or mercantile) and most recreation areas that were identified in the image through visual interpretation were individually digitized by drawing polygons that define their boundaries. This was done using the Draw tool in ArcView. The resulting

polygon features were saved as shapefiles in ArcView and were converted later into raster grid files. Water bodies were identified by doing a 'Find Like Areas' command on the SPOT2005 NDVI image of the area (ESRI, 1998). Using the NDVI vegetation index algorithms, water bodies could clearly be picked up from the satellite image. This was saved as a shapefile layer; water body polygons and other polygons generated were edited in order to remove unwanted polygons and later converted into a grid layer in ArcView.

2.5 Final Merging of All Layers

In the end a total of thirty-six (36) land use and land cover types/features were generated after applying classification (supervised and unsupervised), manual on-screen digitisation and processing of shapefile data acquired from other sources. This formed the final database from which the final land use map for the area could be generated. But since this land use database was in different formats and compiled from different sources at varying scales, a rigorous data integration effort was necessary to improve data consistency and quality. The land use class layers obtained from the SPOT satellite image were in UTM Zone 34 South projection and other vector layers obtained from other data analysis and data sources (e.g., City of Cape Town) were in a different projection (WGS 1984 Zone 19 and 21). Therefore before the final merging, the grids obtained from other means (digitisation from aerial photographs and buffered polyline vector layers) were re-projected to the projection of the satellite image. Each re-projected grid layer was merged with the grid layer generated from the satellite image using the merge command or Con request of ArcView Spatial Analyst extension. Finally, the grid cell values were given appropriate attribute descriptions in text form (as seen in Figure 1). The final land use grid having 36 land use/land cover classes (Figures 1 and 2) was finally achieved.

The area statistics of each land use/land cover unit is illustrated in Table 1. From the table it is evident that vineyards constitute over 35 % of the total area followed by Fynbos (indigenous vegetation) (12.48%), open hard rock area (5.83%), riparian forest (5.21%), mountain forest (4.98%), scrubland (4.38%) and improved grassland (3.61%). The residential area is around 14% only. Roads contribute 3.36% of the total area.

2.6 Final Map Accuracy

The preparation of the Kuils-Eerste River land use/land cover map involved the use of remote sensing and GIS techniques which, in turn, involved the use of multiple sources of digital data and other ancillary data sources supported by local knowledge of the area. The quality and accuracy of the output map will therefore be dependent on the quality and accuracy of the input data. However, care was taken to select the most accurate input data available. All the sources that were consulted for these data sets are accredited data distributors who perform high levels of data pre-processing and quality checking before public distribution. However, data layers that were deemed not suitable for use were duly eliminated, or in certain cases further improved.

The processing of data for the production of the detailed land use/land cover map for the Kuils-Eerste river area started in the year 2006 and great effort was made to acquire the most recent imagery at very good spatial and spectral resolutions. A 10m resolution multispectral image acquired by the SPOT 5 satellite in November 2005 was the closest in time that could be procured. The latest products of topographical map sheets of 1:50,000 scales (large scale map) were employed during ground truthing. Equally, Garmap digital maps (that are integrated in GPS devices) were used in the ground truthing process, and in the evaluation of the final land use/land cover map. A general check of the output and available ground truthing data showed a perfect overlap confirming the decisions to group different land use/land cover units and the maximum accuracy during manual digitisation. A few field trips were conducted to identify training sites and the ground truth data collected were compared with the image classification results.

A map accuracy check was performed using 98 randomly selected sampling points and identifying the ground truth information for the sample points, which were later displayed in ArcMap as an event layer. An error matrix was created using the ground truth information collected and map data information obtained from the table. The overall map accuracy (or total map accuracy) was calculated and an overall accuracy of 91% was obtained for the whole map from this exercise. The Kappa value (coefficient of agreement) for the final map as a whole was also calculated which came to 0.89683 (which means that the total map accuracy is 89.68 %).

Procedure of Map Accuracy Estimation: The accuracy estimation was performed using 200 randomly sampled points generated in an Excel spreadsheet using the Analysis ToolPak extension. Minimum and maximum values of x and y coordinates of the land use map were identified using ArcMap and using these values as a range, random data points for 200 locations were generated (because there were thirty six land use classes it was hoped that each class would have at least one accuracy check point) and displayed in ArcMap as an event layer (by adding the table as XY data). It was noticed that only 98 samples fell within the catchment boundary and 24 land use/land cover types were represented from the 98 locations identified. The event layer of sample points falling inside the catchment was exported as a shapefile and an additional field (value) created with a value of one given to all data points of the accuracy check. The ground truth information for the selected sample points were identified through field visits conducted for the accuracy check and previous ground-truthing. The new data point's shapefile, the land use map and the ground truth information were also converted into raster layers/grids. Using the Raster Calculator in Spatial Analyst extension the raster accuracy check point location layer was multiplied by the land use grids and thus two grids of accuracy assessment data were created. The raster data accuracy check points extracted from the land use map was multiplied by a factor of ten and this grid was added to the raster data accuracy check points extracted from the ground truth layer (in raster form). This operation (performed in Raster Calculator) gave a new grid. The values of this grid showed the ground truth information and also the map data class. The attribute table was exported as a dbf file and displayed in Excel. An error matrix was created using the ground truth information and map data information obtained from this table and the overall map accuracy was calculated for the whole map. The overall or total map accuracy was calculated by dividing the total number of correctly classified sample points by the total number of sample points chosen for accuracy estimation.

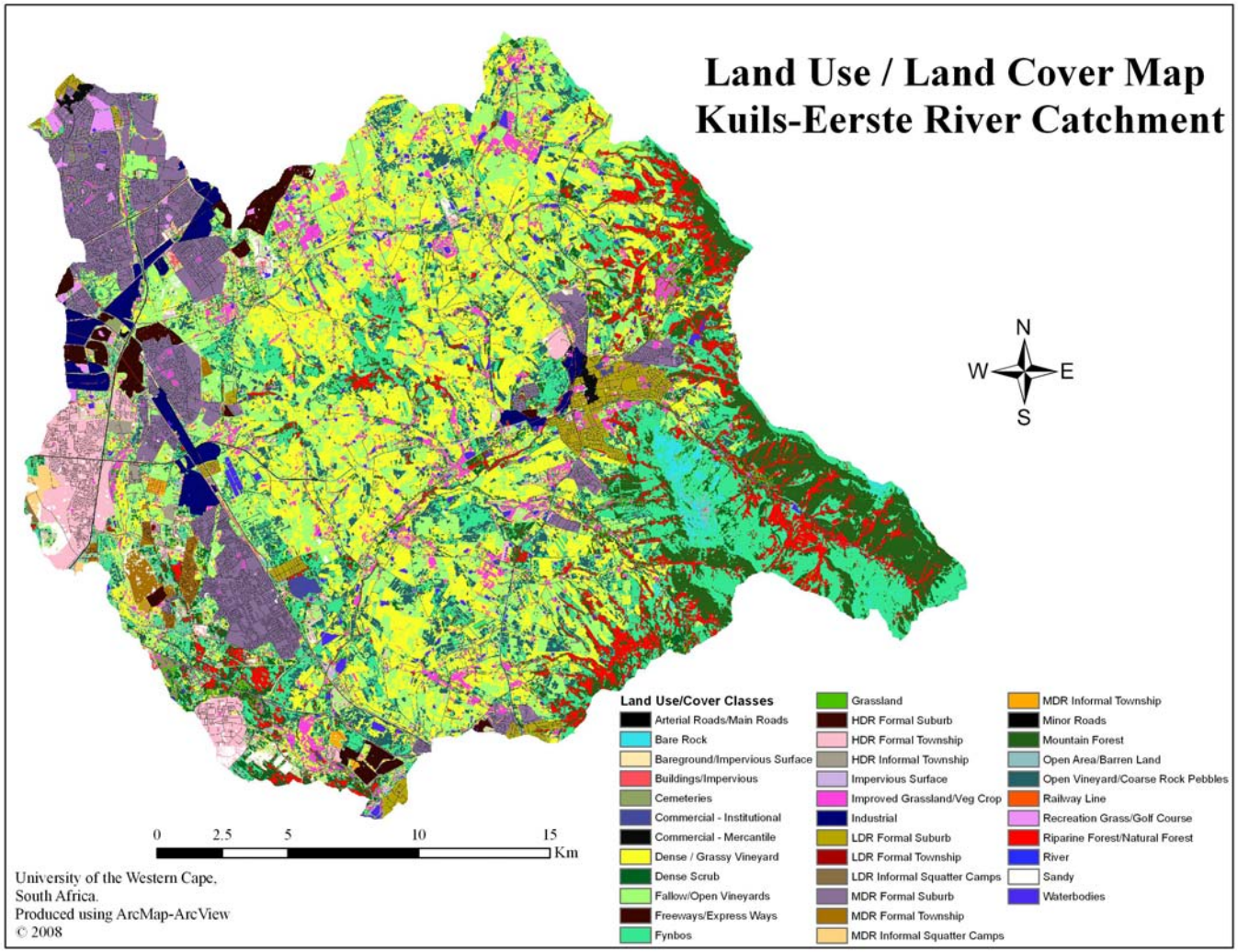

Figure 1 Land Use/Land Cover Map for the Kuils - Eerste River Catchment Area (prepared using an integrated approach).

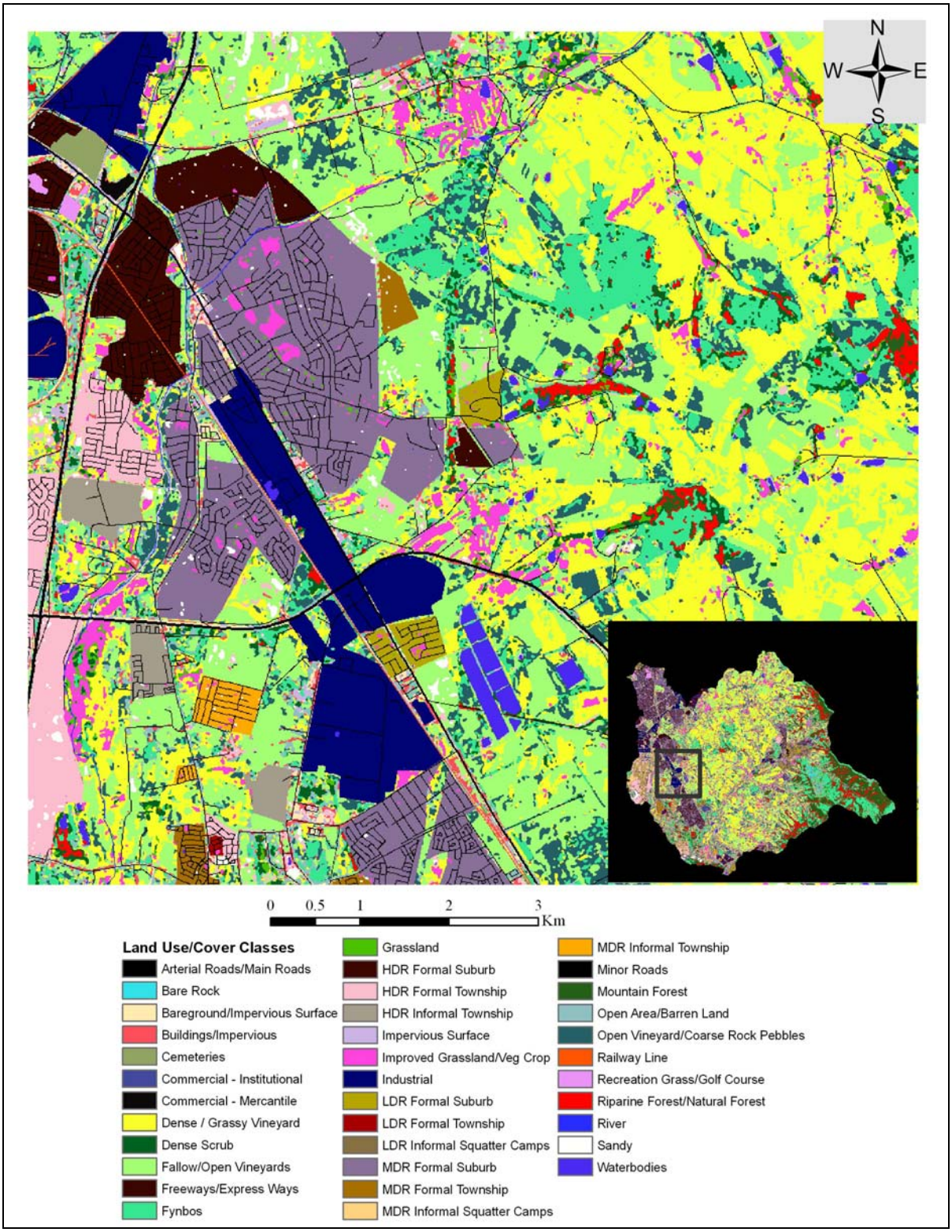

Figure 2 Kuils - Eerste River catchment area at closer view

Table 1 Total area and percentage area of land use/land cover units in the Kuils-Eerste river catchment.

Class No.	Land use type	Cell Counts	Area (m^2)	% Area
1	Mountain Forest	324,131	32,413,100	4.98
2	Riparian Forest/Natural Forest	339,056	33,905,600	5.21
3	Dense Scrub	284,897	28,489,700	4.38
4	Fynbos	812,843	81,284,300	12.48
5	Grassland	115,790	11,579,000	1.78
6	Impervious Surface	41,335	4,133,500	0.63
7	Railway Line	8,649	864,900	0.13
8	Bareground/Impervious Surface	35,773	3,577,300	0.55
9	Bare Rock	36,133	3,613,300	0.55
10	Open Vineyard/Coarse Rock Pebbles	379,872	37,987,200	5.83
11	Open Area/Barren Land	116,675	11,667,500	1.79
12	Improved Grassland/Vegetable	234,823	23,482,300	3.61
13	Buildings/Impervious	49,299	4,929,900	0.76
14	Dense/Grassy Vineyard	1,329,204	132,920,400	20.42
15	Fallow/Open Vineyard	937,630	93,763,000	14.40
16	Recreation Grass/Golf Course	23,781	2,378,100	0.37
17	Freeways/Express Ways	5,206	520,600	0.08
18	Arterial Road/Main Road	23,538	2,353,800	0.36
19	Minor Roads	189,969	18,996,900	2.92
20	Sandy	59,206	5,920,600	0.91
21	Waterbodies	73,820	7,382,000	1.13
22	HDR* Formal Suburb	94,178	9,417,800	1.45
23	MDR* Formal Suburb	455,611	45,561,100	7.00
24	LDR* Formal Suburb	93,700	9,370,000	1.44
25	HDR Formal Township	217,399	21,739,900	3.34
26	MDR Formal Township	34,738	3,473,800	0.53
27	LDR Formal Township	236	23,600	0.00
28	HDR Informal Township	9,861	986,100	0.15
29	MDR Informal Township	6,701	670,100	0.10
30	MDR Informal Squatter Camps	14,990	1,499,000	0.23
31	LDR Informal Squatter Camps	4,280	428,000	0.07
32	Commercial- Mercantile	12,426	1,242,600	0.19
33	Commercial- Institutional	14,365	1,436,500	0.22
34	Industrial	115,054	11,505,400	1.77
35	Cemeteries	2,091	209,100	0.03
36	Rivers	13,572	1,357,200	0.21
	Total	**6,510,832**	**651,083,200**	**100**

* HDR=High Density Residential; MDR=Medium Density Residential; LDR=Low Density Residential

3. CONCLUSION

A detailed land use/ land cover map containing 36 classes that could be used for assessing non-point source pollution could be generated through an integrated approach involving the use of remotely sensed data and further GIS analysis. The final land use/land cover map that was generated reflected the very complex land cover character of the catchment. It extends from urban and suburban settlement plus industrial and commercial activities in the west through extensive open agricultural fields, mainly vineyards in the central parts of the catchment, to mainly forest tree plantation and naturally vegetated areas in the eastern section of the catchment. The relief is generally flat in the western part of the catchment changing to gently undulating hills around the centre to extremely rugged relief with very high mountain ranges in the eastern part. One should take into consideration that, due to both human errors and computer software limitations, there would certainly be some misjudgements in the assigning of certain identities to certain land classes.

4. ACKNOWLEDGEMENTS

The authors would like to thank the Storm Water Division and the Geomatics Division of the City of Cape Town for providing various spatial data such as aerial photographs, Landsat ETM image, vector data layers etc, the GIS division of the Western Cape Provincial Government for providing land use information and other data layers, and the Satellite Application Centre of the Council for Scientific and Industrial Research for providing SPOT 5 satellite imagery. We would like to acknowledge with gratitude the help provided by Mr Brian Lawrence, Mr Peter Meyer and Mr MacFaden Kotelo during the field visits for ground truthing.

5. REFERENCES

ESRI, 1998. ArcView Image Analysis on-line help. ERDAS, Inc.

Petersen, C. 2002. *Rapid Geomorphological Change in an urban Estuary: a case study of the Eerste River, Cape Town, South Africa.* Master's Thesis, University of the Western Cape, South Africa.

Taylor, V. 2000. A study of the Influence of the Kuils-Eerste Rivers on the people of Zandvlei and Environment. *Rocknews 2000*. A publication of the Geological Society, University of the Western Cape, Bellville, Cape Town.

Thomas, A., 2001. *A Geographic Information System Methodology For Modelling Urban Groundwater Recharge And Pollution.* Ph D Thesis. University of Birmingham, United Kingdom.

A Method for an Integrated, Object-oriented Land Cover Classification of Medium-resolution Satellite Imagery: a Case Study of the Kafue River Basin (Zambia)

G. D'Hulst [(1)], G. Govers [(2)], M. Gregor [(3)], I. A. Nyambe [(4)]

[(1)] GIM-Geographic Information Management nv/sa, Researchpark Haasrode, Interleuvenlaan 5, B-3001 Heverlee, Belgium, gregory.dhulst@gim.be
[(2)] Physical and Regional Geography Research Group, K.U.Leuven, Geo-Institute, Celestijnenlaan 200 E, B-3001 Heverlee, Belgium, gerard.govers@ees.kuleuven.be
[(3)] GIM-Geographic Information Management sa, 3, rue Jean Pierre Sauvage, L-2514 Luxembourg, mirko.gregor@gim.lu
[(4)] University of Zambia, P.O. Box 32379 Lusaka, 10101 Zambia, inyambe@gmail.com

Information about Land Cover (LC) is needed by managers of public and private lands, urban planners, agricultural experts and scientists for studying such issues as urban expansion, climate change and many others. In this paper an automated, object-oriented image analysis approach for obtaining accurate LC-maps at a regional scale from remotely sensed satellite data is detailed. Simultaneously the potential of the combination of optical data with radar and ancillary GIS-data is investigated.
The study area is focused on the Kafue River Basin, located in Central Zambia. The Kafue River is one of the major tributaries of the Zambezi River. A multi-spectral image of November 2003 from the MERIS-sensor at 320-m resolution is used together with an ASAR Wide Swath time series of the 2003-2004 growing season at 75-m pixel spacing. Also other supportive hydrological information is generated and integrated in the developed rule-sets to facilitate the classification.
An overall accuracy of 85.1% and a kappa statistic of 79.6% of the generated LC-map were achieved. Comparisons with existing small-scale LC products over the region show a clear improvement of accuracy and prove the added value of this innovative multi-source approach.

1. INTRODUCTION

A nation must have adequate information on many complex interrelated aspects of its activities in order to make decisions. Land Use (LU) is only one such aspect, but knowledge about LU and land cover (LC) has become increasingly important as a nation plans to overcome the problems of haphazard, uncontrolled development, deteriorating environmental quality, loss of prime agricultural lands, destruction of important wetlands, and loss of fish and wildlife habitat. LU data are needed in the analysis of environmental processes and problems that must be understood if living conditions and standards are to be improved or maintained at current levels (Anderson et al., 1976).
One of the prime prerequisites for better use of land is information on existing LU patterns and changes in LC through time. The knowledge of the present distribution and area of such forested, agricultural, and urban lands, as well as information on their changing proportions, is needed by legislators, planners and governmental officials to determine better land use policy, to project transportation and utility demand, to identify future development pressure points and to implement effective plans for regional development. As Clawson and Stewart (1965) have stated: "In this dynamic situation, accurate, meaningful, current data on land use are essential". If public agencies and private organisations are to know what is happening, and are to make sound plans for their own future action, then reliable information is critical. Remote sensing data are attractive for deriving LC cartography by means of digital image classification because updated information for continuous time periods and over extensive geographical regions can only be derived from satellite systems.

In this study a method is presented to obtain land use/land cover (LULC) information on a regional scale. The capabilities of a multi-scale, multi-sensor object-oriented image analysis are investigated. Until now, regional small-scale mapping was mostly derived using a pixel-based approach (Mayaux et al., 2004; Tucker et al., 2004). This technique only takes into account the spectral information contained in a single pixel. The great spectral variation of the LULC classes, however, can result in many errors of commission and omission. Much information is contained in the relationship between adjacent pixels (contextual information), including texture and shape information, which allows for identification of individual objects as opposed to single pixels (Thomas et al., 2003). Such an object-oriented approach allows the user to apply locally different strategies for analysis. Incorporating both spectral information (tone, colour) as well as spatial arrangements (size, shape, texture, pattern, association with neighbouring objects) comes closer to the way humans interpret visual information.

As a first step, the complete image has to be segmented into meaningful objects. The next step is to define a set of knowledge-based classification rules to describe each target class. Those rules can contain spectral, spatial, contextual and textural information. Also arbitrary data like existing GIS-vector layers, additional raster images or digital elevation models can be integrated and used as supportive a priori information in the classification process. The final step is to assign each object to the class that fulfils the rules best (Leukert et al., 2004). The software Definiens is used for this task.

This relatively new object-oriented classification approach is, so far, mostly applied to (very) high-resolution imagery (Laliberte et al., 2004; Mitri et al., 2006). Few attempts have been made to apply this technique on medium-resolution imagery. Some studies however have shown promising results (Santos et al., 2006; Yan et al., 2006).

Our objective was to classify a MERIS Full Resolution (FR) image over the Kafue River Basin (Zambia) with the aid of a time series of ASAR Wide Swath (WS) radar images and other existing thematical layers. A second objective was to compare our classification result by means of a sound validation procedure with other existing LULC-products over the regions, which have been derived with a traditional pixel-based approach. Meris FR and ASAR WS were ordered at a 1B processing level to familiarize ourselves with all the different pre-processing steps and to avoid error propagation caused by inherent errors.

2. MATERIALS AND METHODS

2.1 Study area

The study area is located in the Kafue River Basin in Zambia, being a sub-catchment of the Zambezi River Basin and covering an area of approximately 152,000 km² (Fig. 1). The Kafue River has a length of about 1,000 km and discharges on average 10 billion m³/ year into the Zambezi (mean flow rate of about 320 m³/s through its lower half) (Ellenbroek, 1987).

Much of Zambia enjoys a subtropical climate, which is characterized by two seasons (Fig. 2):

1. The cool and hot dry season from May to October. During this season rainfall is absolutely absent. Mean temperatures vary from 16 °C to 21 °C. This season is split into a ‘dry cool period’ from May to July, called midwinter season, that exhibits low temperatures averaging up to 16 °C and a ‘dry hot period’ with a mean temperature of 24 °C.
2. The wet season between November and April is characterized by high amounts of rainfall. December and January/February are the wettest months with 200-250 mm of rainfall in Lusaka. The mean temperature during this season is around 21 °C.

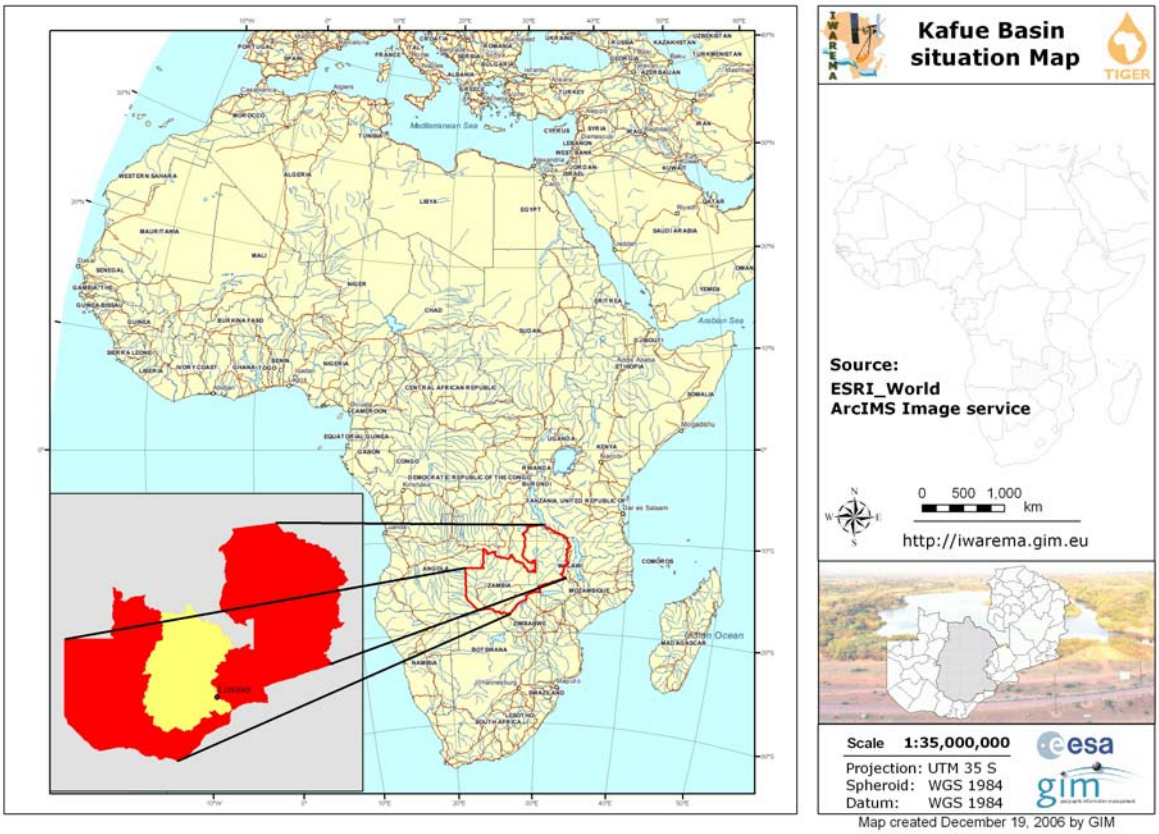

Figure 1 Situation map of the Kafue River Basin (Zambia)

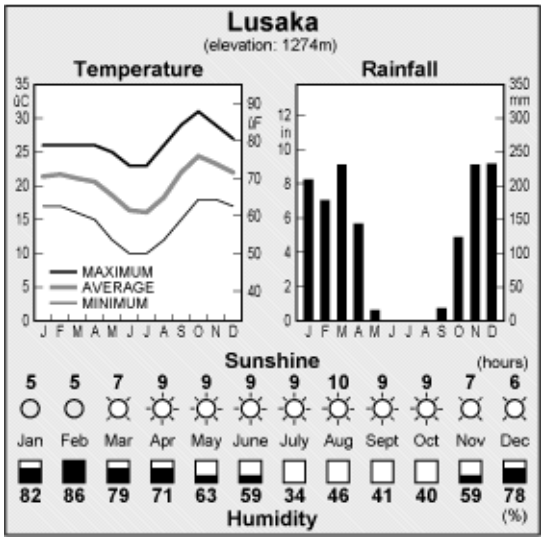

Figure 2 Climatic data of Lusaka (Ellenbroek, 1987).

2.2 Data

2.2.1 MERIS

MERIS is a sensor on board of ESA's ENVISAT environmental satellite, which was launched in March 2002. MERIS is a programmable, MEdium-spectral Resolution, Imaging Spectrometer operating in the solar reflective spectral range. Fifteen spectral bands can be selected by ground command, each of which has a

programmable width and a programmable location in the 390 nm to 1040 nm spectral range. The instrument scans the Earth's surface by the so-called "push-broom" method. Linear CCD arrays provide spatial sampling in the across-track direction, while the satellite's motion provides scanning in the along-track direction. MERIS is designed so that it can acquire data over the Earth whenever illumination conditions are suitable. The instrument's 68.5° field of view around nadir covers a swath width of 1150 km. This wide field of view is shared between five identical optical modules arranged in a fan-shaped configuration (Verstraete et al., 1999).

MERIS products are available in Full Resolution (FR) at 300 m and simultaneously and independently in another data stream in Reduced Resolution (RR) at 1.2 km. A Low-Resolution (LR) atmospheric product for Fast Delivery has also been defined.

One level 1b FR product (575 km × 575 km) was ordered using ESA's EOLI-SA 4.2.8 online catalogue (http://eoli.esa.int/geteolisa/index. html). The image was selected based on the quality and cloud coverage of all available MERIS-scenes over the study area. The selected scene is acquired at 11 November 2003 and covers the whole AOI (so mosaicking could be avoided). Level 1b comprises annotated engineering data, which have been calibrated and contain geolocation data. The data are resampled onto an equal-area MERIS product grid so that each product pixel is of the same size across the swath. The MERIS Level 1b product is Top-Of-the-Atmosphere (TOA) calibrated radiance measured in $mWm^{-2}sr^{-1}nm^{-1}$. The product contains fifteen bands (Tab. 1).

Table 1 Spectral Bands of MERIS.

MERIS FR								
Band	nm		Band	nm		Band	nm	
1	412.5	Blue	6	620	Red	10	753.75	NIR
2	442.5		7	665		11	760,625	
3	490		8	681.25		12	778.75	
4	510	Green	9	708.75		13	865	
5	560					14	885	
						15	900	

While the MERIS sensor measures reflected sun radiation with the help of CCD technique, all spectral measurements are made by individual sets of sensors (of the CCD) for each pixel along an image line. This causes small variations of the spectral wavelength of each pixel along the image line and is known as “smile effect”. For the MERIS instrument, the variations per pixel are in order of 1 nm between adjacent cameras, while they are in order of 0.1 nm within one camera. To avoid disturbances in further processing steps, the image was corrected for this smile effect with ESA’s Level 2 smile correction algorithm as it is implemented in BEAM 3.6 software (www.brockmann-consult.de/). After performing this pre-processing step we obtained MERIS data with normalized wavelengths within one spectral band with respect to the relevant reference wavelengths. All future analyses were performed with these smile-corrected data.

MERIS data are, as all remote sensing data in the optical range of the EMS, affected by atmospheric influences and the variable solar irradiance. To enable to process the image, it’s necessary to convert the sensors Top of Atmosphere (TOA) radiance values into surface reflectance values (SR). For this atmospheric correction we used the SMAC algorithm which is implemented into the BEAM 3.6 software.

SMAC is a Simplified Method for Atmospheric Corrections of satellite measurements (Rahman and Dedieu, 1994). It is a semi-empirical approximation of the radiative transfer in the atmosphere. The signal at the satellite is written as the sum of the following components, which are then expressed in simple analytical terms:

- Two way gaseous transmission
- Atmospheric spherical albedo
- Total atmospheric transmission

- Rayleigh scattering
- Aerosol scattering

The SMAC requires as input, in addition to the measured top of atmosphere radiance, the surface pressure, the ozone content, the water vapour content and, most importantly, the aerosols. The European Centre for Medium-range Weather Forecasts (ECMWF) data that came as metadata with the Meris-scene were used as parameters for the SMAC-algorithm. The aerosol correction requires the selection of an aerosol model and the aerosol optical depth at 550 nm. Pixels that were affected by clouds were avoided during this pre-processing step with the help of the quality flags, which ESA provides within the MERIS Level 1B data.
Fig. 3 shows the spectrum of the same pixel before (left) and after (right) applying the SMAC-algorithm. Notice that the oxygen absorption near 760 nm is fully removed due to this correction and that eventually we get a typical spectral signature of a vegetated pixel.

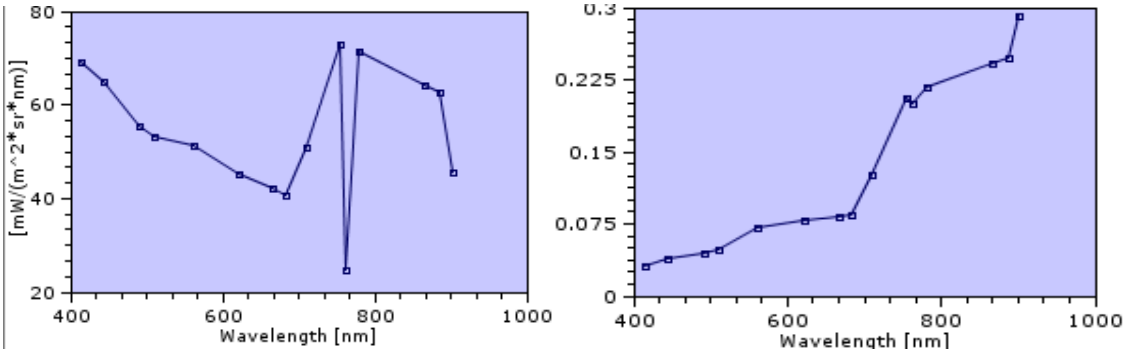

Figure 3 Atmospheric correction using the SMAC-algorithm (left: TOA radiance, right: Surface Reflection (a unitless number, less than one).

According to the MERIS Product Handbook (2006), the MERIS reflectance samples calculated from raw data are relocated to a MERIS Product Grid with a central column oriented along the satellite orbit path projected on the earth surface. Geo-positioning of MERIS samples in the product grid is then accomplished using tie points (every 64 MERIS pixels) derived from the calculated satellite position and arranged so they are evenly spaced along the satellite swath. Using the Map-projection tool in BEAM 3.6 (www.brockmann-consult.de/) the data in the product grid was nearest neighbour resampled from the MERIS raw data by interpolating between these tiepoint positions to the UTM35S projection with the WGS84-datum.
A quick overlay with a geocover ortho mosaic (Dykstra, 2001) showed that the geocoding revealed only suboptimal results. Displacement of several pixels was observed and therefore an enhanced georeferencing was applied. To increase the locational accuracy and to correct for relief displacement of our MERIS-scene an orthorectification was applied in Envi RSI 4.2. The GeoCover Ortho stock mosaic of 2000 was used as reference image and the freely available 3 arc second SRTM-DEM was resampled and used as elevation source (CGIAR-CSI GeoPortal, http://srtm.csi.cgiar.org/).
Twenty-five corresponding points were collected evenly spread all over the scene. Fifteen of them were used as control points and the other ten were used as checkpoints to be able to independently check the accuracy of the calculated transformation parameters. A second order polynomial transformation, using a nearest neighbour resampling technique, was applied which resulted in a sub-pixel locational error (RMSE = 295 m, Fig. 4).
To reduce the dimensionality and the correlation of our 15-band image dataset while retaining those characteristics of the dataset that contribute most to its variance a principal component analysis was applied. Only the first four Principal Components (PC) were selected as they accounted for more than 95% of the variance.

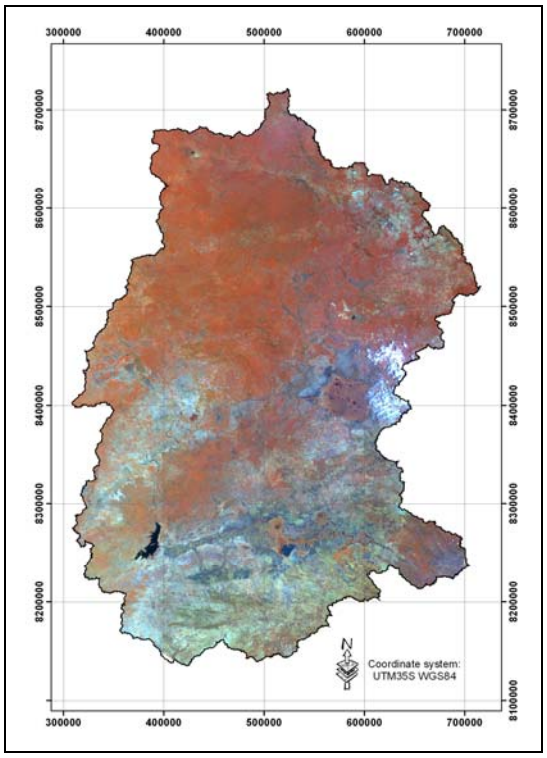

Figure 4 Orthorectified MERIS FR image (RGB: 13-5-1).

2.2.2 ASAR

ESA's ENVISAT satellite also carries the Advanced Synthetic Aperture Radar (ASAR) instrument. According to the ASAR Product Handbook (2006) the ASAR-instrument, operating at C-band (5.331 GHz, ~6 cm), can be regarded as an advanced version of the SAR instruments on board the ERS1 and ERS2 satellites. Its beam elevation steerage allows the selection of different swaths at different incidence angles, providing swath coverage of over 400-km wide using ScanSAR techniques. In alternating polarisation mode, transmitting and receiving polarisation can be selected allowing scenes to be imaged simultaneously in two polarisations.

In the image mode, ASAR operates in one of seven predetermined swaths (100 km swath width) with either vertically or horizontally polarized radiation; the same polarisation is used to transmit and receive (i.e. HH or VV). The ground resolution is about 30 m (three looks), sampled at pixel spacing of 12.5 m. Pixel spacing represents how much area each pixel covers, while pixel resolution indicates the smallest object you could pick out in an image.

In the alternating polarisation mode (in one of seven possible swaths), two images in two polarisation modes (HH & VV, or HH & HV, or VV & VH) are acquired. The ground resolution is about 30 m (1.8 equivalent number of looks), sampled at 12.5-m spacing.

When operating in the ScanSAR mode, a wide swath of > 400 km can be achieved, at a ground resolution of about 150 m (11.5 equivalent number of looks), sampled at 75 m pixel spacing.

Because of the vastness of the study area, wide swath mode ground range amplitude level 1B products were chosen. The products were selected and ordered using the EOLI-SA catalogue (ASA-WSM-1P).

Two acquisition periods were considered during the ordering. One at the end of the dry season (beginning of Growing Season (GS)) of 2003 and another at the end of the rainy season (end of GS) in early 2004. This would enable us to take the time-variability (phenology) of the Zambian landscape into account and would facilitate the classification of our MERIS-scene (acquired at 11-nov-2003).

SARscape 2.3 was used for pre-processing the SAR-images. SARscape is designed as a specialized software package for processing of SAR data, and perfectly complements ENVI's functionality for analysing and visualising remote sensing data of any kind. It is an add-on module for ENVI (also available for ArcView) and is particularly useful for ENVISAT or RADARSAT applications, where dedicated SAR processing is required in combination with data fusion techniques for SAR and optical data.
A first and fundamental step of the processing chain is to import the datasets in a correct way. The measurement datasets and the major processing parameters, including the orbit state vectors are automatically extracted from the ASAR medium resolution images by SARscape.
The imported ASAR WS images were first speckle filtered using the frost filter. This adaptive filter is primarily used to remove high frequency noise while preserving high frequency features (edges). It is an exponentially damped convolution kernel, which adapts itself to features by using local statistics. The adaptive filter computes a set of weight values for each pixel within the filter window surrounding each pixel. The filter dimensions were set to 5.
To transform the data from ground range radar coordinates into the cartographical reference system (UTM35S WGS84), a nominal geocoding operation was applied. A nominal geocoding means that there are no ground control points used during the geocoding but only the nominal parameters (orbit state vectors) which were extracted during the data import step. To achieve a geocoding of sub-pixel accuracy also the corresponding DORIS-files were downloaded from the ESA-website. DORIS or Doppler Orbitography and Radio-positioning Integrated by Satellite instrument is a microwave tracking system on board of the ENVISAT satellite. These files provide highly accurate information, which enhances the geocoding substantially.
When radar data are acquired for the quantitative study of land use and land cover, it is important that data get calibrated, since this allows image brightness values to be more directly related to target backscatter. When, like in our case, radar data are acquired over a number of time periods and under different geometry (ascending and descending) it is essential that data get calibrated. Image calibration for change detection for example, ensures that any changes in the image are the result of a change in the target and not from a change in the sensor.
The radiometric calibration, which is simultaneously carried out during the geocoding in SARscape, is based on the exploitation of the radar equation (e.g. antenna pattern, range-spread loss). Because we had a DEM available, also radiometric distortions related to terrain influences (foreshortening) could be corrected for.
Due to the large incidence angle variability within the ASAR WS-scenes (from ~15° to ~46°), a normalisation is necessary for correcting for these resulting radiometric distortions. A normalisation angle of 8 degrees gave us the most rewarding results (Fig. 5).

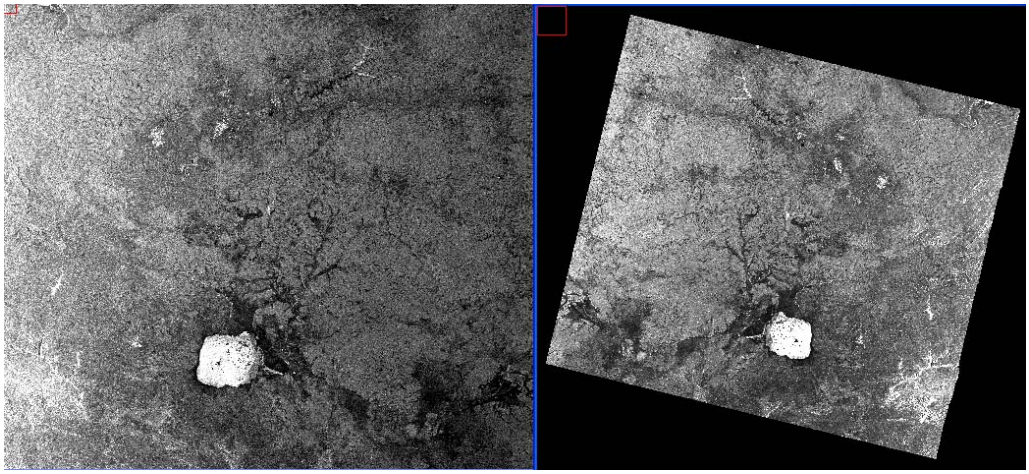

Figure 5 ASAR WS image 01 Oct 2003 – left (raw) image and right (processed image).

In order to obtain an entire coverage of the AOI, the individual pre-processed SAR amplitude images were mosaicked per point in time (start of GS and end of GS). To create a consistent mosaic the frames were seamlessly joined using a gradient mosaicking technique. This method refines the geometry and radiometric calibration by comparing the images to be mosaicked in the overlapping areas
The two available mosaics per point in time were combined into one image using a layer-stacking technique. Band one was assigned to the mosaic of the end of the 2003-2004 GS, band two to the mosaic of the start of the 2003/2004 GS and band three was assigned to the subtraction of both layers (mosaic end of GS2003/2004 – mosaic start of GS2003/2004).

2.2.3 Hydrology data

Supportive data useful for the classification were generated using the hydrology tool within the spatial analyst toolbox of ArcGis 9.0. A stream network and watershed was derived from the hole-filled 3 arc second SRTM-DEM. The workflow for deriving these datasets is illustrated in the flowchart of Fig. 6.

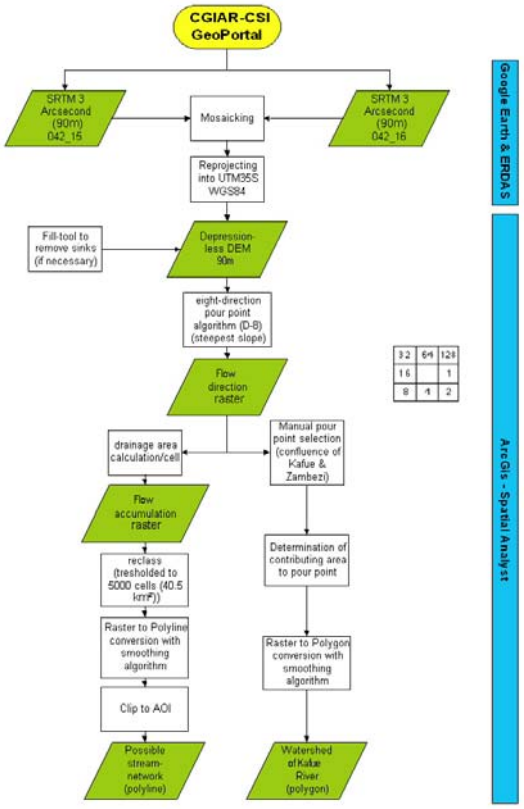

Figure 6 Flowchart for deriving stream network and watershed.

A threshold value of 5,000 pixels (90 m×90 m×5,000 = 40.5 km²) was applied for delineating the final stream network. The confluence of the Kafue and the Zambezi River was selected as the starting point for the calculation of the contributing area which is necessary for deriving the watershed.
In order to overcome the variable pixel-resolutions of our input layers and to avoid errors of omission in the water/wetland class during the classification process, the stream network was buffered using a distance of one kilometre. Due to the coarse resolution of our DEM and the major wetland areas occurring in our study area (Lukanga swamps, Busanga Swamps and Kafue flats -> extremely flat terrain) some streams were far away from the truly observed ones. Some manual editing was applied to resolve these problems

2.3 Analyses

2.3.1 Image segmentation

Segmentation is the first and important phase in the Definiens software and its aim is to create meaningful objects. This means that the shape of each object in question should ideally be represented by an according image object (a pond, a forest…). This shape combined with further derivative colour and texture properties can be used to initially classify the image by classifying the generated image objects. Thereby the classes are organized within a class hierarchy. Each class can have a sub- or super-class and thus inherit its properties from one or more super-classes or to its subclass(es). With respect to the multi-scale behaviour of the objects to detect, a number of small objects can be aggregated to form larger objects constructing a semantic hierarchy. Likewise, a large object can be split into a number of smaller objects which basically leads to two main approaches of image analysis: A top-down and a bottom-up approach (Benz et al., 2003).

In the segmentation phase, following parameters should be assigned as accurate as possible, of course, suiting with the reality (Definiens Professional 5 - User Guide, 2006):

Scale parameter: this parameter indirectly influences the average object size. In fact this parameter determines the maximal allowed heterogeneity of the objects. The scale parameter is the stop criterion for the optimisation process. Prior to the fusion of two adjacent objects, the resulting increase of heterogeneity f is calculated. If this resulting increase exceeds a threshold determined by the scale parameter, $t = \Psi$ (scale parameter), then no further fusion takes place and the segmentation stops. The larger the scale parameter, the more objects can be fused and the larger the objects grow.

Colour/Shape: with these parameters the influence of colour vs. shape homogeneity on the object generation can be adjusted. The higher the shape criterion the less spectral homogeneity influences the object generation.

The increase of heterogeneity f has to be less than a certain threshold (Eq. 1).

$$f = w_{colour}.\Delta h_{colour} + w_{shape}.\Delta h_{shape} \qquad (1)$$

with $w_{colour} \in [0, 1]$, $w_{shape} \in [0, 1]$, $w_{colour} + w_{shape} = 1$

The weight parameters (w_{colour}, w_{shape}) allow adapting the heterogeneity definition to the application. The spectral heterogeneity allows multi-variant segmentation by adding a weight w_{colour} to the image channels c. Difference in spectral heterogeneity Δh_{colour} is defined as shown in Eq. 2.

$$\Delta h_{colour} = \sum w_c \, (n_{merge}.\ \sigma_{c,merge}) - (n_{obj\_1}.\ \sigma_{c,ojb\_1} + n_{obj\_2}.\ \sigma_{c,obj\_2}) \qquad (2)$$

with n_{merge} number of pixels within merged object

n_{obj_1} number of pixels in object 1

n_{obj_2} number of pixels in object 2

σ_c standard deviation within object of channel c.

Subscripts merge refer to the merged object, object 1 and object 2 prior to merge, respectively.

Smoothness/Compactness: when the shape criterion is larger than 0 the user can determine whether the objects shall become more compact (fringed) or more smooth.

The shape heterogeneity Δh_{shape} is a value that describes the improvement of the shape with regard to smoothness (Eq. 3) and compactness (Eq. 4) of an object's shape.

$$\Delta h_{shape} = w_{compt}.\ \Delta h_{compt} + w_{smooth}.\ \Delta h_{smooth}, \text{ with } \Delta h_{smooth} = n_{merge}.(l_{merge}/b_{merge}) - ((n_{obj\_1}.(l_{obj\_1}/b_{obj\_1})) + (n_{obj\_2}.(l_{obj\_2}/\ b_{obj\_2})) \qquad (3)$$

$$\Delta h_{compt} = n_{merge}.(l_{merge}/(sqrt(n_{merge}))) - ((n_{obj\_1}.(l_{obj\_1}/\ (sqrt(n_{obj\_1})) + (n_{obj\_2}.(l_{obj\_2}/(sqrt\ (n_{obj\_2})) \qquad (4)$$

with l being the perimeter of the object
b the perimeter of the object's bounding box.
Thus, the smoothness heterogeneity equals the ratio of the de facto border length l and the border length b given by the bounding box of an image object parallel to the raster. The compactness heterogeneity equals the ratio of the de facto border length l and the square root of the number of pixels forming this image object. The weights w_c, w_{colour}, w_{shape}, w_{smooth}, w_{compt} are parameters, which can be selected in order to get suitable segmentation results for a certain image data stack and a considered application.
In our study only the principal components of the MERIS-image were considered during the segmentation process. The segmentation scale parameter was adjusted to best delineate homogeneous area (25). The final criteria of segmentation consisted of spectral homogeneity (colour) and geometric indices (shape) with the weights of 0.9 and 0.1, respectively. The two geometric indices, compactness and smoothness, were assigned with weights of 0.9 and 0.1, respectively.

2.3.2 Classification

The segmentation phase is followed by the classification of objects. Definiens software offers two basic classifiers: a nearest neighbour (NN) classifier and fuzzy membership functions. Both act as class descriptors. While the NN classifier describes the classes to detect by sample objects for each class which the user has to determine, fuzzy membership functions describe intervals of feature characteristics wherein the objects do belong to a certain class or not by a certain degree. Thereby each feature offered by Definiens can be used either to describe fuzzy membership functions or to determine the feature space for the NN classifier. A class then is described by combining one or more class descriptors by means of fuzzy-logic operators or by means of inheritance or a combination of both (Definiens Professional 5 – Reference book, 2006).
In this study, a combination of both classifiers has been used. Instead of the fuzzy logic approach of the membership functions, however, hard classification rules (threshold values) were chosen to get a more straightforward result.
In a first step the different classes were created according to the descriptions provided by the local end-users. The NN classifier was associated with all these classes.
NN classifier is a supervised non-parametric classification method. It classifies image objects according to its nearest neighbouring training object in feature space. Its principle is: after (pure) sample objects have been selected for each class, the algorithm searches for the closest sample object in the feature space for each image object (Fig. 7). If an image object is the closest sample object belongs to class A, the object will be assigned to class A (Eq. 5).

$$d = \sqrt{\sum_f \left[\frac{v_f^{(s)} - v_f^{(o)}}{\sigma_f} \right]^2} \qquad (5)$$

with: d the distance between sample object s and image object o,
$v_f^{(s)}$: feature value of sample object for feature f
$v_f^{(o)}$: feature value of image object for feature f
σ_f: standard deviation of the feature values for feature f

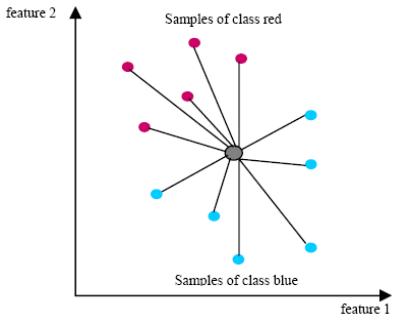

Figure 7 The principle of nearest neighbour classification (Hardin, 1999).

NN is not widely used for pixel-based classification, partially due to its notoriously slow speed of execution (Hardin, 1999). Unlike Maximum Likelihood Classification (MLC), where training data are statistically condensed into covariance matrices and mean vectors, the NN classifier requires that the actual training vectors participate in each classification. However, for the object-based approach used in this study, the segments are the classification primitives, instead of the individual pixels. The amount of classification primitives is greatly reduced through the segmentation process. Therefore, the execution speed is not problematic.

In our study, the nearest neighbour feature space consisted of the four PC's of the MERIS-scene. For the artificial, wetland and grassland class, however, also the Radar TS image bands were taken into account for the feature space definition as variations in radar backscatter provide important additional information for the separation of these classes as they show clearly distinct variations in backscatter over time.

Because of the lack of ground-truth data at that time, existing ancillary datasets were used as reference data to collect our sample-objects. The objects were exported from Definiens and overlaid with GeoCover ortho stock data (Dykstra, 2001) to identify sample objects for each class. The sample selection was an iterative process and for some classes totally pure sample-objects were non-existent.

Because of the large overlap of the wetland sample objects in feature space with sample objects from other classes, an extra criterion was defined for this class to improve the separability. This criterion takes into account that wetlands should be within a short distance of the stream network as we reasoned that wetlands of at least 320×320 m (most objects however consisted of more then 1 pixel) could only exist near a permanent water supply. This criterion was fulfilled by adding a hard membership function to the wetland class that states that an object could only be assigned to this class if at least a part of this object overlap with the thematic layer, which is the buffered stream network layer (logical AND-operation). This criterion was also applied to the water- class to avoid misclassifications with shadowed regions.

3. RESULTS

3.1. Classification map

Fig. 8 shows the result of the classification over the Kafue River Basin. Notice the transition from lush green forested vegetation in the North to the savannah vegetation (grasslands and shrubland) in the South.

The man-made Ithezi-Thezi lake (located in the Southwest of the basin), the nearly circular-shaped Lukanga Swamps (Central East) and the high concentration of lakes in the Kafue Flats (East of the Ithezi-Thezi dam) are the main water reservoirs within the basin. Due to the great (spectral) variability of these wetlands and floodplains throughout the year especially the RADAR-Time series helped us to uniquely identify them.

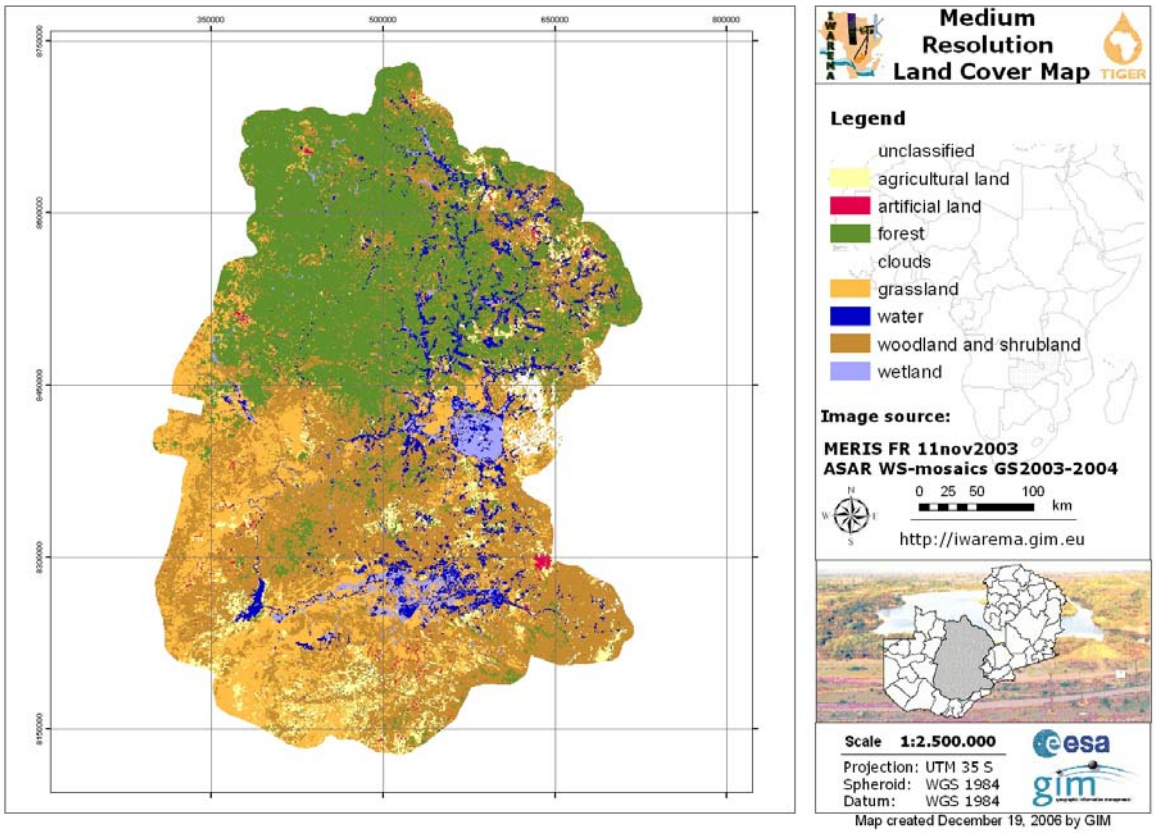

Figure 8 Classification map.

In Fig. 9 the high explanatory value of these time series is illustrated. This figure displays the Lochinvar Lake area within the Kafue Flats. Many different features can be identified in this image. The purple-red regions on the image correspond to grasslands. These regions are characterized on our radar images by high backscatter values at the end of the rainy season (lush green vegetation) and low backscatter values at the end of the dry season (bare soil). A second striking detectable landcover is the Lochinvar Lake (orange region). This area is characterized by higher backscatter values at the end of the dry season in comparison to the backscatter at the end of the rainy season. This area gets totally inundated during the rainy season, which results in a low backscatter while at the end of the dry season a vegetated cover has been formed on the dried out lake bed resulting in a high backscatter.

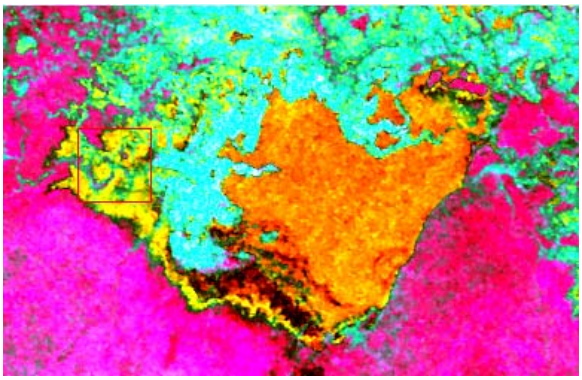

Figure 9 RADAR TS layer stack over the Lochinvar Region (Kafue Flats) (R: end of GS-start of GS, G: start of GS and B: end of GS).

These observations correspond with the climatic data of the 2003/2004 rainy season when high amounts of precipitation have been recorded throughout the basin. Due to this particular wet rainy season the floodgates of the Ithezi-Tezhi Dam (made to store water for the hydroelectric power station of the Kafue Gorge Dam downstream) were exceptionally opened to their full extent allowing the Kafue Flats to flood (Mumba et al., 2005).

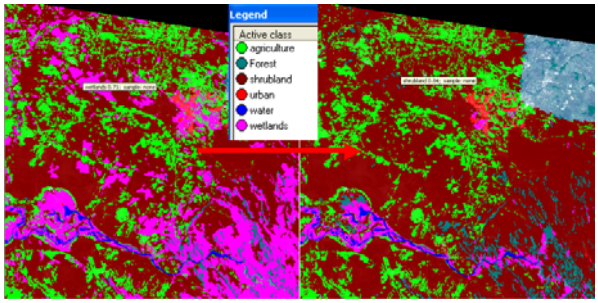

Figure 10 Classification results over the Lusaka area, without (left) or with (right) the use of RADAR TS and thematic layer.

In Fig. 10 the added value of the multi-source approach is illustrated. On the left, the original classification result over the Lusaka area is displayed. One can clearly notice the overestimation of the wetland class. On the right the classification is carried out again using the same sample objects but now applied to the extended feature space (including the RADAR-bands) and taking into account the additional thematical criteria (vicinity of stream). A visual comparison already shows clearly the improved result.
In Fig.10's classification map only the Lusaka urban area can be easily identified. Other smaller cities are omitted due to the coarse resolution of the MERIS-image. The agricultural areas are mainly located around the Lusaka-area (Central plateau) and on the Southern plateau between the Kafue Flats and Lake Kariba further south.

3.2. Quality assessment

Because image selection was undertaken after examining lists of archived images, it was impossible to undertake collection of ground reference data concurrently with the acquisition of the images. Instead thirty-six field points were collected during two field campaigns carried out by the end-users in 2006/2007. The South of the basin was visited in November 2006 and the North in March 2007. Together with the GPS locations of the points, pictures were taken and field questionnaires were filled in providing information about the landcover. The visited points are visualized in Fig. 11.

All this information was summarized in a spreadsheet and imported in ArcGIS where a vector-shapefile was created. This shapefile consisted out of 5 fields. The ID, the X&Y coordinates the field description (class name) and the MR-class name (empty).
An overlay was made with the produced MR-classification map (Fig. 10) and every single record was visited while the corresponding class was filled in the MR-class name field.

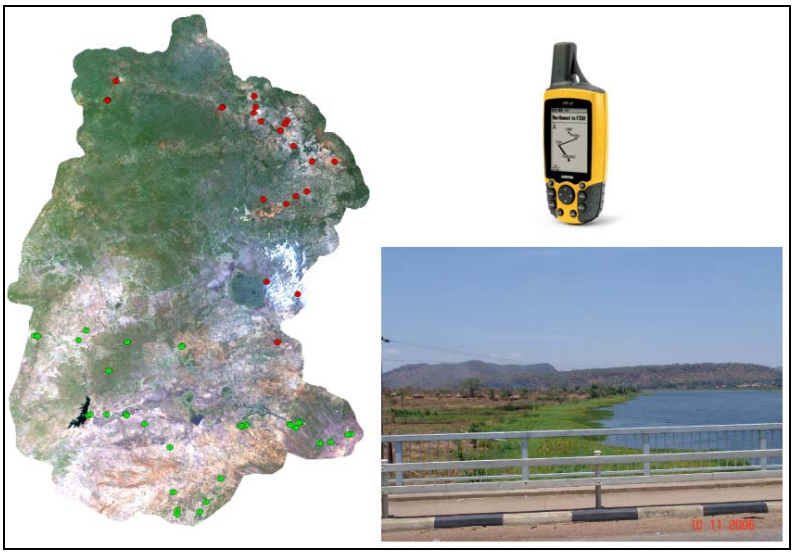

Figure 11 Collected field points (green points were visited in November 2006 and red points were visited in March 2007) visualized on the MERIS FR image (RGB – 752).

Because of the limited amount of field-points that could be collected during the field campaigns the ground truthing database could not be considered to be representative. We therefore decided to collect additional information. Four hundred sample points were generated that were randomly distributed over the Kafue River Basin. Because of the lack of reference data for these points a visual interpretation of Google Earth (GE) images was carried out to obtain the true ground cover for these points.

Over the basin most images displayed on GE were the GeoCover-Ortho stock mosaics of 1990 but some of them were very high resolution QuickBird images from 2003. Only points for which this classification was unequivocal were retained in the further analysis.

The result of the validation is summarized in a contingency matrix (Tab. 2). An overall accuracy of 85.1% and a kappa statistic of 79.6% were obtained.

The highest errors are observed in the agricultural land class with an omission error of 32.5% and a commission error of 18.2%. Probably the main reason for this is the inherent fuzziness of this class resulting in misclassifications (for instance into woodland and shrubland (7)). Another reason could be the lack of a unique spectral signature of this class (Fig. 12).

Figure 12 GE screenshots illustrating the fuzziness and the large spectral variability of the African agricultural land class (displayed areas are approximately 1 (left) and 4 (right) MERIS FR pixels).

Due to the small area fraction of the artificial land class only six of all the sample points were collected in this class.

Note that the total sum of the field and sample points are smaller than the expected 436. This is because the points, which were distributed over cloudy and unclassified areas, were omitted during the quality assessment.

To have an idea about the quality of our classification map in relation to other existing landcover maps over the Kafue River Basin, two additional contingency matrices were produced (using the same points). One for the Geo-cover LandCover product, which is derived from an unsupervised pixel-based classification of Landsat TM images (Tab.3) and another one for the GLC2000 product, which is derived from a pixel-based unsupervised classification of SPOT VGT data (Tab.4))
The first thing that catches the eye is the lower overall accuracy of both products in comparison with our product. Especially the GLC2000 classification map with an overall accuracy of only 56.7% reveals clear deficiencies. Most likely the very coarse resolution (1000m) of the source images will be the main reason for this poor result. However the assessment of the Geo-Cover LandCover product, which is derived from high-resolution (28.5m) Landsat images also results in higher classification errors (overall accuracy of 76.1%). These errors are mainly caused by misclassifications in the grassland and artificial land classes with omission errors of 74.2% and 60.0%, respectively (commission errors of 57.9% and 0.0%). Note that in our classification method, where we took the RADAR-information into account for these classes during the NN-classification, we get significantly better producer's accuracies of 92.9% and 80.0%, respectively.

Also note that for the water and wetlands class, where we also made use of ancillary datasets (RADAR and stream network), again the producer's accuracy improved (producer's accuracy from 76.5% to 80.0%). It seems that the high temporal variability and the fuzzy spectral signal of these classes cause the pixel-based classifiers to fail. In our method these issues could be partially resolved by applying an object-based classification approach combining the optical data with radar time series and ancillary GIS-data.
Another reason for the lower accuracies of the existing products could also be that the errors have been introduced while merging the classes necessary to compare all the different legends (see original classnames in Tab. 5)

4. DISCUSSION

The integration of remote sensing, GIS and expert system techniques for developing an automated object-based land cover classification are resulting in increasingly intelligent information systems. The traditional pixel-based methods, which only use the spectral information of pixels, will in the nearby future be replaced by these smart techniques, described in this paper. Our study, which is one of the first applications of this technique at a regional scale using medium-resolution data, shows that significantly better results can be obtained than with classical pixel-based image classification.

The penetrating power of microwave makes SAR remote sensing a unique tool that can be widely applied to obtain additional information. Especially in areas with a substantial cloud cover, like the tropics, these data have an enormous potential. In our case, optical data were combined with radar amplitude time series, which resulted in significantly improved classification results. Due to the gradient mosaicking of the ASAR-WS scenes, which was necessary for a full coverage of the study area, the original backscatter values could no longer be retained. Therefore the capabilities of our RADAR images could not be fully exploited. In future research, it would be interesting to focus on one image in particular and to search for coregisterable radar image pairs ready for interferometric applications (coherence). By all means, the ongoing progress in radar RS development offers interesting prospects in land cover classification, but additional research is necessary.

Table 2 Error Matrix of MR LC-classification Map over the Kafue river basin.

	Reference (field observation + Visual interpretation of (V)HR Google earth imagery)						Total N	user's accuracy
MR-classification	Woodland and Shrubland	Forest	Grassland	Water and Wetlands	Agricultural land	Artificial land		
Woodland and Shrubland	133	14	0	1	7	0	155	85.8%
Forest	3	118	0	0	2	0	123	95.9%
Grassland	10	1	26	1	2	0	40	65.0%
Water and Wetlands	10	1	2	46	0	0	59	78.0%
Agricultural land	3	0	0	2	27	1	33	81.8%
Artificial land	0	0	0	0	2	4	6	66.7%
Total N	159	134	28	50	40	5	416	Overall accuracy: 85.1 %
Producer's accuracy	83.6%	88.1%	92.9%	92.0%	67.5%	80.0%		Kappa statistic: 79.6 %

Table 3 Error Matrix of the GeoCover LandCover product over the Kafue river basin.

	Reference (field observation + Visual interpretation of (V)HR Google earth imagery)						Total N	user's accuracy
Geo-cover(label)	Woodland and Shrubland	Forest	Grassland	Water and Wetlands	Agricultural land	Artificial land		
shrub (3)	110	2	3	8	9	1	133	82.7%
evergreen(2)+ deciduous forest(1)	34	130	18	0	3	2	187	69.5%
grassland(4) + barren vegetation (5)	5	1	8	4	1	0	19	42.1%
water(11) + wetlands(9)	2	0	2	39	2	0	45	86.7%
agriculture(7) + paddy crops(8)	4	1	0	0	36	0	41	87.8%
urban/built-up(6)	0	0	0	0	0	2	2	100.0%
Total N	155	134	31	51	51	5	427	Overall accuracy: 76.1 %
Producer's accuracy	71.0%	97.0%	25.8%	76.5%	70.6%	40.0%		Kappa statistic: 66.9 %

Table 4 Error Matrix of the GLC2000 product over the Kafue river basin.

	Reference (field observation + Visual interpretation of (V)HR Google earth imagery)						Total N	user's accuracy = 1-Commision error
GLC2000 (label)	Woodland and Shrubland	Forest	Grassland	Water and Wetlands	Agricultural land	Artificial land		
Deciduous wood(10) & shrubland (11&12)	113	35	3	29	21	4	205	55.1%
Forest (9)	21	99	18	6	1	0	145	68.3%
Grassland (13-14-15)	0	1	0	0	0	0	1	0.0%
Water (26) and Wetlands (17)	0	2	0	9	4	1	16	56.3%
Croplands (18)	24	0	8	6	23	0	61	37.7%
Cities (27)	0	0	0	0	2	0	2	0.0%
Total N	158	137	29	50	51	5	430	
Producer's accuracy = 1-(Omission Error)	71.5%	72.3%	0.0%	18.0%	45.1%	0.0%		Overall accuracy: 56.7% Kappa statistic: 37.9 %

Table 5 Original labels and class names of the GeoCover LandCover and GLC2000 products occurring in the Kafue River Basin.

GeoCover LandCover Legend Label + Class name				GLC2000 African Legend Label + Class name			
2	evergreen forest	11	Water	10	Deciduous woodland	26	Waterbodies
3	shrub	5	barren vegetation	9	Closed deciduous forest (dense Miombo)	27	Cities
1	deciduous forest	8	paddy croplands	11	Deciduous shrubland with sparse trees	13	Closed grassland
9	wetlands	6	urban/built-up	18	Croplands (>50%)	14	Open grassland with sparse shrubs
7	Agriculture	13	cloud/shadow	12	Open deciduous shrubland	25	Salt hardpans
4	grassland			17	Swamp bushland and grassland	15	Open grassland

When developing a method for land cover classification it is of great importance that the developed rule-sets are transferable. The Definiens software package offers different tools to achieve this. Unfortunately, within this research project, time and data were not available to elaborate this. Studies, however, are necessary to develop rule-sets based only on membership functions to avoid time-consuming training sampling and to maximize transferability. Ideally, this would enable users to re-use developed rule-sets on other images of different times and even maybe on images of other comparable regions. Going through all the described pre-processing steps is of course a prerequisite for a successful classification. A protocol like this would reduce working load tremendously and would enable to produce near real-time highly accurate land cover datasets. Many study fields would of course benefit from this evolution and could integrate the generated datasets in their GIS for further spatial analysis.

5. CONCLUSIONS

In this paper a method for an integrated LC-classification of medium-resolution satellite imagery over the Kafue River Basin was elaborated. The capabilities of the relatively new object-oriented image analysis technique were investigated on a remotely sensed image using complementary datasets. The different pre-processing steps of the used datasets were thoroughly detailed allowing further studies to experiment with the developed rule-sets. A sound quality accuracy assessment summarized in error matrices revealed high accuracies of the derived regional scale land cover map and a significant improvement over pixel-based classification.

The combination of an optical MERIS multi-spectral image with C-band radar time series and complementary ancillary datasets allowed us to resolve some major classification confusions that occur when only optical data were used. The additional temporal, spatial and contextual information proved to be very useful for example in distinguishing between grasslands and wetlands, urban areas and grasslands, etc.

The benefit of object-based classification presented here over the classical pixel-based classifiers is that the image objects contain more information than just spectral information provided by single pixels. In addition to spectral information, summarized from the collection of pixels composing the image object, each image object also contains information regarding the texture, size, shape and context of that image object to surrounding image objects. The spectral and spatial attributes of each image object can be used to assign the object to a specific classification category, paralleling somewhat the human visual cognitive process. Advantages to this technique are a more robust classification due to the increased information, reduction in the number of units (pixels versus objects) to be classified and the elimination of the “salt-and-pepper” effect which is common in per-pixel classifiers.

6. ACKNOWLEDGEMENTS

This work has been carried out within the IWAREMA Zambia project which has been funded by the European Space Agency under the ESRIN Contract No.19416/05/I-EC in the framework of the TIGER Initiative as an Innovator project. Image data have been provided by ESA, the local ancillary data were provided by the Zambian users and the international ancillary data by MDA Federal (GeoCover), EC-JRC (GLC-2000) and USGS (SRTM). The support of the Zambian Department of Water Affairs, Ministry of Energy and Water Development (in particular Mr. Adam Hussen - Director and Mr. Jack Nkhoma), and Mr. Kawawa Banda, Geology Department, University of Zambia is also acknowledged. Finally we wish to thank all colleagues at GIM and in Zambia, who are not listed in the author’s list for their support

7. REFERENCES

7.1 Papers and books:

Anderson, J. R., Hardy, E. E., Roach, J. T. and Witmer, R.E. 1976. *A Land Use And Land Cover Classification System For Use With Remote Sensor Data*. Washington D.C, United States Government Printing Office.

Benz, U. C., Hofmann, P., Willhauck, G., Lingenfelder, I. and Heynen, M. 2003. Multi-resolution, object-oriented fuzzy analysis of remote sensing data for GIS-ready information. *ISPRS Journal of Photogrammetry & Remote Sensing*, Vol. 58, pp. 239-258.

Clawson, Marion and Stewart, Charles L. 1965. *Land use information. A critical survey of U.S. statistics including possibilities for greater uniformity.* Baltimore, Johns Hopkins Press for Resources for the Future, Inc.

Dykstra, J. D. 2001. "The GeoCover Ortho Program". *GeoInformatics*, Volume 4. January/February 2001.

Ellenbroek, G. A. 1987. *Ecology and Productivity of an African Wetland System: the Kafue Flats, Zambia*. Dordrecht, Dr. W. Junk Publishers.

Hardin, P.J. 1999. Neighborhood methods for image classification. *Proceedings of IEEE International Geoscience and Remote Sensing Symposium (IGARSS '99)*, Hamburg, Germany, 25 – 29 July 2005. 2, pp. 1274–1276.

Laliberte, A.S., Rango, A., Havstad, K.M., Paris, J.F., Beck, R.F., McNeely, R. and Gonzalez, A.L. 2004. Object-oriented image analysis for mapping shrub encroachment from 1937 to 2003 in southern New Mexico. *Remote Sensing of Environment*, Vol. 93, pp. 198-210.

Leukert, K., Darwish, A. and Reinhardt, W. 2004. Transferability of Knowledge-Based Classification Rules. *Proceedings of the ISPRS 2004 Annual Conference*, Istanbul, Turkey, 12 – 23 July 2004.

Mayaux, P., Bartholomé, E., Fritz, S. and Belward, A. 2004. A new land-cover map of Africa for the year 2000. *Journal of Biogeography*, Vol. 31, No. 6, pp. 861–877.

Mitri, G.H. and Gitas, I.Z. 2006. Fire type mapping using object-based classification of Ikonos imagery. *International Journal of Wildland Fire*, Vol. 15, pp. 457–462.

Mumba, M. and Thompson, J.R. 2005. Hydrological and ecological impacts of dams on the Kafue Flats Floodplain system, southern Zambia. *Physics and Chemistry of the Earth*, Vol. 30, pp. 442-447.

Rahman, H. and Dedieu, G. 1994. SMAC : a simplified method for the atmospheric correction of satellite measurements in the solar spectrum. *International Journal of Remote Sensing*, Vol. 15, No. 1, pp. 123-143.

Santos, T., Tenedório, J. A., Encarnação, S. and Rocha, J. 2006. Comparing pixel vs. object based classifiers for land cover mapping with ENVISAT- MERIS data. *Proceedings of the 26th Annual Symposium of the European Association of Remote Sensing Laboratories (EARSeL)*, Warsaw, Poland, 29 May - 2 June 2006, pp. 251–264.

Thomas, N., Hendrix, C. and Congalton, R. G. 2003. A comparison of urban mapping methods using high-resolution digital imagery. *Photogrammetric Engineering and Remote Sensing*, Vol. 69, No. 9, pp. 963–972.

Tucker, C. J., Grant, D. M. and Dykstra, J. D. 2004. NASA's global orthorectified Landsat data set. *Photogrammetric Engineering and Remote Sensing*, Vol. 70, No. 3, pp. 313-322.

Verstraete, M., Pinty B. and Curran P. 1999. MERIS potential for land applications. *International Journal of Remote Sensing*, Vol. 20, No.9, pp. 1747-1756.

Yan, G., Mas, J.F., Maathuis, B.H.P., Xiangmin, Z. and Van Dijk, P.M., 2006. Comparison of pixel-based and object-oriented image classification approaches - a case study in a coal fire area, Wuda, Inner Mongolia, China. *International Journal of Remote Sensing*, Vol. 27, No. 18, pp. 4039-4055.

7.2 Manuals:

ASAR Product Handbook, issue 2.1, 2006. ESA. http:\\ENVISAT.esa.int

Definiens Professional 5 - Reference Book, Document Version 5.0.6.1., 2006. Definiens Imaging.

Definiens Professional 5 - User Guide, Document Version 5.0.6.1. 2006. Definiens Imaging.

Envi 4.2. User's Guide, 2005. ITT Visual Information Solutions.

EOLI-SA catalogue User Manual, 2006. ESA. http://eoli.esa.int/geteolisa/index.html

MERIS Frequently Asked Questions, Issue 1.0., 2006. ESA. http:\\ENVISAT.esa.int

MERIS Product Handbook, issue 2.0., 2006. ESA. http:\\ENVISAT.esa.int

Detecting Water Bodies and Water Related Features in the Niger Basin (Niamey Area) Using SAR Data: the ESA TIGER WADE Project

A.Arledler[(1)], P.Castracane[(1)], A. Marin[(1)], S.Mica[(1)], G.Pace[(1)], M.Quartulli[(1)], G. Vaglio Laurin[(1)], I.Alfari[(2)], H. Trebossen[(2)]

[(1)] Advanced Computer Systems S.p.A., Via della Bufalotta, 378 - 00139 Rome (Italy) E-mail: g.pace@acsys.it; p.castracane@acsys.it
[(2)] Centre Régional AGRHYMET 0425 Bd de l'Université BP 11011 Niamey (Niger) E-mail: i.alfari@agrhymet.ne

Abstract The availability of timely and reliable maps of transient water bodies in arid African countries is an asset of crucial importance for their efficient exploitation. The ESA TIGER WADE project has been developed to provide local authorities with support tools for this aim. The local users, represented by Agrhymet, a Regional Center of the Permanent Interstate Committee for Drought control in the Sahel, have been actively involved mainly in the service requirements' definition and validation campaign execution.
Efficient mapping of water bodies is implemented by SAR systems through the ERS/ENVISAT datasets and well-established, reliable techniques of calibration and classification. An additional service, that exploits watershed modelling GIS tools coupled with automatic linear features extraction, provides maps of probability of groundwater occurrence along draining fault lines. The prototype services are implemented over an area of approximately 30,000 km^2, centred around the city of Niamey, during several months of the rainy season, spanning a time period starting from 1993 up to 2007.

1. INTRODUCTION

The aim of the project TIGER WADE is mapping and monitoring of superficial and underground water resources with SAR imagery in arid and semi-arid regions in Africa. In particular, the area around the city of Niamey (Niger) has been selected for this preliminary study.
SAR data are suitable for mapping water bodies, as the signal is principally sensitive to moisture and to surface roughness. These data can be preferred to the optical ones taking into consideration the cloud penetration capabilities that are fundamental when mapping transient waters typically associated to rainy periods. Despite the large data archive of ERS-1/2 and ENVISAT-1, the investigation on the availability of SAR data in the area of interest of the Niger basin has shown that the time series over the same frame is, in general, quite sparse and that there are only a few tandem[1] acquisitions in the study area. It was therefore decided to try and take as much information as possible from a single SAR acquisition in order to map water bodies with good accuracy.

2. SAR DATA QUALITY CHECK

From SAR raw data, the "de-speckled" backscattering, obtained by the procedure described in the following section, has been analyzed. The visual inspection of this backscattering amplitude, supported by high resolution optical images and by the ground truth data validation, highlighted a certain complexity in some SAR data: an example is illustrated in Fig 1, which shows a portion of the Niger River. The snapshots are chronologically ordered and they appear completely different also at closer time periods (see e.g. sequences 08-08-2004 – 15-09-2004 and 12, 29, 31 July 2007) This behaviour certainly is not related to the presence/absence of water because of the very short time difference, moreover the analysis of the dates does

[1] A "tandem mode" acquisition is a double observation of the same scene, by different satellites (e.g. ERS1 and ERS2), minimising the time gap between the acquisitions.

not show a particular trend which could indicate, for example, that during the dry season there is less water and, therefore a different return signal.

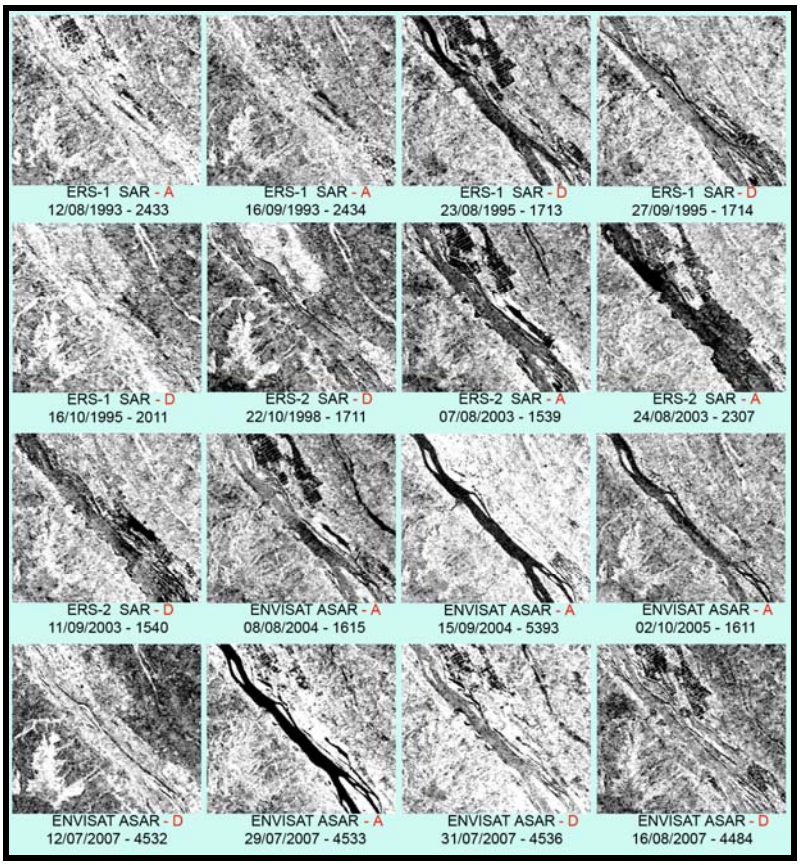

Figure 1 Example of a portion of the Niger River with different dates (section of the river South of Niamey from 13°26'50''N, 2°08'00"E to 13°23'50"N 2°1050"E). The sub-images in this figure have been named according to the following sequence: Satellite, Sensor, Direction (A: ascending, D: descending), Date, Orbit Number (e.g. ENVISAT ASAR A 29/07/2007 -4533).

A similar variable behaviour is represented in Figure 2 which shows some clearly identified water bodies in SAR frames acquired at different times with the same polarisation, mode and geometry. This snapshot is really interesting, as the water bodies show a dramatically changing signal return, whereas the surrounding area is rather stable in backscattering. The stability of the non-water features confirms, moreover, that the variability is not due to processing artefacts or to errors in the data, but is associated to real physical changes in the backscattering targets.

Optical high resolution images (Figure 3) show that this is related to two factors: wind and vegetation. In some cases, also the effect of heavy rain can lead to anomalously high backscattering of the water bodies.
While the backscattering differences over the rivers (< 10dB) can be compatible with the effect of wind over the water surface (as indicated by the analysis of Ulaby et al., 1986), on the other hand, the very high backscattering over the water bodies (e.g. ERS1 16-09-1993 -2446 versus ERS1 21-10-1993 2442 express a difference of about 20dB over the surface of the water bodies), does not seem to be compatible with the effect of wind, as also indicated by the references utilized in the CMOD5 model (currently used in ESA for the measurement of wind speed using scatterometer data) and reported in Hersbach (2007).

After the analysis, we have concluded that:

- Difference in the river water backscattering values are compatible with the typical values of wind (< 10dB)
- in the water bodies, the high backscattering is due to the presence of vegetation-induced roughness
- the water appears particularly bright in some cases, especially if compared with the surrounding area which is very arid

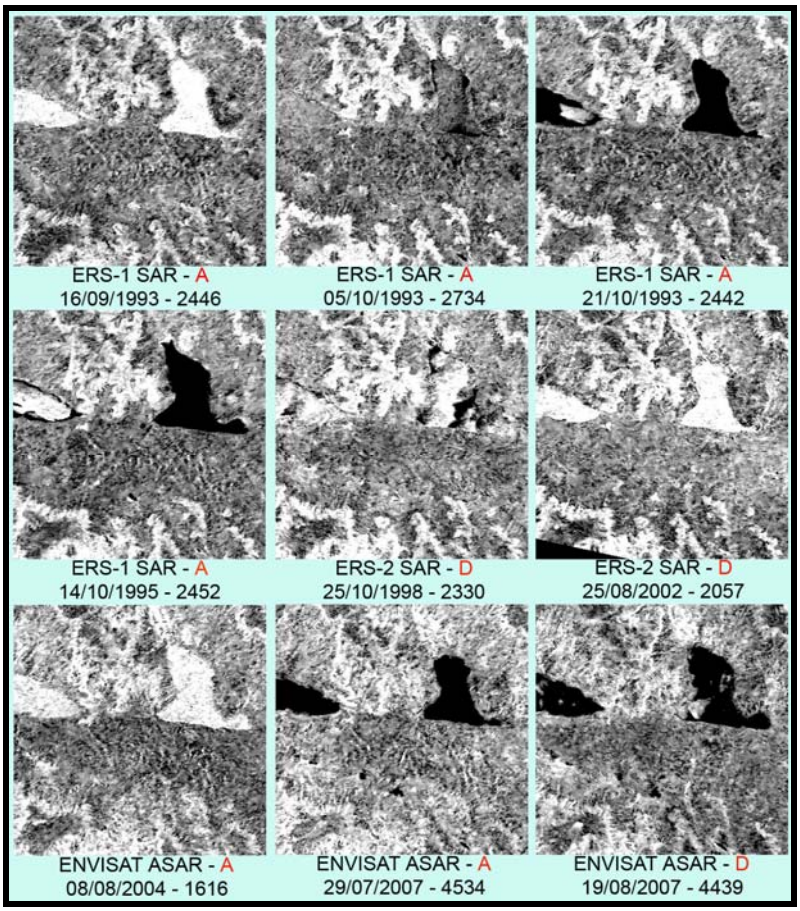

Figure 2 Example of water bodies taken during various time periods (North of city of Tillabery: 14°20'57"N 1°28'14"E). The sub-images in this figure have been named according to the following sequence: Satellite, Sensor, Direction (A: ascending, D: descending), Date, Orbit Number (e.g. ENVISAT ASAR A 29/07/2007 -4533).

Based on the above analyses, it has been concluded that:

- the water body mapping algorithm is well reliable when there is no disturbing effect, such as the presence of dense surface vegetation or the presence of strong wind
- when a significant disturbance is present, the level of confusion induces to completely disregard the data

The consistency of the hypotheses above is confirmed by the fact that images of the same date have always been consistently used (or rejected). Although the influence of vegetation on the water body is not expected to change rapidly with time, the effect of wind can significantly vary from one day to another. So, in

principle, even images of the same area, from two consecutive days, could be treated differently due to strong wind effects.

Figure 3 Example of water bodies with different amounts of vegetation (High-resolution optical image: Alumadi - Nigeria).

3. MAPPING SURFACE WATER BODIES

From the previously described quality analysis of SAR dataset, it has been decided that only the most reliable images are processed, corresponding to the dates where no disturbance was present. Out of the overall 77 frames selected, 36 have been finally used and grouped per year.

3.1 Algorithm Summary

This project was focused on the usage of single SAR scenes, in order to explore its capabilities to detect water bodies. The approach is based on two fundamental steps:

1. robust probabilistic descriptor extraction from speckle-degraded SAR data
2. supervised data classification in multidimensional descriptor spaces

The Enhanced Model Based Despeckling (EMBD) algorithm (Datcu et al., 1998; Schroeder, 1998; Walessa and Datcu, 2000) has been used to de-speckle the data and to extract texture in the classification of the data for detecting the water bodies. The texture supports the water detection as it allows distinguishing between targets which may have a backscattering behaviour similar to that of water. Based on the pre-processing, we obtain a set of layers, out of which the most important ones are listed in Table 1.

Table 1 Layers extracted from the pre-processing.

ID	Type	Scale
B1	De-speckled backscatter amplitude	1 (16m x 16m)
B2	GMRF[2] texture norm	1 (16m x 16m)
B3	Model evidence	1(16m x 16m)
B4	Local noise level	1(16m x 16m)
B5	De-speckled backscatter amplitude	2 (32m x 32m)
B6	GMRF texture norm	2 (32m x 32m)
B7	Model evidence	2 (32m x 32m)
B8	Local noise level	2 (32m x 32m)

The scale is defined by the kernel that is used for the pre-processing activities. Scale 1 represents the highest resolution that can be obtained with the input data used (approximately 16 m), scale 2 is half the resolution of scale 1 (32 m) and so on. After some tests carried out against the ground truth data, using the layer combination B1-B6-B7 in Tab. 1 has been identified as the best approach. This layer combination indicates that, while for the de-speckled amplitude the scale with the highest resolution is desirable, a coarser resolution allows for capturing more texture features of the targets.

A Maximum Likelihood classifier has been applied to the layer combination mentioned above for the scenes not affected by evident disturbances. Four types of classes have been adopted in the classification, representing *water*, *bright targets*, *dark targets* and *very dark targets*. The training samples have been selected by photo interpretation using high resolution optical data. A clump and sieve algorithm has been applied to the final classification maps, in order to have a minimum mapping unit of 0.8 hectares (90 m resolution). This resolution is compatible with the accuracy of the geo-location based on orthorectification built upon the SRTM 90 m DEM.

The level of multi-temporal coverage of the various scenes and the geographical locations of the study area is represented in the following Fig. 4.

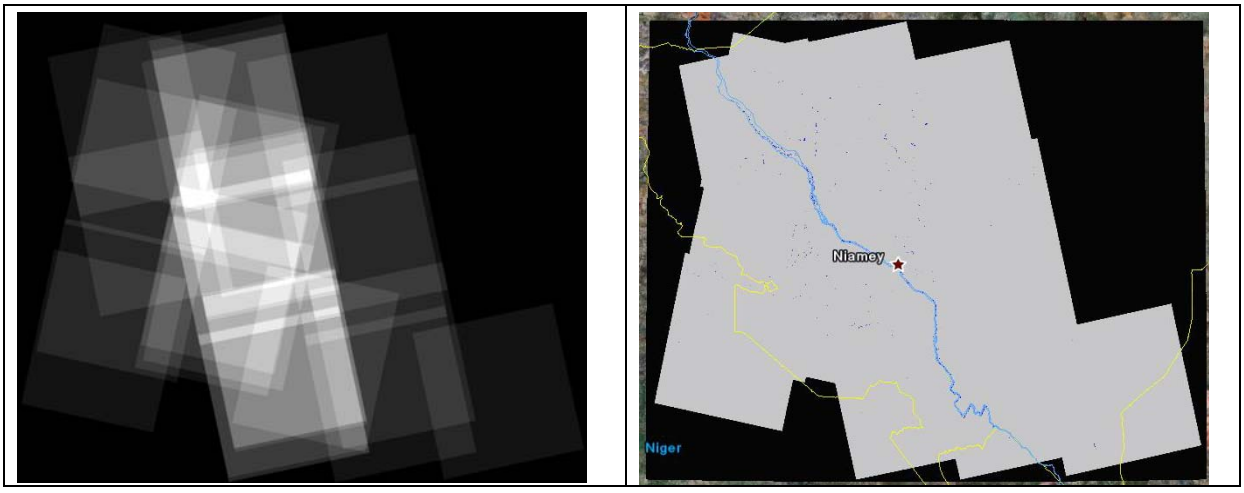

Figure 4 Left: representation of the frame coverage in the study area, including all times and all years: highest value (white) corresponds to 15 occurrences. Right: water body map of the study area.

[2] GMRF: Gauss Markov Random Field

The map on the left in Fig.4 represents the number of occurrences of a frame over each area (white indicates the highest number, which is 15). From the image it can be seen that the level of coverage of the various zones is quite heterogeneous.

3.2 Example of Results

Given the small number of frames for each year and the heterogeneity of time coverage, we have decided to generate a unique map for each year (rather than a series of monthly maps with very limited mapping areas). The following approach has been adopted for producing the final map:

1. We have generated a water body classification map (water/non-water) for each scene used and for each year.
2. For each year we have mosaicked all available water body maps, produced as per point (1) above, using the criterion indicated in point (3) below.
3. In the areas of overlay of more than one water map, we have used a configurable threshold[3] (for each given pixel, the final map will have water, if at least a number greater than the threshold of the overlaid maps indicate water)

So, for each year we delivered the following range of products:

1. The final water body map for that year (see e.g.Fig.6)
2. A map with the number of occurrences of water in the overlaid maps (e.g. Fig.5)
3. A map of the number of scene coverage of the areas (e.g**.** Fig.4, left)

By normalising map (2) and map (3) we obtain a sort of confidence of each area in the final water map (e.g. a value of 0.8 corresponds to 4 occurrences out of 5 scenes). Moreover, a sort of a general water map has also been generated by merging all scenes corresponding to all dates available.
It would be interesting to try and evaluate the variability of the position and extension of water bodies throughout the year, as it is known that they vary during the seasons. Unfortunately, due to the scarce availability of significant SAR data time series, we decided to rely on an average water map for the whole year.

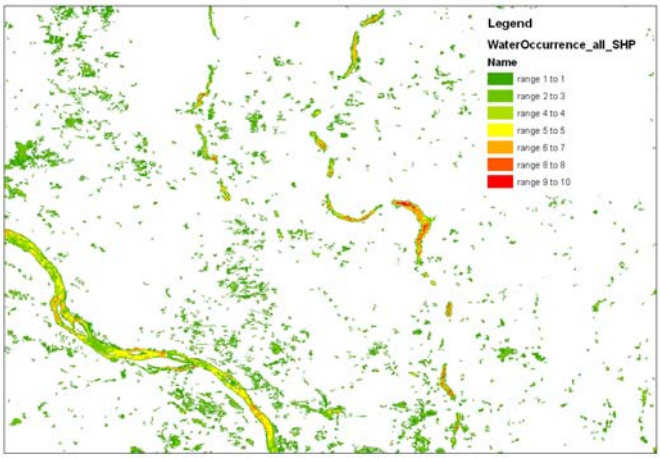

Figure 5 Zoom over the water coverage map ranges (range from 1: 1 occurrence - green to 10:10 occurrences –red)

[3] The optimal threshold should maximize the correct detection and minimize the commission errors. In case of available ground truth, the user can calibrate the system obtaining the best choice of this threshold, otherwise a simple majority criterion (50%) is applied as default.

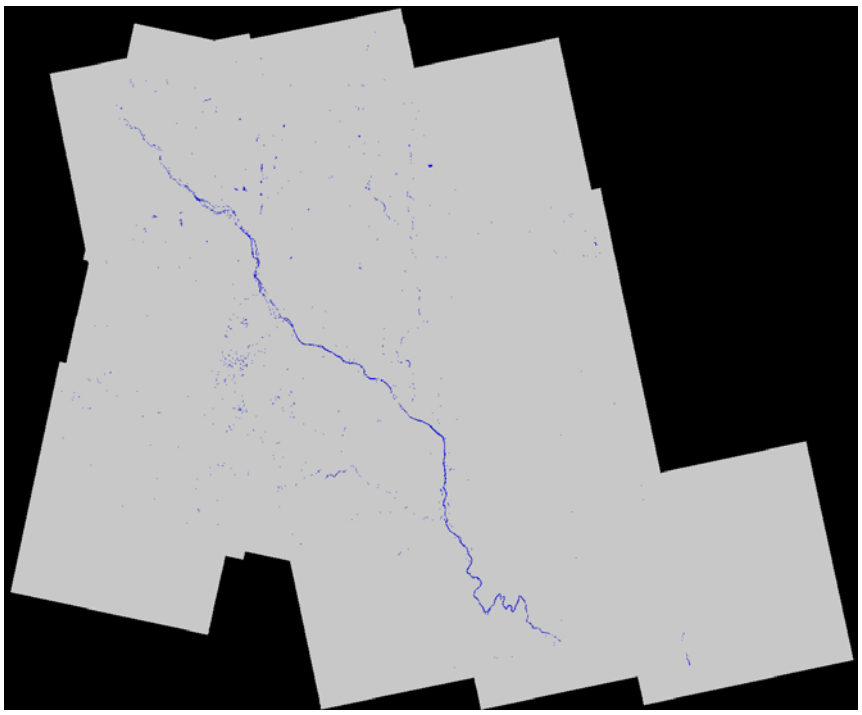

Figure 6 Water map (merge of all years)

4. MAP OF SUITABILITY OF GROUND WATER

The map of suitability of ground water is a prototypal product which has been implemented over an area of approximately 40,000 km^2 around the Niamey city. It is derived from a mosaic of 8 SAR frames selected over the area.

4.1 Algorithm Summary

The procedure, based on the works of Kageyama et al. (2000) and Saint-Jean and Singhroy (2000) is briefly summarized hereafter:

- Input data are SAR image and the Digital Elevation Model (SRTM 90 m)
- The main assumptions, based on the literature, are hereafter:
  - suitability for presence of groundwater is linked to the amount of water which actually overflows a certain area
  - the probability of groundwater accumulation points is higher in areas with presence of fault lines
- fault lines can be detected over SAR images by searching lineaments that often correspond to dried out river beds, which normally appear particularly bright in the image

In fact it is known that rivers tend to find their way in correspondence of fault lines, due to the rock fracturing. Rivers with permanent water flow have not been considered here as we focus on subsurface water.

Obviously this analysis could be improved if additional layers were employed. For example a lithological map could be used for extracting the runoff coefficients to be used for estimating the relative fractions of runoff and infiltrating water. In addition other parameters could be used such as the slope and presence of vegetation, which play an important role in the hydrological modelling. In fact this study is not meant to

implement any quantitative modelling (which would require complex calibration and validation parameters and procedures) but just a preliminary analysis, based solely on SAR data and DEM.

The following procedure is applied:

- Starting from the DEM, we calculate the flow accumulation points, using a dedicated watershed analysis GIS procedure.
- The areas with highest flow accumulation are extracted from the DEM.
- Within these areas, the points with statistically highest backscattering are identified.
- Among these points, the lineaments are searched using a *Hough transform*-based algorithm Gonzalez and Woods (1992).

The result is a map which has no specific geophysical value, but can be considered to indicate suitability for groundwater presence. The final map, normalized between 0 and 100, shall be evaluated in relative terms (100 being highest relative suitability in the study area).

4.2 Example of Results

The final map, covering an area of 40,274 km^2 is overlain with the DEM in Fig.7.

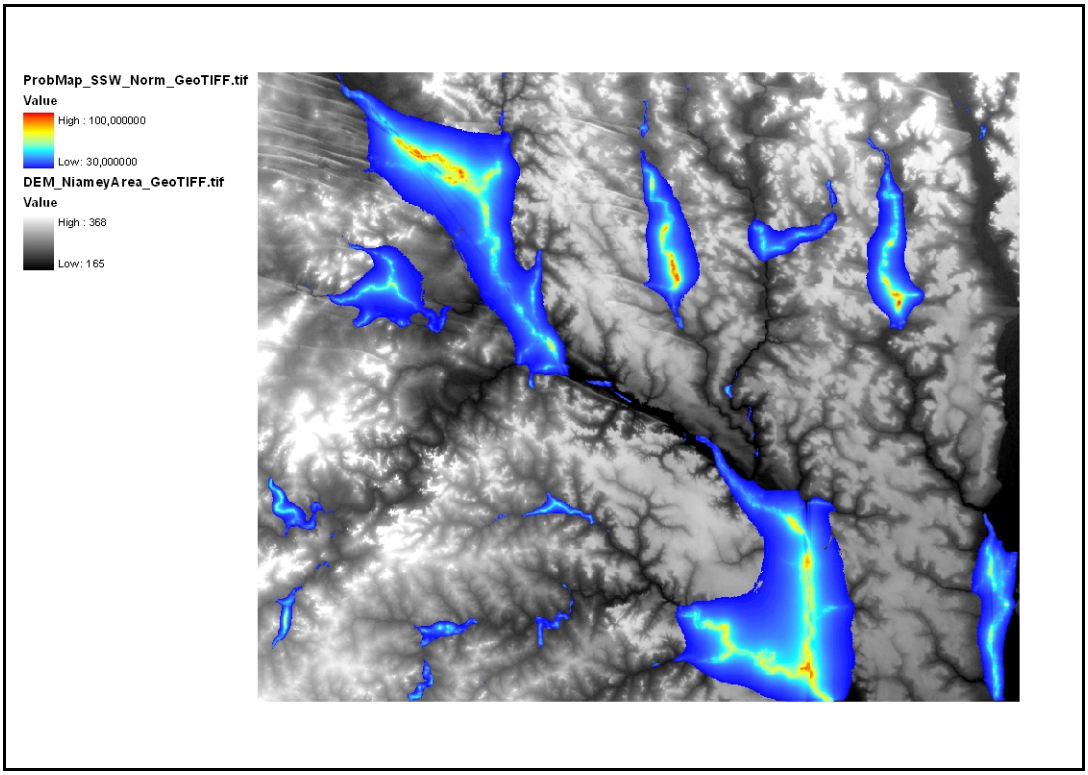

Figure 7 Overlay of the map of suitability for groundwater occurrence with the DEM.

5. VALIDATION

The water body maps have been validated using ground truth data provided by Agrhymet. The validation campaign has been carried out from 27 August to 5 September 2007 during the rainy season that usually occurs from the end of June to the beginning of October. It consists of 89 ground validation points, whereby 12 points represent Permanent water and the remaining 75 are defined as Semi-Permanent water. The validation points have been generally taken on the boundary of their corresponding water bodies. This shall be taken into account during a comparison with the resulting water classification, considering the following:

- The possible inaccuracy of the orthorectification.
- The size of the ponds and the fact that the sampling points have been taken on the boundary of the pond and not in the middle of the pond.

We have decided to define a search area around the GCP identified in the validation campaign. The search area has been defined taking into account the misregistration error and the mean radius of the pond, thus defining a search radius of 170 m (~ 11 pixels). Whenever at least two pixels, classified as water, fall inside this area, matching between GCP and the water bodies map is considered successful.
The analysis if the ground truth has highlighted that:

- The water body maps produced by our algorithm matched all permanent ponds' validation points.
- The water body maps produced by our algorithm matched about 2/3 of the non permanent ponds. The errors are probably due to the time decorrelation between images.
- Visual inspection validation points with the support of very high resolution maps (in the area around Niamey where high resolution imagery are available over the web), shows that the system has a good capability of detecting semi-permanent water (see Fig.8).

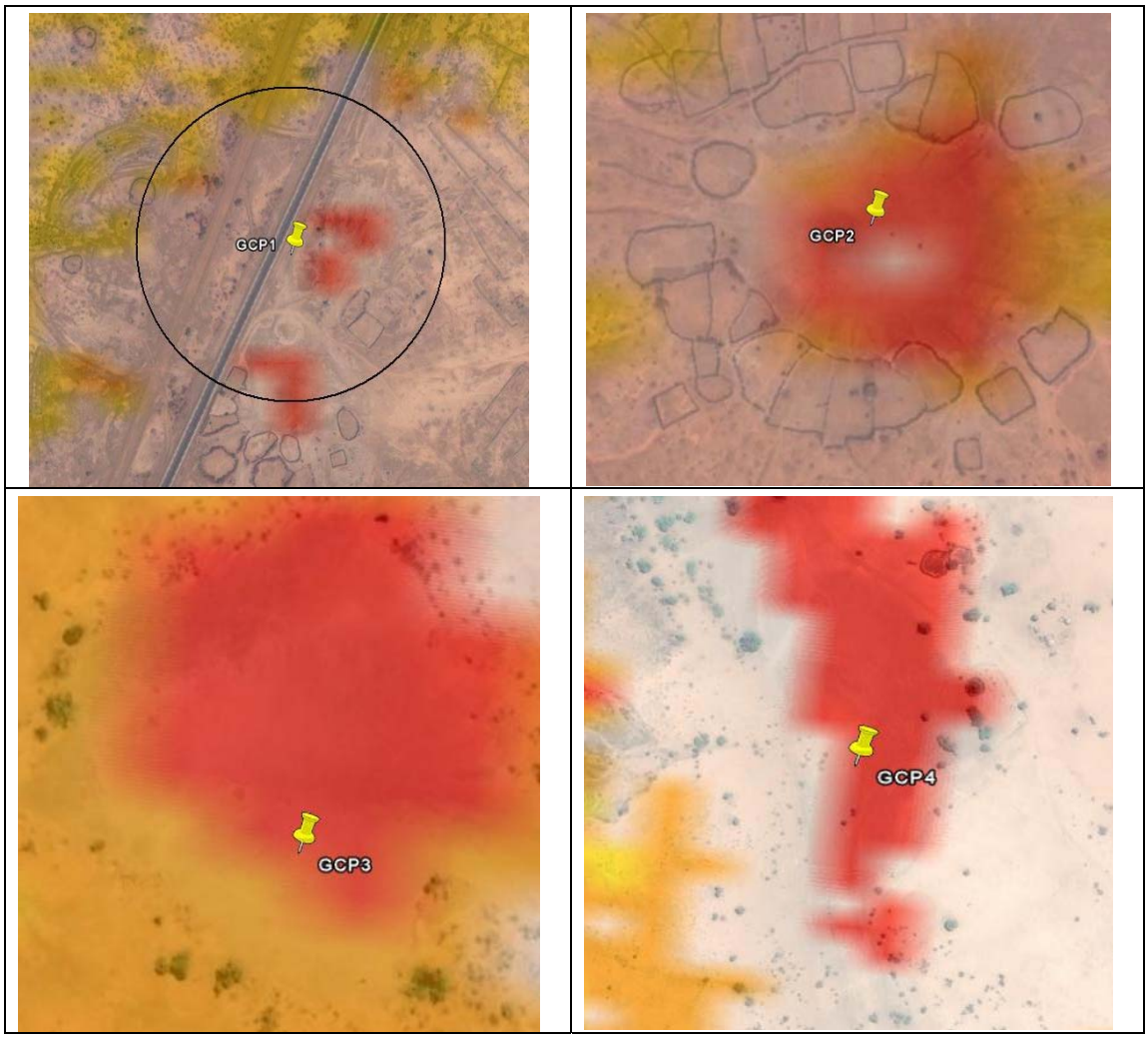

Figure 8 Examples of superimposition of the classification map (water = red) over the very high-resolution images corresponding to four ground control points.

The quality of the map of suitability for groundwater occurrence has been preliminarily assessed by comparing it against the field piezometric measurements. For this comparison, very few reference data were used, corresponding to measurements made in May 2005. Basically May is the month when the groundwater is at its lowest level. Fig. 9 shows a good correlation between these measurements and the suitability map.

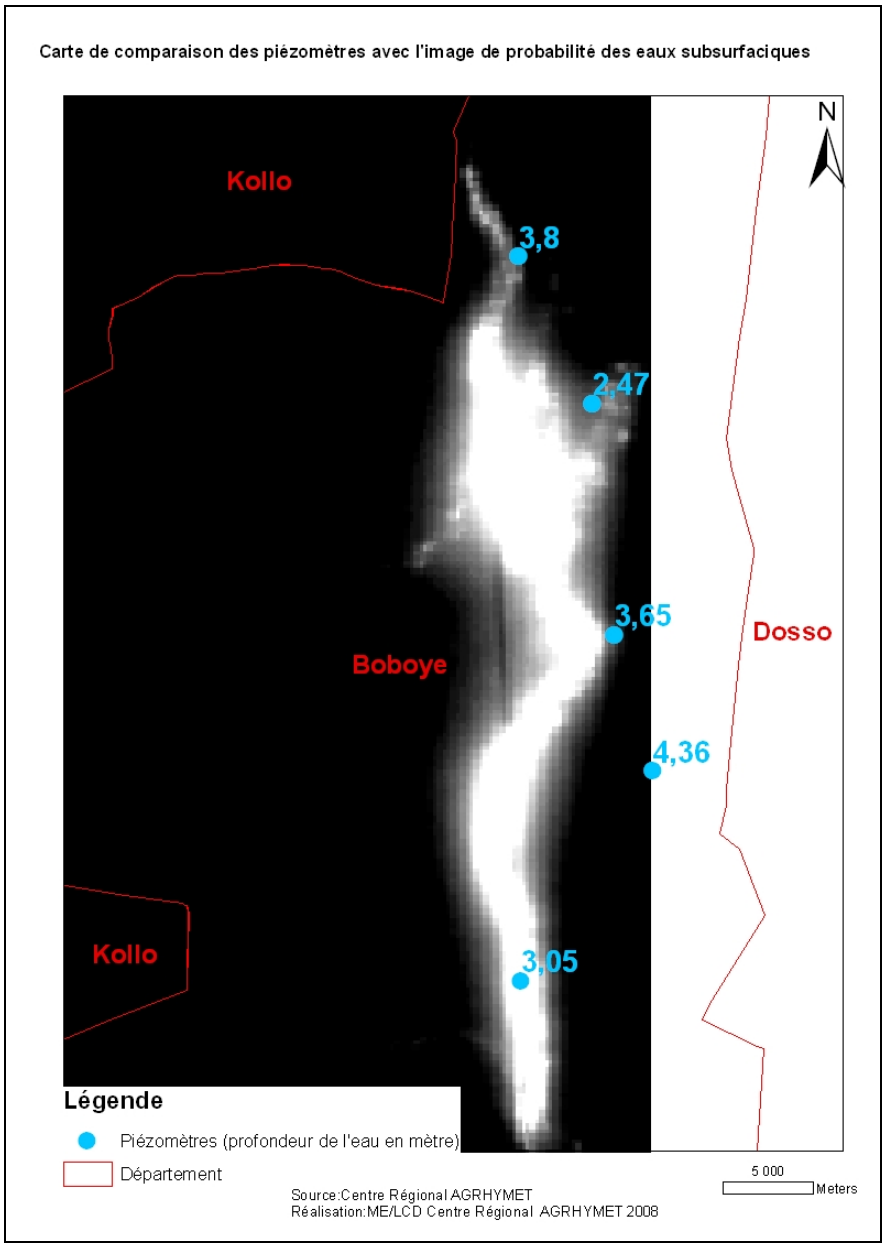

Figure 9 Superimposition of the ground piezometric measurements over the map of suitability for ground water occurrence. Brighter colours in the map indicate higher suitability values.

6. CONCLUSION

At the conclusion of the ESA TIGER WADE project, it is important to highlight the quality of the results achieved but also the critical points encountered in terms of data availability and methodology. More than 50% of the available scenes have been discarded because they were affected by strong disturbances mainly due to the combination of superficial vegetation and wind effect on the surfaces of the water bodies. The

preliminary visual inspection over the backscattering amplitude described in the first section of this article represents an indispensable step in the procedure. This significant reduction of the available data also decreases the statistical significance of the results. Moreover, due the limited sample of frame used, the temporal variation of the water bodies in terms of monthly or seasonal variation has not been monitored. In this light, the results obtained have to be considered partial, conclusions are preliminary and further investigations are considered necessary. Nevertheless the methodology for mapping water bodies provided high accuracy results as confirmed by validation campaign conducted by Agrhymet during summer 2007 and by the comparison with the high resolution optical images.
The map of suitability for groundwater occurrence represents an innovative prototypal service. Although a methodology to validate this product has not been yet set, some preliminary comparison against ground water levels shows an encouraging correlation.

7. ACKNOWLEDGEMENT

We would like to thank Prof. Nazzareno Pierdicca of the Department of Electronic Engineering of the University of Rome La Sapienza for his precious suggestions and support during preliminary analysis of SAR data backscattering phenomena.

8. BIBLIOGRAPHY

Datcu, M., K. Seidel, and M. Walessa. 1998. *Spatial information retrieval from remote sensing images - Part I: Information theoretical perspective*. IEEE Trans. Geosci. and R.S., Vol. 36, No. 5, pp. 1431–1445.

Gonzalez, R.C., and R.E. Woods. 1992. *Digital Image Processing*. Reading, MA: Addison Wesley.

Hersbach, H., A. Stoffelen and S. de Haan, 2007. *An Improved C-band scatterometer ocean geophysical model function: CMOD5* J. Geophys. Res., 112.

Kageyama, Y. Nishida, M. and Oi, T., 2000. *Analysis of the segments extracted by automated lineament detection*, Geoscience and Remote Sensing Symposium, Proceedings. IGARSS 2000. IEEE 2000 International.

Saint-Jean R. and Singhroy V., 2000. *Hydrogeological Mapping in the Semi-arid Environment of Eastern Jordan Using Airborne Multipolarized Radar Images*; First Joint World Congress on Groundwater, Fortaleza-Ceara, Brazil, July 31 to August 4.

Schroeder M., H. Rehrauer, K. Seidel, and M. Datcu. 1998. *Spatial information retrieval from remote sensing images - Part II: Gibbs Markov fields*. IEEE Trans. Geosci. and R.S., Vol. 36, No. 5, pp1446–1455.

Ulaby, F. T., R. K. Moore, and A. K. Fung, 1986. *Microwave Remote Sensing: Active and Passive, Vol. III Volume Scattering and Emission Theory, Advanced Systems and Applications*. Dedham, Massachusetts, Artech House, Inc..

Walessa M. and Datcu M., 2000. *Model-based despeckling and information extraction from SAR images*. IEEE Trans. Geosci. and R.S., Vol. 38, No. 5, pp. 2258–2269.

Monitoring of Small Reservoirs Storage Using ENVISAT ASAR and SPOT Imagery in the Upper East Region of Ghana

Frank Annor[(1)], Nick van de Giesen [(2)], Jens Liebe[(3)]

[(1)] Kwame Nkrumah University of Science and Technology, Kumasi, Ghana, Department of Civil Engineering, costeryz@yahoo.co.uk
[(2)] Delft University of Technology, Delft, Netherlands, Faculty of Civil Engineering and Geosciences, n.c.vandegiesen@tudelft.nl
[(3)] Center for Development Research (ZEF), Friedrich-Wilhelms Universitaet, Bonn, Germany, jliebe@uni-bonn.de

Abstract Within the framework of TIGER Project 2871, a methodology has been developed that allows for the monitoring of storage in small reservoirs on the basis of ENVISAT ASAR images. ENVISAT ASAR images have the advantage that they can be acquired independent of cloud cover. A robust relation between reservoir areas, which can be observed from space, and stored volumes was developed and tested. The accuracy of the area delineation was tested by outlining reservoirs with a GPS. For a more comprehensive test, a comparison was made between SPOT images and ENVISAT ASAR images. The results show a good correlation and the observed differences were consistent with the dates at which the images were acquired.

1. BACKGROUND

The availability of small reservoirs (<100 ha) increases the coping capacity of the rural population in developing countries with respect to shocks produced from rainfall variations and drought in semi-arid regions around the world. In the Upper East region of Ghana, rain-fed and irrigated agriculture, and fishing are the main sources of income and food. The importance of small reservoirs for the local population in this region can therefore not be over-estimated, especially during droughts. These reservoirs capture excess runoff from late May to early October (rainy season) and make water available from November through early May (dry season).

The efficient management and use of the water stored in these reservoirs have very positive socio-economic impacts on the livelihoods of the inhabitants. One of the key elements in managing scarce resources such as this is to determine the availability and demand for the resource so as to allocate it efficiently and effectively in space and time. For small reservoirs, their water level or storage capacity needs to be correctly estimated and this has to be done either with ground data or by remote sensing. Within the framework of TIGER Project 2871, studies have been undertaken to delineate these reservoirs by remote sensing using Landsat and ENVISAT ASAR imagery in 2002 and 2006 respectively. These efforts were successful, especially in the Upper East region of Ghana, West Africa. Satellite imagery, both optical (Landsat, SPOT) and ENVISAT ASAR, were used to determine the number, spatial distribution and storage volumes of the reservoirs for effective water management and reservoir planning.

This report shows how SPOT imagery could be used to check on a large scale the quantity of water stored in small reservoirs obtained from ENVISAT ASAR imagery or other imagery. SPOT's high spatial resolution (2.5 m) and easy interpretation allows for a very precise delineation of small reservoirs. The reason ENVISAT ASAR is still needed for monitoring small reservoirs over time is that they can be acquired independent of cloud cover and hence could be used all year round. Optical satellite sensors, like SPOT and Landsat are much easier to interpret than ASAR but are affected by cloud cover. In the semi-arid tropics,

100% cloud cover occurs for most of the day, especially during the hydrologically interesting wet season (May-October). Almost all available optical images available for West Africa are, therefore, from the dry season (October-May).

2. RESEARCH METHODOLOGY

2.1 Study area

The study area was the Upper East Region of Ghana, West Africa. The Upper East Region is a relatively poor and densely populated area within Ghana. The development of water resources in this area is of crucial importance. A map and some main characteristics of the area are presented in Figure 1.

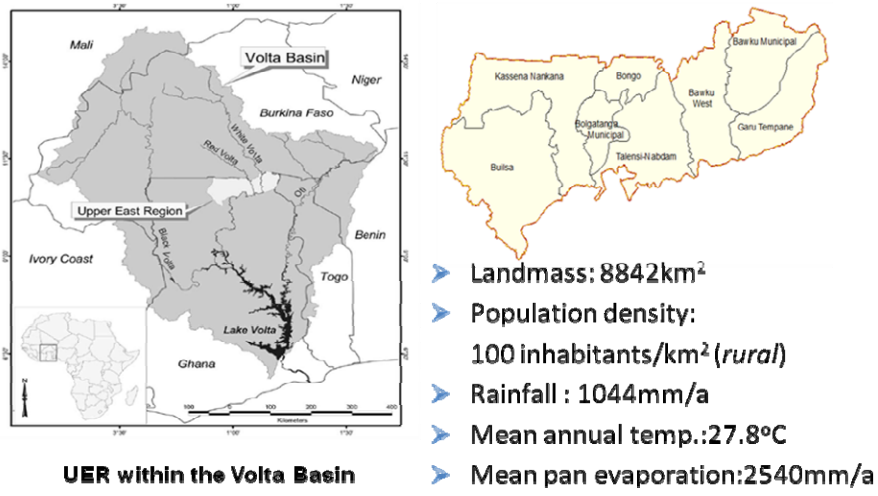

Figure 1 Ghana's Upper East Region.

2.2 Previous work

Liebe et al. (2005) used Landsat images (Fig.2) to delineate small reservoirs in the Upper East region of Ghana. The results show a very good correlation between the Surface area and Volume acquired on the field and that from the satellite imagery (Equation 1 and 2):

$$Area_{field} = 0.9366\, Area_{sat} - 0.7746 \quad (ha) \qquad (1)$$

$$Volume_{reservoir} = 0.00857\, Area_{sat}^{1.4367} \quad (m^3) \qquad (2)$$

A similar study carried out in 2007 using ENVISAT ASAR (Fig.3) produced almost the same results (Annor, 2007) as shown in equations 3 and 4, thereby confirming the robustness of the equations and the usability of satellites for monitoring reservoir areas and volumes:

$$Area_{field} = 0.93\, Area_{sat} \qquad (3)$$

$$Volume_{reservoir} = 0.00875\, Area_{sat}^{1.44}\ (m^3) \qquad (4)$$

The survey, on which Eq. (3) and Eq. (4) are based, was undertaken in February and September 2007. During these measurement campaigns, with a hand-held Garmin76 GPS, a boat and an echo-sounder, the outline and depth (bathymetric survey) of 15 small reservoirs were taken and superimposed on the satellite imagery.

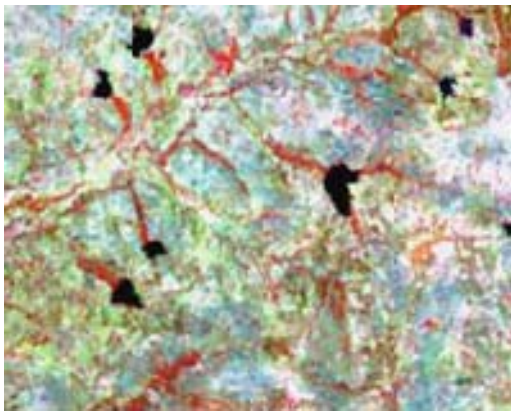

Figure 2 Typical example of small reservoirs (dark shapes) in a Landsat image as used in Liebe et al. (2005).

Figures 2 and 3 emphasize the different characteristics of optical (Landsat) and SAR (ENVISAT ASAR) images. Optical images are relatively easy to interpret and open water tends to stand out as very dark areas. Under wind-free or low wind conditions, water is also dark in SAR images but the contrast is less and the images have a grainy texture that is difficult to interpret.

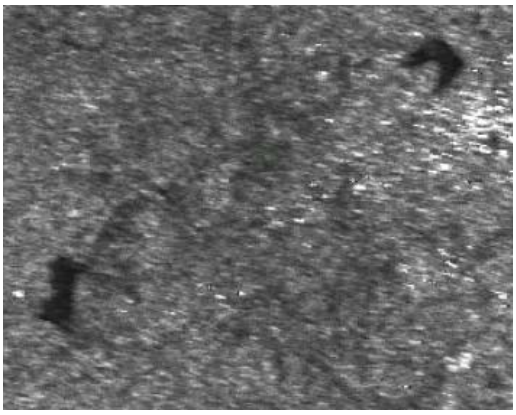

Figure 3 Typical examples of small reservoirs (dark shapes) in an ENVISAT ASAR image as used in Annor (2007).

2.3 Processing of satellite images

Two SPOT images were acquired through the OASIS initiative within the TIGER project. The time of overpass was January 2006 and a small window from these scenes is shown in Figure 4. An important advantage of the optical SPOT images is their high resolution. Because the contrast between land and open water is again very clear, delineation, whether by hand or computer, gives very precise results. The outlines obtained with the SPOT image were superimposed on the outlines obtained in the field and that of the ENVISAT ASAR imagery (with overpass times in February and September). Details on the processing of the ENVISAT ASAR imagery using Erdas Imagine and ArcGIS can be found in Annor (2007).

3. RESULTS

Two comparisons are presented here. The first comparison concerns the one between areas observed in the SPOT images and outlines as obtained by ground observations. The ground campaign was designed to ground truth the ENVISAT images that were acquired in February, whereas the SPOT images were acquired in January. The correlation between the two sources of information is very strong but the earlier SPOT

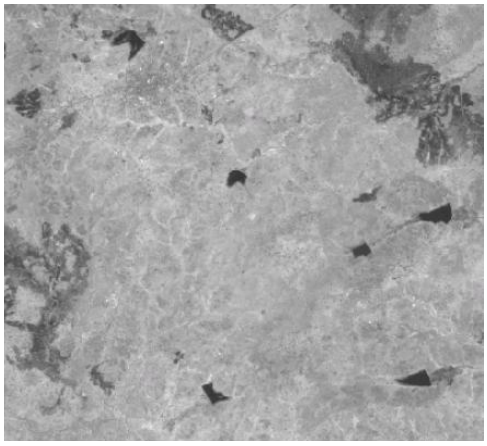

Figure 4 Typical examples of small reservoirs (dark shapes) in a SPOT image as used in this study.

images overestimate the ground-based areas with 37%. This is consistent with the fact that this is the time of year in which the water losses from reservoirs through irrigation and evaporation are the highest.

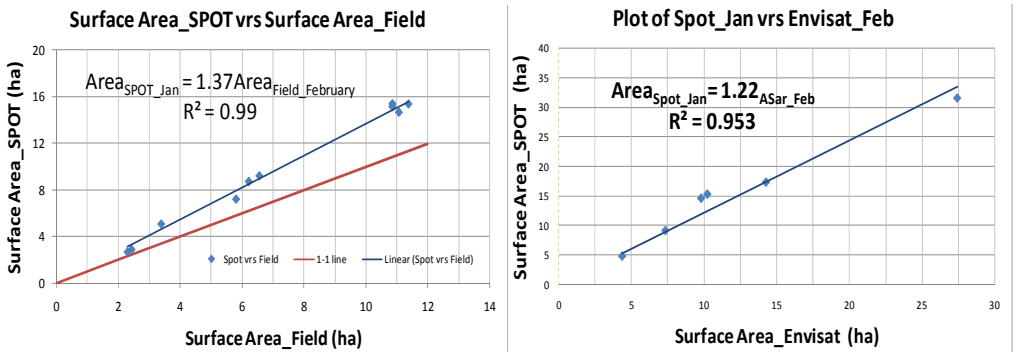

Figure 5 Comparisons between SPOT and field data (left) and SPOT and ENVISAT ASAR data (right).

The second comparison concerns the one between SPOT and ENVISAT ASAR images. A similarly good correlation is found with the January SPOT images giving 22% larger areas than the February ENVISAT ASAR images. This is, again, consistent with the high water use during this part of the year. The difference between the two comparisons points to the fact that the ENVISAT ASAR led to a slight overestimation of the areas as compared to the field observations. It should also be noted that delineation with ENVISAT ASAR is more difficult and prone to larger errors due to the coarser pixels and noisier land/water transition. The comparison over time underlines the usefulness of satellite images for monitoring storage volumes. Using Eq. 2, it can be concluded that almost 40% of the stored volumes are used in the brief period of two months from January to February.

4. CONCLUSION

In accordance with the expectation, the SPOT data correlate well with observations from the field and those based on ENVISAT ASAR images. The ease with which SPOT images can be interpreted and their high resolution would make SPOT the preferred tool for monitoring of small reservoirs over time. Given, however, the fact that cloud cover hinders the acquisition of SPOT images through most of the year makes that the use of ENVISAT remains necessary.

5. ACKNOWLEDGEMENTS

All satellite imagery used for this study was supplied through ESA's TIGER initiative under project 2871 "SAR imagery for the inventory and monitoring of ensembles of small reservoirs in the Volta and Limpopo basins: runoff, evaporation, and irrigation". Field work was supported through the Small Reservoirs Project (www.smallreservoirs.org) of the Challenge Program Water for Food.

6. REFERENCES

Annor F. O. 2007. *Delineation small reservoirs using radar imagery in a semi-arid environment: A case study in the Upper East Region of Ghana*. MSc. thesis, WM.07.06, UNESCO-IHE, The Netherlands.

Liebe, J., van de Giesen, N. and Andreini, M. 2005. Estimation of small reservoir storage capacities in a semi-arid environment: A case study in the Upper East Region of Ghana. *Physics and Chemistry of the Earth*, 30, 448–454.

Recognition of Flooding Patterns in the Okavango Delta using ENVISAT ASAR Images

Philipp Meier[(1)], Christian Milzow[(1)], Lesego Kgotlhang[(1,2)], Wolfgang Kinzelbach[(1)]

[(1)] Institute of Environmental Engineering, ETH Zurich, E-mail: philipp.meier@ifu.baug.ethz.ch
[(2)] Department of Water Affairs, Gaborone, Botswana

Abstract The Okavango Delta, one of the world's largest inland deltas, is a seasonally flooded wetland where most of the incoming water is lost by evaporation. The analysis of the temporal and spatial dynamics of flooding patterns provides valuable information for the evaluation of the performance of hydrological models. In such a large and poorly accessible area, the application of remote sensing techniques provides unique information. The major shortcoming of remote sensing data acquired in the range of visible light or infrared is the dependence on atmospheric conditions and the sun as external radiation source. In this article a method of classification of SAR (Synthetic Aperture Radar) images is presented whose quality is influenced neither by clouds nor by solar radiation. It is shown that this method is capable of classifying inundated areas at a small scale structure level. The seasonal dynamics of the total flooded area is reproduced correctly. Yet the classification of flooded vegetation is afflicted by the superposition of effects due to different surface characteristics if flooded vegetation and open water surfaces are situated within the same pixel. An improvement could be achieved by using reference data or by including the history of a pixel in classification procedures.

1. INTRODUCTION

The Okavango Delta situated in the northern part of Botswana is one of the world's largest inland deltas (Fig. 1). The Okavango has its source in the humid subtropical highlands of Angola and flows after a course of about 1 600 kilometres into the Okavango Graben. By depositing dissolved solids and suspended sediments the Okavango forms a huge alluvial fan in this graben. The permanent swamp and the seasonally flooded areas in the Delta provide the habitat of a tremendous number of species. In the Southern African region pressure on water resources is generally increasing. A growing population, industrialization and a generally higher standard of living demand the development of new water sources.

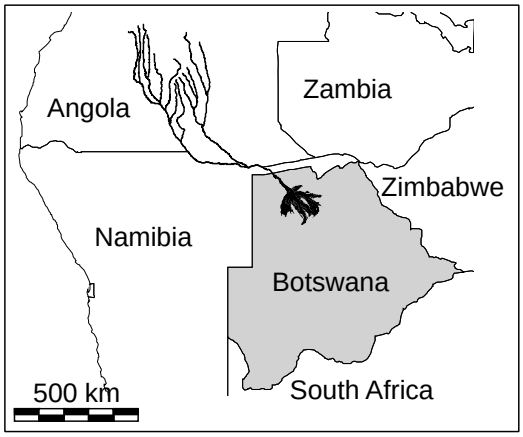

Figure 1 Location of the Okavango Delta.

To assess the impact of water management schemes it is necessary to understand how the flooded area, its spatial distribution and its temporal dynamics are changed by these schemes (Bauer et al., 2006). If these changes are modeled in a distributed manner, the model must be targeted at predicting flooding patterns correctly. Thus a calibration or a performance assessment of the model should be based on that distributed information on the inundation state (Milzow et al., 2008).

The extent of the flooding in the wetlands is driven by strongly seasonal discharge. The movement of the flood wave across the delta is slow: starting from April it takes about four to five months to traverse a distance of 250 km from Mohembo in the north-west to Maun in the south-east of the delta. The low gradient and the limited local relief cause the seasonal flood to spread laterally by overland flow, expanding the area of the wetland (McCarthy et al., 2000). As the flood wave expands, it encounters dry ground and infiltrates, raising the groundwater table. Local summer rains have a more regional influence by raising the water table and consequently reducing the amount of water infiltrating from the river channels. The outflow of the Delta at Maun is a good proxy for the extent of seasonal flooding. A high discharge is an indicator for a wide spread of inundation (McCarthy et al., 2000). However, the spatial distribution of flooding, which is an important parameter for the ecosystem, cannot be derived from a discharge measurement.

The large extent and the limited accessibility of the Delta constrain the direct acquisition of spatial information on the ground. The application of remote sensing techniques therefore is very attractive. Seasonal flooding patterns derived from satellite imagery can provide valuable information. Yet, the applicability of remote sensing data has to be reviewed for each dataset. The exposure of the vegetation to seasonal variation and the small-scale topography result in complex patterns of land cover in the delta. Therefore the data suited for the purpose need to have a relatively high spatial and spectral resolution (Neuenschwander et al., 2005).

The most extensive time series of flooding patterns was obtained by McCarthy et al. (2003) using NOAA AVHRR (Advanced Very High Resolution Radiometer) images from 1972 to 2000. The classification of flooded areas was carried out using an unsupervised clustering algorithm and later evaluated using classified Landsat images. The coarse resolution of 1 km was found to be inhibiting the detection of small-scale structures such as small islands, lagoons and channels. Although the temporal dynamics of the flooding was reliably reproduced, the clustering algorithm leads to an overestimation of the flooded area due to the strong influence of relatively small wet areas on the whole pixel (Milzow et al., 2008). The need for the application of data with higher resolution was also pointed out by Wolski and Murray-Hudson (2006). On Landsat images with a resolution of 30 m, dry and inundated areas could be separated well whereas the large overlap in spectral characteristics of densely vegetated permanent swamp and riparian woodlands did not allow a correct classification.

One major drawback of optical systems is their dependency on an external radiation source and the presence of clouds compromising the data. Active microwave systems such as SAR (Synthetic Aperture Radar) systems provide an alternative to retrieve surface data without being dependent on solar radiation and with almost no influence of clouds. This article presents a method to derive flooding patterns from ENVISAT ASAR (Advanced SAR) satellite images.

2. FLOODED AREAS FROM SAR IMAGES

In this study Wide Swath Level 1 data from the ASAR instrument operating in C-band (5.6 cm wavelength) on board the ENVISAT satellite were used. The data have a pixel spacing of 75 m and the transmitter-receiver polarization HH (horizontal/horizontal) was used. Each data point only consists of the intensity of the backscattered signal. These data are acquired by the satellite approximately once a month.

Radar remote sensing techniques have been proven to be an important data source for monitoring hydrological processes. The sensitivity to open water surfaces and to soil moisture in the top soil layer offer a large potential for mapping changes in earth surface properties related to water while being nearly independent of weather conditions and completely independent of daytime (Bartsch et al., 2004; Rosenqvist and Birkett, 2002).

The interaction of the radar signal with the earth surface is controlled by the parameters surface roughness and dielectric constant. A high dielectric constant leads to high reflectivity whereas a high surface roughness leads to high scattering. Due to the high dielectric constant and the generally smooth surface, open water surfaces are characterized by a low backscattering intensity on radar images (Fig. 2).

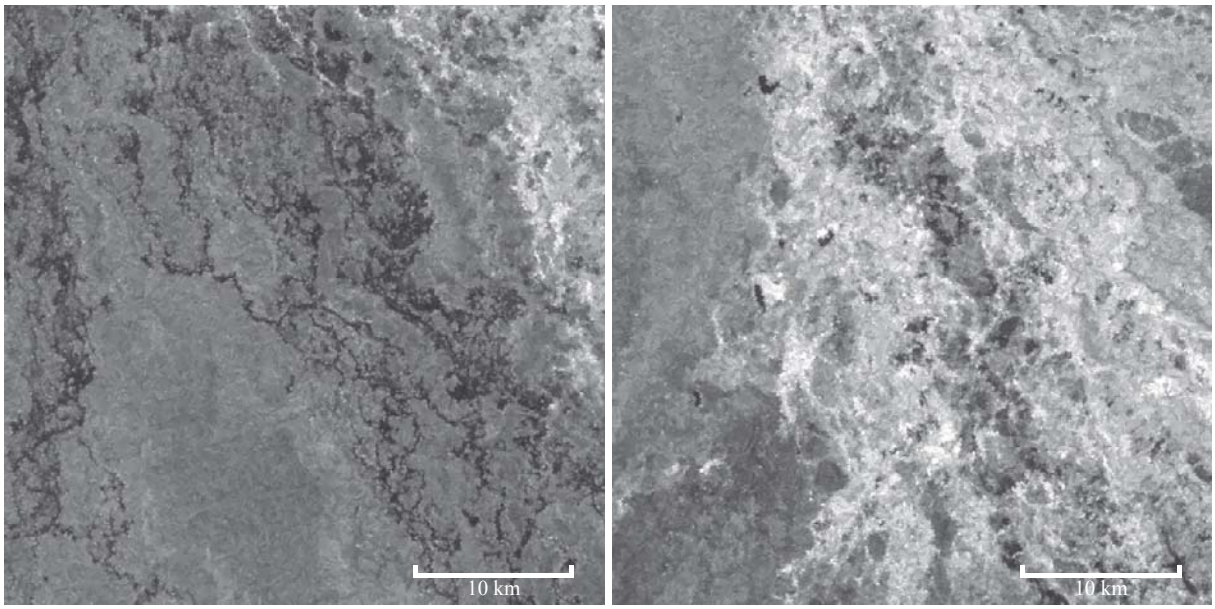

Figure 2 Open water surfaces are characterized by a low backscattering intensity (left) whereas flooded vegetation is represented by a high intensity (right). (Part of the Okavango Delta on an ASAR image acquired on July 11, 2005.)

At wavelengths of 23.5 cm (L-band) or longer, radar signals can penetrate forest canopy which allows to see inundation through plants covering the surface. In forested areas microwave signals interact within the vertical forest profile with branches and trunks. However, the intensity of the backscattered signal depends strongly on ground properties. Dry ground causes a diffuse and attenuated backscattered signal whereas the smooth surface of flooded ground leads to a significantly higher signal due to dihedral reflection between the water and trunks (Rosenqvist et al., 2002).
The effect of dihedral reflection can be observed in the Okavango wetland using C-band radar even if the radar signal does not penetrate vegetation cover. Sparse vegetation and blades of grass surrounded by water are characterized by a high backscattered signal (Fig. 2).

3. CLASSIFICATION

After despeckling and georeferencing, the identification of zones likely to flood is an important task. To be able to cut out these zones, first an approximate mask of the Okavango Delta based on a NOAA AVHRR image was applied. All further calculations are carried out only within this mask which leads to a significantly shorter computing time of the following steps.
Zones with seasonal flooding can be identified under the assumption that they are undergoing a relatively high change in surface properties over one year. Therefore the temporal variance of the backscattering intensity should be high in seasonally flooded areas. The calculation of the zones likely to flood is based on the images of 2005 which is a year known as being relatively wet. For 2005 twelve complete scenes of the area were available whereas for three further scenes a mosaic out of two images is constructed. From the resulting 15 scenes the temporal variance is calculated. Due to the spotted nature of the despeckled image and to the limited availability of images the temporal variance is strongly non-uniform in a space. On a small scale where one would expect for all pixels the same probability of being flooded the values of the temporal

variance differ significantly. To smooth the inhomogeneous appearance of the temporal variance a 5 × 5 median filter was applied. With the availability of a larger number of images this non-uniformity might be reduced and there would be no need to perform the previous step. By normalizing the variance and by applying histogram equalization a probability map was derived where the values correspond more or less directly to the probability of seasonal flooding. To further minimize the number of pixels to be processed a refined mask was derived by clipping all the pixels with a probability value of less or equal to 0.05 (Fig. 3).

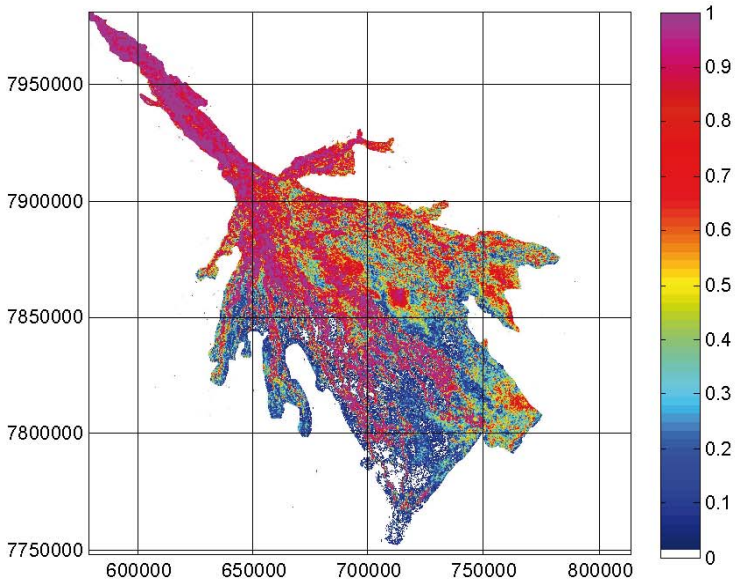

Figure 3 Zones likely to flood calculated from temporal variance. A value of 1 corresponds to a high probability of flooding (Coordinates in UTM, Zone 34).

Although the backscattered intensity of a pixel follows some regularities it is still influenced by a wide variety of determining factors. Therefore a simple classification, using threshold values, leads to unsatisfactory results. On the other hand, classification criteria should be simple enough to be easily implemented in an automatic image classification framework.

For the classification of open water surfaces and flooded vegetation a stepwise approach based on the intensity of the backscattered signal is chosen. The intensity value of a pixel, the temporal variance and the properties of surrounding pixels were taken as basis for classification. A first class of inundated pixels showing unambiguously low or high intensities respectively are classified without applying additional criteria. A second class is formed by those pixels having an intensity value within a close range to the values of the first class. As an additional constraint, the value on the probability map of that particular pixel has to be greater or equal to 0.5. The third class finally is composed of pixels in the medium-low and medium-high intensity range. For this class a stronger criterion for values on the probability map is applied. As a second constraint these pixels are classified only if they belong to a continuous cluster of which at least one is classified in the first or second class. The continuous clusters are selected from the image using a region growing algorithm.

4. RESULTS

Due to limited data availability only data of the year 2005 are distributed more or less equally over time to evaluate the seasonal dynamics of inundation. The classified picture of the maximum flood in 2005 shows that the applied method is capable of evaluating the flooding patterns in the Okavango Delta (Fig. 4). One can see clearly that in this season almost the whole panhandle (the north-western appendix) of the delta is flooded while the flood wave has already reached its southernmost positions. Small scale features like

channels can be identified as well as the permanent islands. These islands are classified as dry even if they were not clipped on the mask based on the temporal variance.

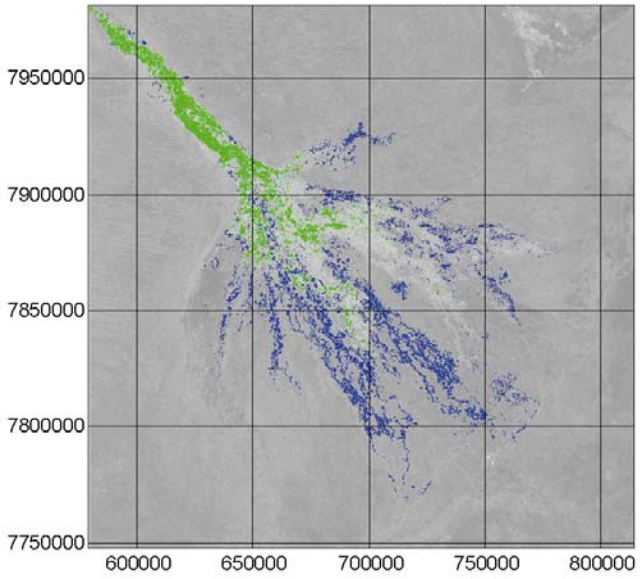

Figure 4 Inundation pattern of the Okavango Delta showing the largest measured flooding extent on June 11, 2005. Regions classified as open water are marked with blue color those classified as flooded vegetation with green colour.

The map of the flooding frequency in 2005 (Fig. 5) shows prevalently flooded areas mainly along the course of the river in the panhandle. Other more channel-like structures in the central part of the delta show a high flooding frequency. Larger continuous flooding takes place only during a short period of time. Generally the flooding frequency decreases towards the south-eastern part of the delta.

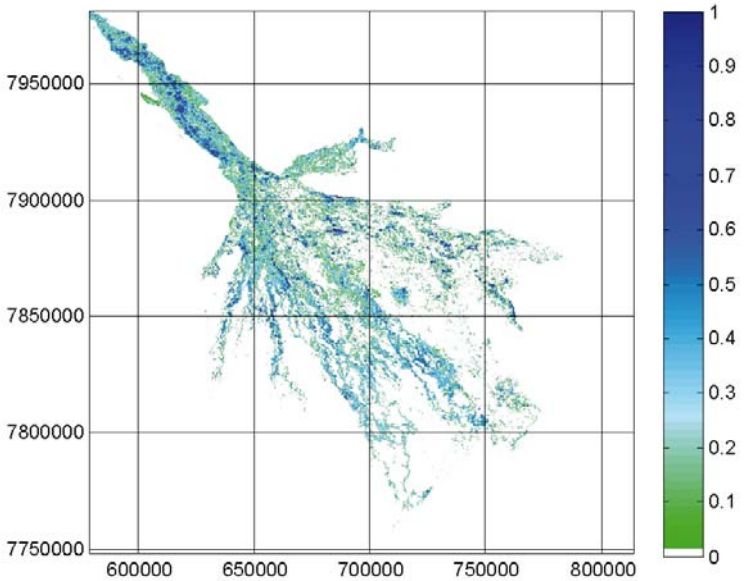

Figure 5 Flooding frequency in 2005.

The seasonal progression of the total flooded area is reproduced reliably. The inundated area increases during the first few months of the year (Fig. 6). After a short period of recession it rises again having a maximum around mid-June. The minimum flooded area is reached by beginning of December. The temporal dynamics of the total flooded area is influenced by two major processes: local rainfalls and the flood wave having its origin in the Angolan highlands. The local rainy season spans from December to March. A part of the water infiltrates directly into the groundwater, another part is running off at the surface forming small ponds and channels. Therefore the total flooded area increases for a short time during the rainy season. The flood wave from the headwater of the Okavango arrives at the delta in April. This causes flooding in large areas. The shifting of the flood wave towards the south takes up to five months with the maximum flood reaching the furthest point by beginning of September.

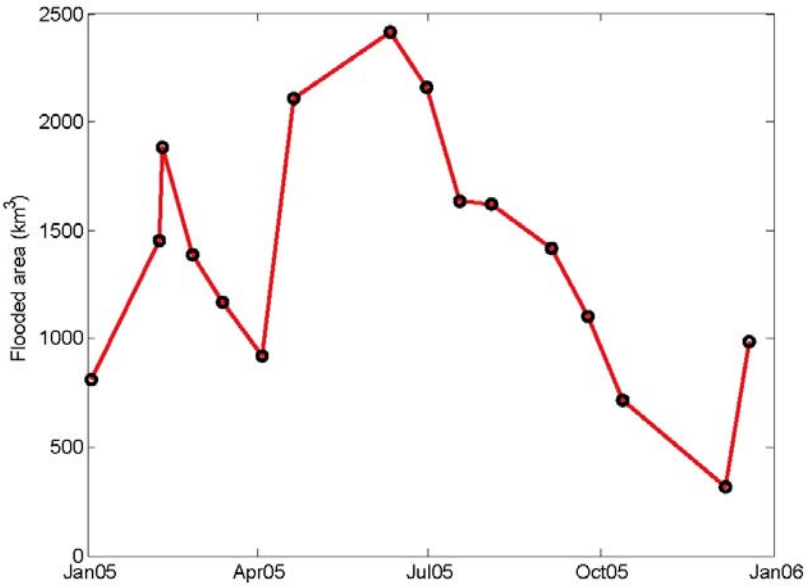

Figure 6 Seasonal progression of the total flooded area in 2005.

At the transition from open water surfaces to flooded vegetation a seam of unclassified pixels can be observed (Fig. 7). Within this area the backscattering characteristics of the water surface and the vegetation are superposed leading to an intermediate backscattering intensity. Due to the limited extension of these areas the error caused by this effect is not very large.

A far more important effect of superposition is caused by the succession of the vegetation in flooded areas. When the flood wave from the headwaters of the Okavango arrives at the delta, large areas, mostly grass land, are first completely inundated and consequently recognized by their low backscattering intensity. After a while, the vegetation starts to grow and slowly shields the water surface. The sparse vegetation, characterized by intermediate backscattering intensities, is turning denser with time until at a certain point the vegetation is dense enough to produce a high backscattering intensity. This process is evaluated for locations where water level measurements were available. In Fig. 8 this dynamics is shown at one place in the delta. As the water level starts to rise the pixel value first decreases. After some time the pixel value starts to increase reaching intermediate values first and later values in the range of those of flooded vegetation while the water is still at a high level. With a receding water level, pixels approach a value typical for dry areas. The process described above takes place in large parts of the seasonally flooded areas. This leads to an underestimation of the total flooded area.

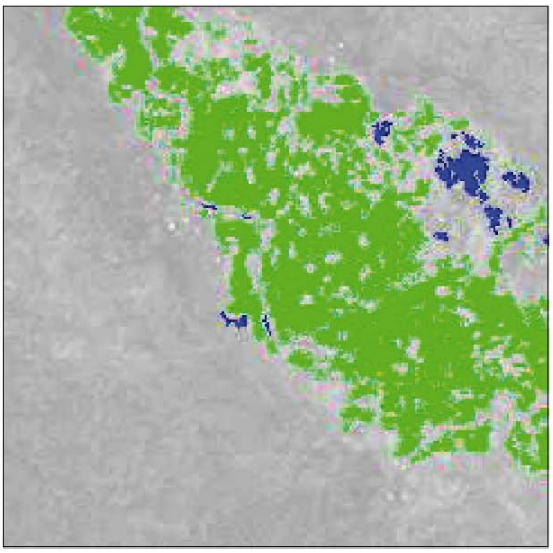

Figure 7 At the transition from open water surfaces to flooded vegetation pixels are not classified due to superposition of reflectivity characteristics.

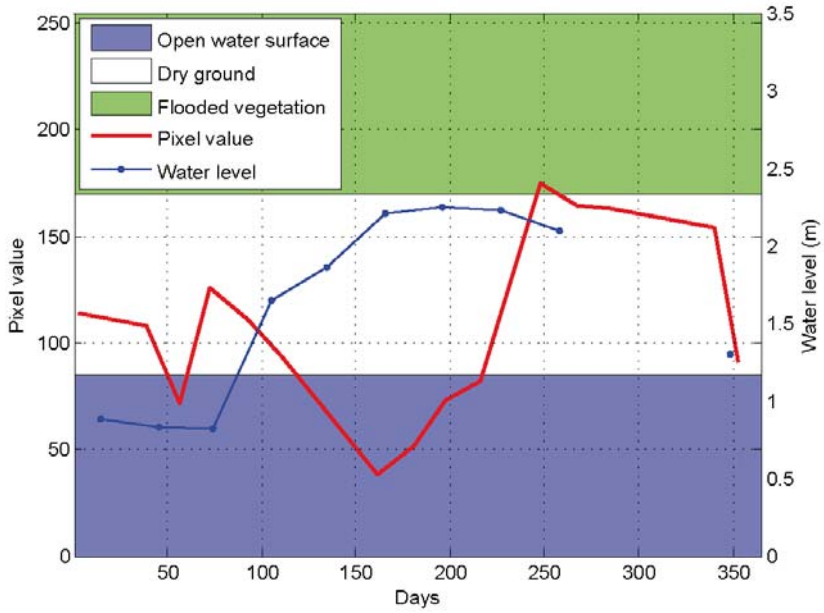

Figure 8 The seasonal trend of the scattering value of a pixel located at a gauging station compared to the water level.

5. CONCLUSIONS

The application of ASAR data is suitable for retrieving flooding patterns. There are some clear advantages compared to the application of data from satellite instruments operating in the visible range of light. The algorithm developed is capable of distinguishing flooded areas from dry areas. Not only is the dynamics of the total area reproduced but also the small-scale structures of inundation patterns. The surface properties of

open water surfaces allow the classification of open water surfaces both unobstructed and densely vegetated. The classification of pixels at the transition from open water surfaces to flooded vegetation remains difficult. The sensitivity of the chosen thresholds for the classification of each pixel can be high. Although the measured size of the total flooded area is plausible, so far no validation was carried out. To retrieve the real flooded area it is necessary to include reference data. The spatial resolution of reference data needs to be at least as fine as the resolution of ASAR data. As a reference, data in the visible light range or infrared radiation data can be used as well as aerial photographs as long as they cover a sufficiently large area. Another option could be to include the evolution of the pixel value over time. If the history of each pixel is known, classification can be based on the typical cycle which was observed in some places in the delta. If a pixel is first classified as open water surface, than as dry ground and later as flooded vegetation the same pixel of the image can be classified as flooded retrospectively on the image in between the first and the last. This approach might be limited if data is not available in a sufficiently high temporal resolution.

6. ACKNOWLEDGMENTS

This research has been supported financially by the Swiss National Science Foundation under project Nr K-21K1-120266. The satellite images were provided by the European Space Agency trough the TIGER initiative under project ID 2977.

7. REFERENCES

Bartsch, A., Kidd, R., Pathe, C., Shvidenko, A., Wagner, W. 2004. Identification of Wetlands in Central Siberia with ENVISAT / ASAR WS Data. *Proceedings of the ENVISAT & ERS Symposium* 6-10 September 2004, Salzburg, Austria.

Bauer, P., Gumbricht, T. and Kinzelbach, W. 2006. A regional coupled surface water/groundwater model of the Okavango Delta, Botswana. *Water Resources Research* 42.

McCarthy, T.S., Cooper, G.R.J., Tyson, P.D. and Ellery, W.N. 2000. Seasonal flooding in the Okavango Delta, Botswana – recent history and future prospects. *S Afr J Sci,* 96, pp. 25-33.

McCarthy, J.M., Gumbricht, T., McCarthy, T., Frost, P., Wessels, K. and Seidel, F. 2003. Flooding Patterns of the Okavango Wetland in Botswana between 1972 and 2000. *AMBIO,* Vol. 32, No.7, pp. 453-457.

Milzow, C., Kgotlhang, L., Kinzelbach, W., Meier, P. and Bauer-Gottwein, P. 2008. The role of remote sensing in hydrological modelling of the Okavango Delta, Botswana. *Journal of Environmental Management* 90(7) 2252-2260.

Neuenschwander, A.L., Crawford, M.M. and Ringrose, S. 2005. Results of the Earth Observing-1 Advanced Land Imager (ALI) data to assess vegetational response to flooding in the Okavango Delta, Botswana. *International Journal of Remote Sensing*, Vol. 26, No. 19, pp. 4321-4337.

Rosenqvist, A. and Birkett, C.M. 2002. Evaluation of JERS-1 SAR mosaics for hydrological applications in the Congo river basin. *International Journal of Remote Sensing*, Vol. 23, No. 7, pp. 1283-1302.

Rosenqvist, A., Forsberg, B.R., Pimentel, T., Rauste, Y.A. and Richey, J.E. 2002. The use of spaceborne radar data to model inundation patterns and trace gas emissions in the central Amazon floodplain. *International Journal of Remote Sensing*, Vol. 23, No. 7), pp. 1303-1328.

Wolski, P. and Murray-Hudson, M. 2006. Reconstruction 1989- 2005 inundation history in the Okavango Delta from archival landsat TM imagery. *Proceedings of Globwetland: Looking At Wetlands From Space*, Frascati Italy, 19-20 October 2006.

Soil moisture dynamics from Synthetic Aperture Radar for Hydrometeorological Applications in the Southern African Development Community

Annett Bartsch[(1)], Daniel Sabel[(1)], Carsten Pathe[(1)], Scott Sinclair[(2)], Theo Vischel[(2)*], Marcela Doubkova[(1)], Wolfgang Wagner[(1)], Geoff Pegram[(2)]

[(1)] Institute of Photogrammetry and Remote Sensing, Vienna University of Technology, Austria, E-mail: ab@ipf.tuwien.ac.at
[(2)] Civil Engineering Programme, University of KwaZulu-Natal, Durban 4041, South Africa
* Now at: Laboratoire d'étude des Transferts en Hydrologie et Environnement (UMR 5564), 38000 Grenoble, France

Abstract A soil moisture monitoring service for the region of the Southern African Development Community (SADC) has been developed within the ESA TIGER Innovator project SHARE (www.ipf.tuwien.ac.at/radar/share). This service addresses one of today's most severe obstacles in water resource management which is the lack of availability of reliable soil moisture information on a dynamic basis. The spatial resolution of the product is 1 km and data are available up to twice per week for southern Africa since December 2004. In this paper the assessment of the new extensive soil moisture dataset is presented. This includes the comparison with other remotely sensed products (precipitation) and ground measurements. River runoff measurements reflect the hydrological state of the upstream basin. Thus, the relationship of relative soil moisture and river runoff has been investigated. Correlations of >0.9 (R^2) are found for subtropical basins with respect to a catchment specific temporal offset. If knowledge is established about this relationship and also the spatial patterns, flood risk assessments can be enhanced. Soil moisture deficits can be identified once a sufficiently long time series becomes available.

1. INTRODUCTION

This document provides an overview of validation activities carried out within the framework of the ESA TIGER Innovator project SHARE. SHARE aims at enabling an operational soil moisture monitoring service for the region of the Southern African Development Community (SADC). The long-term vision of SHARE is to supply soil moisture information for the entire African continent, at a resolution of 1 km, posted on the web, freely accessible to all. Validation is a major prerequisite for such a service.

The soil moisture information system is based on the newest radar satellite technology. The service uses data delivered by ENVISAT's ASAR sensor operated in global mode (GM) and the METOP scatterometer sensors. The synergistic use of both systems allows frequent, medium resolution monitoring of regional soil moisture dynamics.

SHARE provides access to three products: coarse resolution soil moisture, a scaling layer which allows interpretation of the coarse resolution soil moisture product at 25 km resolution and a medium resolution soil moisture product at 1km.

1. Medium Resolution Soil Moisture: The medium resolution soil moisture product is based on ENVISAT ASAR Global Mode data. ENVISAT ASAR Global Mode data allows monitoring of soil moisture for the entire Southern African Development Community (SADC) region on a weekly basis at 1 km resolution, however with a higher noise level compared to the coarse resolution soil moisture product. The ASAR global mode data represent soil moisture in the upper most soil layer (<5 cm) and is developed for applications

such as drought, yield, and flood forecasting or modelling (Figure 1) (Wagner et al., 2007; Pathe, et al. in press; Bartsch et al., 2007).

2. Coarse Resolution Soil Moisture: Global, coarse-resolution soil moisture data (25-50 km) are derived from backscatter measurements acquired with scatterometers on-board of the satellites ERS-1 and ERS-2 (1991 to present) and the three METOP satellites (2006–2020, in near real time via EUMETCast) (Figure 2) (e.g. Wagner et al., 2003; Bartalis et al., 2007).
3. Scaling layer: The scaling layer has been derived from ENVISAT ASAR Global Mode data. The scaling layer allows the interpretation of coarse-resolution soil moisture information as provided by the scatterometer data at 1 km resolution by identifying targets which have similar backscatter characteristics as observed with the scatterometer. The soil moisture variations of these local targets will follow the variations observed in the scatterometer derived soil moisture (Wagner et al., 2008).

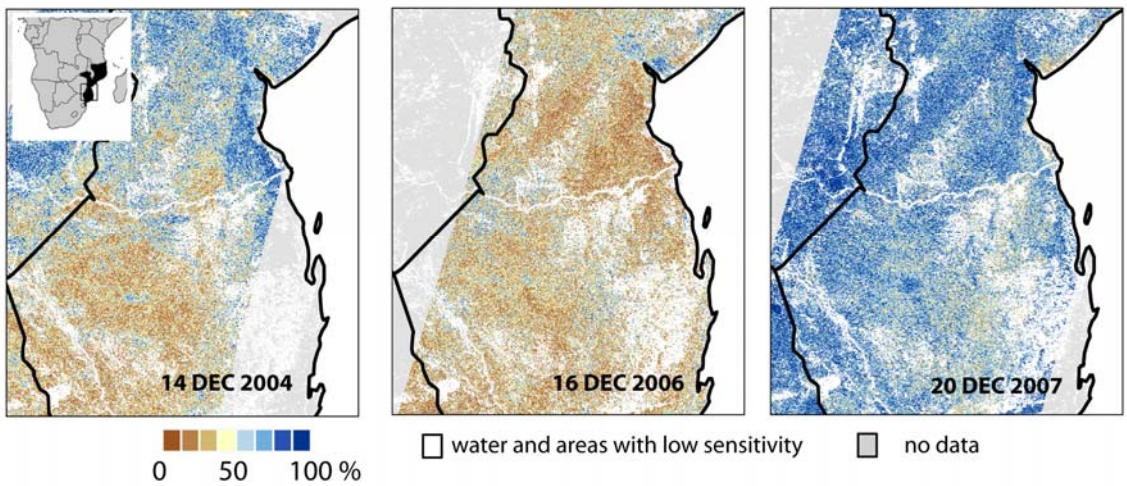

Figure 1 Example maps from the ENVISAT ASAR GM 1km database. Extreme soil moisture conditions in the second decade of December 2007 in central Mozambique can be observed with the 1 km soil moisture product from ENVISAT ASAR. Comparison with other mid-December ASAR GM acquisitions from 2004 and 2006 demonstrates the above-average soil moisture conditions in greater detail.

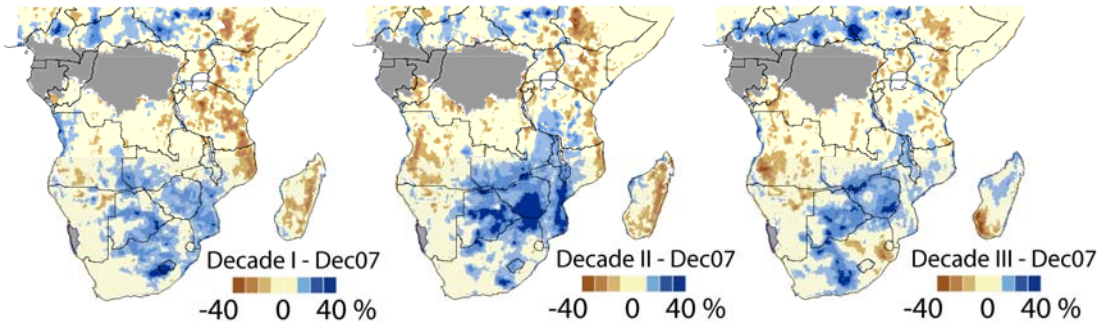

Figure 2 Example for the scatterometer soil moisture database. Above-average soil moisture conditions were encountered over the entire region of southeastern Africa in December 2007. Soil moisture deviations reached 30% above-average in central South Africa and Lesotho during the first decade of December. These conditions extended further north during the second decade of December and caused soil moisture extremes in northern South Africa, Mozambique, Botswana, and Zimbabwe. The soil moisture was still well above-average in southeastern SADC in the third decade of December. However, a declining trend in soil moisture deviations was apparent. Below-average soil moisture conditions were affecting regions of eastern Tanzania, Kenya and Sudan in all three decades of December 2007.

Here we present a summary of the assessment of (1) and (2). The quantitative assessment was based on (a) Transfer of the approach to a different region with ground data availability, (b) Comparison with modelled soil moisture in South Africa, and (c) River runoff comparison on catchment scale in Botswana/Angola. Precipitation data have been used for a qualitative assessment of the 1 km soil moisture product.

2. COMPARISON WITH MODELLED AND IN-SITU SOIL MOISTURE

2.1 Model comparison

TOPKAPI is an acronym which stands for TOPographic Kinematic APproximation and Integration and is a physically-based distributed rainfall-runoff model. TOPKAPI requires ground measurements which have been available in the past in the South African catchment Liebenbergsvlei. Currently sufficient measurements/stations are not available. This assessment approach can therefore only be used for the scatterometer derived soil moisture product which is available from the ERS satellites for 1992-2000.

Hydrological modelling is a suitable framework for providing estimation of the soil moisture fields as an alternative to soil moisture gauging. This approach provides contributions to (i) validation of remotely sensed soil moisture fields on the basis of a physical representation of the hydrological processes, (ii) possibilities for space and time disaggregation of the remotely sensed soil moisture field. In this work the physically distributed hydrological model TOPKAPI (Liu and Todini, 2002) was implemented on a well-documented regional catchment in South Africa (Liebenbergsvlei, 4825 km^2). The Liebenbergsvlei catchment (4825 km^2) is located in the Free State province of South Africa. The climate is semi-arid, characterized by a mean annual rainfall between 600 and 700 mm and a mean annual evapotranspiration between 1400 and 1500 mm. A unique rain gauge network consisting of 45 tipping bucket rain gauges provided 5 minute time step ground rainfall measurement for the period 1993-2002. Two flow gauges are available at the outlet of the catchment and further upstream, with unequal data availability and quality between 1993 and 2001 but both provide good quality data since 2002. External flows that arrive from Lesotho via an inter-basin transfer since September 1997 are recorded at a third station.

The TOPKAPI model has been implemented on the Liebenbergsvlei catchment, South Africa. Because of its physical basis, the model parameters (15 parameters) can be estimated a priori from the catchment characteristics. The spatial resolution for the modelling was imposed by the desire to use a freely available DEM at 1 km. Two seasons of 8 months each were selected during which the rainfall and flow data were both continuous and of good quality. The first season (Season 1) between November 1993 and June 1994 was used to adjust the parameters of the TOPKAPI model. The second season (Season 2) between November 1999 and June 2000 is used further as a model validation period. Four parameters of the model and the catchment initial soil moisture were calibrated during Season 1 in order to ensure that the simulated river flows properly match the observed river flows. Over the two modeled seasons, the only remotely sensed soil moisture estimations available come from the Soil Water Index provided within the ERS1/2 product. A similar Soil Water Index can easily be defined for TOPKAPI by computing the soil saturation at each catchment cell, for each time step of the simulation.

Since the resolution of the hydrological model and the resolution of the scatterometer grid differ (respectively 1 km and 25 km), as a first comparison, (i) a mean modeled SWI was computed at catchment scale by averaging over the catchment the SWI computed at each TOPKAPI cell, (ii) a mean remotely sensed SWI was computed by averaging over the catchment the SWI computed at each scatterometer point grid (average weighted according to Thiessen polygons).

The modeled and remotely sensed mean catchment SWI are compared for the two modeled seasons, at the time step of ten days imposed by the ERS sampling period (Vischel et al. 2008). There is a very good correspondence between the two SWI estimates that is illustrated by the coefficient of determination (R^2) of 0.780 for the first season and 0.922 for the second season. According to the regression equation, a slight bias is observed which seems to be independent of the season. But the order of magnitude of the remotely sensed

and the modeled SWI is similar. As an interesting example, the value of the initial soil moisture, which has been calibrated at 40% according to the river flows for Season 1 (independently of the remote sensing data), could have been better estimated by using the remotely sensed value. This result is very encouraging since the initialization of the hydrological models remains a constant problem in hydrology.
In order to evaluate the relationship between the remotely sensed and the modeled soil moisture at a smaller scale, the SWI is computed at the footprint scale meaning at the original scale of the scatterometer. In order to make a robust comparison, only the three footprints showing the largest covering over the catchment are considered. Figure 3 shows respectively the remotely sensed and the modeled footprint SWI and the associated scatter plots. The results show that the good correspondence already found at catchment scale is retrieved at the smaller scale of the footprint. The correlations are still very good (greater than 0.7), while according to the regression equations, the bias between the two SWI is relatively stable and independent of season and location.

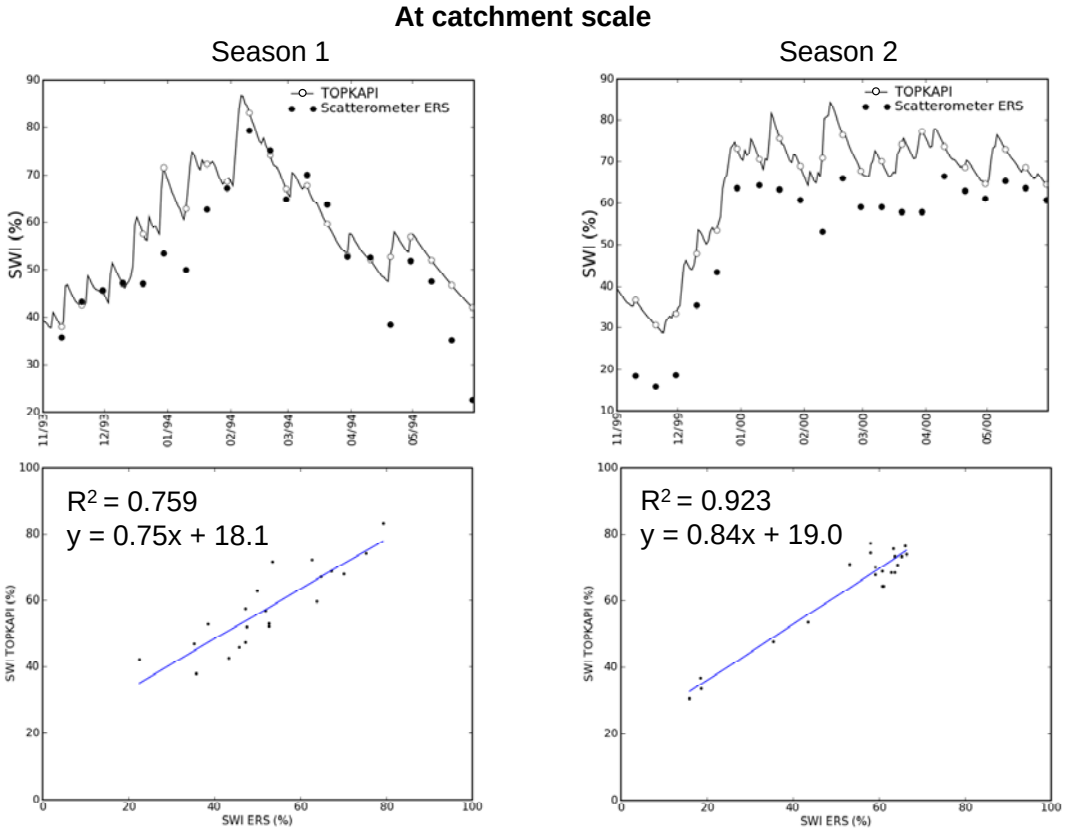

Figure 3 Comparison of the modelled and remotely sensed Soil Water Index (SWI) at the scatterometer footprint scale (from Vischel et al., 2008).

2.2 In-situ soil moisture measurements

A sufficiently large and representative ground measurement network is required when remotely sensed data are compared to in-situ point data. Such a network has not been available for SADC; therefore this kind of validation was carried out over Oklahoma, USA. The Oklahoma Mesonet is a statewide meteorological measurement network operated by the Oklahoma Climatological Survey. Standard meteorological data (e.g. air temperature, precipitation, humidity, etc.) are measured automatically every 5 minutes at 115 stations, at least one in each of Oklahoma's 77 counties. Amongst the sensors installed at each site, there are soil moisture sensors at 4 depths (5 cm, 25 cm, 60 cm and 75 cm) utilizing the heat dissipation method for indirectly measuring the soil matric potential. The soil matric potential is derived from the temperature

difference before and after heating using a second-order polynomial. This conversion requires individual calibration of the soil moisture sensors at each site. Data are collected at regular intervals and are transmitted to a central processing site for archiving and further data analysis (Brock et al., 1995; Illston et al., 2004a; McPherson et al., 2007). To handle the problem of comparability between measurement stations, a new parameter has been developed based on the measurements of the heat dissipation sensors. This parameter is called fractional water index (FWI) and is a normalized version of the actual measurements of the soil moisture sensors. With the FWI a state-wide analysis of soil moisture conditions and comparisons between individual measurement sites is possible. The FWI is a unitless measure ranging from 0 at dry conditions to 1 for saturated soils (Illston et al., 2004b).

Based on a comprehensive archive of ENVISAT ASAR Global Mode data, surface soil moisture values were extracted using a multi-temporal change detection approach. Comparisons of the remotely sensed surface soil moisture m_s to *in-situ* soil moisture showed a good agreement between the two data sets. The ASAR GM surface soil moisture m_s follows temporal trends in the *in-situ* FWI soil moisture data. Extreme high and low soil moisture conditions in the field are reflected in the remotely sensed data. Scatterplots of in-situ soil moisture vs. remotely sensed soil moisture m_s have been generated to characterize the relation between the two data sets (Pathe et al., 2007).

As an example for the Mesonet stations, Figure 4 shows results for station "OKEM". From the time-series plot, it can be seen, that extreme high or low FWI values correspond to extreme high or low GM surface soil moisture values m_s. A linear relation between remotely sensed and *in-situ* soil moisture has been observed. Pearson's linear correlation coefficient R was used to characterize the relation between the m_s and the FWI data for all Mesonet stations. In the case of the station "OKEM", a correlation coefficient of R=0.84 has been calculated. Correlation coefficients R>0.6 were observed for 54% of the stations.

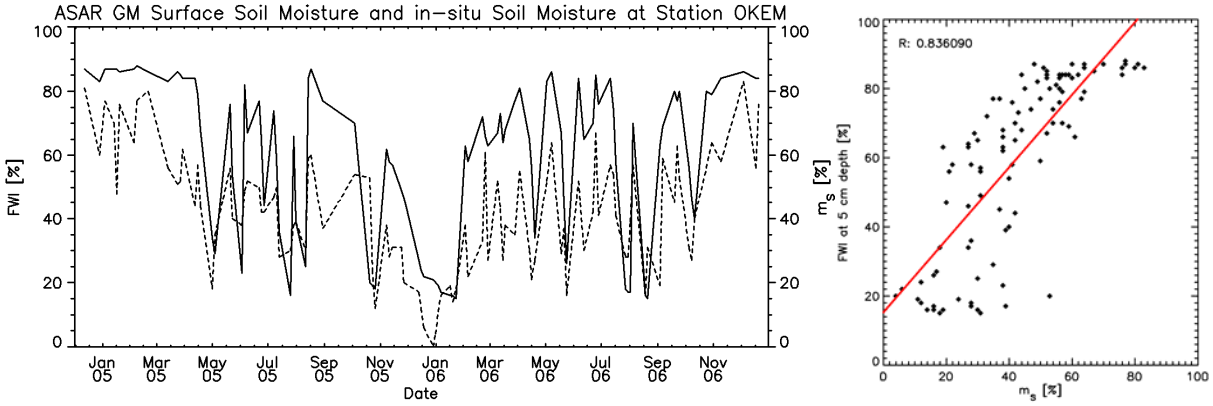

Figure 4 ASAR GM soil moisture m_s (dashed line) and in-situ soil moisture FWI (solid line), time-series (left), scatterplot (right).

3. COMPARISON WITH RUNOFF

River runoff is a point measurement integrating information on the hydrologic status of an entire catchment. To get a representative indicator, soil moisture data can therefore be integrated over all grid points of the sub basins to derive a "Basin Water Index" (BWI) from scatterometer derived Soil Water Index (SWI; Scipal et al., 2005). The SWI is retrieved from temporally filtered near surface soil moisture in accordance with an infiltration modelling approach (Wagner et al., 1999a and 1999b). This results in regular time intervals of 10 days. This cannot be applied to ENVISAT ASAR Global Mode due to the lower and irregular sampling rate. Therefore monthly mean values of the near surface soil moisture have been used to derive the BWI from ENVISAT data. All BWI values are compared to river runoff data which have also been averaged to 10-day or 1-month periods respectively. Both, ERS scatterometer and ENVISAT ScanSAR derived BWI have been

derived for the upper Okavango catchment in Angola and compared to discharge at Mohembo, the entrance to the Okavango inland delta in Botswana. The contribution of Okavango River discharge is essential for the maintenance of the complex wetland area which constitutes the delta. Depending on basin size a delay between BWI and measured river runoff (source: Global Runoff data Centre - GRDC) can be observed. Taking this offset into account a correlation between river runoff and BWI can be found. The relationship can be described by a logarithmic function. Correlations are 0.88 (R^2=0.77) for the entire upper active Okavango River basin (Figure 5a).

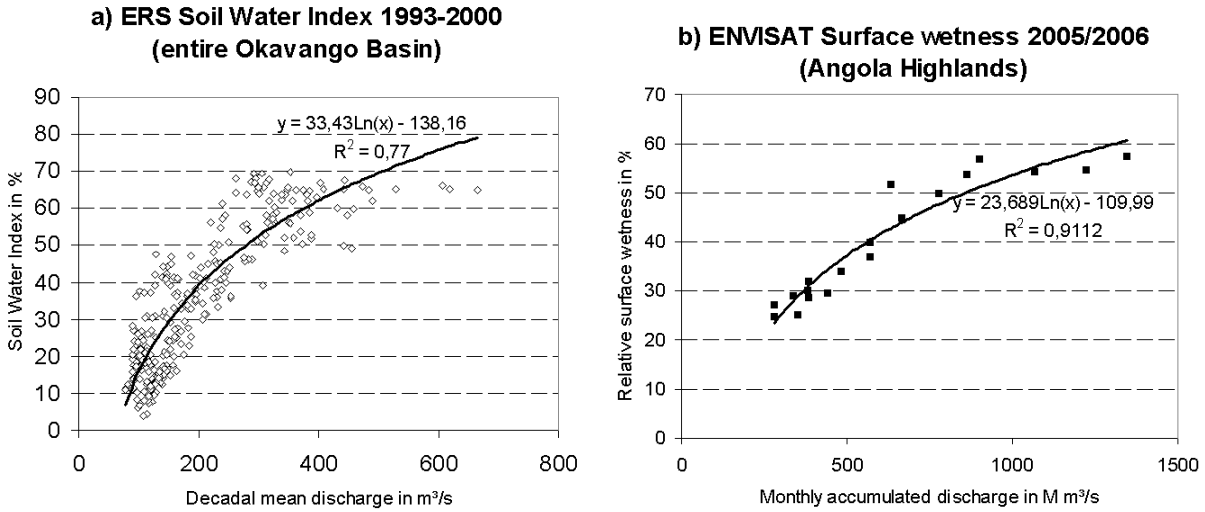

Figure 5 Satellite data derived relative soil moisture integrated for catchment upstream from Mohembo (the entrance of the Okavango river to the delta) in comparison with discharge measurements (a) Soil water index (10 day intervals) from scatterometer (50 km). (b) Relative Surface Soil moisture (monthly mean) from ENVISAT ASAR GM (1km).

Monthly averages have been derived from the 1 km ENVISAT ASAR Global Mode product for the years 2005 and 2006. Monthly discharge measurements at Mohembo have been provided by the Harry Oppenheimer Okavango Research Centre, Botswana (HOORC) for these recent years. Furthermore, only the mountain region within Angola is taken into account since the majority of input originates from this area. The correlation between monthly means and river runoff at Mohembo is above 0.9 (Figure 5b). The offset in case of the two monitored years is three months. This value is higher than for the scatterometer example (60-70 days) which is based on data from nine consecutive years. This difference may result from one or several of the following issues:

1. The scatterometer derived BWI is based on SWI values which result from a temporal filtering approach. The ScanSAR derived BWI represents near surface soil moisture before infiltration.
2. The year 2006 was an anomalous year. Precipitation during the rainy season was above average. It also shows a shorter offset in 2005 than in 2006.
3. The time steps differ. The 10 intervals allow capturing variation within single months. This is not possible for ScanSAR (monthly averages).
4. Data coverage with GM varies within the catchment and thus the monthly average may represent differing time periods from point to point.

4. COMPARISON WITH PRECIPITATION DATA

Surface soil moisture patterns reflect recent local precipitation events. Beside the utilization of gauges which deliver point data, rain radar measurements are used in southern Africa. This offers the opportunity to compare spatial patterns of the experimental soil moisture product with precipitation events. Precipitation is

also available from satellite data through i.e. the Famine Early Warning System Network (FEWS NET). These precipitation maps (10 km) are visually compared to the 1 km product on regional scale (monthly means) and local scale (daily estimates).

4.1 Rain radar measurements

Three case studies are provided, which compare the spatial distribution of surface soil moisture with observed rainfall over South Africa as measured by the SAWS rain gauge and weather radar networks. The daily totals of the gauge network have been spatially interpolated using Kriging (Deyzel et al., 2004; Kroese, 2004; Pegram, 2004) and the radar totals are a composite from the SAWS weather radar network.

The case presented is for the wet season (January 2006) and shows a 3-day composite (Figure 6a) of surface soil wetness. Figure 6b shows the observed rainfall from gauges and radar respectively for the two days prior to the soil wetness composite. There is good correspondence between the spatial distribution of the rainfall and the resulting soil wetness as would be expected since the surface soil layer must respond directly to rainfall.

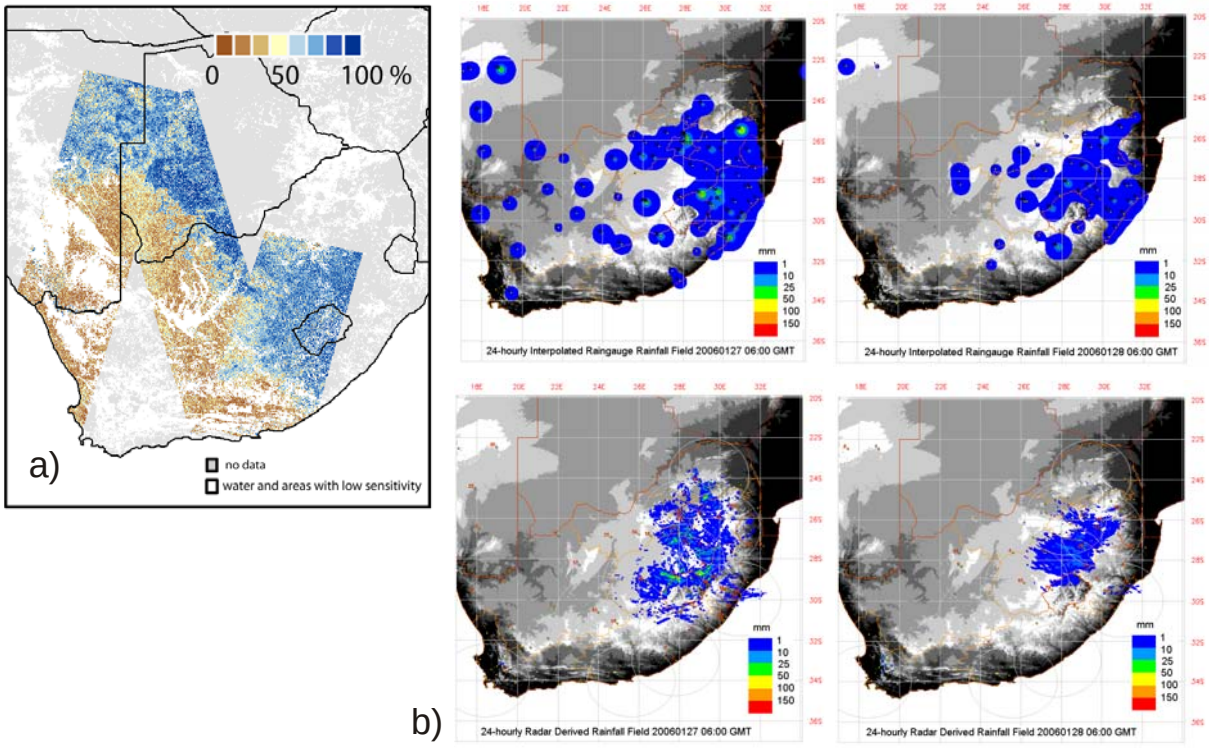

Figure 6 (a) 3-day composite of the 1km surface soil moisture product between 28 and 30 January 2006. The most recent data has been overlaid on the older data. (b) Estimated 24 hour rainfall totals from interpolated rain gauge and radar data for the 24 hour periods ending 06:00 GMT on the 27th and 28th of January 2006 respectively.

4.2 FEWS NET comparison

Rainfall estimates (RFE) available from the Famine Early Warning System Network (FEWS NET) were compared to the ASAR Experimental Soil Moisture data. RFE are produced using the maximum likelihood estimation method, which combines Meteosat and Global Telecommunication System (GTS) data together with station rainfall data (Herman et al., 1997, http://earlywarning.usgs.gov/adds/RFEPaper.php). The newer RFE technique combines latter methods with data from the Special Sensor Microwave/Imager (SSM/I) and the Advanced Microwave Sounding Unit (AMSU) satellite. As of January 1, 2001, RFE version 2.0 has been

implemented by NOAA's Climate Prediction Center. The rainfall estimates are made available in 10 km resolution. Both, monthly and daily values have been examined. Monthly RFE are compared to the monthly composites from ASAR. The spatial patterns of daily estimates are shown on local scale for two selected provinces with frequent ASAR GM coverage. It can be shown that the ASAR GM soil moisture product depicts short term as well as long term features at regional and local scales.
The selected example of monthly rainfall estimates shows the onset of the rainy season (November, Fig. 7). The expanding southern limit of area affected by rainy season is clearly visible. A time lag between precipitation and soil moisture increase can be seen in parts of Angola, Botswana, Zimbabwe and Zambia. While mean precipitation values are increasing after the dry season, the mean monthly soil moisture either stays still relatively low or GM acquisitions are not frequent enough to capture the first precipitation. The storage period of water in the top soil is comparably short immediately after the dry season. This highlights the actual difference between rainfall and soil moisture products. The ASAR GM near surface soil moisture product already represents local conditions (climate and soil) which limit the eventually available water within the top soil.

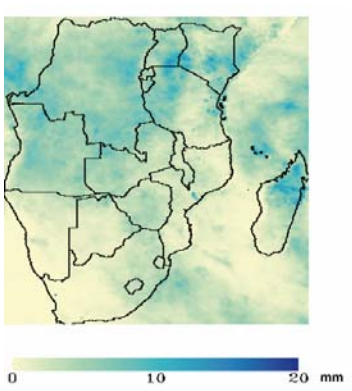

a) FEWS NET

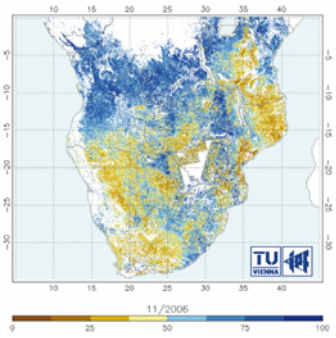

b) ASAR GM

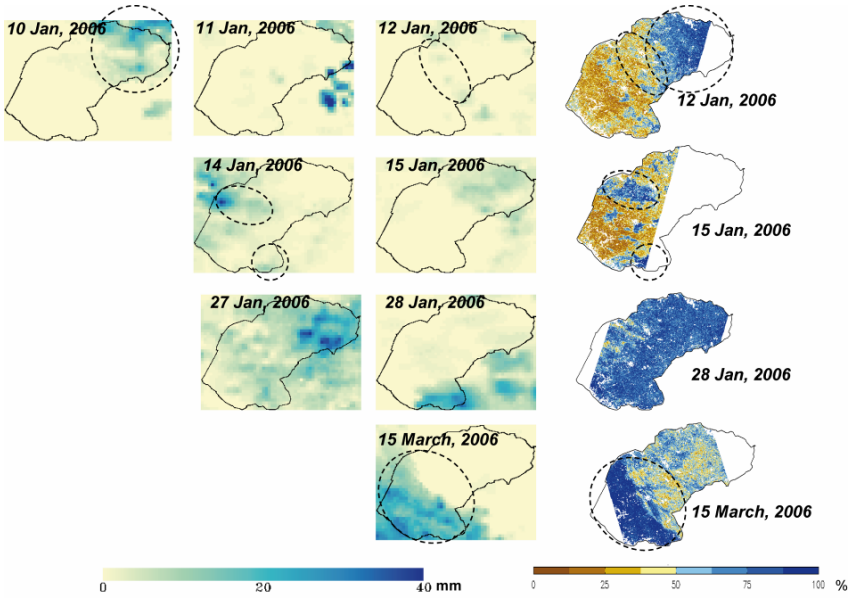

c) day by day comparison FEWS NET – ASAR GM

Figure 7: (a) Monthly rainfall estimates (RFE) from the Famine Early Warning System Network (FEWS NET) and (b) monthly composites (mean) ASAR Global Mode Experimental Soil Moisture from TU Wien for November 2006; (c) Rainfall estimates (RFE) from the Famine Early Warning System Network (FEWS NET) (left) and ASAR Global Mode Experimental Soil Moisture from TU Wien (right) for four selected dates during rainy season in Free State province, Eastern South Africa.

5. SUMMARY

SHARE provides an operational service for hydrometeorological applications in the Southern African Development Community region. Maps of soil moisture dynamics based on satellite data on local and regional scale are made freely available on the internet. Both the coarse resolution product (scatterometer, 25-50 km) and the medium resolution product (ScanSAR, 1 km) have been compared to ground measurements and other remotely sensed datasets for validation purposes. The results have been assessed by comparison with modelled soil moisture and river runoff measurements. In case of the latter, Pearson correlation was >0.9 for scatterometer as well as ScanSAR derived relative soil moisture. A basin specific temporal offset can be observed which yields potential for river discharge forecasting. If knowledge is established about this relationship and also the spatial patterns in gauged and un-gauged basins, flood risk assessments could be enhanced.

There is a very good correspondence between the SWI estimates and modelled soil moisture fields (from TOPKAPI) what is illustrated by the coefficients of determination (R^2) between 0.78 and 0.922 in the Liebenbergsvlei, RSA. As an interesting example, the value of the initial soil moisture, which has been calibrated at 40%, could have been estimated by using the remotely sensed value (Vischel, et al. 2008). This result is very encouraging since the initialization of the hydrological models remains a constant problem in hydrology.

A comparison between monthly means of Fractional Water Index (FWI) and GM surface soil moisture has been carried out. The FWI was derived from a station which is part of the Oklahoma Mesonet (USA). A linear correlation coefficient of r=0.6 can be observed for more than 50% of the 115 stations. Visual comparison between precipitation maps and relative near surface soil moisture maps highlighted the actual difference between rainfall and soil moisture products. The remotely sensed near surface soil moisture product represents also local ground conditions (climate and soil) which limit the actual water content within the top soil.

The scatterometer based data provide long time series (since 1992) which are needed for detection of deviations from mean conditions that may result in flooding and droughts. Here, the third SHARE product, the scaling layer, becomes important. It can be used to transfer the gained knowledge from regional (25-50 km) to local (1 km) scale. The synergy of both datasets allows for advanced monitoring and forecasting on continental scale.

6. REFERENCES

Bartalis, Z., Wagner, W., Naeimi, V., Hasenauer, S.., Scipal, K., Bonekamp, H., Figa, J. and Anderson, C. 2007. Initial soil moisture retrievals from the METOP-A Advanced Scatterometer (ASCAT). *Geophysical Research Letters* 34, L20401.

Bartsch, A., Scipal, K., Wolski, P., Pathe, C., Sabel, D. and Wagner, W. 2007. Microwave remote sensing of hydrology in southern Africa. *Proceedings of the 2nd Göttingen GIS & Remote Sensing Days: Global Change Issues in Developing and Emerging Countries, 4 – 6 October, 2006:* pp. 269-277.

Brock, F. V., Crawford, K. C., Elliot, R. L., Cuperus, G. W., Stadler, S. J., Johnson, H. L. and Eilts, M. D. 1995. The Oklahoma Mesonet: A Technical Overview. *J. of Atmos. and Oceanic Tech.,* Vol. 12, pp. 5-19.

Deyzel, I., Pegram, G., Visser, P., and Dicks, D. 2004. Spatial Interpolation and Mapping of Rainfall (SIMAR) Volume 2: Radar and satellite products, *Water Research Commission, Report No. 1152/1/04*, Pretoria.

Herman, A., Kumar, V. B., Arkin, P. A. and Kousky, J. V. 1997. Objectively determined 10-day African rainfall estimates created for famine early warning systems. *Int. J. Rem. Sens.,* Vol. 18, No. 10, pp. 2147-2159.

Illston, B. G., Caldwell, J. C. and Bodnar, s. G. 2004a. Representativeness of Soil Moisture Conditions in Central Oklahoma During the Enhanced Drying Phase. *Proc. American Meteorological Society-18th Conference on Hydrology*; Jan 11-15, Seattle, Washington.

Illston, B. G., Basara, J. B. and Crawford, K. C. 2004b. Seasonal to Interannual Variations of Soil Moisture measured in Oklahoma. *Int. J. Climatology,* Vol. 24, pp. 1883-1896.

Kroese, N. 2004. Spatial Interpolation and Mapping of Rainfall (SIMAR), Volume 1: Maintenance and upgrading of radar and rain gauge infrastructure, *Water Research Commission, Report No. 1151/1/04*, Pretoria.

Liu, Z. and Todini, E. 2002. Towards a comprehensive physically-based rainfall-runoff model. *Hydrology and Earth System Sciences,* Vol. 6, No. 5, pp. 859-881.

McPherson, R. A., Fiebricha, C. A., Crawford, K. C., Elliott, R. L., Kilby, J. R., Grimsley, D. L., Martinez, J. E., Basara, J. B., Illston, B. G., Morris, D. A., Kloesel, K. A., Stadler, S. J., Melvin, A. D., Sutherland, A. J., Shrivastava, H., Carlson, J. D., Wolfinbarger, J. M., Bostic, J. P. and Demko, D. B. 2007. Statewide Monitoring of the Mesoscale Environment: A Technical Update on the Oklahoma Mesonet. *J. of Atmos. and Oceanic Tech.,* Vol. 24, pp. 301-321.

Pathe, C., Wagner, W., Sabel, D., Doubkova, M. and Basara, J. (2009): Using ENVISAT ASAR Global Mode data for surface soil moisture retrieval over Oklahoma, USA. *IEEE Transactions on Geoscience and Remote Sensing* vol.47, No. 2, pp.468-480.

Pathe, C., Wagner, W., Sabel, D., Bartsch, A., Naemi, V., Doubkova, M. and Basara, J. 2007. Soil moisture information from multi-temporal ENVISAT ASAR ScanSAR data over Oklahoma, USA. *Proceedings of Bio- GeoSAR 2007*, Bari.

Pegram, G. 2004. Spatial Interpolation and Mapping of Rainfall (SIMAR) Volume 3: Data Merging for rainfall map production, *Water Research Commission, Report No. 1153/1/04*, Pretoria.

Scipal, K., Scheffler, C. and Wagner, W. 2005. Soil moisture-runoff relation at the catchment scale as observed with coarse resolution microwave remote sensing. *Hydrology and Earth System Sciences,* Vol. 9, 3, pp. 173-183.

Vischel, T., Pegram, G., Sinclair, S., Wagner, W. and Bartsch, A. 2008. Comparison of soil moisture fields estimated by catchment modelling and remote sensing: A case study in South Africa. *Hydrol. Earth Syst. Sci.* 12, pp. 1-17.

Wagner, W., Lemoine, G., Borgeaud, M. and Rott, H. 1999a. A Study of Vegetation Cover Effects on ERS Scatterometer Data. *IEEE Trans. Geosci. Rem. Sens.* Vol. 37, No. 2, pp. 938-948.

Wagner, W., Lemoine, G. and Rott, H. 1999b. A Method for Estimating Soil Moisture from ERS Scatterometer and Soil Data. *Rem. Sens. Environ.* 70, pp. 191-207.

Wagner, W., Scipal, K., Pathe, C., Gerten, D., Lucht, W. and Rudolf, B. 2003. Evaluation of the agreement between the first global remotely sensed soil moisture data with model and precipitation data. *J. Geophys. Res. Atmos.* 108(D19): 4611.

Wagner, W., Pathe, C., Sabel, D., Bartsch, A., Künzer, C. and Scipal, K. 2007. Experimental 1 km soil moisture products from ENVISAT ASAR for Southern Africa. *Proceedings of the ENVISAT Symposium, Montreux 2007*.

Wagner, W., Pathe, C., Doubkova, M., Sabel, D., Bartsch, A., Hasenauer, S., Blöschl, G.,Scipal, K., Martínez-Fernández, J. and Löw, A. 2008. Temporal stability of soil moisture and radar backscatter observed by the Advanced Synthetic Aperture Radar (ASAR). *Sensors,* Vol. 8, No. 2, pp. 1174-1197.

List of Acronyms and Abbreviations

ABD	AbdelMoumen
ABHSM	Agence du Bassin Hydraulique de Souss Massa
AGNPS	Agricultural Non-Point Source
AHP	Analytical Hierarchy Process
AMSU	Advanced Microwave Sounding Unit
ANRH	Agence Nationale des Ressources Hydrauliques
AOI	Area Of Interest
ASAR	Advanced Synthetic Aperture Radar
AVHRR	Advanced Very High Resolution Radiometer
AWF	African Water Facility
BWI	Basin Water Index
CCD	Charge Coupled Device
CDM	Conceptual Data Model
CHES	Coupling Human and Environmental Systems
CMOD	Compact Meteorological and Oceanographic Drifter
CNTS	Centre National des Techniques Spatiales
CRTS	Centre Royal de Télédétection Spatiale
CSA	Canadian Space Agency
CWR	Crop Water Requirement
DEM	Digital Elevation Model
DN	Digital Number
DORIS	Doppler Orbitography and Radio-positioning Integrated by Satellite
DSS	Decision Support System
EC-JRC	European Commission Joint Research Centre
ECMWF	European Centre for Medium-range Weather Forecasts
EMBD	Enhanced Model Based Despeckling
EMS	Electro Magnetic Spectrum
ENVISAT	Environment Satellite
EO	Earth Observation
ERS	European Remote Sensing satellite
ESA	European Space Agency
ET	Evapotranspiration
ETM	Enhanced Thematic Mapper
FAO	Food and Agriculture Organization
FAPAR	Fraction of Absorbed Photosynthetically Active Radiation
FCC	False Colour Composite
FEWS Net	Famine Early Warning System Network
FR	Full Resolution
FWI	Fractional Water Index
GCP	Ground Control Point
GDE	Gestion de la Demande en Eau
GIS	Geographical Information System
GLC	Global Landcover Classification
GM	Global Mode
GPS	Global Positioning System
GRDC	Global Runoff Data Centre
GTS	Global Telecommunication System
GUI	Graphical User Interface
HH	Horizontal/Horizontal polarisation
HIS	Intensity Hue Saturation
HV	Horizontal/Vertical polarisation
HOORC	Harry Oppenheimer Okavango Research Centre
IDSS	Integrated Decision Support System
IFS	International Foundation for Science
IWR	Irrigation Water Requirement
LC	Land Cover
LCCS	Land Cover Classification System
LR	Low Resolution
LU	Land Use
LULC	Land Use and Land Cover
MCE	Multi-Criteria Evaluation
MDA	Macdonald Dettwiler and Associates
MERIS	Medium-spectral Resolution Imaging Spectrometer
METOP	Meteorological Operational Satellite
MLC	Maximum Likelihood Classification
MNT	Modèle Numérique de Terrain
MSG	Meteosat Second Generation
MTCI	Meris Terrestrial Chlorophyll Index
NASA	National Aeronautics and Space Administration
NDVI	Normalized Differenced Vegetation Index
NN	Nearest Neighbour
NOAA	National Oceanic and Atmospheric Administration
NPS	Non-Point Source
ORMVA SM	Office Regional de Mise en Valeur Agricole du Souss-Massa

OSS	Observatoire du Sahel et du Sahara
PC	Principal Components
RADAR	Radio Detection And Ranging
RADARSAT	Radar Satellite
RFE	Rainfall Estimates
RMSE	Root Mean Square Error
RR	Reduced Resolution
RSA	Republic of South Africa
SADC	Southern African Development Community
SAI	Système Aquifère d'Iullemeden
SAR	Synthetic Aperture Radar
SASS	Système Aquifère du Sahara Septentrional
SAWS	South African Weather Service
SIAD	Système Intégré d'Aide a la Décision
SIG	Système d'Information Géographique
SMAC	Simplified Method for Atmospheric Corrections
SPOT	Satellite Pour l'Observation de la Terre
SR	Surface Reflectance
SRTM	Shuttle Radar Topography Mission
SWI	Soil Water Index
TAUDEM	Terrain Analysis and Using DEM
TM	Thematic Mapper
TOA	Top Of the Atmosphere
TOPKAPI	Topographic Kinematic Approximation and Integration
TS	Time Series
TU Wien	Vienna University Of Technology
UNESCO	United Nations Educational, Scientific and Cultural Organization
USGS	U.S. Geological Survey
USLE	Universal Soil Loss Equation
UTM	Universal Transverse of Mercator
VGT	Vegetation
VV	**Vertical/Vertical polarisation**
WDM	Water Demand Management
WEAP	Water Evaluation And Planning
WGS	World Geodetic System
WMO	World Meteorological Organisation
WS	Wide Swath
YBT	Youssef Ben TachFine

Contact information

INTERNATIONAL HYDROLOGICAL PROGRAMME (IHP)
UNESCO/Division of Water Sciences (SC/HYD)
1 rue Miollis
75732 Paris Cedex 15
France
Tel: (+33) 1 45 68 40 01
Fax: (+33) 1 45 68 58 11
Email: ihp@unesco.org
http://www.unesco.org/water/ihp